



Willis, Miranda Jane (2014) *Prostate cancer: the significance of the cAMP signalling pathway*. PhD thesis.

<http://theses.gla.ac.uk/5410/>

Copyright and moral rights for this work are retained by the author

A copy can be downloaded for personal non-commercial research or study, without prior permission or charge

This work cannot be reproduced or quoted extensively from without first obtaining permission in writing from the author

The content must not be changed in any way or sold commercially in any format or medium without the formal permission of the author

When referring to this work, full bibliographic details including the author, title, awarding institution and date of the thesis must be given

Enlighten:Theses
<http://theses.gla.ac.uk/>
theses@gla.ac.uk

Prostate Cancer: The Significance of the cAMP Signalling Pathway

A thesis submitted in fulfilment of the Degree of

Doctor of Philosophy
in
Integrated Biology

To The



**University
of Glasgow**

Institute of Cardiovascular and Medical Sciences
College of Medical, Veterinary and Life Sciences

Miranda Jane Willis

Abstract

Prostate cancer is the leading form of male cancer in western countries. However, despite a great deal of interest from the scientific community, the cause still remains elusive. What is clear, is that androgenic signalling is important within prostate cancer progression, with early cancer under androgenic control and androgen regulated genes, such as PSA, commonly used for patient prognosis and progression.

3',5'- cyclic adenosine monophosphate (cAMP) is an important second messenger signalling molecule, which has been extensively studied within the field of oncogenesis. cAMP signalling effects are transduced via its effector molecules, PKA and EPAC, and the temporal and spatial control of cAMP dynamics are orchestrated by phosphodiesterase enzymes (PDEs). This signalling pathway has been implicated in a wide range of cellular processes such as, cellular differentiation, transcription, proliferation, apoptosis and learning and memory. In addition, it has also been linked to steroid receptor signalling such as oestrogen, progesterone, and androgen receptors.

PKA can be expressed as 2 forms (PKA-I and PKA-II) depending on the regulatory unit isoform content of the enzyme. In the field of cancer research, PKA-I and PKA-II expression profiles have been shown to be linked to the phenotype of the cancer, i.e. overexpression of PKA-I is linked to a more proliferative cancer. Furthermore, other protein intermediates within the cAMP signalling pathway, including PKAC isoforms (PKA catalytic unit) and PDEs, change with respect to isoform expression and regulation during cancer progression.

In this thesis, I have described my original research in which I endeavoured to understand the role of several components of the cAMP signalling axis in human prostate cancer. I have profiled the isoforms of PKA in androgen sensitive and insensitive prostate cancer, identifying isoforms that are dysregulated in the androgen independent disease stage. In particular, I found a down regulation of PKARIIB and PKACB isoforms in AI prostate cancer compared to AS. The function of these isoforms are not well categorised in prostate cancer. Due to the higher expression of these isoforms in AS cells, I went on to scrutinise these isoforms in relation to their interaction with androgenic signalling. Here, I have uncovered

previously undiscovered aspects of PKA signalling, including the direct interaction of PKAR1B and PKAC β isoforms with the androgen receptor (AR), and that PKA can phosphorylate the AR at site S791. Further analysis of this putative phosphorylation site would be beneficial to isolate a functional output.

In addition, following previous work in the laboratory that identified PDE4D7 as a potential biomarker in prostate cancer, I have investigated novel-PDE4D7 controlled signalling pathways using cutting edge techniques. This data allows a better understanding of the mechanism behind the alteration of PDE4D7 driven signals and their significance during prostate cancer progression. Given more time and scrutiny, changes in these identified novel-PDE4D7 controlled signalling pathways, such as N-MYC, could show sites for exciting study into prostate cancer progression.

Table of Contents

ABSTRACT	2
LIST OF FIGURES	8
LIST OF TABLES	10
ACKNOWLEDGEMENT	11
AUTHOR'S DECLARATION	12
DEFINITIONS/ABBREVIATIONS	13
1 INTRODUCTION- CAMP SIGNALLING AND PROSTATE CANCER	15
1.1 CYCLIC NUCLEOTIDE SIGNALLING	15
1.2 PROTEIN KINASE A	17
1.2.1 STRUCTURE	17
1.3 PHOSPHODIESTERASES: OVERVIEW	20
1.3.1 PDE4	21
1.3.1.1 Structure	21
1.4 PKA, PDE AND DISEASE	23
1.5 HUMAN PROSTATE GLAND	25
1.5.1 FUNCTION	25
1.5.2 STRUCTURE	26
1.5.2.1 Peripheral Zone	27
1.5.2.2 Central Zone	28
1.5.2.3 Pre-Prostatic/Transition Zone	28
1.5.2.4 Fibromuscular Stoma	28
1.6 HORMONE SIGNALLING	28
1.6.1 TESTOSTERONE AND DIHYDROTESTOTERONE	29
1.6.2 AR	30
1.6.2.1 Function	30
1.6.2.2 Structure	31
1.7 PROSTATE DISEASES	36
1.7.1 BENIGN PROSTATIC HYPERPLASIA	36
1.7.2 PROSTATITIS	37
1.7.3 PROSTATE CANCER	37
1.7.3.1 Epidemiology	37
1.7.3.2 Hormone signalling and Prostate Cancer Progression	39
1.7.3.3 Later Stage- Androgen Independence	40
1.8 CURRENT DIAGNOSTICS AND PROCEDURES	40
1.8.1 DIAGNOSIS	40
1.8.1.1 PSA	40
1.8.1.2 Gleason Scoring	41
1.8.2 TREATMENTS	43
1.8.2.1 Hormone therapy	43
1.8.2.2 Prostatectomy	43
1.8.2.3 Radiotherapy	44

2.1 CELLS CULTURE	45
2.1.1 CULTURE	45
2.1.1.1 Sub-culture of cell lines	45
2.1.1.2 Storage of Cell Lines	46
2.1.2 TRANSFECTION	46
2.1.2.1 Lipofectamine 2000 [®]	46
2.1.2.2 X-treme GENE HP [®]	47
2.1.2.3 Polyfect [®]	48
2.1.3 LYSATE HARVESTING	48
2.1.4 LUCIFERASE REPORTER ARRAYS	49
2.1.4.1 Luciferase Assay Calculation	50
2.2 WESTERN BLOTTING PROCEDURES	50
2.2.1 BRADFORD ASSAY	50
2.2.2 SDS-PAGE	50
2.2.3 WESTERN BLOTTING	51
2.2.4 IMMUNO-PRECIPIATION	52
2.2.5 PEPTIDE KINASE ASSAY	52
2.3 PCR	53
2.3.1 EXTRACTION AND PURIFICATION OF RNA	53
2.3.2 NUCLEIC ACID QUANTIFICATION	54
2.3.3 cDNA SYNTHESIS	54
2.3.4 QUANTITATIVE REAL TIME PCR	55
2.3.4.1 Primer Design (TaqMan [®])	55
2.3.4.2 RT-qPCR Protocol (Taqman [®])	55
2.3.5 SYBRGREEN cDNA SYNTHESIS	56
2.3.5.1 RT-qPCR Protocol (SybrGreen [®])	57
2.3.6 CALCULATING RELATIVE EXPRESSION	57
2.3.6.1 The $\Delta\Delta C_t$ Method to Calculate Comparative Expression	58
2.4 HARVESTING OF PLASMID DNA	59
2.4.1 TRANSFORMATION	59
2.4.2 GLYCEROL STOCKS	59
2.4.3 PLASMID DNA PURIFICATION	59
2.5 CELLSPOT[™] PEPTIDE ARRAYS	60
2.6 PURE PROTEIN KINASE ASSAY	60
2.7 PROTEIN ISOLATION AND OVERLAY	61
2.8 PDE ASSAY	62
2.9 MICROSCOPY	63
2.9.1 CONFOCAL MICROSCOPY	63
2.10 STATISTICAL ANALYSIS	63
2.10.1 STUDENTS T-TEST	63
2.10.2 MANN-WHITELY TEST	64

3.1 INTRODUCTION	65
3.1.1 PKA SUBUNITS IN HORMONE RELATED CANCERS	65
3.1.2 PKA SUBUNITS IN PROSTATE CANCER	66
3.2 RESULTS	68
3.2.1 RT-qPCR PROFILING VS WESTERN BLOTTING	68
3.2.1.1 Western blotting	68
3.2.1.2 Antibody selection	68
3.2.1.3 RT-qPCR	69

3.2.1.4	TaqMan Probes	69
3.2.1.5	Use of Relative Quantification	70
3.2.1.6	Housekeeping Gene Selection	70
3.2.2	SELECTION OF CELL LINES	72
3.2.2.1	AS cell lines	73
3.2.2.2	AI cell lines	73
3.2.2.3	Normal prostate epithelial	74
3.2.3	EXPRESSION PROFILE OF PKA SUBUNITS IN PROSTATE CANCER CELL LINES	74
3.2.3.1	Western Blotting	74
3.2.3.2	RT-qPCR	76
3.2.4	PKA SUBUNIT EXPRESSION IN PROSTATE CANCER SAMPLES	78
3.2.4.1	Regulatory Subunits	80
3.2.4.2	Catalytic Subunits	81
3.2.5	REGULATION CHANGE OF PKA SUBUNITS TOWARDS ANDROGEN INDEPENDENCE	83
3.2.6	PKA SUBUNIT EXPRESSION IN A NORMAL PROSTATE EPITHELIAL CELL LINE	84
3.3	DISCUSSION	86
4	<u>STUDY OF PUTATIVE PKA PHOSPHORYLATION SITES ON THE ANDROGEN RECEPTOR</u>	90
4.1	INTRODUCTION	90
4.1.1	AR AND POSTTRANSLATIONAL MODIFICATIONS	90
4.1.2	AR AS A PHOSPHO-PROTEIN	90
4.1.3	THE EFFECT OF FSK TREATMENT ON AR	92
4.2	RESULTS	94
4.2.1	INVESTIGATIONS INTO THE PHOSPHORYLATION OF AR BY PKA.	94
4.2.2	PEPTIDE ARRAY ANALYSIS OF NOVEL PHOSPHO-ANTIBODIES	98
4.2.3	DETECTION OF PUTATIVE PHOSPHORYLATION SITES USING NOVEL PHOSPHO-ANTIBODIES IN CELLS	101
4.2.3.1	Androgen Receptor transfected HEK293 model	102
4.2.3.2	Prostate cancer cell lines	105
4.2.3.3	DHT	108
4.2.4	R11B AR INTERACTION	113
4.2.4.1	R11 β AR IP	114
4.2.4.2	Confocal analysis of proposed R11 β and AR interaction	115
4.3	DISCUSSION	118
5	<u>EXPOSING THE ROLE OF PDE4D7 IN PROSTATE CANCER PROGRESSION</u>	122
5.1	INTRODUCTION	122
5.1.1	PDE4S AND LINKS IN PROSTATE CANCER	122
5.1.2	PDE4D7	123
5.2	RESULTS	125
5.2.1	USING VCAP AS A MODEL TO INVESTIGATE PDE4D7 FUNCTION IN PC.	125
5.2.2	PDE4D7 CONSTRUCTS	125
5.2.3	THE USE OF HIGH –THROUGH-PUT SCREENS	126
5.2.4	RT-qPCR	127
5.2.4.1	Sybr-green vs Taq-man	127
5.2.4.2	RT ² Profiler™ PCR arrays	128
5.2.4.3	CAV	134
5.2.4.4	CASP3	135
5.2.4.5	BCL2	135
5.2.4.6	IL6	137
5.2.4.7	Validation of candidates using RT-qPCR	137
5.2.5	LUCIFERASE REPORTER ARRAYS	139

5.2.6	RPPA	145
5.2.7	CELLUSPOT ARRAYS	147
5.2.7.1	APC	149
5.2.7.2	N-Myc	150
5.2.7.3	Glutamate Receptor Subunit Zeta1	150
5.2.7.4	Ret	151
5.2.7.5	CD136	152
5.3	DISCUSSION	153
6	DISCUSSION	157
6.1	AIMS	157
6.2	cAMP SIGNALLING MOLECULES AND PROSTATE CANCER	157
6.2.1	PKA SUB-UNIT REGULATION CHANGE	157
6.2.1.1	Regulatory subunits	157
6.2.1.2	Catalytic subunit	158
6.3	PKA RIIb AND PKACb AS BIOMARKERS	160
6.4	PDE4D7 COMPARTMENTALISED SIGNALLING DYNAMICS AND INTERACTIVE PATHWAYS	161
	APPENDICES	163
	LIST OF REFERENCES	171

List of Figures

Figure 1.1 Example of cAMP signalling cascade	16
Figure 1.2 PKA activation	18
Figure 1.3 PDE4 Family Structures	22
Figure 1.4 Anatomical view of the prostate gland	26
Figure 1.5 Prostatic Structure (zone model).....	27
Figure 1.6 Schematic of basic androgen receptor signalling	31
Figure 1.7 Predicted structural model of the AR. Adapted from [82, 83]	32
Figure 1.8 Crystal structure of DHT-bound androgen receptor LBD in complex with the first motif of steroid receptor coactivator 3	35
Figure 3.1 GAPDH and 18S rRNA expression in prostate cancer samples.	71
Figure 3.2 PDE4D7 was assessed against GAPDH and 18SrRNA.	72
Figure 3.3 PKA isoform protein expression profile of AS LNCaP cell line	75
Figure 3.4 PKA isoform protein expression profile of AS VCaP cell line	75
Figure 3.5 PKA isoform protein expression profile of AI DU145 cell line.....	75
Figure 3.6 PKA isoform protein expression profile of AI PC3 cell line.....	76
Figure 3.7 PKA isoform mRNA expression profile of AS LNCaP cell line.....	76
Figure 3.8 PKA isoform mRNA expression profile of AS VCaP cell line.....	77
Figure 3.9 PKA isoform mRNA expression profile of AS DUCaP cell line	77
Figure 3.10 PKA isoform mRNA expression profile of AI DU145 cell line	77
Figure 3.11 PKA isoform mRNA expression profile of AI PC3 cell line	78
Figure 3.12 PKA isoform mRNA expression profile of AI PC133 xenograph.....	78
Figure 3.13 PKA expression of AS vs AI cell lines	79
Figure 3.14 Box and whisker plot showing analysis of the PKA isoform protein expression in AS and AI prostate cancer samples	82
Figure 3.15 Box and whisker plot showing analysis of PKA isoform mRNA expression in AS and AI prostate cancer samples	82
Figure 3.16 Androgen dependent regulation of PKA RII β and C β in CSS incubated LNCaP cells.....	84
Figure 3.17 PKA isoform mRNA expression profile of PNT1a normal epithelial prostate cell line	85
Figure 4.1 PKA C β phosphorylation of AR	95
Figure 4.2 Peptide array, overlaid with active PKA catalytic unit	96
Figure 4.3 Peptide arrays overlaid with novel antibodies.....	99
Figure 4.4 Truncated peptide arrays overlaid with novel pS791 antibodies.....	100
Figure 4.5 Testing of novel phospho antibodies in HEK 293 cells	103
Figure 4.6 Testing of novel phospho antibodies in using AR IP.....	104
Figure 4.7: Time course of Forskolin\IBMX treatment in transfected PC3 cells.....	106
Figure 4.8: Time course of Forskolin\IBMX treatment in transfected LNCaP cells	107
Figure 4.9: Treatment of transfected HEK 293 and LNCaP cells with both DHT and FSK\IBMX.....	109
Figure 4.10: 24hr Treatment of transfected HEK 293 cells with both DHT and FSK\IBMX.....	112
Figure 4.11: Overlay of pure RII β protein on a AR peptide array.....	114
Figure 4.12: Co-immuno-precipitation of AR and PKA RII β subunit in LNCaP cells.....	115
Figure 4.13: Co-localisation experiments using confocal microscopy.....	116
Figure 5.1 PDE activity of PDE4D7 constructs transfected into HEK293.....	126
Figure 5.2 Expression of PDE4D7 constructs transfected into VCaP cell.....	128
Figure 5.3 Diagram explaining RT ² Profiler TM PCR array technique.....	129
Figure 5.4 Fold regulation of RT ² Profiler TM prostate cancer PCR array	130

<i>Figure 5.5 Fold regulation of RT² ProfilerTM cancer pathway finder PCR array</i>	131
<i>Figure 5.6 Fold regulation of RT² ProfilerTM focal adhesion PCR array</i>	133
<i>Figure 5.7 Validation of the genes isolated for potential interaction with PDE4D7</i>	138
<i>Figure 5.8 Diagram demonstrating the layout and procedure for the use of luciferase reporter arrays (SA Biosciences®)</i>	140
<i>Figure 5.9 Luciferase reporter array results</i>	143
<i>Figure 5.10 Positive and negative controls for the Luciferase reporter arrays</i>	144
<i>Figure 5.11 Diagram outlining the Reverse Phase Protein Array procedure</i>	145
<i>Figure 5.12 PDE4D7 transfected VCaP RPPA protein expression profile</i>	146
<i>Figure 5.14 CelluSpot peptide array phosphorylation analyses with PDE4D7 transfected VCaP lysates</i>	149
<i>Figure 7.1 Quantification of VCaP cells transfected with PDE4D7 constructs</i>	163
<i>Figure 7.2 Validation of the genes isolated for potential interaction with PDE4D7 (18s HKG)</i>	163
<i>Figure 7.3 Validation of the genes isolated for potential interaction with PDE4D7 (β-actin HKG)</i>	164
<i>Figure 7.4 PDE4D7 transfected VCaP RPPA protein expression profile (Full Screen Part 1)</i>	165
<i>Figure 7.5 PDE4D7 transfected VCaP RPPA protein expression images (Full Screen Part 1)</i>	166
<i>Figure 7.6 PDE4D7 transfected VCaP RPPA protein expression profile (Full Screen Part 2)</i>	167
<i>Figure 7.7 PDE4D7 transfected VCaP RPPA protein expression images (Full Screen Part 2)</i>	168
<i>Figure 7.8 PDE4D7 transfected VCaP RPPA protein expression profile (Full Screen Part 3)</i>	169
<i>Figure 7.9 PDE4D7 transfected VCaP RPPA protein expression images (Full Screen Part 3)</i>	170

List of Tables

<i>Table 1.1 Overview of the Gleason scoring system for prostate tumours</i>	<i>42</i>
<i>Table 3.1 Showing the regulation status of the PKA isoforms from AS to AI phenotype.....</i>	<i>81</i>
<i>Table 4.1 Summary of AR phosphorylation sites</i>	<i>91</i>

Acknowledgement

First I would like to give my thanks to my supervisor Prof. George Baillie, for giving me this opportunity to do my PhD and his guidance throughout the project. I would also like to thank Dr Ralf Hoffmann from Philip research for the opportunity and resources to carry out my PhD.

A big thankyou to Dr. Elaine Huston, Dr. Frank Cristian and Dr. David Henderson, their expertise and guidance throughout my PhD has been resolute. I am forever indebted to your patience and teaching skill. I wish to also thank the Gardiner laboratory members past and present for all their time, chats and kind ear. You are all amazing people and wonderful colleagues and I feel privileged to have worked alongside you.

I would like to say thanks to Dr. Krishna Yalla, Craig Livie, Dr Eirini Vagen, Dr Tamara Martin, Louisa Lee for all the late nights in the laboratory definitely would not have been as much fun without you 😊. To all my friends who have supported me throughout my PhD I would like to say a big thank you for all your kind words and encouragements, for lending an ear when needed and making my precious time outside the laboratory so much fun. I am so blessed to have you all in my life and I am truly grateful to you all.

Last but not least I wish to thank my family. Thankyou for all your patience, kind words and unconditional love. You are the unwavering scaffold on which I build my hopes and dreams and it is to you that I dedicate my thesis.

Author's Declaration

I hereby declare that the work in this thesis is my own composition and that it is a record of work performed personally. It has not been submitted for consideration in any previous application for a higher degree or award.

Miranda Jane Willis

Definitions/Abbreviations

AC	Adenylyl Cyclase
AKAP	A-kinase Anchoring Protein
AI	Androgen Insensitive/Independent
AMP	Adenosine Monophosphate
ARE	Androgen Response Element
AR	Androgen Receptor
AS	Androgen Sensitive
ATP	Adenosine Triphosphate
bp	Base Pair
BPH	Benign Prostatic Hyperplasia
cAMP	Cyclic Adenosine Monophosphate
cDNA	Complementary DNA
CRE	cAMP Response Element
CREB	cAMP response element binding (protein)
DN	Dominant Negative
dNTP	deoxy nucleotide triphosphates
DISC1	Disrupted in Schizophrenia 1
DHT	Dihydrotestosterone / 17 β -diol-glucuronide
DMEM	Dulbecco's modified eagle's medium
DMSO	Di methyl Sulfoxide
DNA	Deoxyribo nucleic acid
DTT	Dithiothreitol
ECL	Enhanced chemiluminiscence
EPAC	Exchange protein for activated cAMP
FAK	Focal Adhesion Kinase
FBS	foetal bovine serum
gDNA	Genomic DNA
GOI	Gene of Interest
GPCR	G-protein coupled receptor
GST	Glutathione-s-transferase
GTP	Guanosine triphosphate
kDa	Kilo Dalton
IP	Immunoprecipitation
mRNA	messenger ribonucleic acid
MW	Molecular Weight
PAGE	Polyacrylamide gel electrophoresis
PAP	Prostatic acid phosphatase
PI3	Phosphotidyl inositol-3
PDE	Phosphodiesterase
PKA	Protein Kinase-A
PKC	Protein Kinase C
PSA	Prostate specific antigen (gene: KLK3)
SDS	Sodium-dodecyl-sulfate
siRNA	small interfering ribonucleic acid
TBE	Tris Buffered EDTA
TBST	Tris Bufferes Saline-Tween
TE	Tris-EDTA
RACK1	Receptor of activated C-kinase
RNA	Total ribonucleic acid
UCR	Upstream conserved region

VSV

Vesicular Stomatitis Virus

1 Introduction- cAMP signalling and Prostate Cancer

1.1 Cyclic Nucleotide Signalling

Eukaryotes have an elaborate signal transduction system by which information from external, extracellular sources, can be converted to intracellular information that regulates the interworking of the cell [1]. While some molecules can diffuse across the membrane and activate cytoplasmic receptors directly, many rely on messenger systems. Here, first messenger molecules such as hormones, neurotransmitters or signalling peptides, activate plasma membrane receptors, which in turn activate intracellular proteins and secondary messengers, thus allowing the transduction of extracellular signals across the membrane. One such secondary messenger is 3', 5' cyclic adenosine monophosphate (also known as cyclic AMP (cAMP)).

Cyclic AMP (cAMP) was the first second messenger molecule discovered in signal transduction [2], and since its discovery it has been linked to a multitude of cellular processes. The cAMP signalling pathway is a paradigm in signal transduction and a key pathway in the conversion of information from external signalling molecules. Binding of ligands to their specific receptors (GPCR) located at the plasma membrane of the cells activates GTP-binding proteins (G-proteins) that are coupled to the membrane receptors. Certain G-proteins called $G_{\alpha s}$ -proteins, activate predominantly membrane bound adenylyl cyclase (AC), to convert ATP to cAMP [3, 4]. This, in turn, activates effector proteins like cAMP-dependent protein kinase (also known as protein kinase A (PKA)) [5]. This intracellular pathway is diminished by the degradation of cAMP by cyclic nucleotide phosphodiesterases (PDEs) (see figure 1). Within this pathway, different GPCR and AC isoforms can be activated within different regions of the cell. The location of the point source of cAMP and the discrete localization of PDEs underpin the spatial complexity of these signals. Indeed, it is now thought that the compartmentalisation of the cAMP signalling system, in this manner, underpins the specificity of receptor action [6], especially amongst different receptor types that all use cAMP as their signalling molecule of choice. PDEs are crucial for creating cAMP gradients within cells and these are activated via PKA when the threshold for activation is reached [4, 7].

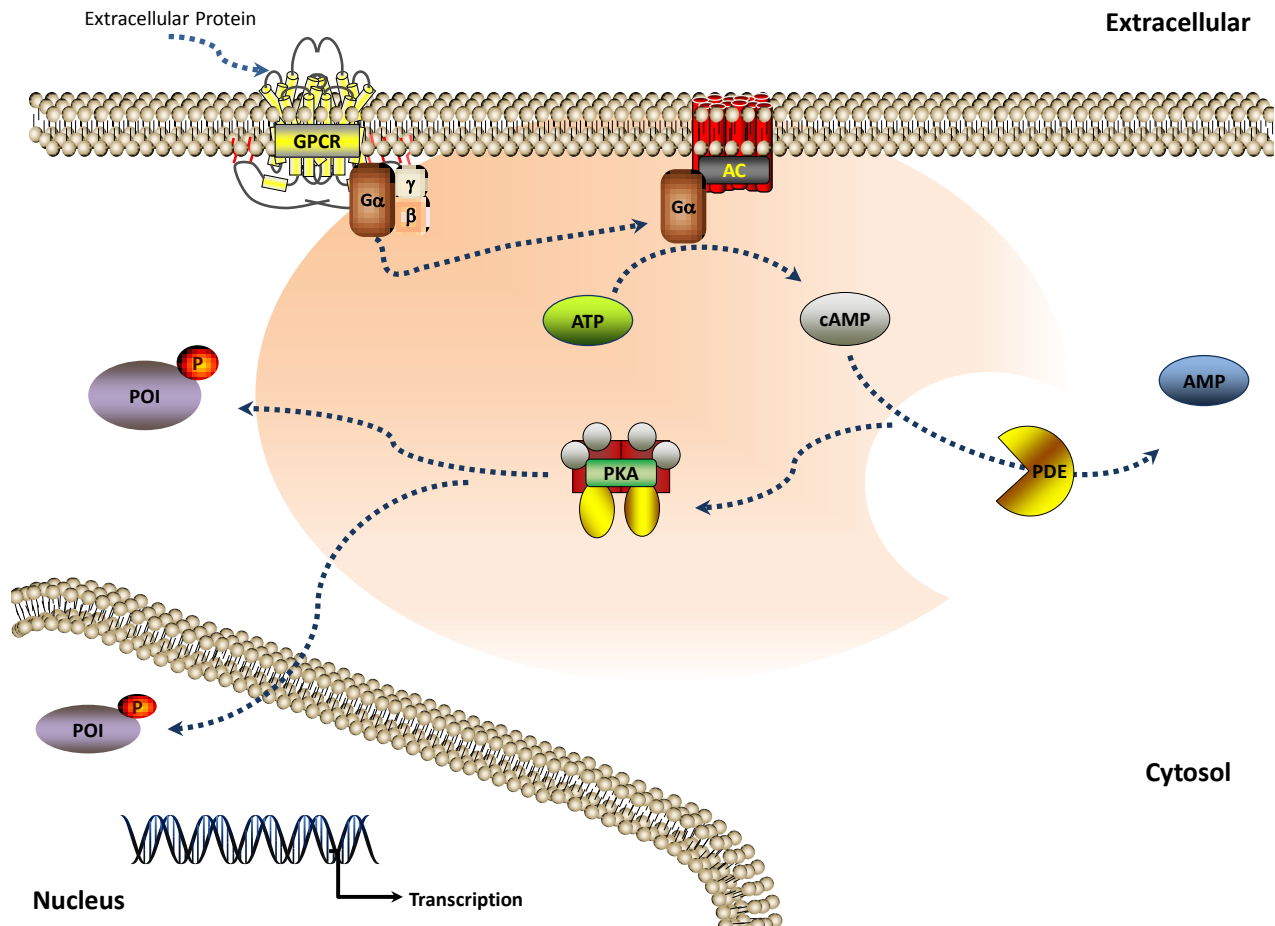


Figure 1.1 Example of cAMP signalling cascade

An example cAMP signalling through PKA activation. Classical Gs-coupled GPCR is activated, leading to subsequent activation of adenylyl cyclase. This leads to cAMP generation (orange gradient) and attenuation by PDEs. PKA activation by cAMP results in phosphorylation of the protein of interest (POI) downstream signalling events e.g. transcription.

PKA and PDE families are made up of multiple isoform variants that exhibit tissue and cellular specific localisation patterns. Furthermore, many different isoforms of these enzyme families can be expressed within a cell and localised to isoform specific signalling complexes and intracellular positions [10-13]. The outcome of this dynamic isoform expression is a number of compartmentalized cyclic nucleotide gradients that modulates the response to extra-cellular signalling molecules. Compartmentalization of cyclic nucleotide gradients and thus downstream signalling cascades allows multiple signalling events to occur simultaneously, controlling molecular interactions and signalling within the intracellular space [12].

1.2 Protein Kinase A

Approximately 2% of the mammalian genome encodes for protein kinases, making this one of the largest gene families. Protein kinases regulate a wide array of cellular processes e.g., they are an integral part of learning and memory, growth, development and differentiation and are essential in the orchestration of cell death and activated in the response to stress signals [8-11]. This means that protein kinase functions are directly related to many diseases and hence represent attractive targets for drug discovery. One of the first discovered proteins from the kinase family was cAMP-dependent protein kinase (PKA), the classical effector molecule of the cAMP signalling cascade.[12, 13].

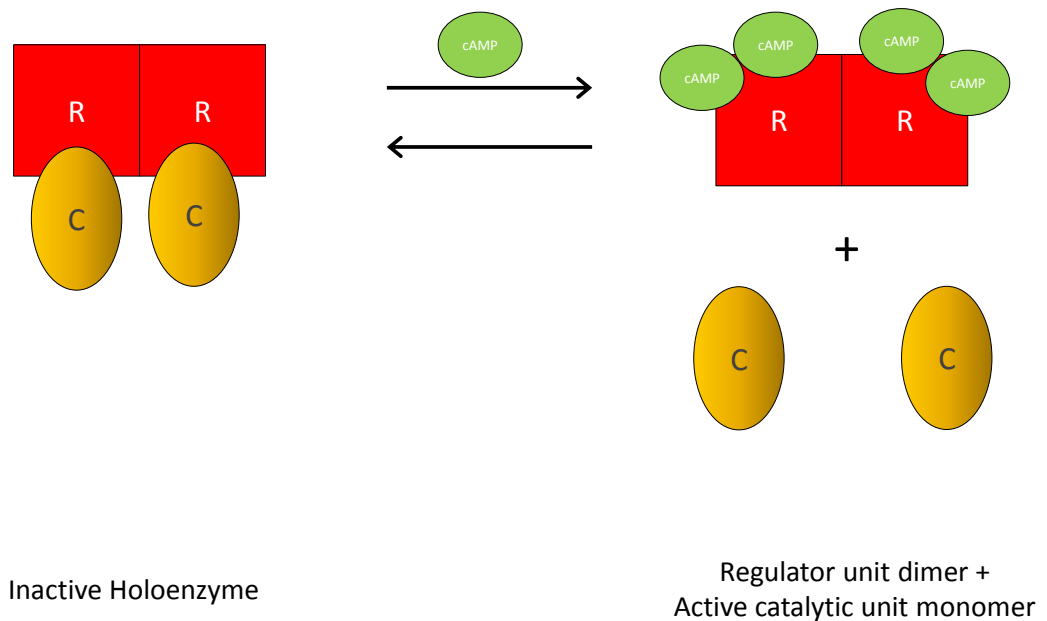
PKA, like other kinases, carries out its function via binding to its substrate and transferring one γ -phosphate group from ATP to its protein substrate. PKA activity is specific to the phosphorylation of serine/threonine residues located within an RxxS/T motif [1, 9].

1.2.1 Structure

When PKA is in its inactive state, the PKA molecule is a tetrameric holoenzyme, made up of 2 regulatory subunits (R), and 2 catalytic (C) subunits. Variation of PKA subunit composition allows for a degree of signalling complexity and is denoted via transcription of four isoforms of the R units: RI α , RI β , RII α , RII β . Additionally there are 3 isoforms of the C subunit: C α , C β , C γ , and mRNA spliced variant of C β have been reported [9, 11]. PKA is often referred to as PKA I or PKA II denoting the R unit composition of the holoenzyme. The differential transcription of the holoenzyme variants allows the regulation of different signalling cascades, in differing cellular locales, leading to diverse outcomes of cAMP compartmentalising dynamics.

The R units contain two, tandem cAMP binding domains at the carboxyl terminus and a dimerization/docking (D/D) domain at the N-terminal. The D/D domain is comprised of four anti-parallel α -helices, which creates a high affinity binding site for A kinase anchoring protein (AKAP) binding and also helps with R-unit dimerization [14, 15]. In addition, a flexible linker region, which joins the D/D and C-terminus, acts as a pseudo-substrate site for the active site of the catalytic subunit [15].

PKA R subunits are highly versatile proteins that exhibit multiple functions. Their main purpose is to inhibit the activity of the catalytic subunit via binding to the pseudo-substrate site within the linker region. When cAMP concentrations increase above activation threshold levels, cAMP binds to the C-terminal of the R subunits causing a conformational change in this hinge region, resulting in dissociation and release of the active C subunit into two monomeric units, leaving the R unit as a dimer (See figure1.2) [11].



1

Figure 1.2 PKA activation

A diagram depicting PKA activation. PKA inactive holoenzyme is disbanded when cAMP concentrations increase above threshold levels and bind to the C-terminal of the R subunits. This results in the release of the active C subunits, leaving a R unit dimer.

The C and R units primarily interact via the pseudo-substrate site, however, there is a peripheral docking site that consists of the residues of the cAMP binding site A and allows higher affinity binding [16]. While the R units share a highly conserved carboxyl terminus, the amino terminus can vary between isoforms. One of the key variations between the RI and RII subunits is within the C subunit binding site. RII subunits contain an auto-phosphorylation site in the inhibitor region, where the RI units contain a high affinity ATP binding site [15,

17]. This change has been shown to be important in holoenzyme conformation as well as R and C unit dissociation. In addition, the molecular shape of the tetramer differs depending on the R units present in the holoenzyme. The RII units, in dimer formation, form an elongated rod-like shape whereas RI units are more Y shaped [15, 18].

Although the R units show some structural homology, they can differ in function and cellular expression. It has been shown in mouse knockout models that RII α is embryonically lethal, however RII β knockouts have resistance to obesity and diet-induced diabetes. Furthermore, RII β knockout resulted in a compensatory increase in RII α expression and an associated decrease in neural plasticity. This balance between type I and type II PKA expression also plays an important role in cell growth and differentiation and has been implicated in several disease mechanisms including breast and prostate cancers [19-22].

Another notable feature of R subunit architecture include the R subunit D/D domain, which allows binding of scaffold proteins known as A kinase anchoring proteins (AKAPs). This protein family adds another degree of compartmentalisation and PKA specificity of action through the targeting of R units of the PKA tetramer to different cellular sites, which are in close proximity to a specific protein substrate [9]. Furthermore, AKAP anchoring can also cause localisation with enzymes that can degrade cAMP (PDEs), leading to deactivation of PKA [1]. This negative feedback loop can be used to produce transient cellular signals within the cell. In order to bind the regulatory subunits, AKAPs contain an amphipathic helix. Initially, it was thought that R subunit/ AKAPs interactions were RII specific, however it has been shown that RI can also bind AKAPs but with lower affinity [1, 10, 23].

The C subunits of PKA contain a small ATP binding site at the amino terminal and a larger C- terminal docking site to bind the protein substrate. Within the C subunits, residues 40-300 of the unit makes up the conserved kinase core, in addition, 40 residues at the amino terminal and 50 at the carboxyl wind around the lobes of the protein and dock with the hydrophobic pocket on the surface of the smaller amino terminal lobe; this acts to stabilize the catalytic subunit [24, 25].

PKA subunit isoforms have shown differences in their expression profiles and tissue distribution, implying specificity of function. For example, mice models lacking splice variant C β 1, while still viable, have deficiencies in cAMP dependent processes which result in long-term depression, even though other splice variants and isoforms are still expressed [1, 26].

Protein Kinase Inhibitors (PKI) are a family of small proteins that are able to inhibit the catalytic subunit of PKA and are encoded for by 3 genes, giving rise to 3 isoforms α , β , and γ . These isoforms show different tissue distribution. PKI association with C units results in the deactivation of the C subunit and promotion of nuclear exportation [27].

1.3 Phosphodiesterases: Overview

In the early 1980s, Brunton and colleagues [28] proposed the concept of cAMP compartmentalisation. At the time this concept was met with scepticism, however, it has stood the test of time, with new supporting data, resulting from novel technically advanced experimental procedures, like FRET probes, which detect real time, spatial and temporal changes in intracellular cAMP concentrations [29]. One major finding from these studies was that the compartmentalization of cAMP responses are underpinned by the action of the only known enzymes to degrade cAMP, phosphodiesterases (PDEs).

Phosphodiesterases (PDEs) are a superfamily of enzymes that are encoded by 20 human genes and divided into eleven families [30]. These 11 families are characterised by their specific structural elements, sequence homology, inhibitor sensitivity and their ability to hydrolyse cyclic nucleotides. PDE4, PDE7 and PDE8 are cAMP specific, PDE5, PDE6 and PDE9 are cGMP specific and the other 5 families (PDE1, PDE2, PDE3, PDE10 and PDE11) have dual specificity with differing affinities for both types of cyclic nucleotide. Most of these families contain various isoforms or splice variants and exhibit tissue specific localisation patterns [31]. In addition to this, multiple isoforms of the PDE family can be expressed within the same cell, leading to a differential compartmentalisation of cyclic nucleotide gradients, enabling independent but simultaneous signalling events to occur [32, 33]. This paradigm of compartmentalised cyclic nucleotide signalling is altered in many disease states. This has led to interest in the regulation and function of cyclic nucleotide signalling pathways. Recently, there

has been much interest in the PDE4 family, as a PDE4 inhibitor (roflumilast) has been licensed in Europe and the USA for the treatment of severe chronic obstructive pulmonary disease (COPD) [34].

1.3.1 PDE4

PDE4s are one of the most important enzyme families for the degradation of cAMP in cells, and they have been associated with many disease states such as schizophrenia, stroke and cancer [7, 35, 36]. They are encoded by 4 genes (A,B,C,D) and these give rise to at least 25 different proteins (6 PDE4A forms, 5 PDE4B forms, 3 PDE4C forms and 11 PDE4D forms) via mRNA splicing and promoter diversity. Each isoform is distinguishable via its unique N-terminal, which is involved in targeting the PDE4 to specific intracellular signalling complexes and it is this consensus sequence that is thought to be one of the major factors that promotes compartmentalisation of cAMP signalling [7, 37]. The study of the PDE4 family has been key for the understanding of intracellular targeting of cAMP hydrolysis. As all the PDE4 isoforms display similar K_m s and V_{max} for cAMP hydrolysis [6], PDE4 research has resulted in the concept that PDE function depends on the cellular location, interaction with other signalling proteins and post-translational modifications of the PDE.

1.3.1.1 Structure

Like all other PDE families, PDE4s have a complex modular structure, consisting of a conserved catalytic domain, sub-family specific C-terminal domain, dual regulatory domains called upstream conserved region 1 (UCR1) and upstream conserved region 2 (UCR2) and an isoform specific N-terminal region [37]. The tailoring of compartmentalised cAMP signals by individual PDE4 isoforms are conferred by the unique localization sequences that are contained within isoform-specific N-terminal regions. This unique binding region allows the direct association of PDE4 family members with a variety of inert scaffolds, lipids or active proteins, resulting in specific PDE4 isoform localised signalling. Signalling scaffold proteins associated with PDE4 binding include, but are not limited to; AKAP18, RACK1, disrupted in schizophrenia 1 (DISC1), heatshock protein 20 (HSP20) and the scaffold protein β -arrestin [29, 36, 38-41].

The PDE4 isoforms can be further categorised with the presence of the UCR domains, which are located N-terminally to the catalytic domain. With respect to the UCR domains, these isoforms can be divided into 3 basic classes (Figure 1.3). Long forms have UCR1 and UCR2 regions; short isoforms lack the UCR1 region but retain the UCR2 region; and super-short forms lack the UCR1 region and contain a truncated UCR2 region [42].

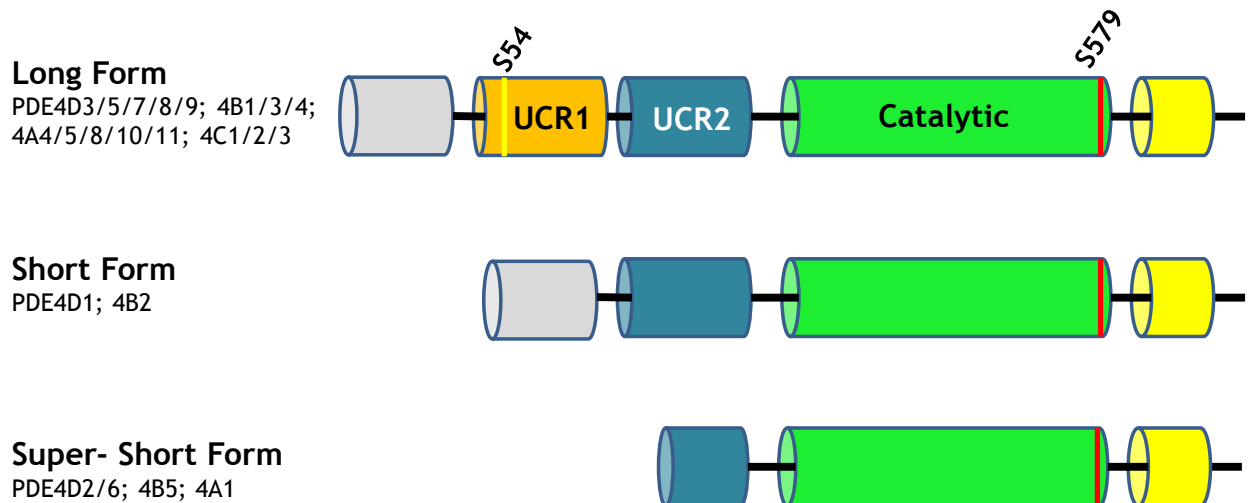


Figure 1.3 PDE4 Family Structures

The domain structure of PDE4 isoforms, showing the differences in UCR region expression (Figure adapted from [7])

PDE4s can coordinate enzymatic changes upon regulatory phosphorylation by kinases like PKA and ERK. The UCR regions dictate the type of activity change that result from such phosphorylations and thus are a contributor in PDE4 enzymatic regulation. UCR1 includes a PKA phosphorylation site and is connected to UCR2 by linker region 1 (LR1) [43]. UCR2 has a hydrophilic N-terminal region, which interacts with the hydrophobic C-terminal portion of UCR1 and is connected to the catalytic domain via linker region 2 (LR2) [42, 44]. In long form PDE4s the interactions between UCR1, UCR2 and their phosphorylation status is

important in understanding PDE4 enzymatic activity. Phosphorylation of UCR1 by PKA causes an alteration between UCR1 and UCR2 interactions [43]. Alone the UCR2 is thought to act as an auto-inhibitory domain of the catalytic unit, the change in interaction between UCR1 and UCR2 caused by the phosphorylation is proposed to remove this auto-inhibitory effect. Furthermore, PDE4s are phosphorylated by extracellular signal-regulated kinase 2 (ERK2) upon the C terminus. This phosphorylation has been shown to differ in its effect depending on UCR presence, for example the enzyme activity of long form PDE4s (containing both UCR regions) was inhibited via this phosphorylation, whereas short forms lacking UCR1 exhibited activation by the same phosphorylation [44, 45]. Long form PDE4s have also been shown to undergo dimerization through the intermolecular interactions of the UCR1 regions, thus short and super-short forms only exist as monomers [44, 45].

1.4 PKA, PDE and Disease

Michael Gottesman, in 1986, predicted that ‘...sustained expression of the PKA catalytic subunit, either because of high cAMP levels from an altered adenylyl cyclase or phosphodiesterase system, or because of mutations in R or C, could act like an oncogene product in certain cell types’. He had also said that cAMP had reappeared in the study of tumorigenesis ‘like a Halley’s comet’ [46]. At a time when the importance of cAMP as a messenger in many hormonal systems was established and the complexity of its functions was becoming apparent, human diseases that were linked to abnormal cAMP responses, such as irregular cell growth and proliferation, were beginning to be elucidated.

Recently, mutations in *PRKAR1A*, the gene encoding R1 α , the regulatory subunit type 1A of cAMP-dependent protein kinase A (PKA), has been shown to be linked to carney complex (CNC), which is a multiple endocrine neoplasia (MEN) syndrome and thus has a major effect on the endocrine system [47]. This was the first time that cAMP-dependent PKA was found to be directly involved in oncogenesis in an inherited disease.

Furthermore, R1 α has been shown to associate with transcription factor, RIAZ. Members of the family of BTB/POZ domain zinc finger proteins, including PLZF and BCL6, are associated with oncogenesis and RIAZ is shown to be aberrantly

expressed in breast cancer cell lines. Co-transfecting GFP-RIAZ with R1 α results in cytoplasmic localization. The presence of cAMP causes GFP-RIAZ to translocate from the cytoplasm into the nucleus. Deletion of the C-terminus of RIAZ abolishes its interactions with R1 α and GFP-RIAZ localizes in the nucleus thus suggesting that the R1 α subunit (and potentially the other subunits) of PKA may have functions independent of the normal kinase activity [48]. In addition, it has also been demonstrated that mutation in the R1 α , but not the C subunit, is associated with increased resistance to the DNA-damaging anticancer drug cisplatin [49].

In mammalian cells, two types of PKA are expressed, type I and type II, distinguishable by the expression of different R subunits. During development, differentiation and transformation, ratios of PKA I and PKA II can change dramatically and this change in expression has been shown to be a feature of carcinogenesis. Cho et al [50] showed that PKA-I was over expressed in various cancer cells and cells with high RI:RII are associated with poor prognosis in terms of early disease recurrence and death. In breast cancer cell lines, increased expression of PKA could change sensitivity to estrogens and antiestrogens in cancer cells. In a model system of breast cancers, exposure to antisense R1 α oligonucleotides slows cell proliferation and tumour growth, linking of PKA with cancer. This evidence of PKA mutation and links to cancer, make this holoenzyme a clear target for novel cancer therapies.

In addition to PKA signalling, data suggest that cyclic nucleotide phosphodiesterases (PDEs) are relevant in various cancer pathologies [51]. Many tumour cells interestingly have PDE4, as the major regulator of cAMP-hydrolysing activity. PDE4 inhibitors have been shown to inhibit growth and to increase differentiation and/or apoptosis in pancreatic cancer cells, colon cancer cells and malignant melanoma cells [52-54] Inhibition of PDE4 by the selective inhibitor rolipram is also shown to suppress tumour growth and augments the anti-tumour effects of chemotherapy and radiation therapy in medulloblastoma, glioblastoma [55] and in several hematological malignancies [56]. Why PDE4 isoforms are overexpressed in so many different tumour types remains elusive. However, like PKA, with major links to carcinogenesis, it is a clear target for exploitation in the fight against cancer.

1.5 Human Prostate Gland

The prostate gland is a small gland located in the lower pelvis. It sits below the bladder and encompasses the proximal part of the urethra as it leaves the bladder. The prostate gland weighs approximately 20g and is 10-20cm³ in volume [57].

1.5.1 Function

The prostate gland is an integral part of the male reproductive system. Its primary function is production and secretion of prostatic fluid. This fluid makes up 20-30% of semen, which protects and carries the spermatozoa after expulsion. It is an alkali solution to counteract the acidic environment of the urethra and the vagina, and thus ensuring the gametes stay viable. Electrolytes that are important for the function of the spermatozoa while en-capsuled in the seminal fluid, originate from the prostatic fluid. The prostatic secretions also contain important proteins such as seminal plasmin, which is an antibiotic that helps prevent urinary tract infections, as well as kallikrein-related peptidase 3 (KLK3 (also known as Prostate specific antigen (PSA)) and prostatic acid phosphatase (PAP), which are important secretory enzymes [58, 59]. PSA participates in the lysing of seminal proteins in order to maintain seminal fluidity [60]. PAP is a member of the small protease family and degrades acidic molecules like lysophosphatidic acid (LPA) [61]. LPA is present in the seminal fluid and is also linked with aberrant cellular proliferation and tumourigenesis in many contexts, including prostate cancer [62, 63].

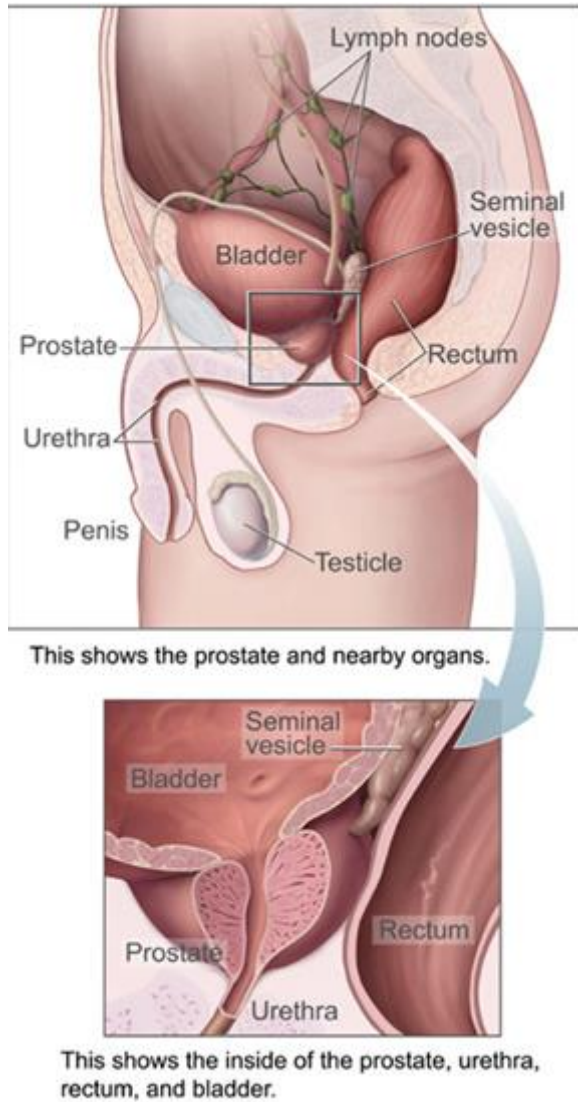


Figure 1.4 Anatomical view of the prostate gland
Image shows the regional anatomy of the Prostate gland (Image taken from www.cancer.gov)

1.5.2 Structure

The prostate gland is a small capsule about 4cm in diameter. It is a lobular capsule subdivided into 3 glandular zones: peripheral, central, and pre-prostatic, which is encapsulated by a thin fibroelastic, non-glandular layer, known as the fibromuscular stroma [57, 64].

Within the prostate gland there are two basic cell types, epithelial and stromal. The glandular zones are comprised of two major types of epithelial cells; luminal secretory and basal cells, but also contain a small amount of neuroendocrine

cells. In all the glandular zones, there is a layer of basal cells beneath the secretory lining, which surrounds the ducts and acini of the zone [65]. The fibromuscular stroma surrounding the glandular sections of the prostate is comprised of fibroblasts and smooth muscle cells [66].

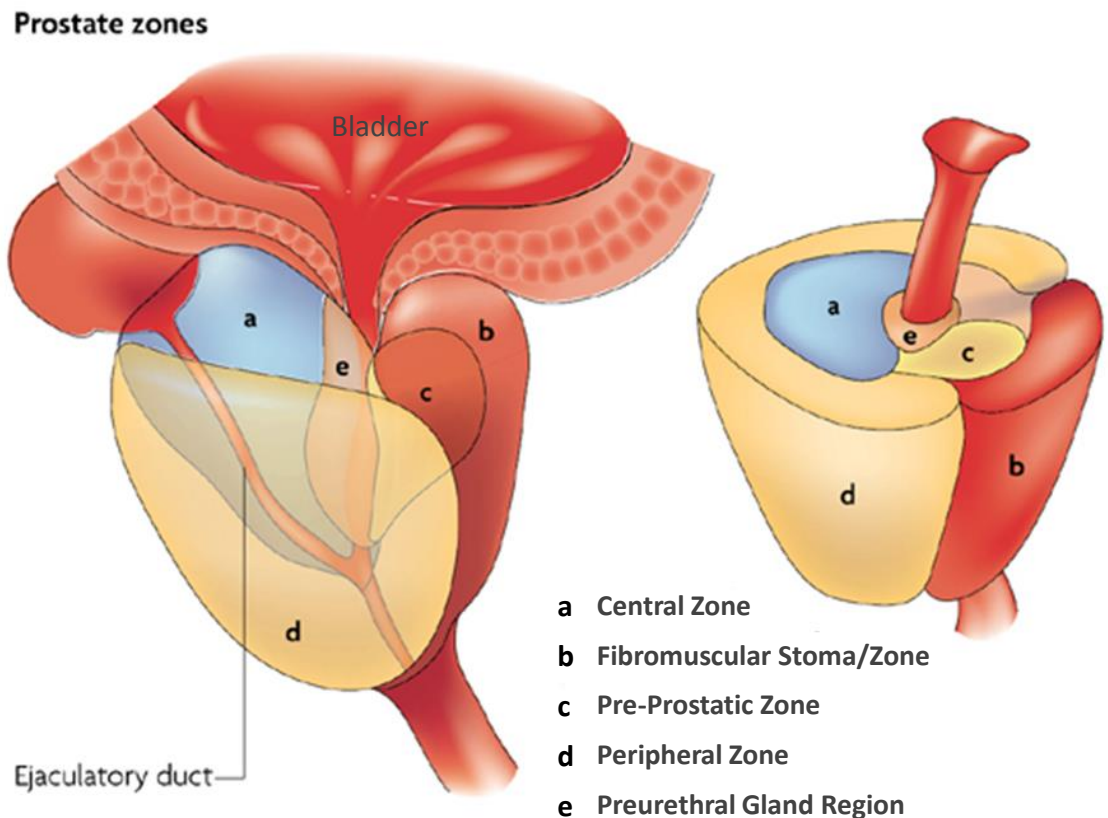


Figure 1.5 Prostatic Structure (zone model)
Diagram depicting the zonal structure of the prostate gland (Figure adapted from [67])

1.5.2.1 Peripheral Zone

The peripheral zone makes up over 70% of the glandular part of the prostate and is the part of the prostate from which most cancers originate. Nearly 80% of all adenocarcinomas arise in this zone [64], which is located towards the rectal side of the prostate. The peripheral zone is also the main contributor to the secretory epithelial of the prostate, which synthesises the prostatic fluid.

1.5.2.2 Central Zone

The central zone makes up approximately 25% of the glandular prostate in young male adults. It is a cone shaped region and is located close to the ejaculatory ducts and borders the peripheral zone. It should be noted that, although in close proximity, the peripheral and central zones display histologic differences that suggest these zones have important biological differences [64]. The central zone is less likely to develop carcinomas compared with other zones of the prostate. In fact, only approximately 1-5% of carcinomas originate from this area [65]. Although the incidence of cancer in this area is reduced, cancers in this region often have poorer outcomes than cancers derived from other prostate zones [68].

1.5.2.3 Pre-Prostatic/Transition Zone

The preprostatic zone is located proximally to the urethra. It composes about 5-10% of prostate volume. In this zone, major ducts do not feature, though there is small transition region, and several tiny ducts in which benign prostate hyperplasia (BPH) often originates [64]. Approximately 20% of adenocarcinomas arise from this zone, however, the morphologic and growth pattern of the cancer suggests that it is less aggressive than cancers derived from other zones.

1.5.2.4 Fibromuscular Stroma

Surrounding the glandular prostate is a fibromuscular stromal layer. This comprises mainly of fibroblasts, smooth muscle, nerves, and lymphatic cells. This zone is responsible for the functional contractions of the prostate gland.

Prostate growth and development is associated with cell-cell communication, notably stromal-epithelial interactions [60] and the production of growth factors. However these interactions are still poorly understood.

1.6 Hormone Signalling

Steroid hormones are diverse class of molecules derived from cholesterol and include androgen, oestrogens, progesterone and corticosteroids. Androgens, also known as the male sex hormones, are important in a large amount of biological

processes throughout the body including the maintenance and function of the sexual tissues in an adult and differentiation and development in male adolescents. They exert this action through the activation of the androgen receptor (AR), which is part of the steroid receptor family of transcription factors. These androgens and their action on the androgen receptor can also affect the development and progression of male pathologies such as BPH and PC [60].

1.6.1 Testosterone and Dihydrotestosterone

The primary sex hormone in an adult male is testosterone. It is secreted via the Leydig cells of the testes in response to luteinising hormone from the pituitary gland [69]. It is the most abundant androgen in the serum of males. 97% is bound to sex-hormone binding globulins and albumin, leaving 3% as free and biologically active, circulating testosterone [70]. Testosterone is the precursor molecule for locally metabolised effector molecules at peripheral tissues. The mechanism of this uptake into tissues is still poorly understood [71]. The most bioactive of the 'effector' molecule for AR activation is dihydrotestosterone (DHT) which has a 2-5 time higher binding affinity for the AR than testosterone itself [72]. DHT is important in the differentiation and growth of the prostate gland, male external genitalia and growth of facial and body hair at puberty.

Conversion of testosterone into DHT requires the action of the 5α -reductase enzyme, which is expressed in high amounts within the prostate gland [70, 73]. Three forms of 5α -reductase are described in the literature. Type 1 and 2 are expressed differentially in liver, genitals and nongenital skin, prostate, epididymis, seminal vesicle, testis, ovary, uterus, kidney, exocrine pancreas, and brain. Type 1 is usually located within the nucleus, whereas type 2 is located within the cytoplasm of the cells. In the prostate gland, type 2 has an increased expression within epithelium (especially basal cells) compared to type 1. Type 3 is ubiquitously expressed in all tissues [71].

During normal development, DHT promotes the differentiation of the foetal prostate and the development of the male genitals. In adults, DHT is the main modulator of prostatic function and contributes to the homeostatic effects of the AR [69].

1.6.2 AR

The androgen receptor belongs to a superfamily of nuclear receptors that mediate the action of steroid hormones. The androgen receptor has a molecular weight of 110kDa and is a member of the NR3 subfamily of the nuclear hormone receptor family. It is encoded by a gene located on the X chromosome (xq11-12) and contains 8 exons which encode 3 protein domains [74].

1.6.2.1 Function

The function of the androgen receptor is to mediate the effects of androgens via the regulation and transcription of specific genes. The unliganded androgen receptor resides in the cytoplasm, associated with heat-shock proteins through interactions with the ligand binding domain of the receptor (Figure 1.6). The HSP/AR complex acts to induce a high-affinity conformation in the AR for ligand binding. Upon ligand binding, the AR undergoes several conformational changes that allows, dissociation from heat-shock proteins, phosphorylation and dimerization, and also exposure of the AR nuclear localisation signal and translocation to the nucleus [70, 73]. In the nucleus, the AR associates with nuclear androgen receptor elements (AREs) on the DNA of various androgen receptor target genes [75, 76]. Transactivation of these AR-regulated genes often requires the recruitment of cofactors and transcriptional machinery as well as the binding of the AR [77]. The most studied of these genes is PSA, a component of seminal fluid and currently the main biomarker used for monitoring PC development and progression [58, 73].

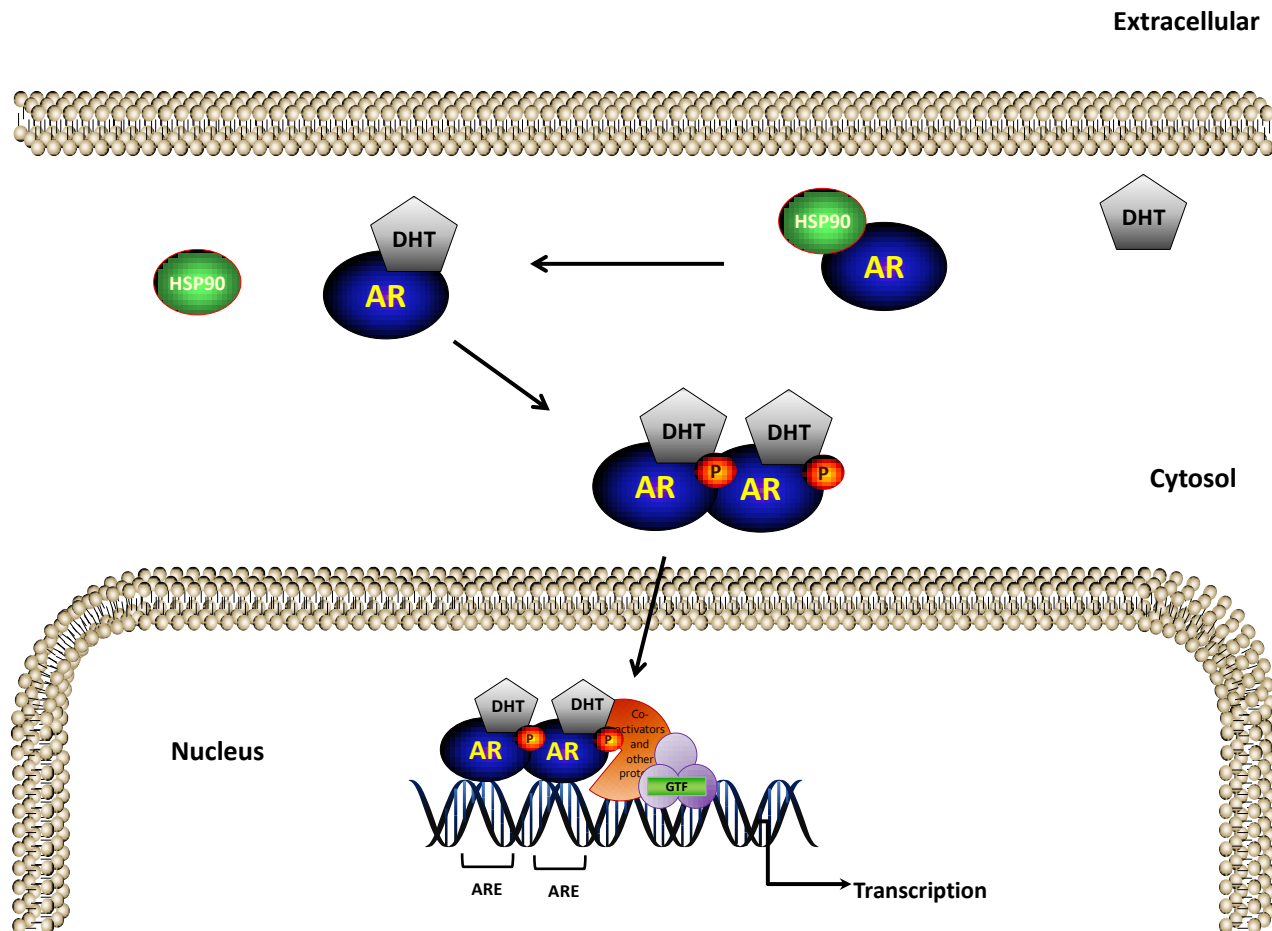


Figure 1.6 Schematic of basic androgen receptor signalling

1.6.2.2 Structure

The receptor family to which the androgen receptor belongs, have distinct functional domains; a ligand binding domain (LBD) located at the carboxyl terminus, a conserved DNA binding domain (DBD) which contains 2 zinc finger motifs and an amino-terminal domain (NTD) that is poorly conserved within the receptor family and contains the transcriptional activation sequences [76, 78]. The androgen receptor fits nicely into this family (see Figure 1.7) as it contains; an amino terminal domain (NTD) that modulates transcription activity via its transcriptional activation function sequence (AF-1), a conserved DNA-binding domain (DBD) that recognises the (androgen) response elements (ARE) in the target sequence and C-terminal containing a ligand-binding domain (LBD), which modulates ligand recognition, and binding of the co-activator binding sequence (AF-2) [70, 79, 80]. 3D structures of the LBD, hinge region and DBD have

currently been determined via X-ray crystallography. However, NTD, the most unique region of the receptor, still has an undetermined 3D structure [59]. Surprisingly, most of the posttranslational modifications of the AR, determined via mutation studies, have been reported to lie in this region [81].

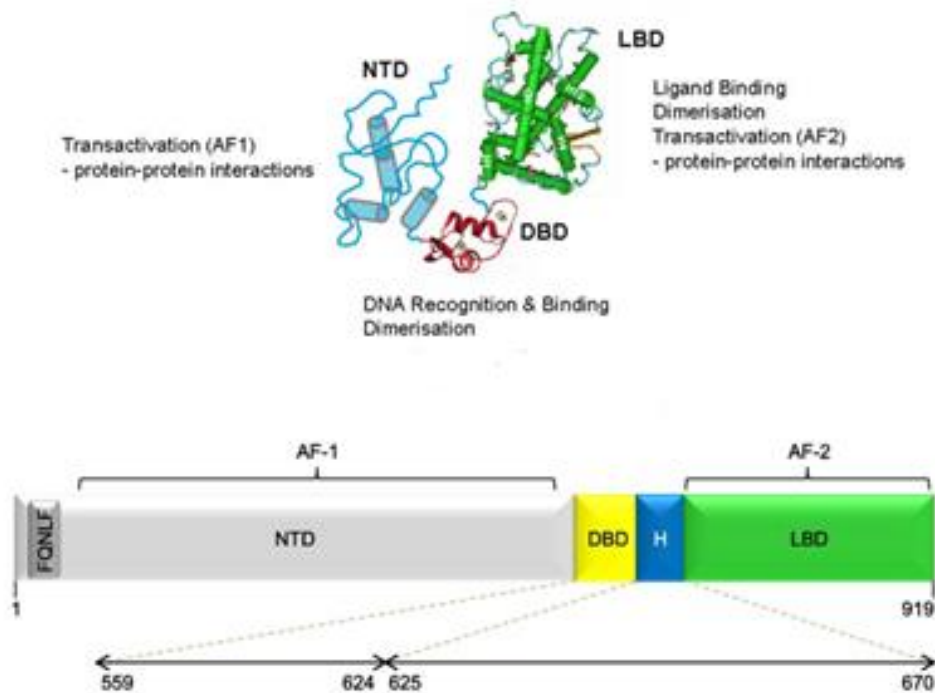


Figure 1.7 Predicted structural model of the AR. Adapted from [82, 83]

1.6.2.2.1 AF-1 and NTD

The NTD is the most unique domain in the androgen receptor structure, with approximately 15% of homology with other steroid receptors [82, 84]. Unlike other domains of the receptor, the NTD has no published crystallographic or NMR-based structure. However, the transcription transactivation of the AR has been shown to be dependent on contributions from this domain, despite LBD activation [82].

The NTD of the AR contain the *FQQLF* motif that is important for the interaction with the LBD. This motif is located in the first 25 amino acids of the domain and is involved in a 'charge clamp' that forms between the LBD and the NTD [85].

The AF-1 region is located within the NTD. This domain is thought to have limited structure and be highly disordered. It is made up of amino acids 142-485 of the androgen receptor. Within the NTD AF-1 region, several transactivation domains have been defined; Most notably, the TAU-1 (amino acids 101-370) and TAU-5 (amino acids 360-528) domains.

A 'core' of the TAU-1 domain between amino acids 173 and 203 in the AR was described during mutational analysis of the α -helices. The hydrophobic side chains and the negative charges of the amphipathic helix are suggested to be important in the trans-activating capacity of the AR [86]. The region around this core has also been shown to change in confirmation when interacting with co-factors. This change in structure has been suggested to be the natural active confirmation of the AF-1 region, as mutations of these helical structures decreases the activity of the AR [82, 84]. Another motif (amino acids 234-247) which is located towards the carboxyl-terminal end of the TAU-1 core sequence, is highly conserved within the species and is the interaction site for the Hsp70-interacting protein E3 ligase CHIP [85], and so overexpression leads to a down-regulation to the steady state of AR. It is also noteworthy that both TAU-1 and CHIP-interacting motifs have been shown to have mutations, which increase the AR activity.

TAU-5 domain was first described by Jenster et al in 1995 [87], and has been suggested to allow the AR to retain its activation potential in the absence of the LBD. It is an autonomous activation domain that is targeted by many co-activator proteins [84, 86]. The TAU-5 domain also contains two SUMO-1 modification sites at positions 385 and 511 respectively. This SUMOylation has been suggested to be in response to agonists and mutation studies of K385, these show an effect on the co-operativity of the receptor when forming a complex at the ARE [86].

1.6.2.2.2 DBD and the hinge region

The DBD is the region responsible for DNA interactions. This domain is highly conserved between steroid receptors, with the receptors sharing the same DNA recognition sequence (CGSCKVF) [88]. Despite the conservation of the DNA binding sequence between steroid hormone receptors, different steroid hormones can elicit different biological responses. The mechanism of exactly how this occurs is largely unclear, however, differential receptor and cofactor expression, cell-type- specific chromatin organization or hormone metabolism may account for many physiological situations where a gene is specifically regulated by steroid hormones. The DBD region is approximately 80 amino acids in length, and is composed of two zinc motifs, which contain three helices each. The first helix extends from the C-terminal of the first zinc-finger and contains amino acids responsible for the specific recognition of the DNA. The second helix lies in the tip of the second zinc-finger and borders the receptor dimerization surface. The third helix is important for the overall three dimensional structure of the DBD. Each of the zinc motifs are composed of a zinc ion which is surrounded by four cysteine residues [88, 89].

The region located between the LBD and the DBD is known as the hinge region. It is composed of amino acids 625-670 and is poorly conserved. This region of the AR contains a nuclear localisation signal motif (amino acids 617-634) which overlaps with the DBD [90]. This localisation signal motif binds importin- α at residues 629-634 [84]. The nuclear import of the AR is mediated via an importin α/β complex [83]. Although this region was initially thought to be a simple linker region, it is now linked to many control factors of the AR as well as its import. These factors include, nuclear export (as well as import), DNA affinity and selectivity, co-factor interaction and the ARs transactivation abilities. The mechanisms of action for these factors still remain to be described fully [83, 84].

1.6.2.2.3 AF-2 and LBD

The C-terminal contains the LBD and the AF-2 sequences and unlike the NTD its structure (when in a complex with a variety of ligands) has been solved. The mechanistic function of the LBD is to bind androgens (ligand) in the ligand binding pocket, causing a conformational change which induces the formation of

the AF-2 co-activator binding surface. This is the function which is exploited during PC treatment.

The LBD domain has a very similar structure to other members of the nuclear receptor family. However, the LBD of the AR is comprised for 11 α -helices instead of the usual 12. These 11 α -helices make up the binding pocket of the LDB in a 3 layer, antiparallel sandwich structure (Figure 1.8). 18 amino acids, within 10 of the α -helices, directly interact with the ligand and the final helix stabilises the ligand in the binding pocket by acting as a flexible lid [91, 92]. This conformational change of the helices results in the formation of a hydrophobic region on the surface of the LBD known as AF-2.

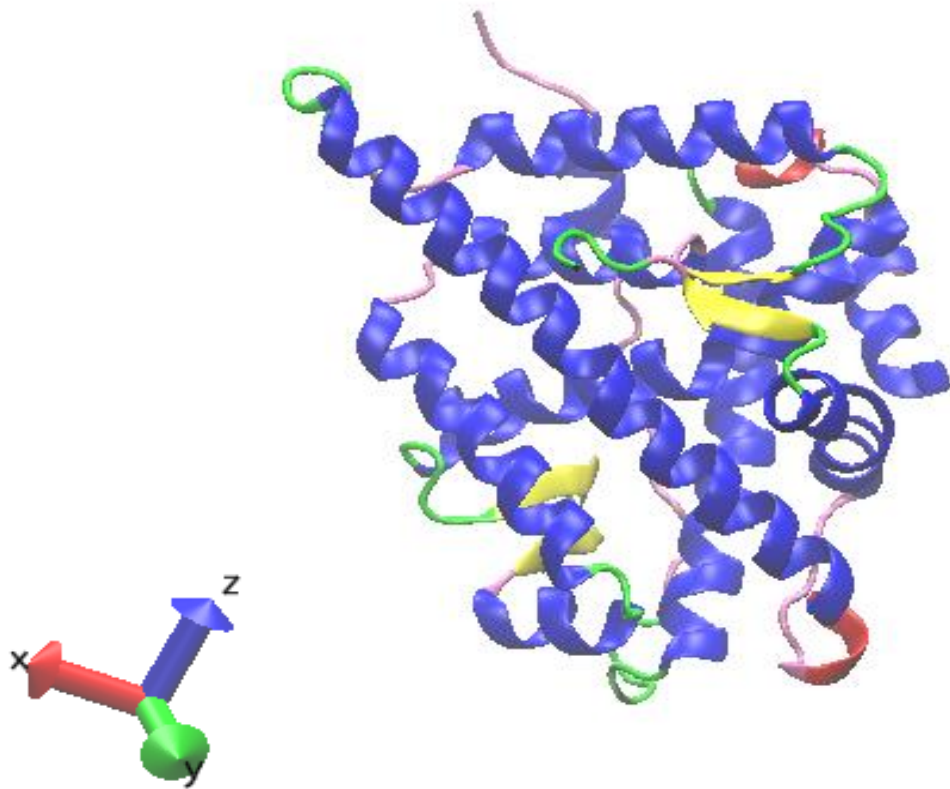


Figure 1.8 Crystal structure of DHT-bound androgen receptor LBD in complex with the first motif of steroid receptor coactivator 3
Protein bank database ID 3L3X. Graphical represented using visual molecular dynamics (VMD) software.

The AF-2 surface is a hydrophobic region, with areas of positive and negative charge. As suggested the AF-2 region acts as a docking site for co-regulators via a conserved LxxLL motif. Studies into the recruitment of co-activators has shown that residues within the helices of the LBD act as clamps to stabilize the co-

activator interaction with the AF-2 region, however the exact role of co-regulation recruitment by the AF-2 surface is still unclear [78, 93]. The boundaries of the AF-2 domain in the androgen receptor ligand-binding domain have not been determined as yet, but it is known to contain a defined core region. This AF-2 activation domain (AD) core region, contains a conserved sequence aa 884-888. Mutations in this region result in a decrease in activation without affecting the ligand-binding capability. This indicates that the amino acid residues of the AF-2 AD core region are not directly involved in ligand-binding, but are part of, or are determinates of the interaction surface [94].

In several of the nuclear receptor families, a communication between the LBD and the NTD has been shown. For the AR receptor, this interaction is very strong and thus, its physiological importance has been called into question. This communication is conducted via the binding of the LxxLL binding motifs in the LBD and the FQNLF motif in the NTD. The NTD/FQNLF motif is of great importance for this interaction as illustrated by mutation or deletion studies that have resulted in ablation of the NTD-LBD interaction. Ablation of this interaction subsequently affects AR trans-activation and kinetics of ligand binding [85].

1.7 Prostate Diseases

1.7.1 Benign Prostatic Hyperplasia

Benign Prostatic hyperplasia (BPH), a noncancerous enlargement of the prostate gland, is a common prostatic disease in men. It affects over 50% of men over 50 years of age, and 80% of men over the age of 70 [95]. It is an age related, regional prostate disorder that normally develops in the peripheral and transition zones of the prostate gland. BPH develops from a simple micronodular hyperplasia to a macroscopic volume enlargement of the prostate gland and progression to clinical symptoms [96, 97]. As BPH progresses, it is associated with symptoms such as decreased urinary flow, due to the enlarged gland causing a constriction to the urethra. This leads to lower urinary tract symptoms (LUTS), which include symptoms such as urinary hesitancy, frequent urination, thin urine flow and urinary retention. In severe cases, delayed treatment could

lead to worsening symptoms and complications that may result in surgery [98, 99].

The causes and mechanism behind BPH occurrence is generally not understood. The current theory is that there is a general unbalancing of the factors that are associated with cell growth and apoptosis, and so the importance of androgens in BPH has been well established [99, 100].

1.7.2 Prostatitis

Prostatitis is the inflammation of the prostate gland which can be separated into 4 clinical categories; acute and chronic bacterial prostatitis, rare infectious diseases of the prostate gland, chronic prostatitis/chronic pelvic pain syndrome (CP/CPPS) and asymptomatic inflammatory prostatitis. The majority of prostatitis relates to the CP/CPPS category.

Diagnosis of prostatitis is increasingly being linked with the later development of BPH and also prostate cancer. In a study on approximately 2500 men in the USA, patients that had been diagnosed with prostatitis were associated with a 2.4 fold increase in the probability of being diagnosed with BPH at a later date [101, 102]. Additionally, a meta-analysis study conducted by Dennis et al, showed that the association between prostatitis and PC is significant [103]. Other studies have also shown links between these diseases [104, 105].

1.7.3 Prostate Cancer

Prostate Cancer is the leading cause of death among men in Western Europe and the United States. In an autopsy study, 64% of men between 60 and 70 years of age were shown to have small prostatic carcinomas [106, 107].

1.7.3.1 Epidemiology

The specific cause of prostate cancer is unknown but the primary risk factors include family history, diet, age and weight. The incidence of prostate cancer varies significantly with ethnicity, with African-Americans having the highest incidence rates in the world, followed by Caucasian-Americans and Asians exhibiting the lowest incidence [108]. <0.1% of cancer cases occur before the

age of 50 and risk then, rapidly increases with age [109]. However, in the US only one in six men diagnosed with prostate cancer will eventually die from it. The number of patients that are diagnosed with the disease has increased dramatically in the past few decades due to an ageing population and the introduction of new screening methods, leading to earlier diagnosis [110]. Another major risk factor is diet. Increased fat intake has been strongly correlated to the incidence of prostate cancer, with the main risk foods being, animal and saturated fats, and red and processed meats, with the consumption of oily fish been associated with reduced risk [111]. Although the causes of prostate cancer still remain mostly elusive, epidemiological studies have provided important insights into the potential risk factors of prostate disease.

1.7.3.1.1 Prostatic Intraepithelial Neoplasia

Prostatic Intraepithelial Neoplasia (PIN) is a suggested precursor of prostatic adenocarcinoma. A study by Bostwick et al has also suggested this close relationship, indicating that the occurrence of PIN seems to run in parallel with the occurrence of prostate cancer, with prostate cancer lagging about 10 to 20 years behind the appearance of PIN [112]. PIN is detected via biopsy, as it doesn't often affect PSA levels and cannot be detected with ultrasound. The incidence of PIN detection in the US averages at approximately 9% of all biopsies carried out and like prostate cancer, the possibility of occurrence increases with the age of the patient [113].

PIN is characterised by cellular proliferation within pre-existing ducts and glands with cytological changes that mimic cancer [112]. Like cancer, PIN is mostly located within the peripheral zone of the prostate, but unlike cancer, retains an intact or fragmented basal layer which becomes increasingly disrupted into higher grades and finally into carcinoma. Early stromal invasion, which is indicative of early progression into carcinoma, occurs at sites of glandular outpouching and basal cell disruption [113]. Furthermore, PIN is associated with progressive abnormalities in phenotype and genotype, which are intermediates between normal epithelium and cancerous tissue. As expected, PIN is shown to be hormone dependent, with a marked reduction with androgen deprivation therapy. However, patients with PIN are not typically treated with hormone therapy but are subjected to further studies to search for concurrent invasive

carcinoma. In addition, follow-up biopsies are suggested at 3- to 6-month intervals for 2 years, and thereafter at 12-month intervals for life [112-114].

1.7.3.2 Hormone signalling and Prostate Cancer Progression

As earlier discussed, androgens and the androgen receptor are fundamental in the development and function of the prostate gland. The most significant function of this pathway is the regulation of apoptosis vs proliferation. Therefore, because of this function, this pathway and related proteins are, unsurprisingly, often changed in prostate cancer, and are key to its progression.

The androgen receptor was first shown to have a role in the pathogenesis of PC in 1941, showing that orchiectomy or treatment with oestrogen could effectively treat the metastatic disease. Since this pioneering work, androgen ablation is still the main systemic treatment for PC [115]. As this study suggests, the cross talk between oestrogen and androgen signalling has been shown to be of significance in prostate signalling [116, 117]. In addition, the ratio of these hormones has also been shown to decrease with age, and this altered ratio correlates with the onset of disease, such as BPH and PC [118, 119].

Furthermore, up-regulation of the oestrogen receptor related receptor α (ERR α) expression in malignant epithelial and stromal cells subsequently increased production of oestrogen from testosterone during prostate progression [120, 121].

The androgen reducing enzyme, 5- α reductase enzyme, is present in the prostate in 3 isoforms. It is generally thought that the expression of type 1 is increased and type 2 decreased in malignant cancers, compared to benign prostate and BPH [122-124]. In addition, 5- α reductase type 3 was recently shown to increase in malignant prostate cancers compared to BPH [125]. Furthermore, a study showed that 5- α reductase type 2 expression decrease in PC was a result of methylation on its promoter sequence [126]. The change in expression patterns of these enzymes means that it is possible for DHT levels to increase, eliciting effects on the prostate stroma and secretory epithelium. Increases in DHT levels, subsequently lead to an increase in AR transcriptional activity in the epithelium of BPH and in early prostate cancer.

1.7.3.3 Later Stage- Androgen Independence

One of the major side effects of androgen ablation therapies is that, over time, prostate cancer invariably progresses to an androgen independent phenotype [127]. The theory is that the removal of androgens from the sensitive cancers results in the selection of cells which are no longer androgen reliant [128]. This phenotype of PC is a fatal manifestation, which is resistant to all other known treatments and further androgen ablation. The cells within the AI phenotype show an increase in proliferation, invasiveness and rate of metastasis compared to their AS counterparts [129]. Therefore significant effort has been focused on understanding this stage of the disease and its progression from androgen dependent PC.

1.8 Current Diagnostics and Procedures

1.8.1 Diagnosis

The ARs importance in prostate cancer and other disease states of the prostate has long been exploited for the detection of the disease. Currently, the detection of prostate-specific antigen (PSA) is used as a biomarker for the detection of prostatic diseases, response of cancers after ablation therapy and recurrence after treatment [79, 130]. Early detection of the disease is paramount to treatment outcome. As clinical symptoms often do not surface until late aggressive stages of the disease, the introduction of PSA testing has improved survival rates [131].

1.8.1.1 PSA

PSA is a serine protease from the tissue kallikrein family and is produced by prostate epithelial cells. PSA is an androgen sensitive gene, and thus is upregulated in PC due to the increase in AR activity [132]. This significant increase in expression levels leads to the excretion of PSA into the circulatory system. Here, PSA can be monitored via a simple blood test [133]. PSA protein is synthesized with a leader sequence which is cleaved to produce an inactive form of PSA. Further cleavage from the N-terminal of 7 amino acids results in an active enzyme [59]. The majority of PSA that enters the peripheral blood stream is intact and is complexed with a protease inhibitor [134]. However, some forms

do exists as free inactivated PSA, due to internal cleavage of the enzyme, and thus has an inability to form the PSA/inhibitor complex. These free, inactive forms are decreased in PC cells and consequently can be used to aid the discrimination between normal and PC [59].

Prior to the routine screening of men with PSA, diagnosis was conducted via physical examination and trans-rectal ultrasound coupled with a biopsy. As a result, patients weren't often diagnosed until after the manifestation of clinical symptoms, mostly in the later stages of the disease [135]. PSA came into routine use in the early 90s and it is the most studied androgen receptor target [136, 137]. It is also the most widely used cancer marker for diagnosis and follow up [79, 130]. It has also revolutionised patient care. Where previously, patients were often diagnosed in aggressive late stages of the disease, testing via PSA has given the opportunity for treatment with hormone and radiotherapy, extending survival times and decreasing mortality rates [138, 139]. However, it is not without controversy, as it can frequently produce false positives, causing unnecessary treatment and often inducing\ accelerating cancer growth. In the latest report for the U.S. Preventive Services Task Force, its co-chair Michael LeFevre stated "Prostate cancer is a serious health problem that affects thousands of men and their families. But before getting a PSA test, all men deserve to know what the science tells us about PSA screening: there is a very small potential benefit and significant potential harms" (www.uspreventiveservicestaskforce.org/prostatecancerscreening.htm). Thus, in recent years it has become advantageous to find a new, more reliable biomarker for this disease [140]. The regulation of the PSA transcription is initially androgen-related and thus declines after castration or ablation therapy. However, in the case of androgen independent PC, PSA levels are continually increased through a currently undefined mechanism [141]. Once the disease regresses to the castration resistant, androgen independent form, patients usually succumb to the disease in 2 years [142].

1.8.1.2 Gleason Scoring

Gleason scoring was first created in 1966 and is a unique grading system for prostate cancer based solely on the tissue architectural pattern in the tumour [143, 144]. Gleason originally described this system based on 270 US veterans,

later this study was expanded to include 1032 men, with further refinements to the system shown even today [144-147]. This scoring system was designed to give clinicians a system on which to relate prognostic symptoms and is based upon the level of differentiation observed at biopsy. All tumours were classified into a 5-grade system representing the progressive complex morphologies. Tumours are assigned grades based on a two-step process. The tumours are first assigned a primary grading between 1-5 based on the most prevalent tissue pattern (i.e. the majority of the tumour contains this type of architectural pattern), then they are assigned a secondary grading between 1-5 based on the second most common tissue pattern. These 2 scores are added together to give a 'Gleason score'. Patients with low Gleason scores (<6) often undergo 'watchful waiting' and active surveillance treatments, where patients have an increase in PSA monitoring and symptom progression. This is to monitor potential cancer progression and facilitate early intervention for progressive disease [145, 148]. Patients with a score higher than 7, receive active therapy. Gleason scores 8-10 are associated with treatment with radiation and androgen therapy [145]. The table shows a brief overview of the Gleason scoring system (see table 1.1) [143].

Gleason Grade	Description of Observed Tissue
1	Simple round glands, close-packed in rounded masses with well-defined edges. Closely resembles normal tissue.
2	Simple rounded glands, loosely packed in vague, rounded masses with loosely defined edges
3A	Medium sized single glands of irregular shape and irregular spacing with ill-defined infiltrating edges
3B	Very similar to 3A, but small to very small glands, which must not form significant chains or cords
3C	Papillary and cribriform epithelium in smooth, rounded cylinders and masses; no necrosis
4A	Small, medium, or large glands fused into cords, chains, or ragged, infiltrating masses
4B	Very similar to 4A, but with many large clear cells, sometimes resembling "hypernephroma"
5A	Papillary and cribriform epithelium in smooth, rounded masses, more solid than 3C and with central necrosis
5B	Anaplastic adenocarcinoma in ragged sheets

Table 1.1 Overview of the Gleason scoring system for prostate tumours
Adapted from [143]

1.8.2 Treatments

1.8.2.1 Hormone therapy

Prostate tumours are initially under hormonal control, and so respond well to androgen ablation therapies and physical and medical castration. Androgen ablation is often achieved by using a combination of AR antagonists and 5 α -reductase inhibitors [149]. For most AR antagonists, the target sequence is the LBD. This prevents nuclear translocation and the conformational changes that causes the exposure of the AF-2 surface [150]. This in-turn causes the AR to promote co-repressor molecules to AR-regulated gene promoters, overall decreasing AR activity [77, 151]. Furthermore, suppression of luteinizing hormone releasing hormone (LHRH) in the hypothalamus also acts to decrease androgen levels [152]. LHRH activation mediates the production of testosterone in the testes. Therefore, by suppressing expression of LHRH, medical castration can be imposed [152, 153].

However, as discussed, androgen withdrawal treatment regimens invariably result in the regression of AS cancers into a more aggressive AI phenotype [129].

1.8.2.2 Prostatectomy

Prostatectomy is the removal of the prostate gland (either partial or complete). Due to the invasive nature of these procedures, prostatectomy of the prostate is usually only conducted in younger patients. Prostatectomies can be carried out via 3 procedures.

Laparoscopic radical prostatectomy is used for the complete removal of the prostate gland, to decrease the invasiveness of open prostatectomy surgery by using small incisions and robotics aids [154]. Open prostatectomy, in contrast, is a highly invasive procedure.

Trans-urethral resection of the prostate or TURP, is the least invasive of the 3 procedures and as such can be employed in high-grade BPH. Here, a cystoscope is inserted into the urethra and removal of prostatic tissue is carried out to alleviate pressure on the urethra [155].

1.8.2.3 Radiotherapy

Radiotherapy has long since been used in the treatment of prostate cancers and is thought to be paramount in the treatment of high grade tumour control [156]. Treatment of prostate cancer with radiotherapy can be administered via 2 methods; External beam radio therapy and brachytherapy [157]. External beam radiotherapy is based upon directed beams of targeted radiation generated outside the body, whilst brachytherapy involves the implantation of radioactive isotopes into the tumour mass [156]. Radiotherapy combined with androgen ablation therapy is usually used to treat patients with high Gleason scores, as warranted by the fact that dual treatment of androgen therapy with radiotherapy improves survival of patients compared to single treatments [158].

In light of the information above, the main scientific thrust of my thesis was directed towards two major cAMP signalling molecules in the context of prostate cancer development. Hence the main aims of my thesis were divided into two sections: 1) the profiling of PKA isoform expression in prostate progression and subsequent characterisation of the direct effects on AR; 2) the isolation of interacting pathways with PDE4D7 in advancing prostate cancer, to establish how changes in PDE4D7 regulation can effect prostate cancer signalling.

2 Materials and Methods

2.1 Cells Culture

All cells were grown at 37°C in 5% CO₂. All sub-culture of cells was conducted in a sterile environment using laminar flow hoods and 70% ethanol to sterile hands and working surfaces just prior to use. All culture media and additives were source from Sigma- Aldrich and all plastics were sourced from Corning unless stated below. Growth media was changed every 48 hours unless otherwise stated. All cells were sourced from ATCC, with the exception of PC133 which was a kind gift from Dr. Guido Jenster of the Erasmus Medical Centre in Rotterdam.

2.1.1 Culture

HEK293 cells (Human Embryonic Kidney Cells) were cultured in Dulbecco's modified Eagle Medium (DMEM) supplemented with 10% foetal bovine serum, 2mM L-glutamine and penicillin-streptomycin. Cells were received with a passage number between 5-11.

DU145 cells were cultured the same as HEK293 cells. Cells were received with a passage number between 53-62.

LNCaP cells were cultured in RPMI1640 medium and supplemented the same as DMEM. Cells were received with a passage number between 21-28.

VCaPs and PNT1a cells were all cultured the same as LNCaP cells. Cells were received with a passage number between; VCaPs (35-39), PNT1a (19). PC-3 cells were cultured as LNCaP cells but with only 5% foetal bovine serum supplemented into the medium. Cells were received with a passage number between 9-13.

2.1.1.1 Sub-culture of cell lines

Cells lines were sub-cultured when they reached the confluence of approximately 70-80%. Cells were washed twice in warm (37°C) PBS. Subsequently, cells were incubated with 4ml of 1% trypsin-EDTA (for a 75cm³ flask) to cleave the extracellular anchoring proteins attaching the cells to the

plastic. Once all cells had been dislodged from the tissue culture plastic, 8mls of appropriate growth media was added to the flask. The resulting 12ml cell suspension was transferred to a 15ml tube.

Cell suspensions were then centrifuged at 800 x g for 3 minutes to pellet the suspended cells. The trypsin/growth media mixture was then removed from the tube and the cell pellet was re-suspended in 10mls of growth media. Cells required to be precisely seeded were counted using a Millipore® Scepter. For sub-culture cells were re-seeded at a density of approximately 30%.

2.1.1.2 Storage of Cell Lines

Samples of the cell lines used within this study were prepared for liquid nitrogen storage for future use. All samples were prepared for storage by suspending cells in 10% DMSO in appropriate growth media and transferring the suspension to a cyro-vial suitable for liquid nitrogen storage. Cells were frozen at -80°C prior to transfer to liquid nitrogen storage.

Cells were retrieved from storage by incubation of the frozen sample at room temperature prior to the addition of 5ml of growth media, also at room temperature. Cells were centrifuged at 800 x g for 3 minutes and the supernatant removed. Cells were then re-suspended in 12mls of growth media and plated out in a 75cm³ culture flask.

2.1.2 Transfection

2.1.2.1 Lipofectamine 2000®

All prostate cell lines (ATCC) were transfected with DNA constructs using Lipofectamine 2000® (Invitrogen®) transfection reagent, as per the manufacturer's instructions (with the exception of during the high-through-put screens in chapter 3). Transfections were typically performed when cell cultures were 80% confluent. Outlined below is the procedure for a single well of a 6-well plate, which was scaled up or down depending culture vessel surface area.

Growth media was replaced with Opti-MEM® (Invitrogen®) 2 hours prior to transfection. Transfection complexes were formed in 15ml polypropylene tubes.

250µl of Opti-MEM was added to each of two separate tubes. 4µg of plasmid DNA was then added to one tube whilst 10µl of Lipofectamine 2000® reagent was added to the other. Both tubes were gently agitated to ensure mixing. Tubes were then incubated at room temperature for 5 minutes before the Lipofectamine 2000® mixture was added to the diluted plasmid DNA. Transfection complexes were allowed to form for 25 minutes. During this time the cell culture media was replaced with 1.5ml of fresh Opti-MEM®. Transfection complexes were gently added to the culture vessel by pipetting directly into the Opti-MEM® culture media. Transfection complexes were incubated with cells for 4 hours and then normal growth media was added. Cells were harvested 24- 48 hours after transfection according to the experimental design. A typical transfection efficiency of 30-40% was achieved for the VCaP cell line whilst all other prostate cell lines exhibited an efficiency of 50-60%.

2.1.2.2 X-treme GENE HP ®

For all the high-through-put screens in chapter 3 the following protocol was followed, with the exception of luciferase reporter arrays for which the protocol is outlined in section 2.1.3. The X-treme GENE reagent was used after a screening of transfection reagents was carried out in a hope to increase the transfection efficiently in the VCaP cell line (Appendix 7.1). Lipofectamine 2000® was used as outlined in the protocol above, the other transfection reagents were used as outlined in the 'X-treme' GENE HP' protocol.

VCaP cells were transfected with DNA constructs using X-treme GENE HP® (Roche®) transfection reagent, as per the manufacturer's instructions. Transfections were typically performed when cell cultures were 80% confluent. Outlined below is the procedure for a single well of a 6-well plate, which was scaled up or down depending culture vessel surface area.

Growth media was replaced with Opti-MEM® (Invitrogen®) 2 hours prior to transfection. Transfection complexes were formed in 15ml polypropylene tubes. X-treme GENE HP® transfection reagent was heated to room temperature prior to use. 500µl of Opti-MEM was added to the tube followed by 4µg of plasmid DNA and 12µl of X-treme GENE HP® reagent. The tube were gently agitated to ensure mixing and incubated at room temperature for 25 minutes to allow the

transfection complexes to form. During this time the cell culture media was replaced with 2ml of fresh Opti-MEM®. Transfection complexes were gently added to the culture vessel by pipetting directly into the Opti-MEM® culture media. Transfection complexes were incubated with cells for 4 hours and then normal growth media was added. Cells were harvested 24- 48 hours after transfection according to the experimental design. A typical transfection efficiency of 40-50% was achieved for the VCaP cell line.

2.1.2.3 Polyfect®

For HEK293 cells were transfected with DNA constructs using PolyFect® (Qiagen®) transfection reagent, as per the manufacturer's instructions. Transfections were typically performed when cell cultures were 80% confluent. Outlined below is the procedure for a single well of a 6-well plate, which was scaled up or down depending culture vessel surface area.

Transfection complexes were formed in 15ml polypropylene tubes. 100µl of Opti-MEM was added to the tube followed by 2µg of plasmid DNA and 20µl of PolyFect® reagent. The tube were gently agitated to ensure mixing and incubated at room temperature for 10 minutes to allow the transfection complexes to form. During this time the cell culture media was replaced with 1.5ml of fresh full growth medium. 1ml of full media was added to the transfection complexes and was gently added to the culture vessel by pipetting directly into the growth media. Transfection complexes were incubated with cells until ready to harvest, 24- 48 hours after transfection according to the experimental design. A typical transfection efficiency of 70-80% was often achieved.

2.1.3 Lysate Harvesting

Cell lysates were harvested using 3T3 lysis buffer (25mM HEPES, 10% w/v glycerol, 50mM NaCl, 1% w/v Triton x100, 50mM NaF, 30mM NaPP, 5mM EDTA pH7.4). Complete, EDTA-free Protease Inhibitor Cocktail Tablets were added to the lysis buffer prior to use and PhosSTOP Phosphatase Inhibitor Cocktail Tablets® (both Roche®) were added to the lysis buffer where indicated. Cells were detached from the tissue culture vessel by scraping with a rubber

policeman. Lysates were then pipetted immediately into a 1.5ml Eppendorf® tube and kept on ice. After, lysates were centrifuged at 13000 x g for 5 minutes to remove insoluble material. Concentrations were immediately assessed (Section 2.2.1) and lysates were either used the same day, or snap frozen on dry ice and stored at -80°C for future use.

Lysates used in PDE assays were harvested using KHEM lysis buffer (50mM KCl, 50mM Hepes, 10mM EGTA, 1.92mM MgCl₂, pH 7.4). Protein lysates were passed through a needle several times. As KHEM buffer contains no detergents, physical breaking of the cells was achieved by this process.

2.1.4 Luciferase reporter arrays

Luciferase Signal pathway reporter arrays were purchased from SABioscience® (Qiagen®). Each well of the reporter array contained dried constructs of a pathway-focused transcription factor responsive Firefly luciferase and ‘control’ constitutively transcriptionally active Renilla luciferase constructs in a 1:1 ratio. These plasmids were reconstituted and cells reverse transfected as laid out below.

All arrays were transfected using X-treme gene HP® (Roche). 5ml of Opti-MEM® per plate was added to a 15ml polypropylene tube. To each tube 20µg of plasmid DNA was added and 25µl of Opti-MEM® was added to each well of the 96well array to re-constitute the plasmid DNA, these were then incubated for 5 min at room temperature. 120µl of X-treme gene® transfection reagent was then added to the polypropylene tube and instantly, with a multi-channel pipette, added to the 96 well arrays (for control plates only 60µl of transfection reagent was used). Transfection complexes were formed over 25 minutes at 37°C. During this time VCaP cells were trysonised, added to new Opti-MEM® media and counted as previously described. After 25 minutes 30,000 cells added to each well. Cells and transfection complexes were incubated together for 4 hours, after which 100µl of normal media was added to each well. Cells were incubated for a further 48 hours. After 48 hours, media was removed from the cells and washed with 100µl of ice cold PBS. Quantification of luciferase activity was carried out using a dual luciferase assay kit from Promega®. Cells were lysed by added 20µl of 1x Passive Lysis Buffer (PLB, from the Promega® kit) and incubated by rocking for 1 hour.

The catalytic activities of the luciferase enzymes was measure for 1 second per well using a Mithras® multiplate reader from Berthold® industries as a luminometer. The results were described as a ratio of Firefly luciferase/Renilla luciferase activity.

2.1.4.1 Luciferase Assay Calculation

Results for the dual luciferase assays were expressed as a ratio of Firefly luciferase activity / Renilla luciferase activity, where Firefly activity is the 'test' and Renilla activity is used as a 'control'. This is due to the Renilla plasmid, being constitutively transcriptionally active. This therefore gives a constant baseline expression to which the firefly luciferase can be referenced. This acts to minimize experimental variability between different transfections, and control for factors which can affect the absolute luminescence.

2.2 Western Blotting Procedures

2.2.1 Bradford Assay

Bradford assays were conducted to determine the protein concentration of harvested lysates. Assays were carried out using Bio-Rad® reagents, following the manufacturers instruction and [159]. The absorbance at A590 nm was assessed for each 50µl of a 1/50 dilution of cell lysate. This was compared against a standard curve of absorbance spectra from known amounts of BSA. 0-5µg of BSA in 50µl dH2O were used to calculate the standard curve and samples were run in triplicate wells using 200µl of the protein assay solution.

2.2.2 SDS-PAGE

Sodium dodecyl sulphate-polyacrylamide gel electrophoresis (SDS-PAGE) is the standard method used for protein separation by molecular weight. SDS-PAGE was conducted using the Novex® NuPAGE® SDS-PAGE Gel System from Invitrogen®. Protein samples were separated by electrophoresis in XCell SureLock® XCell II® Blot Module Kits.

Protein samples of 20-100ug were denatured and reduced by diluting in 5x SDS sample buffer (10% SDS, 300mM Tris-HCl; pH 6.8, 0.05% bromophenolblue, 50%

glycerol and 10% β -mercaptoethanol). The samples were boiled for 5 minutes and the loaded directly to a well of a NuPAGE® 4-12% Bis-Tris polyacrylamide gel from Invitrogen® and immersed in Invitrogen® NuPAGE® MOPS SDS running buffer. 5 μ l of Bio-Rad® pre-stained molecular weight protein marker was also loaded to an appropriate well of the gel to allow the molecular weight of the proteins within the sample to be estimated. The gels were run at 160V for 1 hour.

2.2.3 Western Blotting

Western blotting is used to detect proteins, separated via SDS-PAGE, with specifically raised antibodies. These proteins were transferred from SDS-PAGE to nitrocellulose membrane using the XCell® blotting apparatus and NuPAGE® transfer buffer containing 20% methanol. To achieve this, a voltage was applied through the blotting apparatus at 20V for 2 hours. Following the transfer of proteins onto the nitrocellulose membrane, this membrane was then blocked with 5% milk powder (Marvel®) or 5% PhosphoBLOCKER™ (Cell Biolabs Inc.®) in 1x TBST (20mM Tris-Cl pH 7.6, 150mM, NaCl and 0.1% Tween20) as indicated, for 1 hour on an orbital shaker. The primary antibody, at the appropriate dilution, was added to a solution of 1% milk powder/phosphoBLOCKER™ in 1xTBST. The blocked nitrocellulose membrane was then heat-sealed in an airtight bag with the primary antibody solution. This was incubated overnight at 4°C on an orbital shaker. The appropriately raised anti-immunoglobulin secondary antibody conjugated with either horseradish peroxidase (HRP)(Sigma®) or LI-COR Biosystems® fluorophor was added to a solution of 1% milk powder/phosphoBLOCKER™ in 1xTBST at a dilution of 1:10,000. The membrane was washed 3 times with 1x TBST for 5 minutes before being heat sealed in an airtight bag with the primary antibody bound membrane and secondary antibody solution for 1 hour at room temperature on an orbital shaker. Again, the membranes were washed 3 times in 1xTBST. For visualisation of HRP conjugated secondary antibodies, Amersham Biosciences® chemiluminescence (ECL) western blotting kit was used, in collaboration with blue-light sensitive X-ray film (Kodak®) and developed using the Kodak® X-Omat model 2000 processor. To visualise antibodies conjugated with LI-COR Biosystems® fluorophor, membranes were placed face down on the LI-COR Biosystems® Odyssey infrared scanner. Membranes were scanned at either 680 or 800nm wavelength, according to the

secondary fluorophore. The scans were saved as TIF files and were analysed using LI-COR Biosystems® Odyssey® software.

2.2.4 Immuno-precipitation

Co-immunoprecipitation is a method for the confirmation of interactions. Cell extracts (Section 2.1.3) underwent protein determination via Bradford assay (Section 2.2.1) and then adjusted to equal protein amount (1 µg/µl) using 3T3 lysis buffer. After preclearing, the AR (Santa cruz ®) antibody was used to immunoprecipitate (IP) over-expressed AR. The resulting immunocomplexes were captured using Protein G beads (Invitrogen) at 4 °C overnight. The immunocomplexes/beads were centrifugation at 13 000 rpm for 3 min and washed three times with 3T3 lysis buffer. The immunocomplexes/beads pellet was re-suspended in SDS-PAGE sample buffer and boiled in order to elute the bound proteins in the sample buffer. After, centrifugation the supernatant was subjected to SDS-PAGE and Western blotting as described previously (Section 2.2.2, 2.2.3). Negative controls using isotype-matched IgG (Millipore ®) from the same species as the antibody was included to screen for non-specific binding.

2.2.5 Peptide Kinase Assay

The peptide kinase assay was undertaken with a peptide array containing immobilised peptide libraries that encompass the entire sequence of the AR. The array contains 25mer segments of the androgen receptor sequence, each shifted by 5 amino acids at a time (produced in house by Ruth McLeod). This was blocked with 5% BSA in 1xTBST for 1 hour at room temperature on an orbital shaker. 3µg of active catalytic unit of PKA (Millipore®) was added to phosphorylation buffer (20 mM MgCl₂ in TBS [20 mM Tris-HCl pH 7.5, 150 mM NaCl]) plus 10µM of ATP (Cell Signaling®), and overlaid on the slide for 30 minutes at 37°C on an orbital shaker. A negative control was carried out under same conditions but without the addition of the PKA enzyme. PKA consensus site phospho-Serine primary antibody (Sigma®) was added to a 1% BSA in 1xTBST solution at a dilution of 1:1000. The slides were washed 3 times with 1x TBST for 5 minutes before being added to a slide tray containing the primary solution and was then incubated overnight at 4°C on an orbital shaker. Again the slides were washed 3 times in 1xTBST for 5 minutes. Immunoglobulin secondary antibody

conjugated with HRP (Sigma®) was added to a solution of 1% BSA powder in 1xTBST at a dilution of 1:10,000. This secondary antibody solution was added to the slides and incubated for 1 hour at room temperature on an orbital shaker. Again, the membranes were washed 3 times in 1xTBST. For visualisation, Amersham Biosciences® chemiluminescence (ECL) western blotting kit was used as described in Section 2.2.3.

2.3 PCR

2.3.1 Extraction and Purification of RNA

Due to the delicate nature of RNA samples, surfaces were cleaned with 10% chlorinated dH₂O to remove any residual nucleic acids, RNase ZAP (Ambion®) was then used to treat gloves, plastic and metal surfaces in order to deactivate environmental RNase enzymes. Where pipetting was required nuclease free filter-tips (Rannin®) were used and nuclease free water was purchased from Ambion®. Prior to the harvesting of RNA, cells were seeded and grown over 48 hours to 60% confluency in cell culture plates purchased from Corning. Cells were washed with 10mls warm PBS (137 mM NaCl, 2.7 mM KCl, 100 mM Na₂HPO₄, 2 mM KH₂PO₄) before direct lysis. RNA was extracted using RNeasy® Mini kit (Qiagen®), according to the manufactures instructions.

In brief, RLT buffer is added directly to cells for lysis, and homogenised by passing through a needle several times. 70% nuclease free ethanol is then added to the lysate. This mixture is applied to the RNeasy Mini spin column and centrifuged for 15s at 8000 x g. The ethanol creates conditions that cause selective binding of RNA to the RNeasy membrane and the flow through is discarded. The membrane is washed twice with 500µl of RPE buffer and centrifuged for 15s at 8000 x g, removing any contaminants. The RNeasy Mini spin column is then placed into a new collection tube and 30-50µl of nuclease free water is applied to the column. This is centrifuged for 1 minute at 8000 x g eluting the RNA. All bind, wash, and elution steps were performed at room temperature to minimise salt precipitation.

Total RNA sample was then subjected to DNase digestion to ensure no genomic DNA contamination using DNA-free™ Kit (Ambion®). Briefly, if the nucleic acid

concentrations were above 200µg nucleic acid per ml, 10µl of 10X DNase I Buffer and 2µl of rDNase I was added to 50µl of un-treated RNA sample. This was incubated at 37°C for 30 minutes. 10µl of re-suspended DNase inactivation reagent was then added to the sample and incubated at room temperature for 2 minutes, mixing occasionally. The sample was centrifuge at 10,000 × g for 1.5 minutes to pellet the DNase inactivation reagent and the supernatant, which contains the DNA free RNA, was carefully transferred into a fresh tube.

2.3.2 Nucleic Acid Quantification

Purified RNA was assessed for quantity and purity using the Nanodrop spectrophotometer from Thermofisher Scientific®. 2µl of sample was applied to the pedestal on the Nanodrop and RNA concentration was measured by absorbance at A260, where an absorbance of 1 is equal to 40µg/ml of RNA. Purity of the sample was assessed by the A260/A280 nm ratio method. A value of 1.8-2.1 was considered optimal for protein/nucleic acid ratio.

2.3.3 cDNA Synthesis

First strand cDNA synthesis was carried out using Precision nanoScript™ reverse transcription kit (Primerdesign®). In brief, 1µg of total RNA was added to 1µl of random primers and nucleotide free water, to make 10µl total volume. To anneal the RNA and primers the sample was heated to 65°C for 5 minutes in a thermostatically controlled heat block. After 5 minutes the samples was applied straight to ice. To amplify the sample and synthesise cDNA for the RNA, the 10µl sample was added to the following components:

Component	1 reaction
nanoScript 10X Buffer	2.0 µl
dNTP mix 10mM of each	1.0 µl
DTT 100mM	2.0 µl
RNase/DNase free water	4.0 µl
nanoScript enzyme	1.0 µl
Final volume	10 µl

After vortexing, samples were incubated at 25°C for 5 minutes. Amplification of cDNA was carried out at 55°C for 20 minutes followed by a heat inactivation step

at 75°C for 15 minutes. Subsequent dilutions of this preparation were performed in nuclease free water and stored at -20°C until further use.

2.3.4 Quantitative Real Time PCR

2.3.4.1 Primer Design (TaqMan®)

Primers were designed to amplify an 80-120 base region of target cDNA within the gene of interest (GOI). Melting temperature of probe sets were optimally between 55-60°C. Dual labelled probes with TAMRA and FAM labels, 3' and 5' respectively, were used throughout this study. To ensure specificity all oligonucleotides were BLAST searched against the NCBI mRNA database. Where an oligonucleotide showed possible affinity (e.g. 70%) for an off target transcript cDNA it was ensured that cognate two oligonucleotides forming the probe-set showed no homology to the same off-target transcript.

Primer and probe sets were synthesised by Eurofins MWG Operon® and purified using HPLC.

2.3.4.2 RT-qPCR Protocol (Taqman®)

RT-qPCR was carried out using Applied Biosystems® Prism® 7900HT cycler. Reactions were carried out in 15µl volumes with the following reaction mixture composition:

Reagent	Final Concentration / Volume
qRT-PCR Mastermix(Quanta®)	7.5µl
Nuclease free dH ₂ O	2.2µl
Forward Primer	500nM
Reverse Primer	500nM
Probe	500nM
cDNA	5.0µl

Reactions were carried out in 96-well optical plates from Applied Biosystems® using the following reaction protocol:

Segment	Cycles	Temperature	Time
1	1	60°C	30 Seconds
		95°C	2 Minutes
2	40	95°C	15 Seconds
		60°C	1 Minute

Where not indicated, Taqman® probe sets were used throughout this study. Auto adjustment of threshold level means that it was optimally placed within the exponential region of the RT-qPCR amplification curves. Cycle number (Ct) values were taken for each gene of interest (GOI) where the amplification curve intersected the threshold level. The Ct values were then used in the calculations described in 2.3.6.

2.3.5 SybrGreen cDNA Synthesis

For the experiments in which SYBR green is used, cDNA synthesis was carried out using RT² First stand kit (Qiagen ®). In brief, 1µg of total RNA was added to nucleotide free water, to make 10µl total volume. To amplify the sample and synthesise cDNA for the RNA, the 10µl sample was added to the following components:

Component	1 reaction
5x Buffer BC3	4.0 µl
Control P2	1.0 µl
RE3 Reverse Transcriptase Mix	2.0 µl
Nuclease free dH ₂ O	3.0 µl
Final volume	10 µl

After gentle mixing, amplification of cDNA was carried out at 42°C for 15 minutes followed by a heat inactivation step at 95°C for 5 minutes. Subsequent dilutions of this preparation were performed in nuclease free water and stored at -20°C until further use.

2.3.5.1 RT-qPCR Protocol (SybrGreen ®)

RT-qPCR was carried out using Applied Biosystems® Prism® 7900HT cyclers. Reactions were carried out in 25µl volumes with the following reaction mixture composition:

Reagent	Final Concentration / Volume
2x RT ² STBR Green Mastermix	12.5µl
Nuclease free dH ₂ O	11.5µl
cDNA	1.0µl

Reactions were carried out in 96-well optical plates from Applied Biosystems ® using the following reaction protocol:

Segment	Cycles	Temperature	Time
1	1	95°C	10 Minutes
2	40	95°C	15 Seconds
		60°C	1 Minute

The Sybr green protocol was used in chapter 5. Auto adjustment of threshold level means that it was optimally placed within the exponential region of the RT-qPCR amplification curves. Cycle number (Ct) values were taken for each gene of interest (GOI) where the amplification curve intersected the threshold level. The Ct values were then used in the calculations described in 2.3.4.3.

2.3.6 Calculating Relative Expression

Transcript abundance was calculated via the comparative method, where GAPDH was used as internal housekeeping genes to which all genes of interest (GOI) were compared against.

The following mathematical transformation was required to take into account the optimal doubling of PCR product with every round of the PCR.

$$\Delta Ct = Ct_{GOI} - Ct_{HKG}$$

To express GOI relative to HKG

$$\text{Relative quantification (RQ)} = (2^{-\Delta Ct})$$

Error bars were calculated from the standard deviation of a triplicate. This triplicate repeats were combined with the variance from the HKG in order to properly account for Ct variance. The standard deviation, of the triplicate, of the HKG and the GOI were integrated together using this formulation. The integrated standard deviations were then used within the original expression calculation in order to calculate the maximum and minimum potential values, which when compared to the relative expression would give the error bars:

$$\text{Upper error bar} = RQ \cdot (2^{-(x_{\Delta Ct} + \sigma_{\Delta Ct})})$$

$$\text{Lower error bar} = RQ \cdot (2^{-(x_{\Delta Ct} - \sigma_{\Delta Ct})})$$

Where: x = mean of samples

σ = Standard Deviation

2.3.6.1 The $\Delta\Delta Ct$ Method to Calculate Comparative Expression

When comparing two or more samples to assess changes in expression, the $\Delta\Delta Ct$ method was used to quantify the degree of differential regulation between the samples. The $\Delta\Delta Ct$ calculation is based on the ΔCt method of calculating relative expression to the HKG, but expands this calculation to assess fold changes in relative expression between samples. This method requires the use of a control sample. All experimental samples are then compared to this control sample.

$$\Delta\Delta Ct = x\Delta Ct_{\text{Reference Sample}} - x\Delta Ct_{\text{Experimental Sample}}$$

Relative quantification and error bars can be calculated as above substituting ΔCt for $\Delta\Delta Ct$.

Using this method the reference sample will have a value of 1, and the experimental samples will be compared as a fold change in this value i.e. a doubling in expression will have a value of 2.

2.4 Harvesting of Plasmid DNA

2.4.1 Transformation

All transformations performed within this study were performed using competent DH5 α E.coli cells from Invitrogen®. Competent cells were aliquoted into 30 μ l samples in pre-chilled Falcon polypropylene tubes. 10ng of plasmid DNA was gently added to 30 μ l of competent cells. The mixture was incubated on ice for 15 minutes before a 90 second heat shock treatment at 45°C and a return to incubation on ice for 2 minutes. 300 μ l of SOC medium (Invitrogen®) was then added to the transformed cells which were then incubated for 1 hour at 37°C. 150 μ l of the transformed cell suspension was then added to a 10cm³ agar plate containing 100 μ g/ml of the appropriate antibiotic. Plates were incubated for 16 hours at 37°C before colonies were selected using a sterile loop and grown in 10ml LB containing 100 μ g/ml of the antibiotic required for selection. Several colonies were selected per transformation. 10ml cultures were incubated in a shaking incubator for 16 hours before a glycerol stock was created for each colony (Section 2.4.2).

2.4.2 Glycerol Stocks

Glycerol stocks were created from bacterial cultures by mixing 500 μ l of the bacterial cell suspension with 500 μ l of sterile 40% glycerol in dH₂O in a 2ml cryo-tube. The mixtures were then snap-frozen on dry ice before transfer to -80°C storage. When creating new cultures from glycerol stocks, the glycerol was kept on dry ice at all times.

A scrape from the top of the glycerol using a sterile 10 μ l pipette tip was then added to a 10ml sample of LB containing 100 μ g/ml of the required antibiotic, and incubated at 37°C for 16 hours in a shaking incubator.

2.4.3 Plasmid DNA Purification

400ml samples of LB containing 100 μ g/ml of the required antibiotic were inoculated with 10ml suspensions derived from glycerol stocks as described in 2.4.2. The culture was then incubated at 37°C in a shaking incubator overnight. Samples were subsequently centrifuged at 6,000 x g for 15 minutes. The

resulting pellet was lysed, and plasmid DNA purified using the Qiagen® Qfilter Plasmid Maxiprep kit® as per the manufacturer's instruction.

2.5 CelluSpot™ Peptide Arrays

VCaP cells were transfected with the specified constructs and cellular lysates were made after 48hrs. Slides were blocked in blocking buffer (50 mM HEPES, pH 7.4, 150 mM NaCl, 0.05% TX100) and 5% BSA at room temperature for 2 hours. After, the kinase reaction was carried out by incubating the slides with kinase buffer (for Ser/Thr slides; 25 mM Tris-HCl (pH 7.5), 2 mM dithiothreitol (DTT), 1 phosphoStop tablet/10ml, 10 mM MgCl₂, 10μM ATP: For Tyr Slides; 60 mM HEPES, 5 mM MgCl₂, 2.5mM DTT, 5 mM MnCl₂, 1 phosphoStop tablet/10ml, 10μM ATP) which was supplemented with 1% BSA, 400μCi/ml [γ -³²P]ATP and 1 μg/ml of cellular lysate. Peptide array slides were incubated with 1ml of the kinase reaction mixture for 2 hours at room temperature. After incubation the slides were washed 2x 5 minutes with 1xTBST, followed by 3x 5 minutes in dH₂O. The arrays were dried on blotting paper and dried slides were incubated with X-ray film at -80°C and developed via the x-omat 2000 processor.

2.6 Pure Protein Kinase Assay

1μg of pure AR protein (Millipore ®) was incubated with phosphorylation buffer (20 mM MgCl₂ in TBS ([20 mM Tris-HCl pH 7.5, 150 mM NaCl]), 0.5mM DTT and 1mM ATP and pre-heated to 30°C. After, 1μl of PKACβ (Millipore ®) was added along with 4μCi of (γ -³²P)ATP (PerkinElmer ®) and incubated at 30°C for 30 minutes. 5x SDS buffer was added to the solution and the samples were boiled for 5 minutes and then loaded directly to a well of a NuPAGE® 4-12% Bis-Tris polyacrylamide gel from Invitrogen® and immersed in Invitrogen® NuPAGE® MOPS SDS running buffer. 5μl of Bio-Rad® pre-stained molecular weight protein marker was also loaded to an appropriate well of the gel to allow the molecular weight of the proteins within the sample to be estimated. The gels were run at 160V for 1 hour. The gel was then dried for 2 hours and overlaid with blue-light sensitive X-ray film (Kodak®) in a development box. This was place at -80°C for 2 weeks and then developed using the Kodak® X-Omat model 2000 processor.

2.7 Protein Isolation and Overlay

R unit proteins were isolated from a donated mini-preparation (Dr Frank Christian). A scrape from the top of the glycerol using a sterile 10µl pipette tip was then added to a 1L sample of LB containing 100µg/ml of the ampicillin antibiotic, and incubated at 37°C for 16 hours in a shaking incubator. After, 15ml of this solution was added to a new 1L LB flask containing 100µg/ml of the ampicillin antibiotic and the OD of the sample was monitored until 0.6A was reached. 0.5mM IPTG was then added to the solution and incubated at 25°C overnight. Samples were spun at 5000g for 10 minutes, supernatant discarded and the pellet re-dissolved in 10ml of MOPS buffer (Sigma ®). To this solution, 1mM PMSF, 1mg/ml lysozyme, 5mM DTT was added and supplemented with protease inhibitor tablet (Roche ®) and then incubated for 20 minutes at room temperature. After, the solution was sonicated for 10 minutes and centrifuged at 35000g for 1hr, after which the supernatant was removed. 400ul of cAMP agarose beads were washed in MOPS buffer and added to the supernatant. This solution was incubated on the 'end over end' for 2 hours. R units within the solution bind to the cAMP and thus binding to the beads. The solution was centrifuged at 500g for 3 minutes, the supernatant removed and the pellet washed with MOPS buffer. The pellet was then re-dissolved into 2.5ml (3.7mg/ml) of cGMP and incubated at 4°C on the 'end over end' for 1 hour. This excess amount of cGMP causes a displacement of the R units, resulting in the units moving into solution. After centrifugation at 500g for 3 minutes, the supernatant was added to washed salt columns. The R units were eluted by adding 3.5 ml of MOPS solution to the columns. This eluent was added to hydrated dialysis cassettes (pierce ®) and incubated in MOPS buffer overnight at 4°C. The pure protein was then removed from the cassettes. A sample was taken from each protein to determining concentration and to test for purity using SDS-PAGE and western blot procedure (2.2.2, 2.2.3).

After isolation the R unit pure protein was utilised in peptide array overlay experiments. A peptide array containing immobilised peptide libraries that encompass the entire sequence of the AR were used. The array contains 25mer segments of the androgen receptor sequence, each shifted by 5 amino acids at a time (produced in house by Ruth McLeod). The array was blocked with 5% BSA in 1xTBST for 1 hour at room temperature on an orbital shaker. The array was

overlaid with 1 µg/ml of protein diluted in 1% BSA in 1xTBST, overnight at 4°C. After the array was washed 3x in 1xTBST and antibody probed with the appropriate regulatory unit antibody (BD Biosciences ®) as outlined in the western blotting protocol (Section 2.2.3).

2.8 PDE assay

Eppendoff tubes were incubated on ice and protein lysates were added, with or without the PDE4 selective inhibitor, rolipram (4-[3-(Cyclopentyloxy)-4-methoxyphenyl]-2-pyrrolidinone). If rolipram was to be used the protein lysate sample was adjusted to a volume of 40µl and 10µl of the inhibitor was added as a 10 x stock, if no inhibitor was used the protein sample was adjusted to a volume of 50µl by the addition of KHEM lysis buffer. Two control tubes containing only KHEM buffer were prepared for each substrate concentration. A 2 x stock solution of substrate was prepared by adding 3',5'-cyclic adenosine (Sigma®) from a stock solution to the desired concentration in buffer A (20 mM Tris-HCl, 10 mM MgCl₂ pH 7.4). Tritiated cAMP (Sigma®) was then added at 3µCi/ml and mixed thoroughly. 50 µl of substrate was added to the protein samples on ice and mixed briefly by flicking the tubes. The PDE reaction was started by incubating the samples at 30°C for 20 min. Here, ³H-cAMP is linearized to ³H-AMP via the activity of the PDE within the protein lysate sample. The reactions were stopped by transferring tubes immediately to a boiling water bath and incubating for 2 min. Samples were allowed to cool on ice and 25µl of 1 mg/ml snake venom (Sigma®) (diluted 1:10 from a 10 mg/ml stock solution) was added and tubes were mixed thoroughly by flicking. Snake venom is added as it contains a 5' nucleotidase which converts the ³H-5'AMP into ³H- adenosine, thus with a further 10 minutes incubation at 30°C allowed phosphate groups to be removed from AMP. Dowex ion exchange resin (Sigma®) prepared as a 1:1 Dowex: water stock was thoroughly resuspended, diluted 1:2 with ethanol and 0.4 ml added to each tube. This exchange resin allows the displacement of the ³H from the ³H-adenosine within the sample. Tubes were vortexed to mix and incubated on ice for at least 15 minutes before a final vortex. The Dowex resin was pelleted by centrifugation at 13,000g at 4°C for 2 minutes and 150µl of the supernatant (which contains the ³H) was removed to an Eppendorf tube containing 1 ml of Ecoscint® scintillation fluid. 50 µl of substrate was also added to two tubes to enable calculation of specific PDE activities. Tubes were

vortexed thoroughly to mix and counted for 1 minute in a β scintillation counter calibrated for [^3H].

2.9 Microscopy

2.9.1 Confocal Microscopy

Cells were plated onto collagen-coated glass coverslips in 6-well cell culture plates and treated as indicated. Cells were analysed 24-48 hours after plating. Cells were fixed with TBS (20mM Tris-Cl pH 7.6, 150mM, NaCl) containing 4% paraformaldehyde for 5 minutes and then permeabilised with 0.1% Triton X-100 in TBS for 10 min at room temperature. The cells were blocked with 10% donkey serum and 2% BSA (w/v) in TBS by a blocking step comprising three 5-minute incubations. Primary antibodies were diluted to the required concentration in dilutant buffer (blocking buffer diluted 1:1 with TBS) and added to the cells for 2 hours followed by three wash steps with TBS. This step was then repeated for the other primary antibody. After the second primary antibody incubation, cells were incubated with 1:400 diluted secondary antibodies Alexa Fluor 488 donkey anti-mouse IgG and Alexa Fluor 594 donkey anti-rabbit IgG (Molecular Probes) for 1 hour. Following several extensive washes with TBS, the coverslips were mounted onto glass slides with ProLong Gold anti-fade reagent with 4',6-diamidino-2-phenylindole (DAPI) nuclear stain (Invitrogen®). Staining was visualized using a Zeiss Pascal laser-scanning confocal microscope (LSM) 510 Meta and an Axiovert 100 microscope (Carl Zeiss, UK) equipped with an oil immersion objective (63x/1.4 NA plan apochromat lens). Images were captured and processed on Zeiss LSM Image Examiner.

2.10 Statistical Analysis

2.10.1 Students T-test

Where data distribution followed a Gaussian distribution the student's two-tailed t-test was used. Graphpad Prism® (Graphpad® software) was used for two-tailed student's t-tests.

2.10.2 Mann-Whitely Test

Where the distribution of data was observed to be skewed (as observed in box-whisker plots) the Mann-Whitney statistical test was used. A P value of less than 0.05 was considered to be statistically significant.

3 PKA Subunits and Prostate Cancer

3.1 Introduction

3.1.1 PKA subunits in hormone related cancers

As discussed earlier, PKA is the classical effector molecule of the cAMP signalling cascade and, as such, has been implicated in a variety of diseases. This is particularly true in the context of carcinogenesis, where cAMP/PKA is known to modulate cellular growth and proliferation.

In mammalian cells, two types of PKA are expressed, type I and type II, distinguishable by the expression of different R subunits. During development, differentiation and transformation, ratios of PKA I and PKA II can change dramatically and this change in expression has been shown to be a feature of carcinogenesis. Cho et al [50] showed that PKA-I was over expressed in various cancer cells. They went on to show that switching the dominant form of PKA (PKA-I) by over-expressing the RII subunit of PKA, resulted in reversion of the phenotype in these cells. This change in cancer phenotype depending on R unit expression has also been linked to hormone related cancers and is thought to be predictive of patient outcome.

In breast cancer studies, significant increases in epithelial proliferation in breast tissue were correlated to a high RI expression. Furthermore, measurements of regulatory subunits in paired samples of normal and malignant tissues from the breasts of 13 women with breast cancer, displayed a higher expression of RI and RII PKA regulatory subunits in malignant tissues, with the degree of RI subunit overexpression greater than that of the RII subunit [160]. In addition, similar findings have been reported when comparing regulatory subunits in colorectal cancer [161]. In a study of breast cancer patients, it was shown that there were no significant relationships between R subunits and tumour histological grade and patient lymph node positivity, although levels of R subunits were higher in oestrogen receptor-negative tumours. However, in patients presenting with early-stage disease, high levels of R unit expression could be associated with poor prognosis in terms of both disease recurrence and overall survival, and allowed the identification of a small subgroup of patients whose poor outlook

warranted implementation of aggressive systemic therapy [162]. Similar effects were shown in ovarian cancer cell lines. In a microarray study using transfected OVCAR8 cells, $R1\alpha$ transfection resulted in changes in genes for pathways involved in cell growth, whereas the $R11\beta$ up-regulation lead to changes in pathways involved in cellular differentiation [163].

In light of these findings, it is worth noting that increased expression of the PKA catalytic unit, $C\alpha$, has not only been linked to an increase in PKA I expression, but has also shown to be expressed externally by a various cancer cell types. In breast cancer, hormone independent cancers display an increase in internal and external PKA activity compared to the hormone dependant cancer [50]. Furthermore, the increase activation of PKA in breast cancer has been linked to drug resistance, through the increased phosphorylation of the ER leading to reduced drug induced degradation [164]. Due to the discovery of increased extracellular PKA in cancer, it too has been suggested as a potential diagnostic marker for cancer [50].

3.1.2 PKA subunits in Prostate Cancer

Several reports have linked prostate cancer with the action of PKA. Reports suggest that PKA action can modulate androgen dependency of prostate cancer cells [165, 166]. There are numerous papers and reviews [166-169] that focus on the PKA isoform\subunit expression (i.e. PKA I vs II) within prostate cancer. It is clear that changes in PKA I affects cancer cell proliferation and that the increased expression of PKA II is found to correlate with less proliferative cells. This is due to the change in expression of the R subunits. Neary et al [167] showed that up-regulation of $R11\beta$ in prostate cancer cells (PC3M) caused a decreased $R1\alpha$ expression and tumour growth. However, they also found that upon up-regulation of $R1\alpha$, they could not induce the same repression of the $R11\beta$ subunit but instead found that it induced increased protein levels of the catalytic unit. It was later found that cells overexpressing $R1\alpha$ can produce extracellular active catalytic subunit [170].

A study conducted by Kvissel et al [169] found that $R11\beta$ was up-regulated in clinical samples of prostate tissue vs normal, and this expression pattern was mirrored in the LNCaP cell line. Furthermore, they showed a significant increase

of PKAC β 2 protein levels in clinical samples, and also an increase in both PKAC β 2 protein and mRNA in the LNCaP wild type (WT) cell line compared to LNCaP cells subjected to an androgen free environment. This was not evident in androgen insensitive cell lines and when cells were incubated in an anti-androgen environment.

Following on from these studies, investigations into PKA expression in prostate cancer for diagnostic purposes have been undertaken. In 2008, the overexpression of RI α was examined as a biomarker for predicting the outcome of patients in clinical trials [171].

Here, I endeavoured to profile the PKA expression patterns of frequently used prostate cancer cell lines in order to elucidate changes in the regulation of PKA signalling during prostate cancer progression.

3.2 Results

3.2.1 RT-qPCR Profiling vs Western blotting

In this study, I employed both western blotting and RT-qPCR techniques in order to construct a full profile of the PKA subunit expression in advancing prostate cancer. RT-qPCR and western blotting are 2 major biochemical techniques with their own drawbacks and positives. Both were used in this study, where possible, to gain insight into the full profile of PKA subunits in prostate cancer.

3.2.1.1 Western blotting

Western blotting is a standard biochemical technique, which involves antibody probing for the detection of specific proteins. This technique, compared to RT-PCR, has the advantage of displaying the functional levels of a specific protein within a sample. The technique does not involve 'sensitive' RNA and one membrane can be used for concomitantly detecting different sized proteins [172]. However, the production and testing of antibody antisera for this technique can be time consuming and costly. To achieve the optimal sensitivity for each antibody, incubation conditions and working dilutions of the antibody have to be optimised before each experiment to reduce background signals. Western blotting also lacks the sensitivity of PCR techniques, especially with proteins of high or low-molecular mass.

3.2.1.2 Antibody selection

Antibody selection is very important in western blot analysis. The sensitivity of the antibody for its epitope can severely affect the sensitivity of the western blot procedure, as promiscuity of the antibody can markedly increase the false positives within the experiment. Thus, all antibodies used in this procedure should be fully tested before use in the study.

For this screening, PKA regulatory unit isoform antibodies (RI α , RIIB, RII α) were selected from BD bio laboratory® as they are readily available and conditions have been optimised previously within our laboratory (as well as [169, 173]). All these antibodies are mono-clonal and so have increased isotope specificity, reducing interaction within isoforms. RI β has been reported not to be expressed

in LNCaP cells [169], and accordingly, we tested RI β antibodies and detected no protein expression in the cell lines used. PKA catalytic units were detected with a 'pan' monoclonal antibody. This was selected after varying results with isoform specific antibodies. The antibody is also from BD Biolaboratories and has been previously used in the Baillie group.

3.2.1.3 RT-qPCR

Reverse transcription polymerase chain reaction (RT-PCR) is a molecular biology technique for amplifying a specific piece of mRNA. The mRNA molecule is first reverse transcribed into complementary DNA (cDNA), followed by amplification of the resulting DNA by polymerase chain reaction (PCR). RT-qPCR uses primers to amplify a short segment of cDNA usually approximately 100bp in length. These primers are specific to the transcript of interest and it is important that they are validated for 'off target' binding affinity to reduce non-specific amplifications. RT-PCR is widely and increasingly used because of its high sensitivity, good reproducibility, and wide dynamic quantification range [174]. While it is generally accepted that RNA levels correlate to protein expression, it is shown that is not always the case. Post-transcriptional regulation of proteins can cause differences between RNA and protein concentration [175, 176].

3.2.1.4 TaqMan Probes

Taqman[®] probe-sets were used during this study due to previous testing and validation within the Baillie group. These probe sets are composed of forward and reverse primers and a probe that is targeted toward unique sequence between the primer binding sites. The probe is an oligonucleotide that is labelled with a fluorophore (FAM) and a quencher molecule (TAMRA). When bound to the probe, emission from the fluorophore is intercepted by the quencher due to the close proximity. However, during PCR amplification the probe is broken down by DNA polymerase activity. This separates the fluorophore and quencher, leading to an increase in fluorescence level within the reaction [177]. As the probe should only anneal and be broken down at a specific location, no melting point analysis is required, as any off target binding will not be broken down in the amplification process and thus not affect the overall change in fluorescence in the PCR reaction.

3.2.1.5 Use of Relative Quantification

There is two major types of quantification for RT-PCR; absolute and relative [174].

Absolute quantification involves the use of calibration curves. In this method, PCR amplifications are compared to an established standard curve. While these curves are highly reproducible and generate highly specific and sensitive data, the calibration curve has to be thoroughly validated, as this technique relies entirely on the accuracy of the standard curve. Design and production of this standard curve can be highly time consuming and problematic.

Relative quantification determines the change of mRNA levels of a gene of interest and expresses it relative to the levels of an internal control gene. Housekeeping genes such as glyceraldehyde-3-phosphate dehydrogenase (GAPDH) are the most often used internal control genes. This eludes the issues of absolute quantification as a standard curve is not required. However, in this model, gene of interest expression is normalised by a non-regulated reference gene, whose mRNA expression could vary between treatments or individuals. To try and circumvent this more than one reference gene is often selected.

To profile the expression levels of the PKA isoforms by RT-qPCR in this study, we have selected to use the TaqMan® approach, coupled with a relative quantification method, when compared to GAPDH. As discussed, Taqman probes add specificity unavailable in other approaches. Plus use of relative quantification means that no standard curve set-up or validation is needed and it also decreases pipetting errors associated with this method.

3.2.1.6 Housekeeping Gene Selection

GAPDH, was selected as the reference gene used in this study. GAPDH is an enzyme that catalyses glyceraldehydes-3-phosphate to D-glycerate1,3-bisphosphate in the sixth step of the glycolysis pathway. Due to its function it is often ubiquitously and stably expressed in most tissues. It is also resistant to most cellular manipulations that can cause gene expression changes, but gene expression levels have been shown to change between tissue types.

Mori et al [178], using prostate cancer and normal tissue from patients, investigated the usefulness of beta-actin and GAPDH as housekeeping genes. Using AR as the variable gene, expression levels normalised using beta-actin significantly correlated with the expression of GAPDH. This suggests that GAPDH is a suitable reference gene in prostate cancer studies. Furthermore, work carried out by our laboratory on the cell lines used in this study, examined the expression level of GAPDH in relation to 18S rRNA (Figure 3.1). 18S rRNA is a part of ribosomal RNA and is a component of the small ribosomal subunit. It has been often described as a reliable reference gene in PCR. This work showed no significant changes in expression between samples of each of the cell line. In addition, transcript variance was tested by comparison of the expression of genes that vary between cell line samples and each housekeeping gene. In plotting this change, they observed a strong correlation between the two housekeeping genes suggesting that they didn't undergo differential regulation in the prostate cancer cell lines (Figure 3.2).

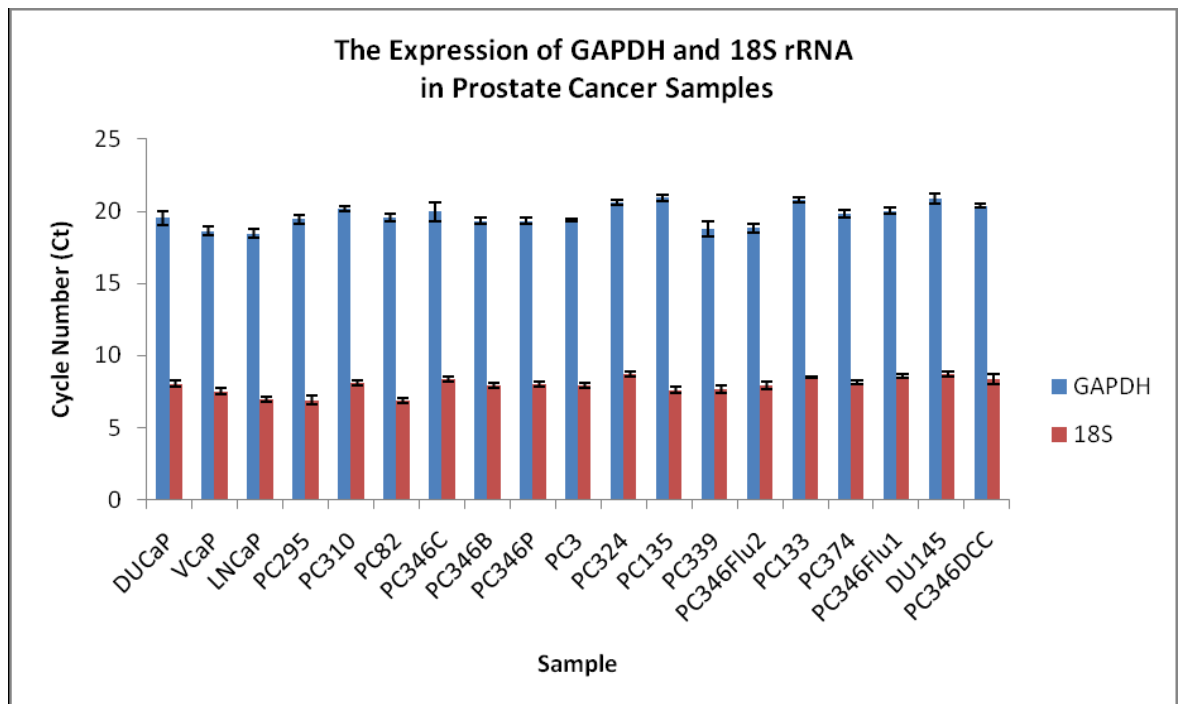


Figure 3.1 GAPDH and 18S rRNA expression in prostate cancer samples. Taken from [179]

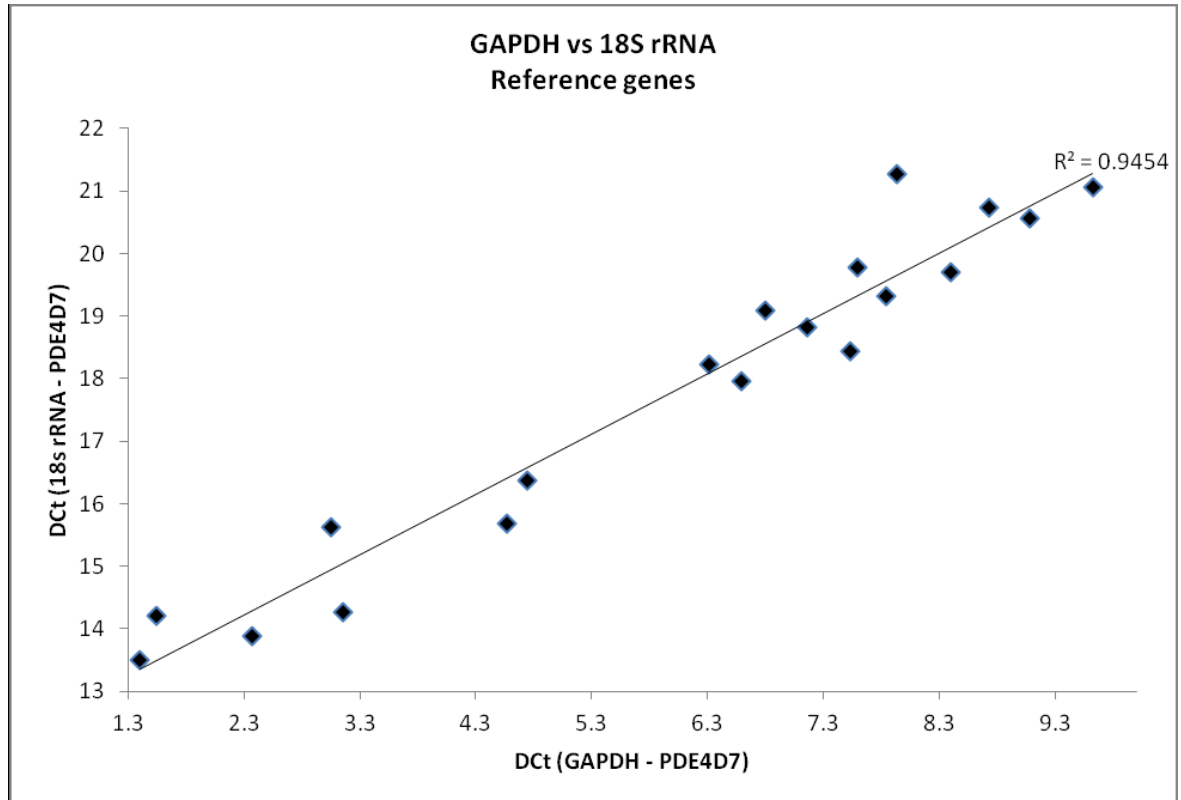


Figure 3.2 PDE4D7 was assessed against GAPDH and 18SrRNA. An R^2 value of 0.94 indicates a good positive correlation using a straight line trend line. Taken from [179]

3.2.2 Selection of Cell Lines

Studying the molecular changes in cancer and its progression is paramount to the identification of novel avenues for the development of effective therapies. While animal models can be beneficial to this cause, they have significant drawbacks, such as ethical concerns and housing costs. To my knowledge there is no animal model that mimics all the aspects of human prostate cancer. To overcome this, significant effort has been put into developing cell culture models that represent various cancer stages. Cell lines selected in this study are well established lines for studying prostate cancer and its progression [180, 181]. I have selected 2 well-characterised androgen sensitive (AS) and androgen insensitive (AI) cell lines for western blot analysis and 3 of each for RT-qPCR analysis, to try and highlight difference in PKA isoform expression as PC progresses towards the AI phenotype. A cell line predictive of ‘normal’ epithelial prostate cells was also included in the final part of the screening to establish changes between “normal” prostate signalling and that during prostate carcinogenesis.

3.2.2.1 AS cell lines

AS cell lines selected were VCaP, LNCaP and DUCaP. VCaPs (along with DUCaP) is the newest of the selected cell lines and was isolated in 2001 from a 60 year old male. It was isolated from a metastatic lesion from the lumbar vertebral region of the patient at post-mortem. This cell line expresses wild type AR, PSA, and PAP; characteristics usual of clinical prostate carcinoma [182].

LNCaP cell line was isolated in 1977 from a needle biopsy of a lymph node metastasis in a 50 year old male. It has been used extensively used as a AS model in prostate cancer, and it can also be grown in the absence of androgens to generate an AI type cell line and also to study prostate cancer progression. This has led to the large number of sub-lines described in the literature. These cells express PSA and AR, however a mutation has been shown in the AR, which results in somewhat promiscuous response to steroids [180, 183].

DUCaPs were isolated from the same patient as the VCaP cell line at autopsy from a metastatic lesion in the dura matter. The tissue was first xenographed into SCID mice and later harvested and plated to derive this cell line. These cells express wild type AR, PSA and PAP [180, 184].

3.2.2.2 AI cell lines

AI cell lines selected were DU145, PC3 (and PC133). DU145 cells were the first cell line established in tissue culture. They were isolated at autopsy from a metastatic tumour from the brain of a 69 year old male. This cell line is described as moderately differentiated and fails to express AR and PSA with low levels of PAP. It is also negative for any neuroendocrine markers [180].

PC3 is classified as one of the 'classical' prostate cancer cell lines and as such is one of the mostly used models for AI prostate cancer. It is classified as a poorly-differentiated cancer cell line and was isolated in 1979 from a 62 year old male lumbar vertebral metastasis. It does not express AR or PSA [180, 185].

PC133 is an AI xenograft that was isolated from bone metastasis in 1981. It doesn't express AR or PSA and was a kind gift from Dr. Guido Jenster of the Erasmus Medical Centre in Rotterdam.

3.2.2.3 Normal prostate epithelial

PNT1a cells are immortalised normal prostatic epithelial cells isolated in 1991 [186]. They have been shown to lose AR expression after 3 weeks in culture and the reduced expression of PAP and PSA is correlated with this loss [187].

3.2.3 Expression Profile of PKA Subunits in Prostate Cancer Cell Lines

Protein and mRNA expression profiles of PKA isoforms are presented for each cell line in sections 3.2.3.1 and 3.2.3.2. The samples have been split into AS and AI, depending on their androgen sensitivity, to correlate with the differential analysis of the PKA isoforms in prostate cancer progression conducted later in this study. For the protein expression analysis RI β was not profiled due to the inability to pick up the protein with the antibodies tested, and previous literature stating that RI β is not present in LNCaP prostate cancer cells. In addition, the expression of all the PKAC isoforms with a molecular weight of 40kDa (C α , C β 1/3/4) were presented together. The protein expression of PKAC β 2 (47kDa) was profiled separately. For mRNA profiles, RI α profile is not presented owing to validation problems with the RI α TaqMan® probe set. PKAC isoforms are split into C α and C β transcripts.

3.2.3.1 Western Blotting

3.2.3.1.1 AS

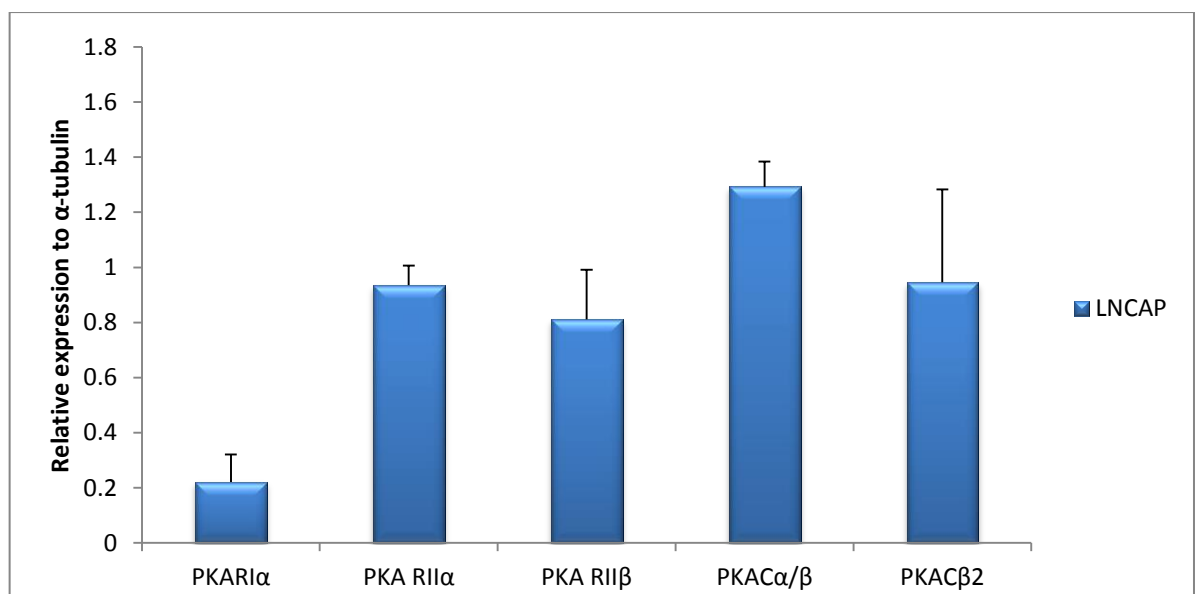


Figure 3.3 PKA isoform protein expression profile of AS LNCaP cell line

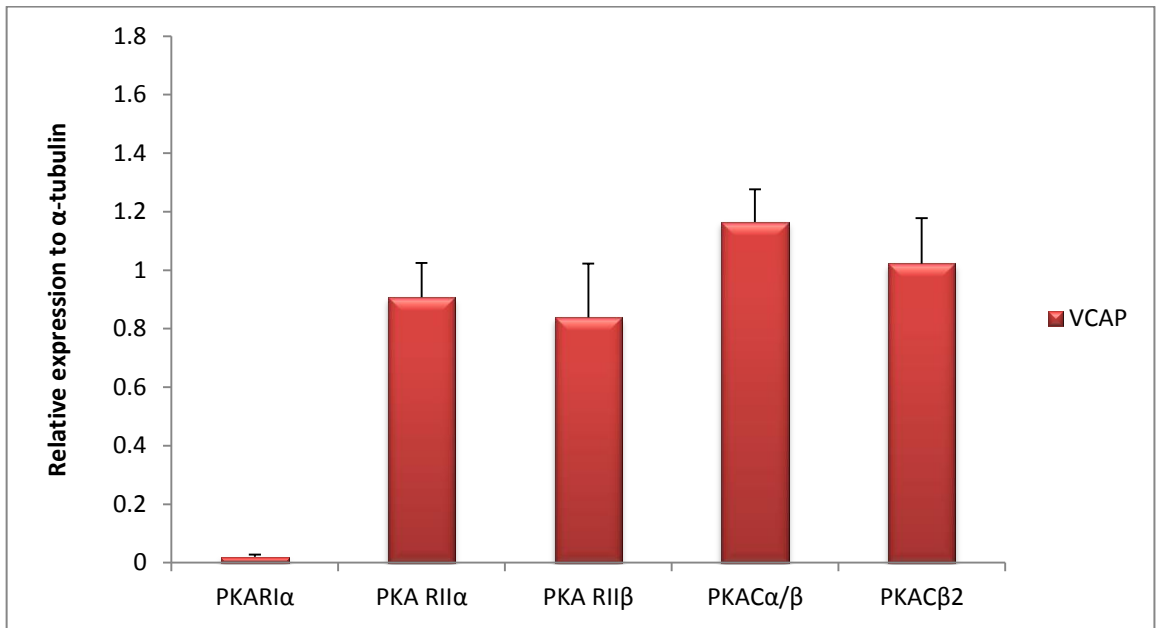


Figure 3.4 PKA isoform protein expression profile of AS VCaP cell line

3.2.3.1.2 AI

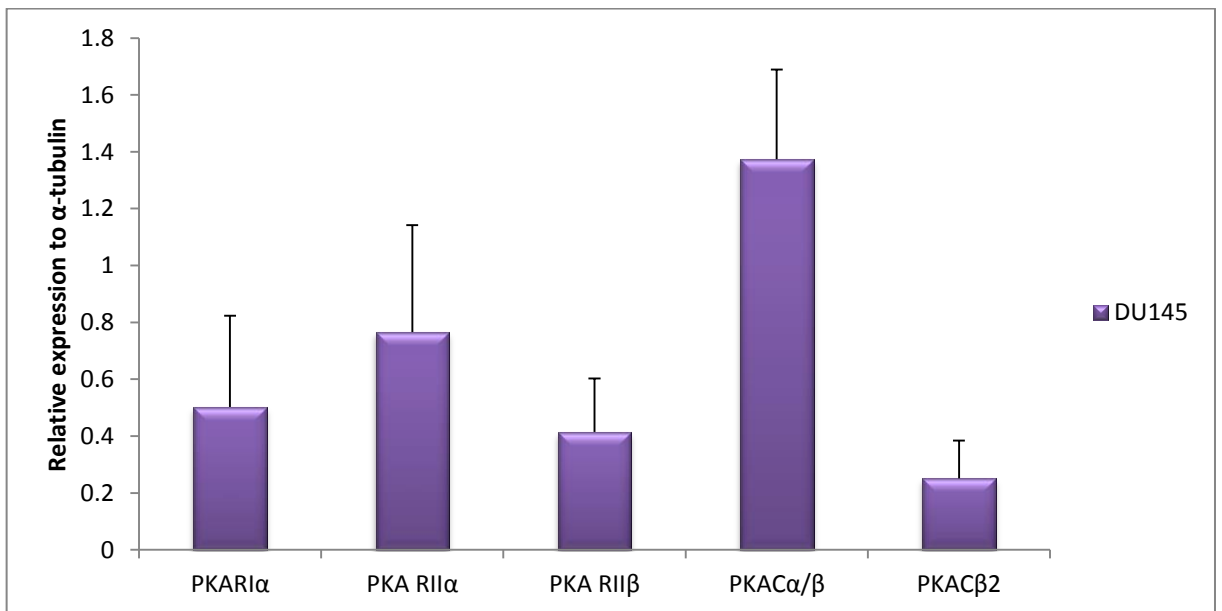


Figure 3.5 PKA isoform protein expression profile of AI DU145 cell line

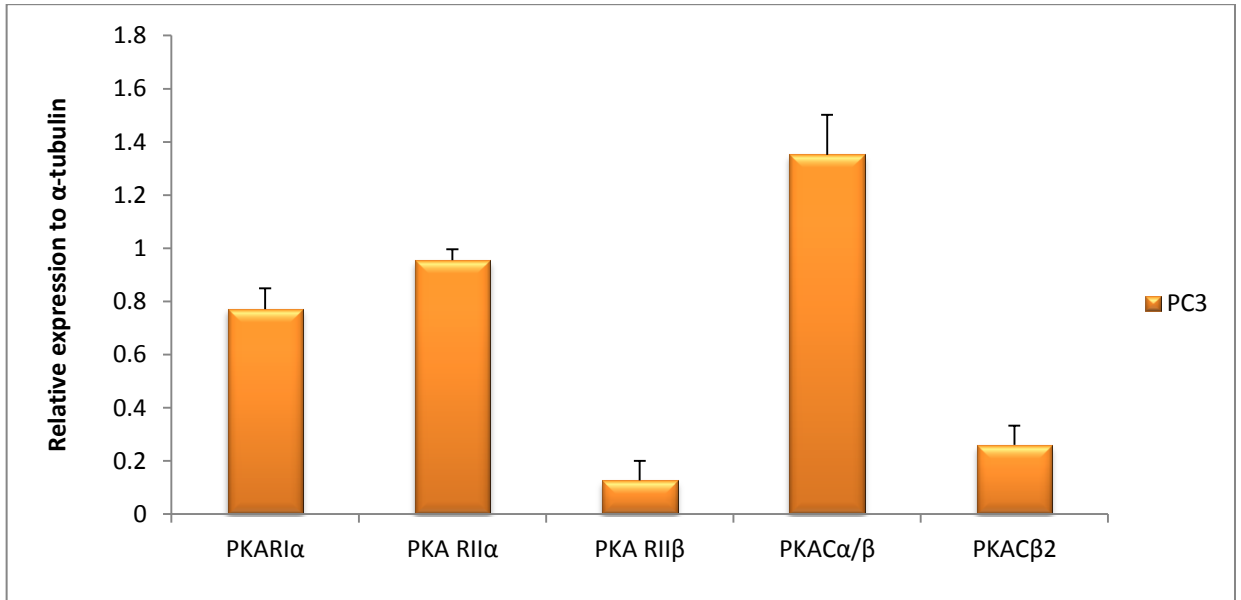


Figure 3.6 PKA isoform protein expression profile of AI PC3 cell line

3.2.3.2 RT-qPCR

3.2.3.2.1 AS

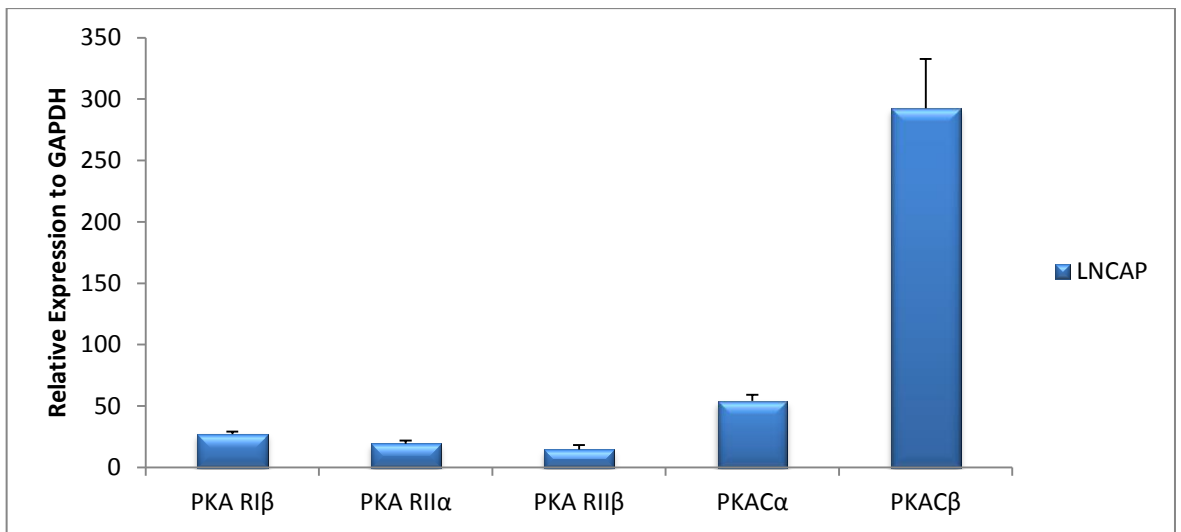


Figure 3.7 PKA isoform mRNA expression profile of AS LNCaP cell line

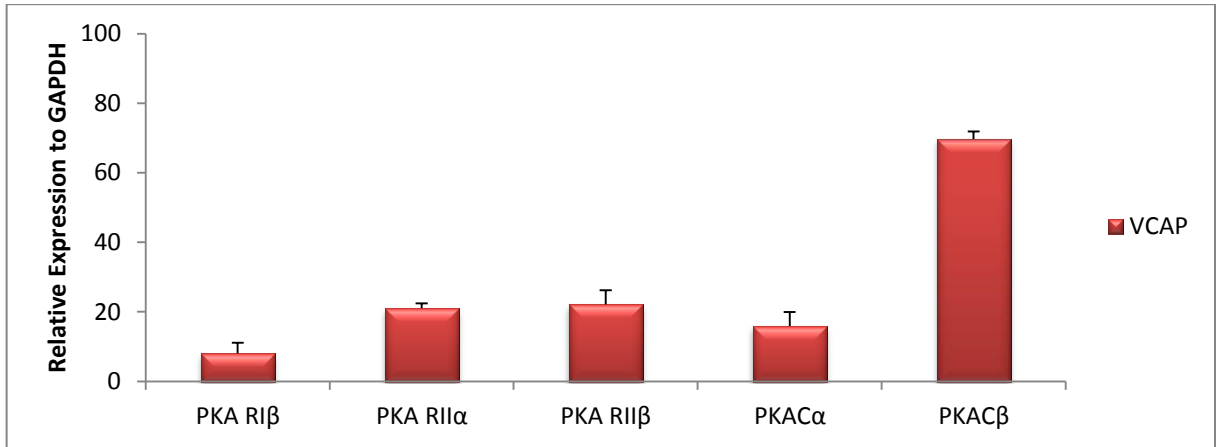


Figure 3.8 PKA isoform mRNA expression profile of AS VCaP cell line

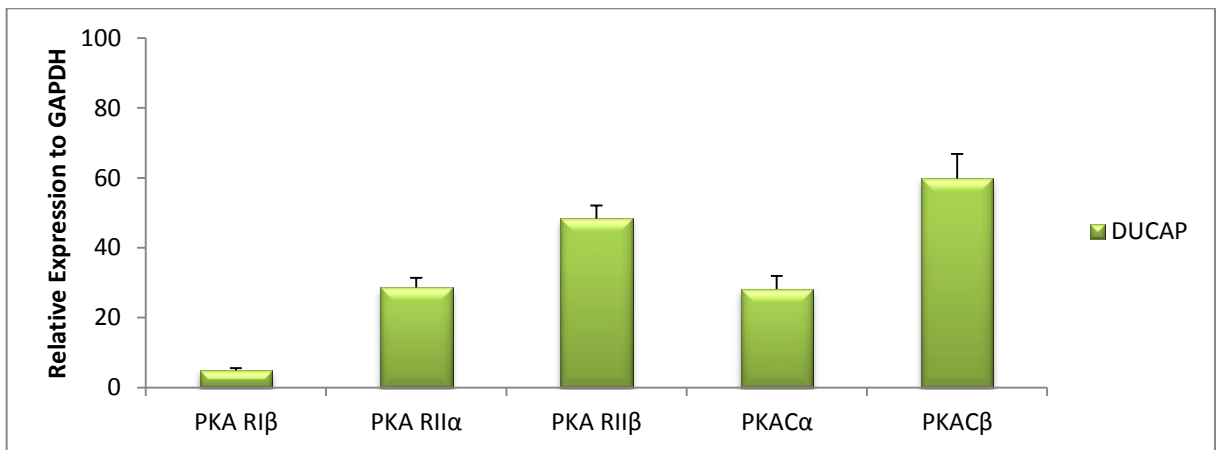


Figure 3.9 PKA isoform mRNA expression profile of AS DUCaP cell line

3.2.3.2.2 AI

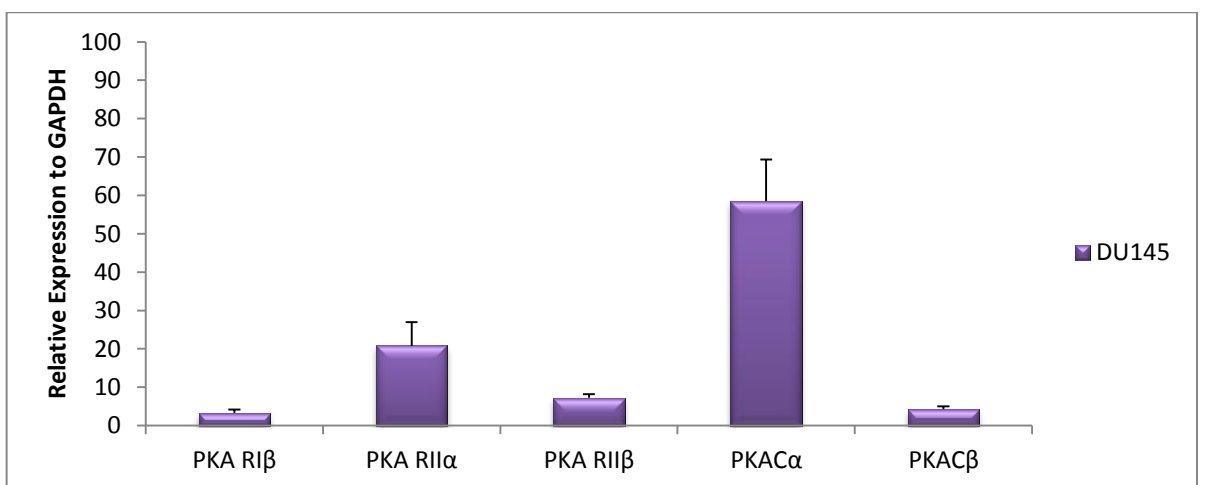


Figure 3.10 PKA isoform mRNA expression profile of AI DU145 cell line

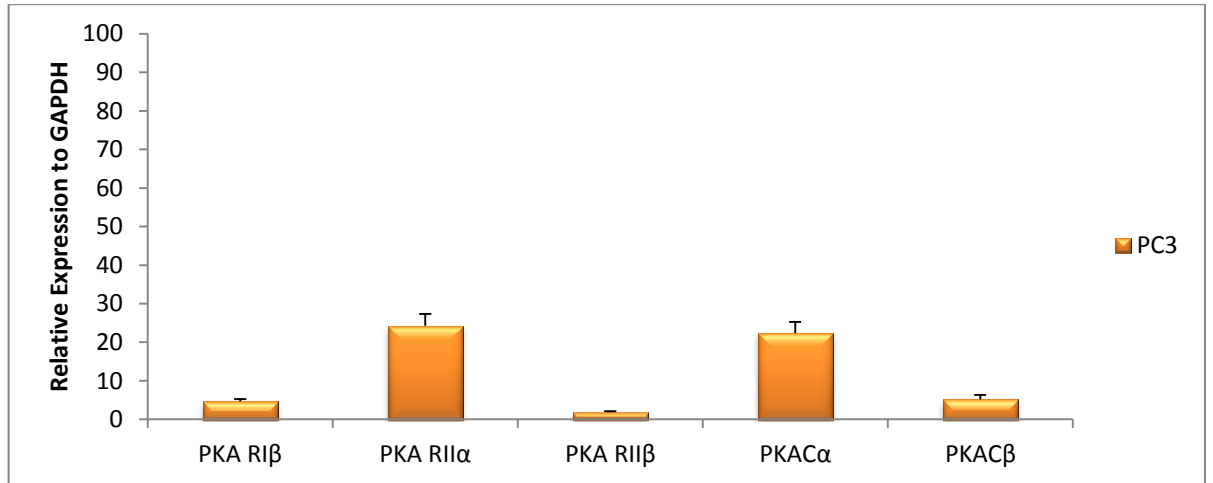


Figure 3.11 PKA isoform mRNA expression profile of AI PC3 cell line

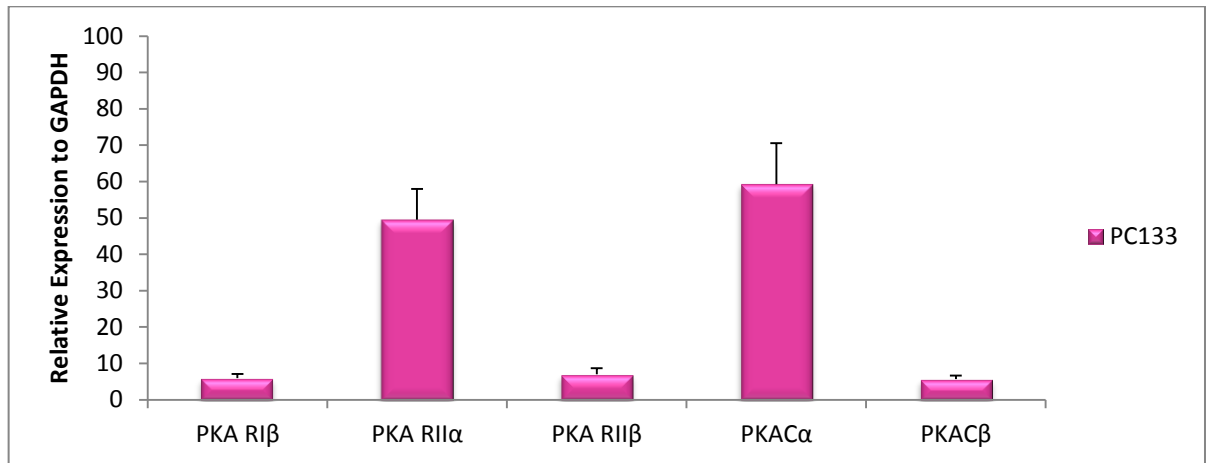


Figure 3.12 PKA isoform mRNA expression profile of AI PC133 xenograph

3.2.4 PKA subunit Expression in Prostate Cancer Samples

By using RT-qPCR and western blot analysis I have investigated the expression of PKA isoforms in prostate cancer cell lines. I found that all PKA isoforms are expressed at mRNA level (with the exception of RI α) including RI β . However, upon western blot analysis, the detection of all isoforms but RI β protein could be detected. This correlates with Kvissel et al who indicated that RI β is not expressed in LNCaP prostate cancer cells [169].

To assess the expression of these PKA isoforms during the transition of prostate cancer the sample set was reorganised into AS and AI groupings (Figure 3.13).

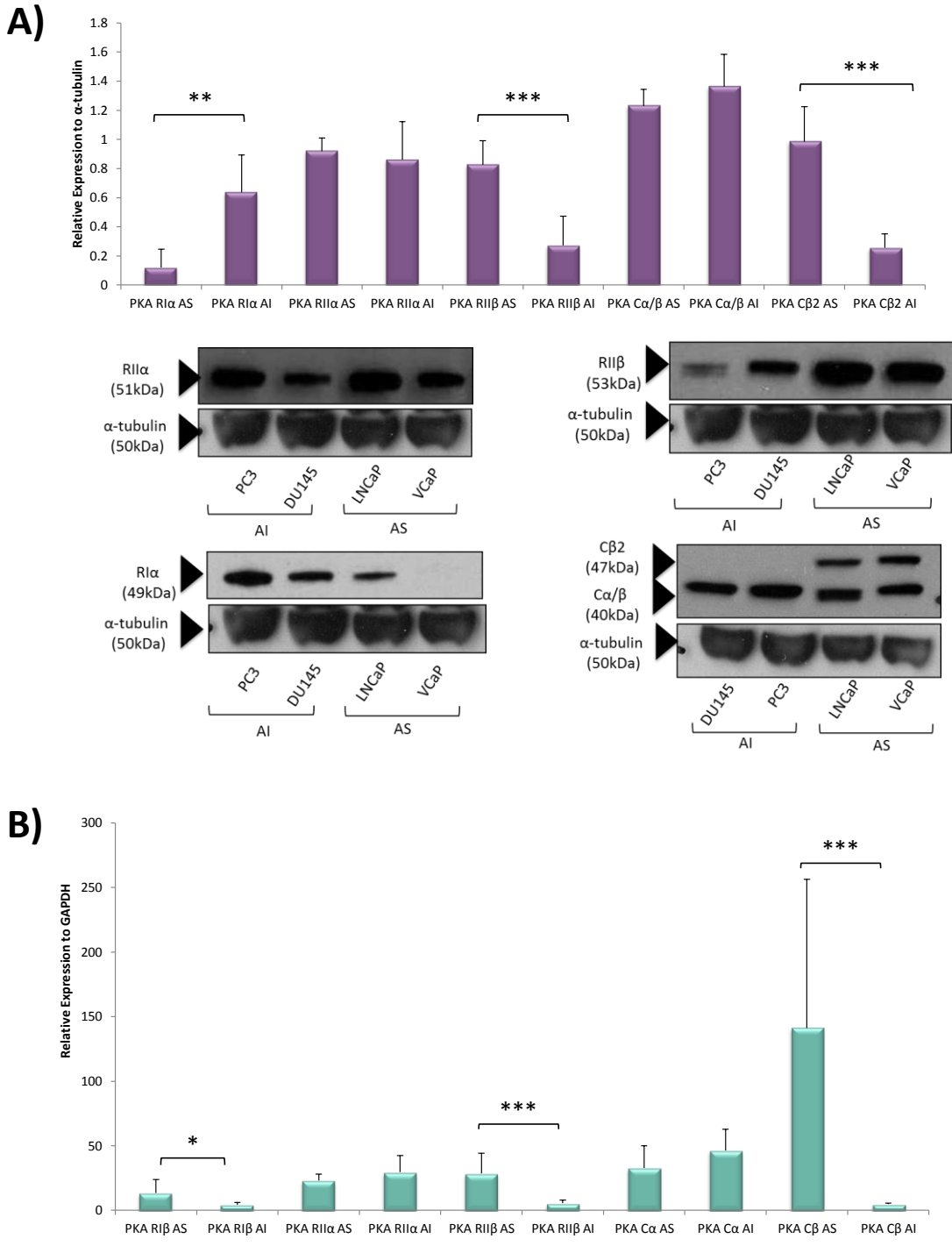


Figure 3.13 PKA expression of AS vs AI cell lines
A) Graph shows western blot analysis of AS vs AI. Blots are representative of PKA expression in prostate cancer cell lines **B)** Graph shows RT-qPCR analysis of AS vs AI

3.2.4.1 Regulatory Subunits

The change in expression of the regulatory (R) subunits of PKA has been described in many cancers and also studied in relation of prostate cancer. As discussed, the change in R unit composition of the holoenzyme can determine the balance between growth and proliferation and therefore can often change in cancer progression. In relation to cancer proliferation, it has been reported that PKA-I is over expressed in growth-stimulated cells, as well as in normal cells in response to physiological stimulation. Conversely, PKA-II is found in normal non-proliferation tissues and in growth arrested cells.

Using student T-test statistics, I showed that PKA RII β is significantly down-regulated in RT-qPCR (P=0.0001) (Figure 3.13B) and western blot analysis (Figure 3.13A)(P=0.0004) in AI cell lines compared to AS. In addition, using western blot analysis I found RI α (P=0.0013) to be significantly up-regulated (Figure 3.13A) and mRNA showed that PKA RI β is significantly decreased (P=0.0066) (Figure 3.13B). This data correlates with other studies into PKA R unit expression within prostate cancer which report an increase in PKA I in prostate tumours. There is also evidence that the PKA I and II isoforms exert different functions in prostate cancer. These studies have reported that PKA RI α is over expressed in prostate cancer and is linked to poor prognosis, and the PKA RII isoform is preferentially found in differentiated tissues. I have shown that RI α and RII β are regulated inversely proportionally with progression from AS to AI prostate cancer suggesting that differently expressed isoforms are employed at different stages of PC progression.

In RT-qPCR studies, I showed that RI β is also significantly decreased in expression from AS to AI. However this finding cannot be correlated to protein levels. Additionally, Kvissel et al also found no protein expression of RI β in LNCaP cell lines, agreeing with my western blot data. RT-qPCR is more sensitive to low level transcription than western blot analysis and thus could show levels of RI β that cannot be isolated via western blotting. However, as post-transcriptional regulation of proteins can cause differences between RNA and protein concentration [175, 176] and as other literature agrees with my observation that RI β is not present at protein level, the function of this change in RI β regulation in prostate cancer may be hard to characterise into a functional output.

3.2.4.2 Catalytic Subunits

The change in catalytic subunit regulation in prostate cancer has also been investigated by Kvissel et al [169]. They investigated the change in PKAC expression in LNCaP incubated in CSS medium to induce differentiation. In addition, they have shown expression in AI cell lines, DU145 and PC3. Here, they found that PKAC β 2 isoform was down-regulated into prostate cancer differentiation and further decreased in the AI cell lines. My data broadly agrees with these findings, as using student T-test statistical analysis showed PKAC β / β 2 are significantly down-regulated in RT-qPCR (P=0.0001) and western blot analysis (0.0001) in AI cell lines compared to AS. In western blot analysis PKAC β 2 (47kDa) shows a statistical decrease in expression while the expression of all other isoforms do not vary, thus in RT-qPCR analysis, where all C β isoforms were examined together, it could be suggested that the change in expression here is also due to PKAC β 2. However, Kvissel et al has suggested a decrease in C β 3/4 isoforms via western blot analysis which were not confirmed by my study.

PKA isoform	Observed change in regulation	RT-qPCR			Western Blot analysis		
		T-Test P-Value	Mann-Whitney P-Value	Significant difference (P<0.05)	T-Test P-Value	Mann-Whitney P-Value	Significant difference (P<0.05)
PKA RI α	Increase	-	-	-	0.0013	0.0087	Yes
PKA RI β	Decrease	0.0066	0.0097	Yes	-	-	-
PKA RII α	None	0.2207	0.3508	No	0.6066	0.7273	No
PKA RII β	Decrease	0.0001	0.0001	Yes	0.0004	0.0022	Yes
PKA C α	None	0.1004	0.1600	No	0.2276	0.3680	No
PKA C β /C β 2	Decrease	0.0001	0.0001	Yes	0.0001	0.0022	Yes

Table 3.1 Showing the regulation status of the PKA isoforms from AS to AI phenotype.

Box-and whisker plots are used in statistics to graphically display differences between the populations, indicating the spread or skewness of the data without making assumptions about the distribution. The data regarding all AS and AI samples, in RT-qPCR and western blot analysis were plotted as box and whisker plots in Figures 3.14/3.15. In brief, the upper box represents the third quartile. The median is represented by the intersection of the upper and lower box and is known as the second quartile. The lower box represents the first quartile. The

upper and lower ‘whiskers’ represents the minimum (lower) or maximum (upper) of all the data.

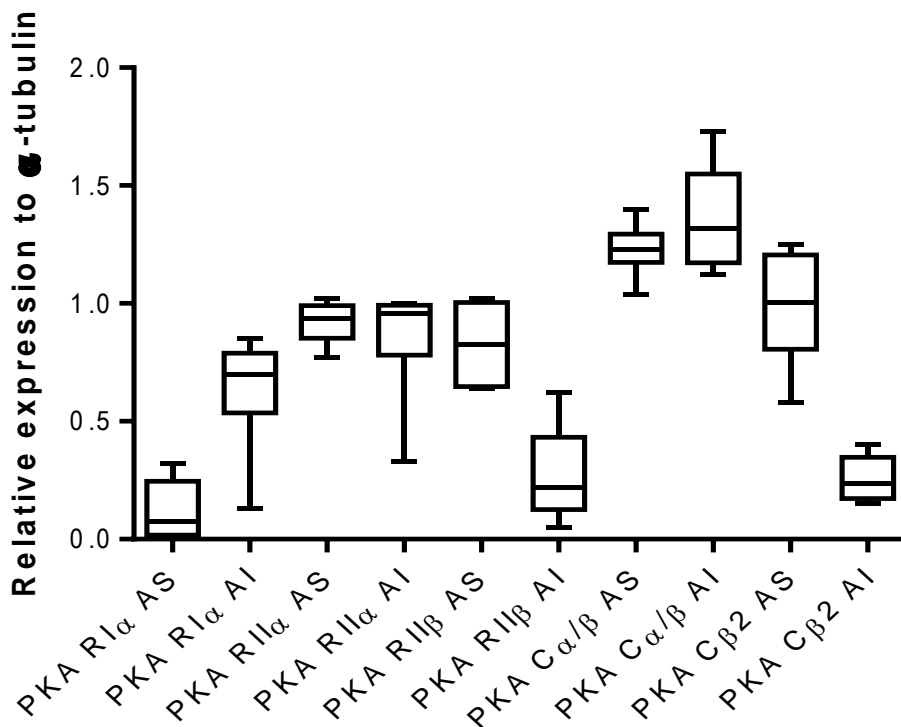


Figure 3.14 Box and whisker plot showing analysis of the PKA isoform protein expression in AS and AI prostate cancer samples

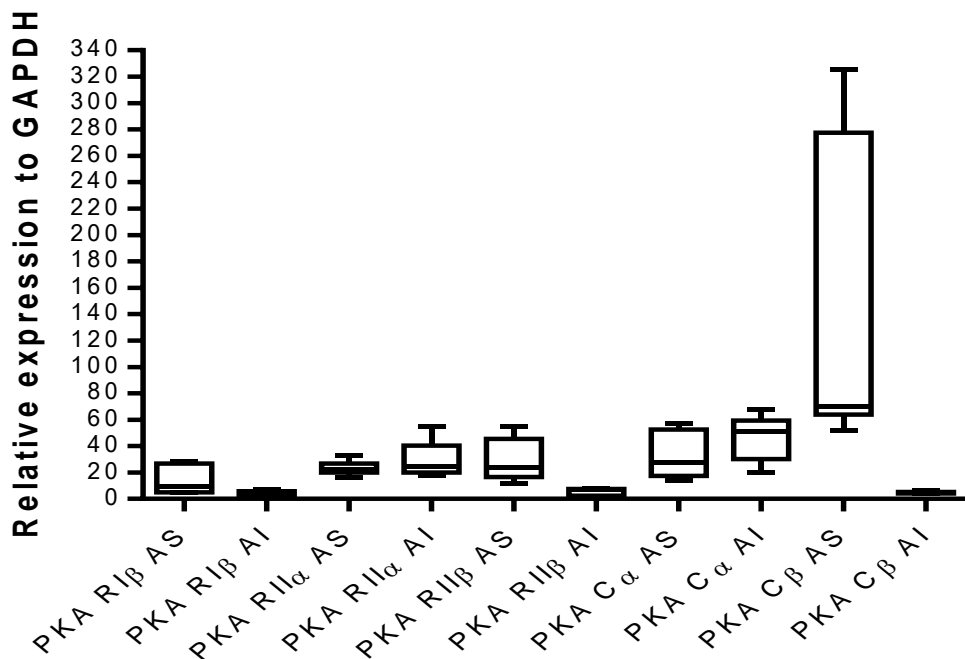


Figure 3.15 Box and whisker plot showing analysis of PKA isoform mRNA expression in AS and AI prostate cancer samples

As some of the data sets do not follow Gaussian distribution, the Mann-Whitney statistical test was used alongside the student t-test to give two tailed p-values (Table 3.1). This shows that the significance of the PKA isoforms differential regulation is not affected by the distribution or spread of the data.

3.2.5 Regulation change of PKA subunits towards androgen independence

I conclude from the data that $R11\beta$ and $R1\alpha$ are expressed in an inversely proportional manner in prostate cancer and $C\beta/C\beta2$ is downregulated in AI cell lines compared to AS. In cancer $R11\beta$ has been linked to neuroendocrine differentiation, and $PKAC\beta2$ has been recently shown to be downregulated in differentiating cells [169].

To explore whether these signalling molecules also change in regulation under an androgen ablated environment and thus are important in the 'switch' from AS to more aggressive AI prostate cancer, LNCaP cells were used as a model system to study prostate cancer progression (Figure 3.16). Androgen ablation is conducted by charcoal stripping of the fetal calf serum (FCS) in the cellular media, which pushes LNCaP cells to trans-differentiate into NE-like cells. Morphological characteristics like neurite extensions and soma compaction appear after 3-5 days in charcoal-stripped FCS (CSS) as well as induced expression of NE-markers like neurotensin and neuron-specific enolase [4]. LNCaP cells were incubated in CSS medium for 2 months or differentiated into AI cells for 4 months. LNCaPs incubated in FCS and CSS+ 10nM DHT were used as controls. Full differentiation of the AI cell line was assessed via RT-qPCR of neurone specific enolase and chromogranin A (carried out by Dr. David Henderson)

Results are expressed in relation to LNCaP grown in FCS medium. $PKAC\beta$ decreases 5 fold in CSS treated cells compared to FCS (Figure 3.16). However, cells incubated in CSS medium containing DHT, display a similar change in mRNA levels compared to CSS only, suggesting the effect may not be due to androgen ablation. However the decrease in $C\beta$ correlates with the data from Kvissel's

study, which showed a 70% decrease in expression of $C\beta 2$ when comparing CCS incubated cells with FSC. In addition, they also showed restoration of this decrease after treatment with R1881 (a synthetic androgen). Interestingly, I have also shown a decrease in mRNA levels in LNCaP AI cells when compared to FCS-WT LNCaP, which correlates with the decrease in expression shown with other AI cell lines. PKARII β has similar mRNA levels in CSS and CSS+DHT treated cells as FCS WT LNCaPs (Figure 3.16). However, this has a high-variability within the data and so no conclusions can be drawn. Furthermore, RII β expression is decreased by 16 fold in AI LNCaP cells compared to FSC WT LNCaPs (Figure 3.16).

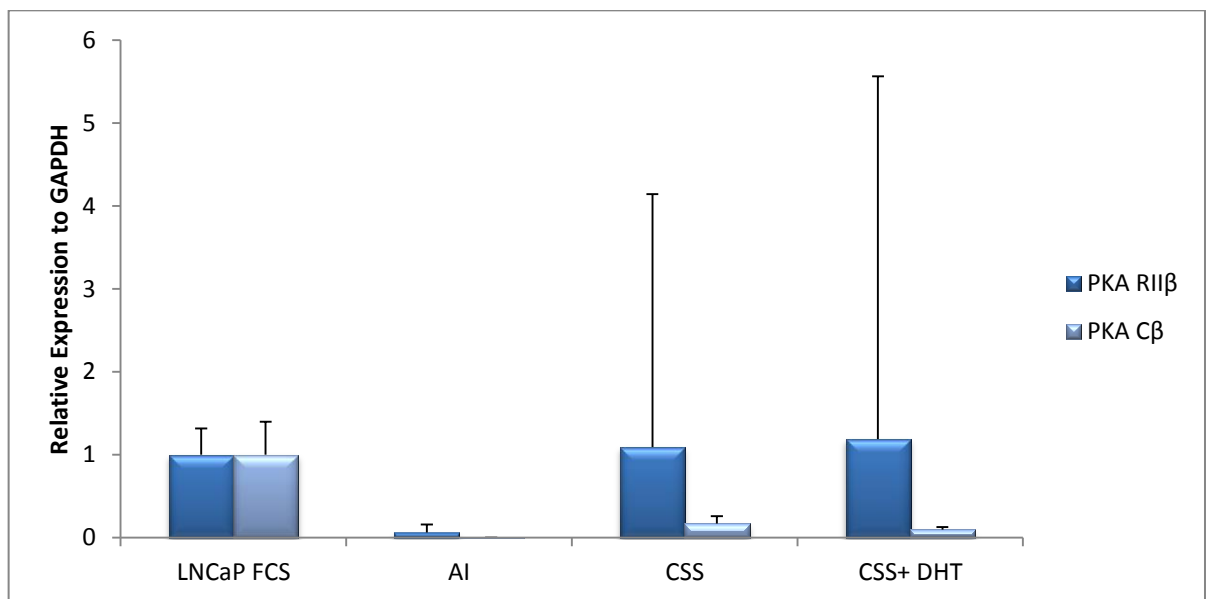


Figure 3.16 Androgen dependent regulation of PKA RII β and C β in CSS incubated LNCaP cells.

LNCaP cells were incubated in a) FCS medium b) CSS medium for approximately 4 months until AI proliferation occurred c) CSS medium for 2 months of differentiation and d) CSS medium + 10nM DHT for 2 months. RNA was isolated and RT-qPCR was carried out as outlined in the 'material and methods' section. Results are relatively expressed to GAPDH.

3.2.6 PKA Subunit Expression in a Normal Prostate Epithelial Cell Line

Thus far, I have shown a decrease in C β and RII β from AS to AI prostate cancer. However, I have not yet addressed the expression of these two isoforms in a normal prostatic cell line. Kvissel showed the expression of C β isoforms within cancer specimens (isolated from localised prostate adenocarcinomas) as compared to normal tissue from radical prostatectomies, showing an up-regulation of PKAC $\beta 2$ in the cancerous tissue. However, this study failed to

elucidate the PKA isoform expression within the differing cell types. In particular, PKA expression within the prostate epithelium is of interest as 95 % of all prostate cancer cases arise from this cell type. In addition, while the cellular ratio of C subunits to R subunits is fairly constant around 1:1, PKA RI and RII subunits show considerable differences in expression between tissues. In order to fill this obvious gap in the experimental protocol, we examined the expression of PKA RII β and C β in a normal epithelial cell line, PNT1a cells, using RT-qPCR. Here (Figure 3.17), RII β expression is significantly down regulated compared to AS cells(P=0.0016), but exhibits similar levels of expression to the AI cell lines used in this study. Furthermore, PKAC β was significantly down regulated compared to both AS and AI cell lines (P=0.0001).

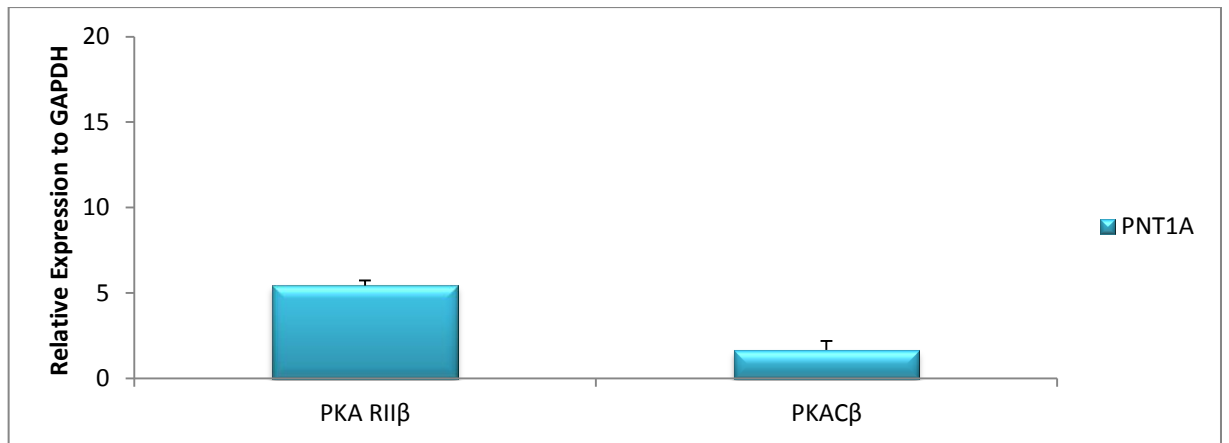


Figure 3.17 PKA isoform mRNA expression profile of PNT1a normal epithelial prostate cell line

3.3 Discussion

One aim of my PhD thesis was to discover putative new biomarkers for advancing prostate cancer. Within this study, I have concentrated on the regulation of the PKA isoforms in prostate cancer and how they change as the cancer develops and progresses. These studies were done on the back of a large amount of evidence that points to cAMP signalling as a key factor in advancing prostate cancer. In several studies, the effects of the differential regulation of the PKA isoforms has been discussed [17, 50, 167, 169, 171, 173, 188-191].

Composition of the PKA holoenzyme has led to two isozyme descriptions of PKA, I and II. As discussed, these R units have high homology in cAMP-binding domains, but vary in structure in the D/D and linker domains. These sequence diversions are yet to be fully understood, however major differences in subcellular localisation and physiological differences have been shown between the R-unit isoforms [19, 192-195]. These changes in physiological function have also been linked to cancer and cancer progression. Expression of the RI and RII isoforms have shown to be high in malignant breast tissues. In addition, the ratio of RI/RII seems to favour RI expression, and this is correlated in many cancers including colorectal and ovarian [160, 161, 163]. RI α expression has been extensively studied in the context of cancer, including prostate cancer. This isoform's constitutive overexpression is associated with increased proliferative cancers and poor prognosis in patients. PKA I expression has also been linked to hormone levels. PKA I activity was shown to decrease by 50% in ventral prostate three days post-castration, whereas PKA II levels did not change, suggesting a potential functional link between the PKA I protein levels and hormone production [50, 196]. Additionally, PKARI α has been studied in the context of prostate cancer progression as a biomarker and also as a potential cancer treatment, e.g. PKA isoform knockdown combined with radiotherapy as a treatment for advanced cancer [171, 191].

Using western blotting and RT-qPCR techniques, I have shown that RII β and RI α are inversely regulated in prostate cancer cells. This correlates with the R unit expression in other cancers [50, 160] and in a study by Kvissel et al [169]. In this study Kvissel and co-workers showed that PKA RII β was upregulated in LNCaP

cells compared to AI cell lines DU145 and PC3. In addition they showed that RII β decreased in regulation in patient samples compared to normal tissue.

In the early stages of prostate cancer, the adenocarcinoma is very slow growing, contrasting with more advanced cancers. RII β (or expression of PKA-II) is found in nonproliferating tissues and growth arrested cells. Moreover, over expression of RII β in AI dominant cells, switches the dominant isoform leading to growth arrest, apoptosis and changes in cancer cell morphology. In my study, I have shown an overexpression of RII β in AS cells compared to AI [50, 167]. AS cancers have also been described as slower growing and less aggressive than their AI counterpart, suggesting that RII β overexpression could be the mechanism behind this phenotype.

However, RII β is shown to be mostly associated with differentiating cells [17, 196]. Differentiation has also been proposed to nucleate the formation of AI growth and provide paracrine proliferative signals which signal the advancement of prostate cancer. NE differentiation is also an important factor in PC progression [197]. Changes linked neuroendocrine differentiation have been associated with the transition into the later, more aggressive stage of prostate cancer [198]. Neuroendocrine cells are found in the lumen of the healthy prostate and secrete a variety of signalling molecules [199]. In cancer, tumours have been shown to form around neuroendocrine cells. Furthermore, secretion of mitogenic peptides from neuroendocrine cells is thought to contribute to cellular proliferation and tumour growth [200]. It is important to note however that epithelial cells that undergo neuroendocrine differentiation in cancer still retain epithelial markers, and so are potentially hybrid of neuroendocrine and epithelial signalling [201].

Increased intracellular cAMP concentrations can lead to neuroendocrine differentiation in some AS prostate cancer models [165]. I have shown that RII β is significantly up-regulated in LNCaP and VCaP AS cells when compared with AI cells. The RII β PKA isoform is associated with differentiating cells, and thus could be the isoform that initiates this change. This correlates with the study by Kvissel which shows overexpression in LNCaPs cells compared to AI. In addition, they demonstrate increased RII β levels during the differentiation process. I have

shown that while RII β levels are the same in LNCaP WT cells as CSS treated cells during the LNCaP differentiation process. However, I also show that when cells are no longer under androgenic control (AI), RII β levels diminish. This suggests that RII β overexpression in AS stage cancers could drive neuroendocrine differentiation through AR dependant mechanisms. I have also shown a decrease in RII β in the normal epithelial prostate cell line. These cells don't, however, express the androgen receptor as it is lost during the immortalisation process. Thus I cannot conclude if this decrease of RII β is due to normally lower expression in the prostate or, as I hypothesise, that RII β is down-regulated due to the loss of AR.

In addition to significant RII β downregulation, PKAC β is also downregulated in AI cells compared to AS. PKA catalytic subunit expression has also been discussed in the context of cancer, but not as extensively [50, 169, 170]. PKAC was shown by Cvijic et al [170] to be present as a free extracellular kinase in the growth media of cultured cancer cells, including prostate cancer. This finding was also linked to an increase in PKA activity of plasma samples of prostate cancer patients. This increase in extracellular PKA activity has been shown to be inversely proportional to hormone-dependency in breast cancer cells e.g. hormone independent cancers have an increase in extracellular activity [50].

Conversely, Kvissel et al [169] showed an increase expression of PKAC β 2 isoform overexpression in AS LNCaP cells. This isoform decreases quickly upon cellular incubation in androgen stripped media (shown by Kvissel and myself (Figure 3.16)) and is significantly down regulated in AI cell lines (Figure 3.13/3.16 and [169]). In addition, Kvissel showed an increase in tumour cells compared to normal prostate tissue. This data suggest that regulation of PKAC β could be androgen sensitive and that PKAC β is correlated with androgen activity in androgen sensitive cancer cells, suggesting that this isoform is potentially important in androgen dependant androgen receptor activity in malignant cells.

In the context of considering PKA RII β and C β isoforms as biomarkers, we have to address how advantageous these markers would be in prostate cancer diagnostics. While there is no doubt about the change in expression of these isoforms between AS and AI prostate cancer, at present, intracellular proteins or

mRNA can only be measured in cases where a prostate biopsy has been taken. If I consider this, would there be an advantage of using these isoforms as biomarkers if a biopsy is required, as prostate cancer assessments from biopsy (or ultrasound) are very accurate in determining the stage and prognosis of the cancer. However, if these problems can be overcome, the use of PKA isoforms as biomarkers for advancing prostate cancer may be incredibly useful. In addition, it may also decrease the reliability on tests currently based on PSA, the use of these isoforms as biomarkers may also allow the identity of the androgen sensitivity of the tumour and its selectivity for AI growth.

4 Study of putative PKA phosphorylation sites on the Androgen Receptor

4.1 Introduction

4.1.1 AR and posttranslational modifications

Like all steroid hormone receptors, activation of the androgen receptor is triggered by the binding of a steroid hormone, in this case, testosterone and its derivatives. In recent years, another level of regulation has come to the fore in the form of a number of posttranslational modifications of the AR. As these modifications are discovered and as their roles emerge, they have been shown to contribute to the regulation of AR activity, stability and structure [75, 202]. With such effects on the AR, it is thought that these modifications are important in normal prostate function and also in prostatic diseases such as cancer. To date there are approximately 23 sites of direct posttranslational modification of the AR via acetylation, methylation, SUMOylation, ubiquitination and phosphorylation [75, 203-206].

4.1.2 AR as a phospho-protein

16 of the 23 modification sites have been shown to be phosphorylation sites (see table 1) [75, 81]. Other steroid hormone receptors have also been shown to be extensively phosphorylated, such as the progesterone, oestrogen and glucocorticoid receptors [207-209]. Several basal phosphorylation sites have been identified on the progesterone receptor, with many of these increasing in phosphorylation levels upon ligand binding. Moreover, sites have also been identified that even with ligand binding, have a delay in becoming phosphorylated [205, 210]. In the case of the glucocorticoid receptor, phosphorylation has been shown to have a prominent role in the receptor turnover [211] and with the oestrogen receptor, phosphorylation at Ser167 helps regulate the transcriptional activity of the AF-1 region of the receptor.

Summary of AR phosphorylation sites.

Phosphorylation Site				Regulation		Function			
Amino acid	ID			DHT Required	Kinases	Transcription	Stability	Localisation	Growth
	S16	MS	Ab	MA	Yes				
S81	MS	Ab	MA	Yes	CDK9, CDK1	Yes	-	-	Yes
S94	MS	Ab	MA	No	-	-	-	-	-
S213	-	Ab	MA	Yes	Akt	Yes	-	-	-
S256	MS	Ab	MA	Yes	-	-	-	-	-
Y267	-	-	MA	-	Ack	Yes	-	-	Yes
T282	-	-	MA	No	Aurora-A	Yes	-	-	-
S293	-	-	MA	No	Aurora-A	Yes	-	-	-
S308	MS	Ab	MA	Yes	CDK11	Yes	-	-	-
Y363	-	-	MA	-	Ack	Yes	-	-	Yes
S424	MS	Ab	MA	Yes	-	-	-	-	-
S515	-	-	MA	-	MAPK, CDK7	Yes	Yes	-	-
Y534	MS	Ab	MA	Yes	Src	Yes	Yes	-	Yes
S578	-	Ab	MA	-	PKC	Yes	-	Yes	-
S650	MS	Ab	MA	Yes	p38, JNK	Yes	-	Yes	-
S791	-	-	MA	-	Akt	Yes	-	-	-

Table 4.1 Summary of AR phosphorylation sites
Adapted from [75]

The 16 phosphorylation sites on the AR have been identified by mutational analysis, with some having additional verification via MS or western blot analysis. In several of the mass spectrophormetry (MS) experiments, phosphorylation of the androgen receptor was shown to increase upon ligand binding [202, 205]. However, several different kinase sites have been identified as the reason behind the increase in AR phosphorylation and no clear functional output has yet been uncovered [202, 205, 212]. Whats more, the accuracy of mutagenesis analysis (MA) has been called into question, with the suggestion that mutagenesis can alter the phosphorylation events on sites distinct from the ones mutated [205].

13 of these 16 sites are located in the N-terminal of the protein, which contains the ligand independent activation domain (AF-1) [213]. This domain is

responsible for target gene transactivation independent of a ligand [70, 202] and this phenomenon has been suggested to be important in unpinning the understanding of androgen independent cancers. However 5 of the 13 sites in the N-terminal have been shown to need ligand binding for induction of phosphorylation [75]. The remaining 3 known phosphorylation sites are located within the other major domains of the receptor. pS578 is located within the DBD, pS650 within the hinge region of the receptor and pS791 within the LBD [75, 81, 214].

4.1.3 The effect of FSK treatment on AR

Several reports have shown that adenylate cyclase activators (like FSK) can activate PKA and serve to increase the phosphorylation of the AR causing its activation. It is known that this activation can occur with or without ligand binding, depending on PKA signalling effects. For instance Gioeli et al [205] reported that treatment of LNCaP cells with FSK, increased the overall phosphorylation of the AR, and Sadar et al [76] showed that treatment with FSK increased PSA mRNA levels, suggesting AR activation. It is also reported that treatment with AR antagonists can block this PKA-dependant activation and downstream PSA increase, suggesting that although activation is driven by PKA, AR is required for transcription [76, 215]. In addition, Janne [216], using ARE and reporter constructs, showed that PKA activating treatments can not only simulate the AR, but also sensitise it to low level androgens. It is also worth noting that modifications such as phosphorylation could affect AR activity by increasing/decreasing protein interactions close to the phosphosite [75].

It is widely thought that aberrant phosphorylation of the AR could promote deleterious mechanisms that underpin certain cases of prostate cancer. Additionally, a considerable amount of evidence now indicates that kinase cascades can affect AR signalling within PC. Many different kinase cascades have been shown to have different effects upon AR signalling at different stages of the pathway. This suggests that these kinase signals are important in regulating AR signalling, and thus changes in these kinase cascades could drive PC progression through their effect on the AR [75, 80, 205].

As shown in the previous chapter, I have found a downregulation of PKA RII β and PKAC β from AS to AI prostate cancer cells. These findings also correlated with several studies that have reported an increase in RII β in less proliferative cancers, and a study by Kvissel et al [169], who found the same expression pattern of PKAC β in cell lines and clinical samples. In addition I have discussed the possibility that PKA RII β and PKAC β could interact with the androgen receptor pathway. In correlation with this hypothesis, as outlined above, there are many reports about the effects of PKA on AR signalling and potential prostate cancer progression, and the direct effect on the AR of other kinase signalling cascades. However, very little is known about the phosphorylation events that mediate AR signalling. Here, I explore whether PKAC β and PKARII β can interact directly with the AR and the potential effect on PC signalling.

4.2 Results

4.2.1 Investigations into the phosphorylation of AR by PKA.

I have hypothesized that PKARIIB and PKACB down-regulation could be used as biomarkers for advancing prostate cancer due to observed expression changes during cancer progression. As discussed, AR is extensively post-translational modified but mainly the full function of these modifications remains mostly unknown. Here I endeavour to tackle these issues by investigating the effects of PKACB and RIIB overexpression on prostate cancer progression.

The AR has a pivotal role in prostate cancer, and many studies have shown that nearly all prostate cancers express AR in the early stages of the disease. In addition, studies have shown a relationship between AR and disease progression to AI cancer [217]. The increase in PSA levels in AI prostate cancer also suggests a restoration of inappropriate AR signalling during this progression [76]. This evolution from a localised hormone-sensitive state to the AI phenotype requires the interplay of a complex network of signalling molecules. Intracellular kinase signalling cascades can initiate cellular processes such as proliferation. The dysregulation of cellular growth that is often observed in cancer can therefore result from the disrupted signalling cascades with alterations in certain kinases.

PKA activation, as discussed earlier, has been shown to modulate AR activity in the absence of androgens, increase mRNA of PSA and increasing the overall phosphorylation levels of the AR [76, 205, 215]. However, no study has effectively isolated the potential sites of PKA phosphorylation on the AR and established their effects on AR transcription and PC progression.

Many of the site directed studies of AR phosphorylation by PKA have been carried out via MS, however this technique is based on peptide fragments. I wanted to examine the ability of PKA to phosphorylate the AR full length protein, with native folding. Therefore I carried out an *in vitro* protein kinase assay, with pure full length AR protein, which was incubated with purified PKACB kinase in a kinase assay mixture containing radio-labelled phosphate. Gratifyingly, I was able to validate the phosphorylation of the full length AR protein by the PKACB isoform (Figure 4.1) as a band was only visible at the AR

molecular weight when active kinase was included. A band was also seen in the positive control lane where another verified PKA substrate, PDE4A4 had been incubated in a similar fashion to the purified AR.

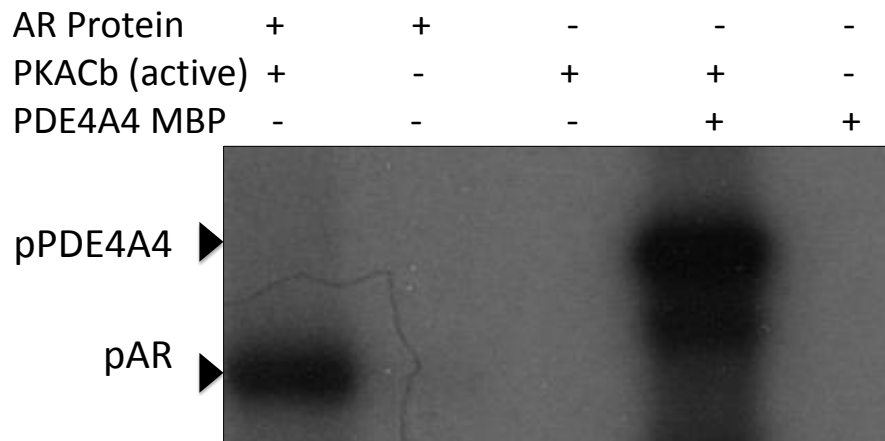


Figure 4.1 PKAC β phosphorylation of AR

Purified androgen receptor protein was phosphorylated with PKAC β enzyme (both Abcam®) using [γ - 32 P] ATP for 30 minutes at 30°C. Lane 1: AR protein plus PKAC β enzyme Lane 2: AR protein Lane 3: PKAC β enzyme Lane 4: PDE4A4 with MBP tag plus PKAC β enzyme Lane 5: PDE4A4 with MBP tag. Data is a representation of 2 independent experiments

The sequence of the consensus PKA phosphorylation site is RxxS*, where x is any amino acid, and S* the target for PKA-mediated phosphorylation. The AR has 4 potential phosphorylation sites in its sequence, 2 located at the N-terminal and 2 located in the LBD. We have identified that AR can be directly phosphorylated by PKAC β (Figure 4.1). However, this does not tell us which site or sites are being modified. As the domains of the AR have different function in AR signalling, different sites of phosphorylation may lead to differences in downstream function. To isolate the phosphorylation site responsible for the PKAC β phosphorylation of AR, novel peptide array technology was employed. This technique uses peptide libraries of known sequences that are covalently linked to macro-molecular cellulose fibres.

The sequence of the AR was, broken down into a series of overlapping 25mer peptides each shifted by 5 amino acids that covered the entire AR. These

peptide segments are synthesised and presented as distinct spots on the cellulose membrane. The membranes can be probed with potential binding partner proteins, or proteins that will covalently modify certain sequences (e.g. kinases). The array was overlaid with an active PKACB enzyme in a kinase assay mix and subsequently probed for modification with a phospho-serine primary antibody and visualised with a secondary HRP conjugate. Distinct regions of phosphorylation were seen in experiments that were overlaid with active kinase (Figure 4.2), whereas no positive spots were detected in the dead kinase control.

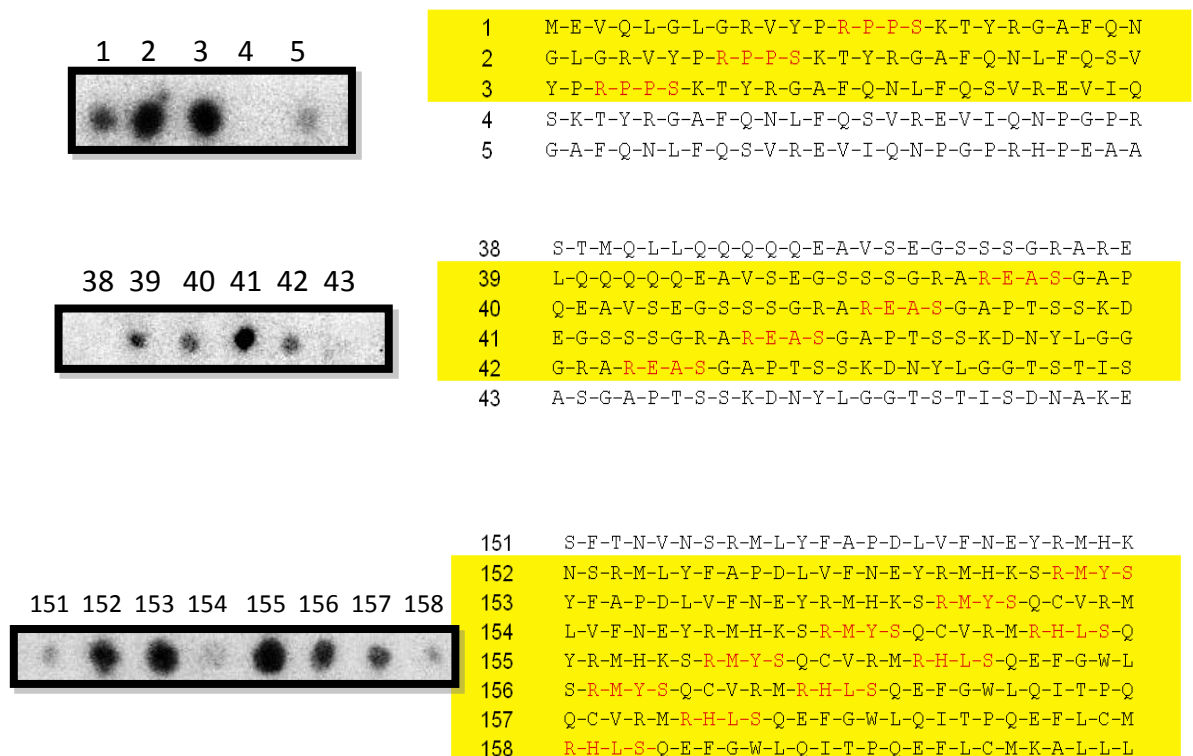


Figure 4.2 Peptide array, overlaid with active PKA catalytic unit
An androgen receptor peptide array was blocked with 5% BSA prior to over lying with activate PKA catalytic subunit, ATP and phosphorylation buffer. This was then subjected to immuno-probing with PKA phospho-serine antibody, anti-rabbit secondary antibody conjugated with HRP and subsequent development using ECL. Data is a representation of 2 independent experiments.

The array exhibited 4 sites of phosphorylation by PKA. Site one, (S16) contained a series of proline's that surround the phosphorylation site, a feature that made it a less than ideal PKA site, and so it was believed that this site would likely not be phosphorylated *in vivo* via PKA. In addition, this site had been shown previously not to be phosphorylated in MS studies that utilised samples isolated

from LNCap cells treated with FSK [205]. Hence, this site was discounted for further analysis. Site 2 (S213) was also discounted. It would have been interesting to study this site due to its location in the NTD, which is shown to modulate transcriptional activity [70] of the AR and has been shown to target gene activation independent of ligand binding and thus may show a link between PKA and androgen free AR activation [70, 202]. However, currently, this domain has no crystal structure and so *in vivo* site surface availability could not be verified.

Peptide array screening can provide a highly efficient way for identifying binding sites and sites of post-translational modification and these results can serve as a base for modelling predictions at the full protein level. This method is successful in the investigation of protein-protein interactions as binding partners often undergo induced fit events upon ligand detection and as a consequence, interactions between purified proteins and immobilised peptides can be similar to the natural situation [218]. That said one must be mindful that the arrays are made up of peptide fragments and thus, cannot form a truly native structure or interactions indicative of a full length protein. In addition, amino acids could potentially become available for interaction, which are not normally available in a fully folded, full length protein. Due to this I utilised modelling VMD software to check the availability of the phosphosites on the surface of isolated crystal structures.

Sites 3 and 4 (S782, S791: Fig 2 lowest panel) look like promising sites for PKA phosphorylation and both are located in the ligand binding domain. The LBD contains the AF2 sequence that has been shown to mediate transactivation [75, 219]. These sites were checked for surface availability using VMD modelling software alluded to above.

AR residue, S650, was also considered as a putative PKA phosphorylation site. Although this site wasn't detected on the peptide array assay, there is strong evidence that phosphorylation of this site is significantly increased following forskolin treatment [205]. S650 is located within the hinge region- linking the DBD and LBD. This region has been shown to regulate AR nuclear localization, DNA binding and co-activator recruitment, and is increasingly thought to potentially be of great importance in prostate signalling [75, 83]. Although this

isn't a PKA consensus sequence, we have included this site to examine the effects of FSK treatment and as a potential positive control within the study.

As sites 3 and 4 (S782, S791) represent novel PKA sites on the AR, I wanted to determine if these were physiologically relevant. To this end, I commissioned the production of phospho-site specific antibodies to these sites.

4.2.2 Peptide array analysis of novel phospho-antibodies

6 phospho- site specific antibodies were raised in rabbits against sequences corresponding to the phosphorylated forms of the 3 unique phosphorylation sites of AR mentioned above (S782, S791, S650). Peptide array technology was used again to examine the specificity and avidity of the novel phospho-antibodies. Arrays were synthesised where the peptide sets comprised of the 20 amino acid antigen for each antibody, with or without phosphorylation of the serine site. In addition alanine 'mutations' of the phosphorylation consensus sequence was included as a negative control. Mutating amino acids to alanine will prevent the antibody binding and thus controlling for false positives. Each of the novel phospho-antibodies were incubated with the arrays and detection of positive interactions was conducted via HRP conjugated secondary antibodies and ECL reagent.

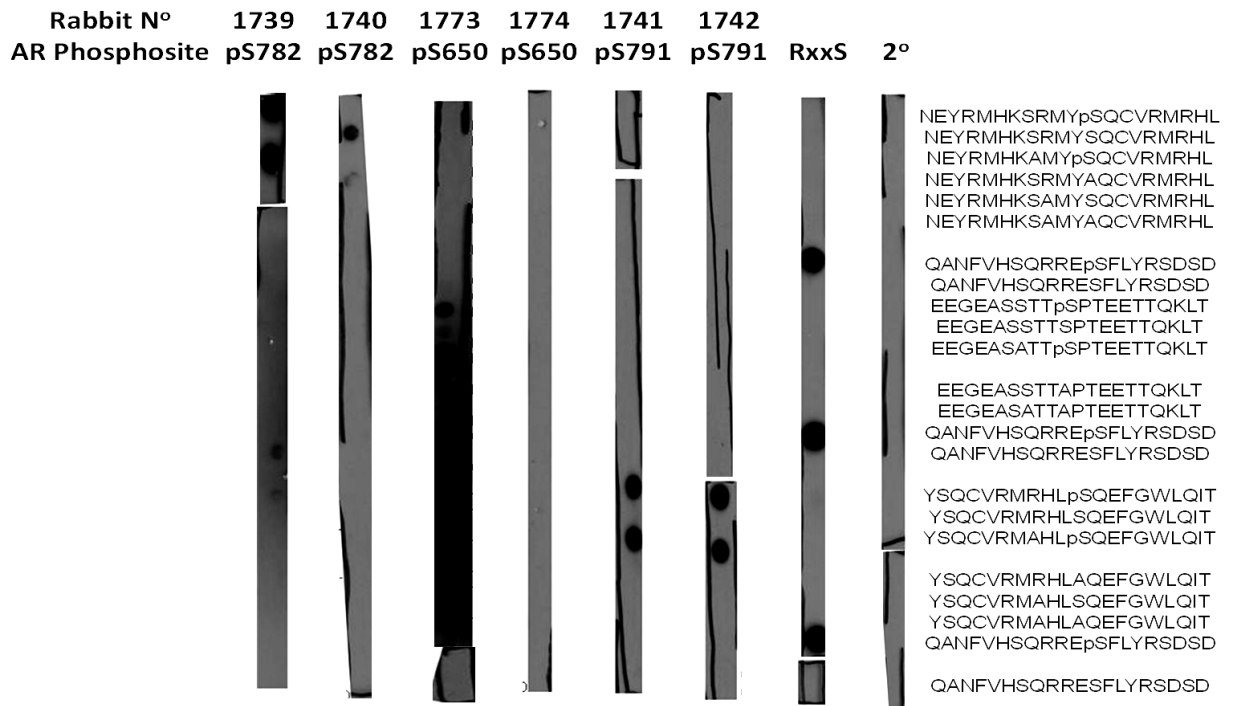


Figure 4.3 Peptide arrays overlaid with novel antibodies. Peptide arrays displaying spotted phosphorylated and non-phosphorylated peptides of novel antibody antigens, plus peptides with alanine substitutions in the PKA consensus sequence.

Antibodies raised in 2 of the 6 rabbits, (numbers 1741, 1742) displayed specific recognition of the indicated phosphosites, discriminating between the phosphorylated and non-phosphorylated consensus sequence. Both these antibodies were raised against a sequence of the AR containing consensus site RHLS* (Site 4, S791).

After, peptide array technology was implemented to examine the specificity of the novel phospho-antibodies identified in figure 4.3, to the phosphorylation of the PKA phosphorylation site. Here, I used peptide arrays that contained ‘truncations’ of the antibody consensus sequence. The 20 amino acid antigen was truncated by one amino acid (from either the left, right or both) at a time and a non-phosphorylated consensus sequence was used as a negative control.

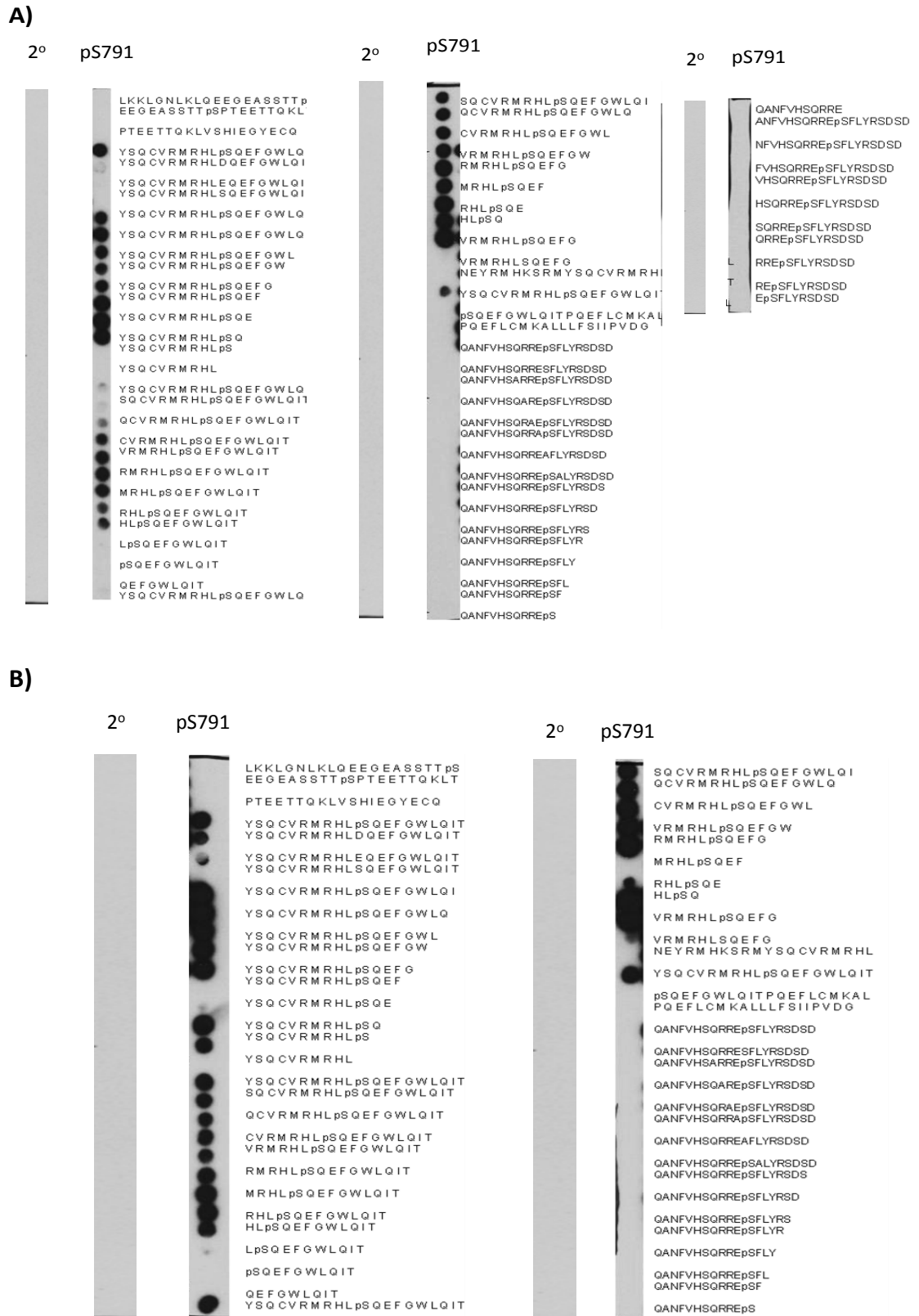


Figure 4.4 Truncated peptide arrays overlaid with novel pS791 antibodies. Peptide arrays displaying 20 amino acid phospho-antibody antigen that was truncated by one amino acid (from either the left, right or both) at a time, overlaid with novel phosphor-antibodies for pS791.

Antibodies (both numbers 1741, 1742) exhibited binding to peptide spots that contained the PKA consensus site and upon ablation of this site binding was lost.

RHLS* (S791) is located within the ligand binding domain of the receptor. One other antibody raised in rabbit number 1739, exhibited strong phosphosite specific binding with very weak non-specific binding in some experiments. The consensus sequence for this antibody is RMYS* (Site 3, S782), and is also located in the ligand binding domain.

The AR ligand binding domain facilitates binding of AR ligands and is recognised as the primary control mechanism for androgen signalling. This domain also contains the AF-2 region, which forms after androgen binding and is crucial in co-factor binding. I hypothesize phosphorylation in this domain could therefore have a potential effects on AR transcription. To further validate these phosphorylation sites and to better understand their function, I investigated the putative phosphosite within a cellular model.

4.2.3 Detection of putative phosphorylation sites using novel phospho-antibodies in cells

Many studies have endeavoured to categorise cAMP-specific effects in prostate cancer. As previously discussed, many studies have used forskolin (FSK) and IBMX treatments to elevate cAMP levels. In keeping with other studies, I too used forskolin/IBMX treatments to elevate cAMP and activate its effector molecule PKA.

Forskolin is a diterpene that is produced by *coleus forskohlii* and is often used to increase cAMP levels. Forskolin activates adenylyl cyclase inducing an increase in intracellular levels of cAMP. This leads to downstream activation of cAMP effector molecules such as PKA and Epac. IBMX is a non-selective PDE inhibitor, which as a consequence leads to an increase in cAMP intracellular levels. IBMX inhibits all PDE isoforms with the exception of PDE8 and 9. In a study using fluorescently labelled PKA subunits and PC12 cells, it was shown that dissociation of PKA subunits occurs within 2 minutes after cAMP stimulation, and nuclear translocation of the catalytic unit begins in 3-5 minutes [1].

4.2.3.1 Androgen Receptor transfected HEK293 model

Peptide array has identified novel putative phosphorylation sites for PKACB on the AR. In order to ascertain if PKACB phosphorylation of the AR can be observed in cells, I utilised the human kidney cell line HEK293. HEK293 or Human Embryonic Kidney Cells were first isolated in 1977 and are commonly used in tissue culture due to a high rate of proliferation and ease of transfection [220]. Due to the anatomical origins of this cell line, they are not classed as a paradigm for prostate cancer, however as they do not endogenous express AR [221] non-transfected cells can act as a good control for antibody testing. In addition, they have been used in many studies as a 'model' system for testing molecules involved in prostate cancer within the literature [221-223].

HEK293 cells, while not expressing endogenous androgen receptor, have been shown to express other hormone receptors such as the glucocorticoid receptor [224]. As the LBD domain, where these phosphosites are located, retains some homology between the hormone receptor family, I conducted a BLAST search of the antibody epitope. Notably however, no protein sequences showed significant homology to residues within the 20 amino acid epitope of the phospho specific antibodies (BLAST searched in the NCBI database against the unique region of each phospho-specific antibody of the AR).

HEK293 cells were transfected with the AR and cAMP levels were elevated by treatment with FSK/IBMX for 10 minutes. The resulting western blots were immuno-blotted with the phospho-specific antibodies for sites pS791 and pS782.

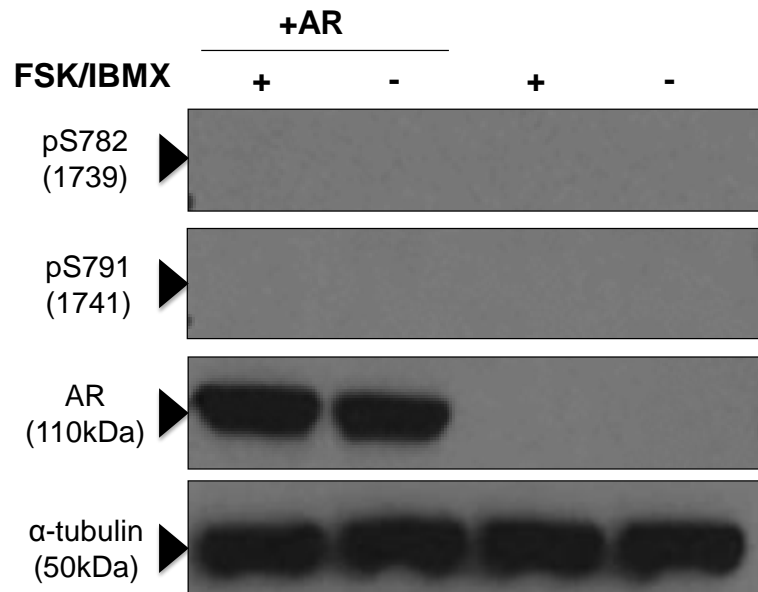


Figure 4.5 Testing of novel phospho antibodies in HEK 293 cells

Testing was carried under normal western blot conditions. HEK 293 cells were transfected with AR (lanes 1+2) or transfection agent only (lanes 3+4) 24-48hrs prior to treatment. Cells were then treated with 100 μ M Forskolin and 100 μ M IBMX (lanes 1+3) or DMSO (lanes 2+4) for 10 minutes and harvested with 3T3 buffer. Western Blots were blocked in 5% milk solution and immuno-blotted with the indicated novel phospho-antibodies.

Unfortunately, no specific phospho-bands were detected by the phospho-antibodies despite good transfection of the AR. In addition, treatment with FSK/IBMX was unable to induce detection of any phospho-bands with the phospho-antibodies used.

To further investigate the phosphorylation of AR in a cellular model, I used immuno-precipitation studies, in which the transfected AR is isolated at high concentrations on IgG beads and the subsequent western blot was probed with pS791 phospho-antibodies.

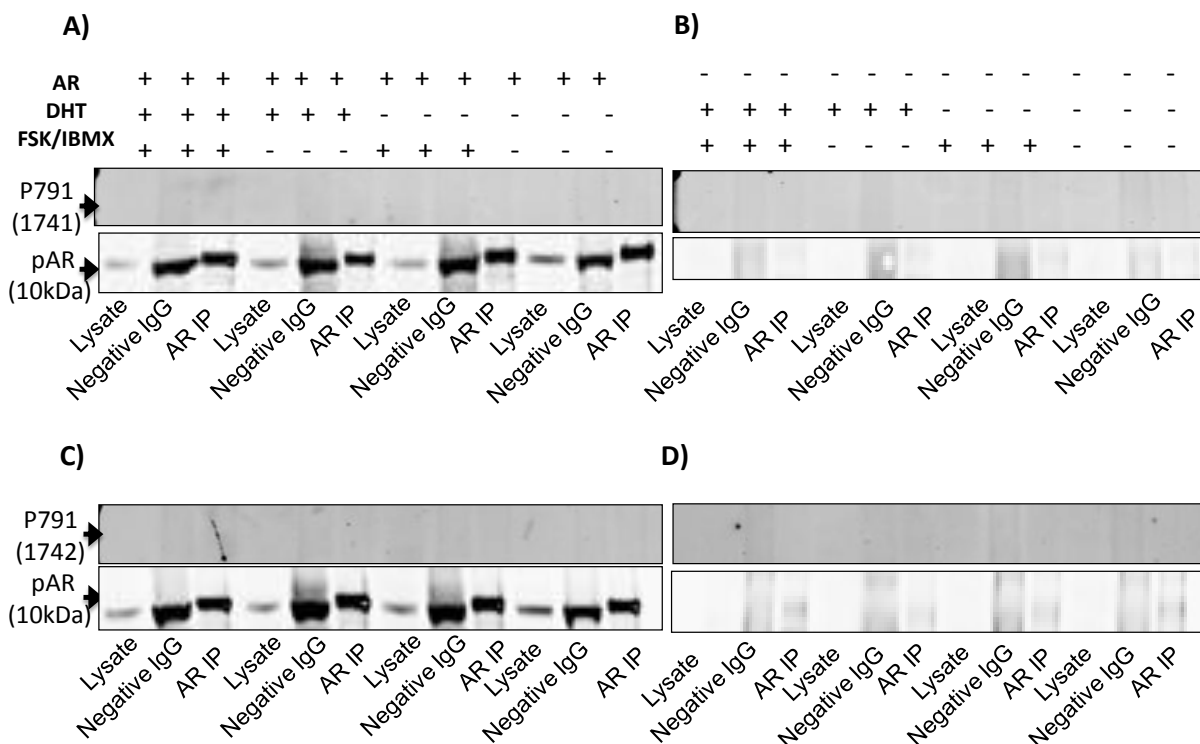


Figure 4.6 Testing of novel phospho antibodies in using AR IP

HEK 293 cells were transfected with AR (blot A and C) or transfection agent only (blot B and D) 24-48hrs prior to treatment. Cells were then treated with 100 μ M Forskolin and 100 μ M IBMX (all blots lanes 1-3 and 7-9) or DMSO (all blots lanes 4-6 and 10-12) for 10 minutes and harvested with 3T3 buffer. 1 μ g of protein was used to conduct AR IP, under normal conditions. Subsequent western blots were blocked in 5% milk solution and immuno-blotted with the indicated novel phospho-antibodies. Data is a representation of 2 independent experiments

Figure 4.6 shows successful immunoprecipitation of the androgen receptor.

Unfortunately the antibodies raised against the novel phosphorylation site S791 was unable to detect phosphorylated androgen receptor under these conditions.

Prostate cancer is a complex array of interacting signalling molecules and as previously discussed, the AR receptor is an integral part of many of these signalling pathways. Therefore it could be assumed that other signalling molecules within the cancer's complex of interacting pathways could be paramount to evoking the phosphorylation of novel phosphosites. If this is true, HEK293 cell, not being derived from prostate, may not contain the required signalling molecules to evoke the PKA phosphorylation. I therefore endeavoured to test these novel antibodies in transfected prostate cancer cell lines.

4.2.3.2 Prostate cancer cell lines

The LNCaP cell line has long been used to investigate different post-translational modifications of the AR including phosphorylation [76, 205, 214, 225]. In addition, LNCaP cells have been used as a model for AS prostate cancer since its description in 1977 [183]. I have previously shown that PKAC β and PKAR1 β are increased in AS prostate cancer cell lines and thus this model of prostate cancer could induce the novel phosphorylation shown in the peptide arrays. The PC-3 cell line has been used as a model for AI prostate cancer since its isolation in 1979 and it does not express the AR [185]. Both these cell lines were used as a transfected model of AR expression.

As the novel antibodies produced poor and unexplainable results in the HEK293 transfected 'model' system, it could be argued that these transfected cells may not possess the required interacting signalling pathways to allow the AR to be phosphorylated at these novel sites. Therefore, testing of the antibodies was also carried in LNCaP cell lines (Figure 4.8) and transfected PC3 (AR independent cell line) model (Figure 4.7).

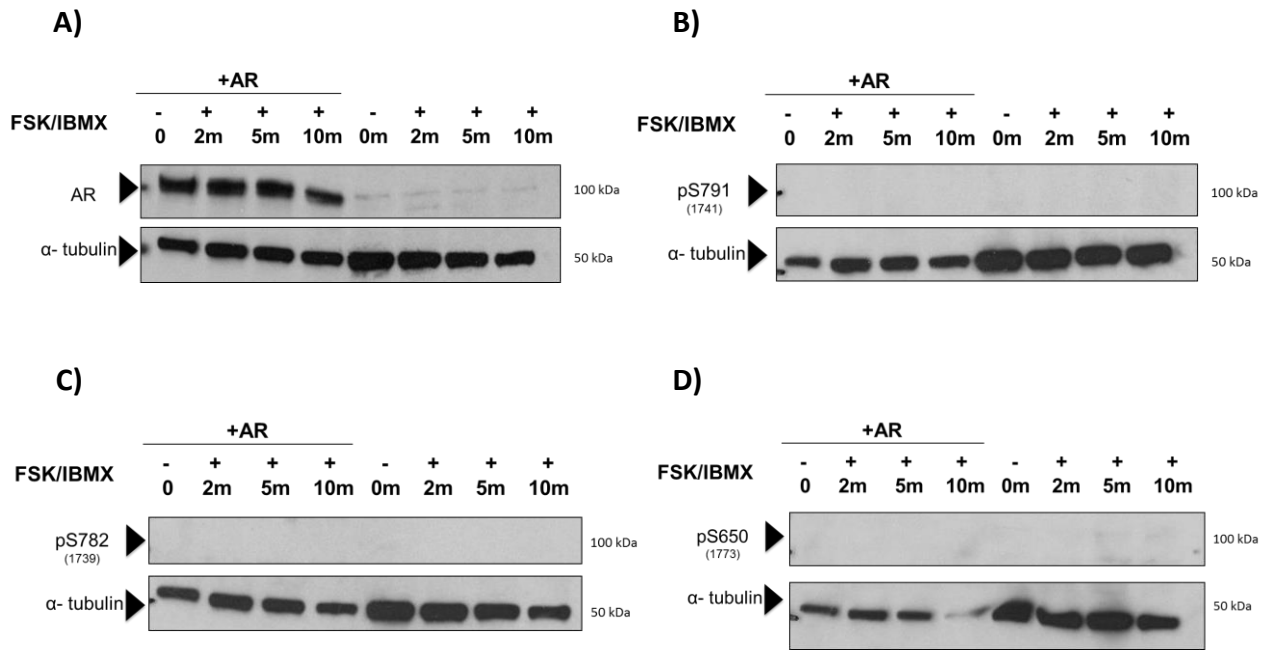


Figure 4.7: Time course of Forskolin\IBMX treatment in transfected PC3 cells
 Testing was carried under normal western blot conditions. PC3 prostate cancer cells were transfected with AR (lanes 1-4) or transfection agent only (lanes 5-8) 24-48hrs prior to treatment. Cells were then treated with 100 μ M Forskolin and 100 μ M IBMX (lanes 2-4, 6-8) or DMSO (lanes 1+4), for 2 min (lanes 2+6), 5 min (lanes 3+7) and 10 min (lanes 4+8) and then harvested with 3T3 buffers containing phosphatase and protease inhibitors. Western Blots were blocked with 5% PhosphoBlocker, and subjected to immune-probing by novel phospho-antibodies (as indicated [B,C, D]), AR [A] and α -tubulin loading control. Data is a representation of 2 independent experiments

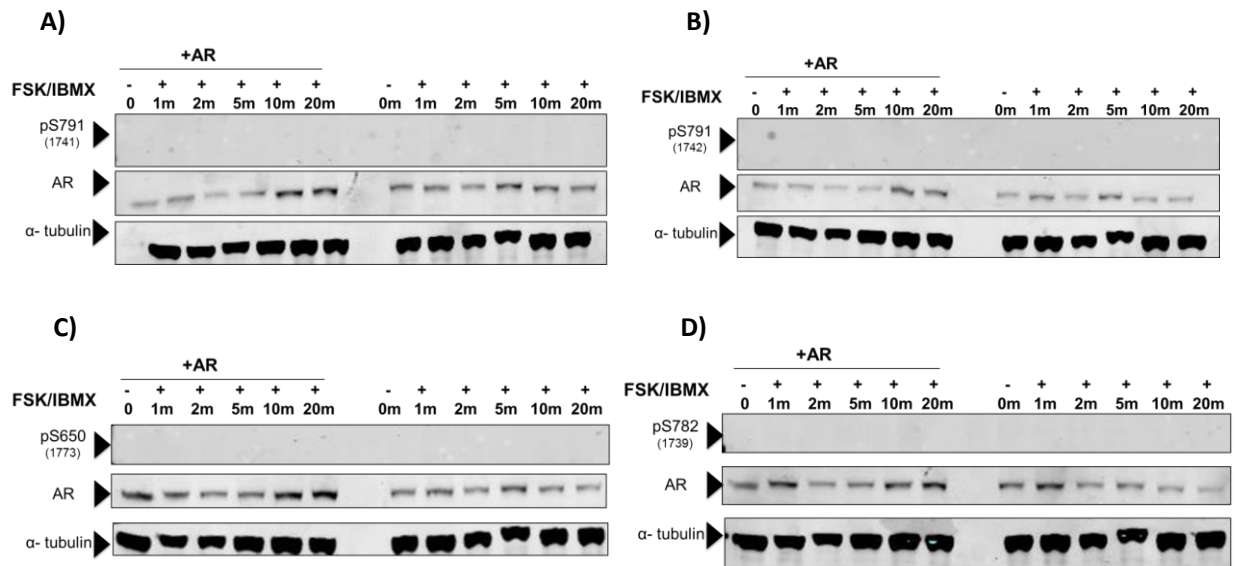


Figure 4.8: Time course of Forskolin\IBMX treatment in transfected LNCaP cells
 Testing was carried under normal western blot conditions. LNCaP prostate cancer cells were transfected with AR (lanes 1-6) or transfection agent only (lanes 7-12) 24-48hrs prior to treatment. Cells were then treated with 100 μ M Forskolin and 100 μ M IBMX (lanes 2-6, 8-12) or DMSO (lanes 1+7) for 1 (Lanes 2+8), 2 (lanes 3+9), 5 (lanes 4+10), 10 (lanes 5+11) and 20 (lanes 6+12) minutes and harvested with 3T3 buffers containing phosphatase and protease inhibitors. Western Blots were blocked with 5% PhosphoBlocker, and subjected to immunoprobining by novel phospho-antibodies (as indicated), and further incubated with a 700nm alexa fluorophore secondary and developed using odyssey. After blots were probed for α -tubulin loading control and AR, incubated with a 800nm alexa fluorophore secondary and developed using odyssey. Data is a representation of 2 experiment.

These experiments yielded little in the way of informative results as no phospho-bands were detected with the novel phospho-antibodies in both LNCaP and PC3 prostate cancer cells lines, despite good transfection of the AR.

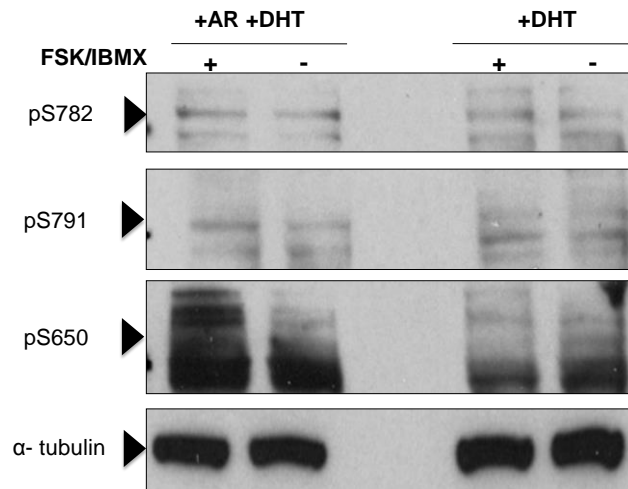
4.2.3.3 DHT

As previously discussed, ligand binding to the LBD causes the AR to undergo conformational changes.

The novel phosphorylation sites identified are located in the ligand binding domain. There is conflicting evidence whether ligand is needed for PKA to cause its effects on the AR [166, 226]. However, other sites of phosphorylation within the AR sequence have been identified as requiring ligand binding for phosphorylation to occur [75]. It is therefore possible that ligand presence maybe needed in order for phosphorylation to occur at the sites identified. If these effects are caused via direct phosphorylation, as I hypothesize, then it is shrewd to test these antibodies with and without ligand present. Furthermore, it has also been suggested that phosphorylation on pS650 occurs or is enhanced in the presence of bound ligand [205].

To test if the novel phosphorylation of the AR is ligand dependant, HEK 293 (Figure 4.9A) and LNCaP cells (Figure 4.9B) were transfected with the AR, treated with DHT for 16hrs and cAMP levels elevated via FSK/IBMX for 10 minutes.

(A)



(B)

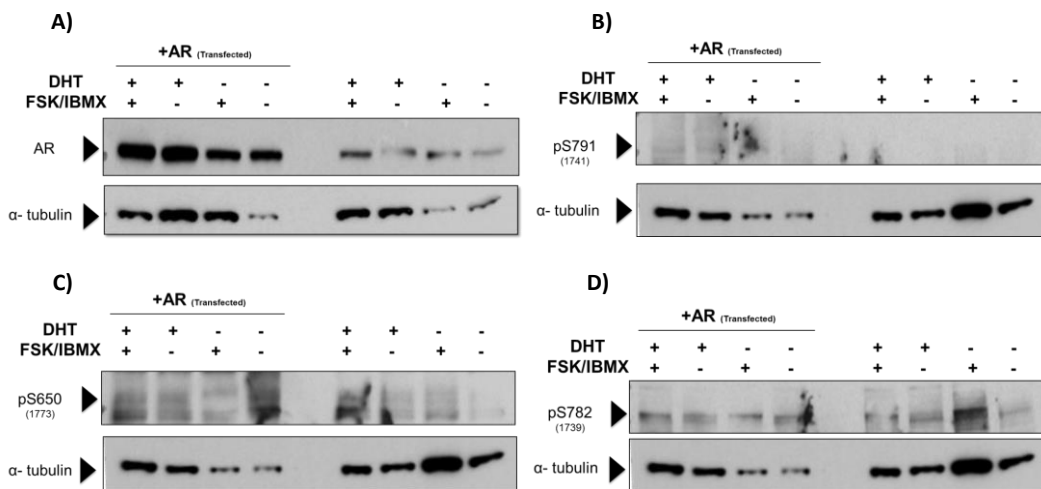


Figure 4.9: Treatment of transfected HEK 293 and LNCaP cells with both DHT and FSK/IBMX
(A) Testing was carried under normal western blot conditions. HEK 293 cells were transfected with AR (lanes 1+2) or transfection agent only (lanes 3+4) 24-48hrs prior to treatment. Cells were then treated with 10nM DHT for 16hrs and subsequently treated with 100µM Forskolin and 100µM IBMX (lanes 2+3) or DMSO (lanes 1+4) for 10 minutes and harvested with 3T3 buffers containing phosphatase and protease inhibitors. Western Blots were blocked with PhosphoBlocker and subjected to immune-probing by novel phospho-antibodies (as indicated), and α -tubulin loading control. Data is a representation of 2 experiments

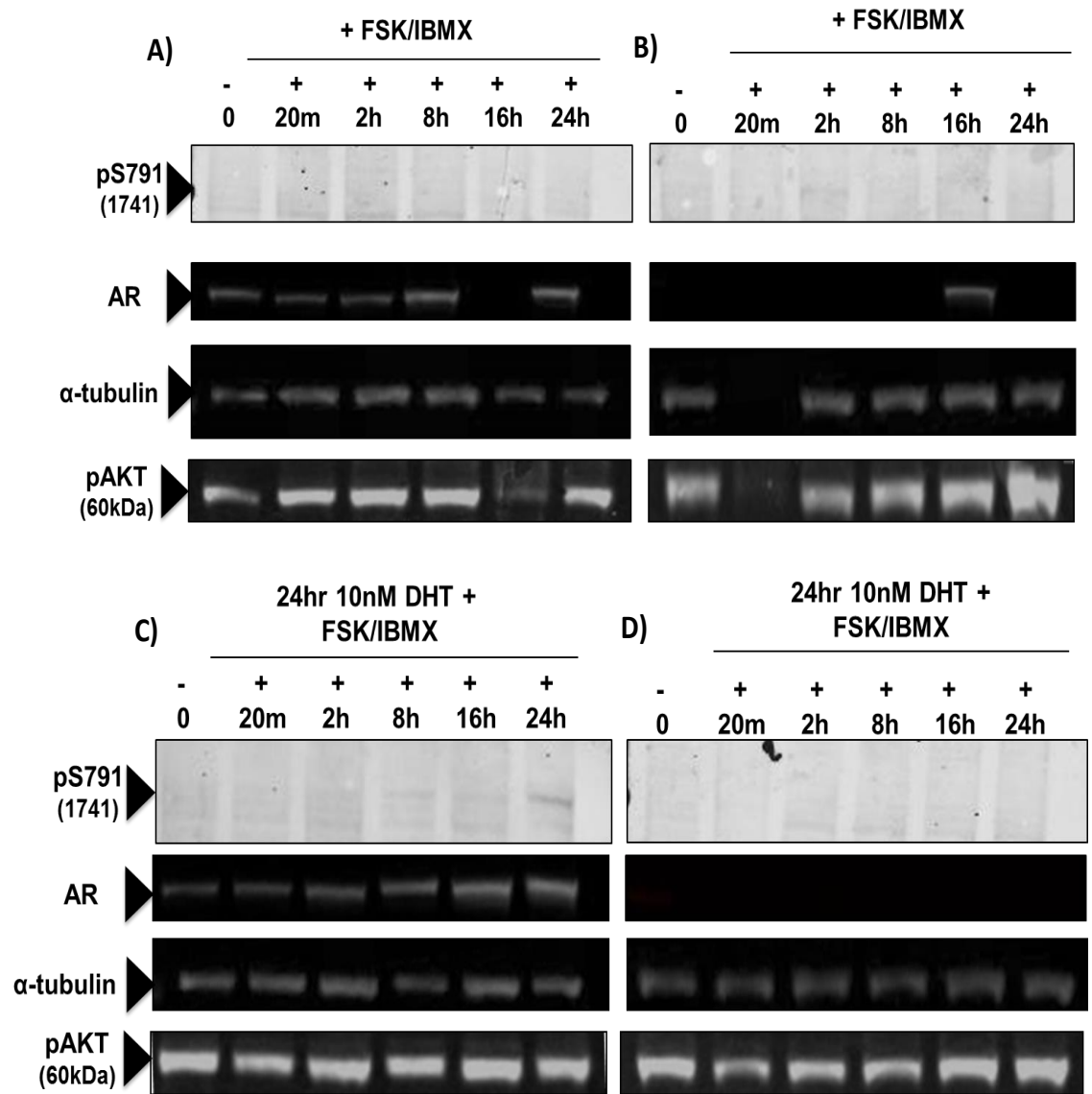
(B) Testing was carried under normal western blot conditions. LNCaP cells were transfected with AR (lanes 1-4) or transfection agent only (lanes 5-8) 24-48hrs prior to treatment. Cells were then treated with 10nM DHT (Lanes 1+2, 5+6) for 16hrs and subsequently treated with 100µM Forskolin and 100µM IBMX (lanes 1+3, 5+7) or DMSO (lanes 2+4, 5+8) for 10 minutes and harvested with 3T3 buffers containing phosphatase and protease inhibitors. Western Blots were blocked with PhosphoBlocker and subjected to immune-probing by novel phospho-antibodies (as indicated), AR and α -tubulin loading control. Data is a representation of 2 experiments

As seen for figure 8, these experiments also produced little in the way of informative results as no phospho-bands were detected with the novel phospho-antibodies in both LNCaP and HEK cells lines following DHT and FSK/IBMX treatment, despite good transfection of the AR.

While nuclear translocation of the PKA catalytic unit begins 3-5 minutes after cAMP elevation, translocation doesn't peak until 30 minutes and levels do not return to basal until after 50 minutes. As it is not determined where in the AR activation pathway phosphorylation occurs, it could be possible that 20 minutes stimulation of FSK/IBMX may not be sufficient to produce an effect that can be detected using our techniques. Phosphorylation of other hormone receptors such as the PR, exhibit a delay in the induction of phosphorylation. Moreover, Sadar et al [166] showed that mRNA levels of PSA increased with FSK treatments. This experiment was carried out over a 48hr period and optimal induction of PSA levels was between 8-16hrs of treatment. These again suggest that 10-20 minute treatment of cells with cAMP simulating agents maybe insufficient to induce PKA phosphorylation.

With this in mind, I transfected the AR into HEK 293 cells and treated them with FSK/IBMX over a 24hr time course. As it is not yet apparent whether the sites I have identified require DHT to become phosphorylated, the cells were also treated with or without DHT for 24hrs.

Surprisingly, a robust and repeatable phosphorylation was detected at site S791 following 24 hours of treatment of FSK/IBMX and DHT (Figure 4.10).



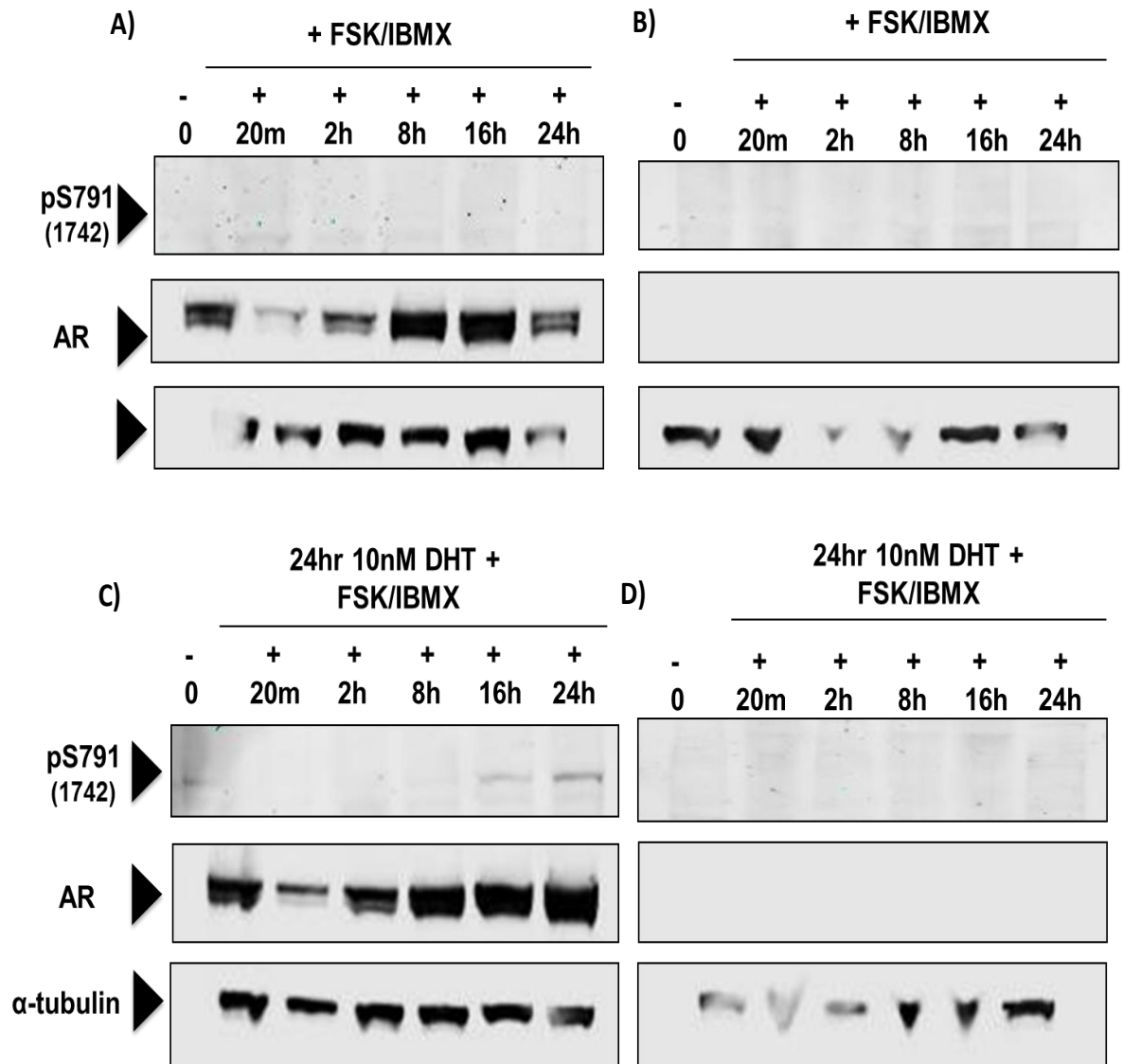


Figure 4.10: 24hr Treatment of transfected HEK 293 cells with both DHT and FSK/IBMX
 Testing was carried under normal western blot conditions. HEK 293 cells were transfected with AR (Blots A and C) or transfection agent only (Blots B and D) 24hrs prior to treatment. Cells were then treated with 10nM DHT for 24hrs (Blots C and D) and subsequently treated with 100 μ M Forskolin and 100 μ M IBMX (Blots A-D) or DMSO (lane 1 of all blots) for the time indicated and then harvested with 3T3 buffers containing phosphatase and protease inhibitors. Western Blots were blocked with 5% PhosphoBlocker and subjected to immunoprobation by novel phospho-antibodies (as indicated), AR, pAKT and α -tubulin loading control (as indicated). Data is a representation of 2 experiments.

4.2.4 RII β AR interaction

As discussed, it has been shown that several components of the PKA signalling pathway are changed at their transcription level in human prostate cancer cells compared to normal prostate cells. This, coupled with preliminary evidence that increased expression of PKA II is found in less proliferative cells and the observation that RII β expression is decreased as the prostate cells move towards androgen insensitivity, led me to the hypothesis that RII β may directly interact with the AR [167, 169].

To investigate this hypothesis, I implemented peptide array technology in order to assess the binding of PKARII β to the AR. As before, the sequence of the AR was broken down into a series of overlapping 25mer peptides which shifted by 5 amino acids at a time and covered the entire AR sequence. These peptide segments are synthesised and presented as distinct spots on the cellulose membrane. This membrane (array) was then overlaid with pure PKARII β protein (produced in house, see materials and methods) and subsequently probed with PKARII β antibody to detect sites of PKARII β /AR binding.

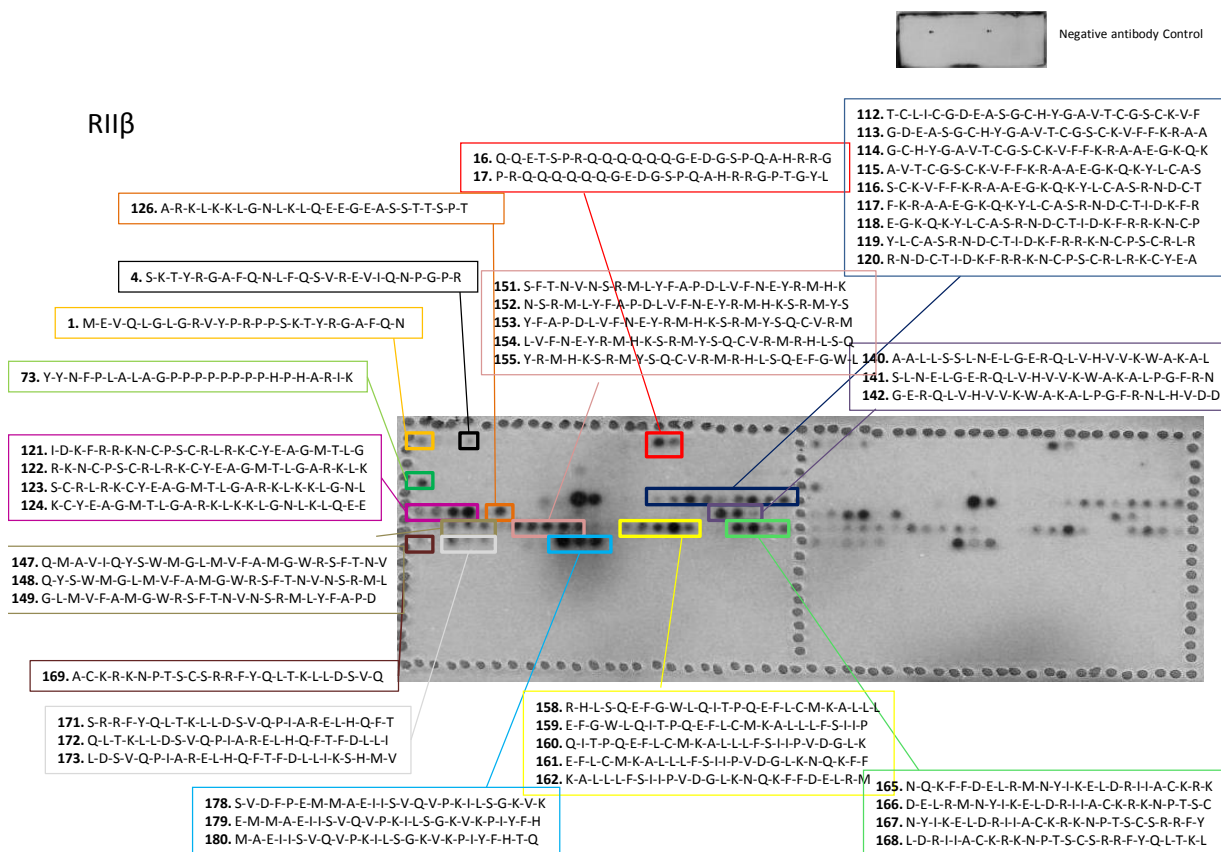


Figure 4.11: Overlay of pure RII β protein on an AR peptide array
 PKA RII β protein was overlaid onto an immortalised AR peptide array. The array was subsequently probed with a PKARII β antibody and processed under usual western blot conditions. Data is a representation of 1 experiment

Figure 4.11 shows possible RII β interacting sites on the AR. While this peptide array study is useful in identifying the binding sites, it is an artificial screening tool that requires validation in a more physiological environment.

4.2.4.1 RII β AR IP

To validate the binding shown using the peptide array technology, I carried out immuno-precipitation experiments to detect possible binding between RII β and AR. LNCaP and VCaPs lysates were immuno-precipitated with AR antibody (Santa Cruz®) and subsequently blotted with a RII β (BD Bioscience®) primary antibody. Detection was achieved via a HRP conjugated light chain only secondary.

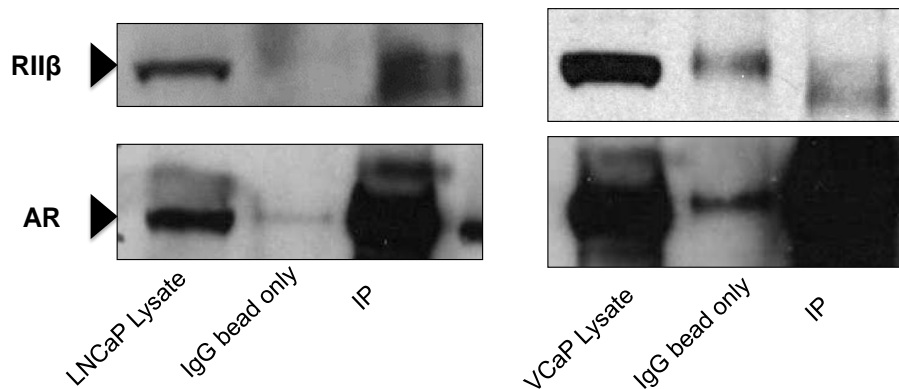


Figure 4.12: Co-immuno-precipitation of AR and PKA RII β subunit in LNCaP cells
 Testing was carried under normal western blot conditions. LNCaP cells were harvested with 3T3 buffers containing and protease inhibitors. Lysates were incubated with 1 μ g of AR (Santa Cruz®) antibody and Protein G beads. Negative control was conducted in the same manner without antibody. Western Blots were blocked with 5% milk protein and subjected to immune-probing by the RII β and AR as indicated. This was followed by a mouse light-chain only secondary and subsequent development by ELC. Data is a representation of 3 independent experiments

This experiment shows a reliable and reproducible interaction of the AR with RII β in LNCaP and VCaP cells lines. Suggesting that RII β can interact directly with AR.

4.2.4.2 Confocal analysis of proposed RII β and AR interaction

To confirm the co-immunoprecipitation experiments and assess localisation of PKA RII β and AR in prostate cancer cells, confocal imagery using LNCaP cells was carried out (Figure 4.13). Cells were treated with or without FSK/IBMX for 10 minutes prior to fixing with 4% formaldehyde and subsequently immunostained using the protocol highlighted in 'materials and methods' section. AR (abcam®) and RII β (BD Bioscience®) antibodies were used.

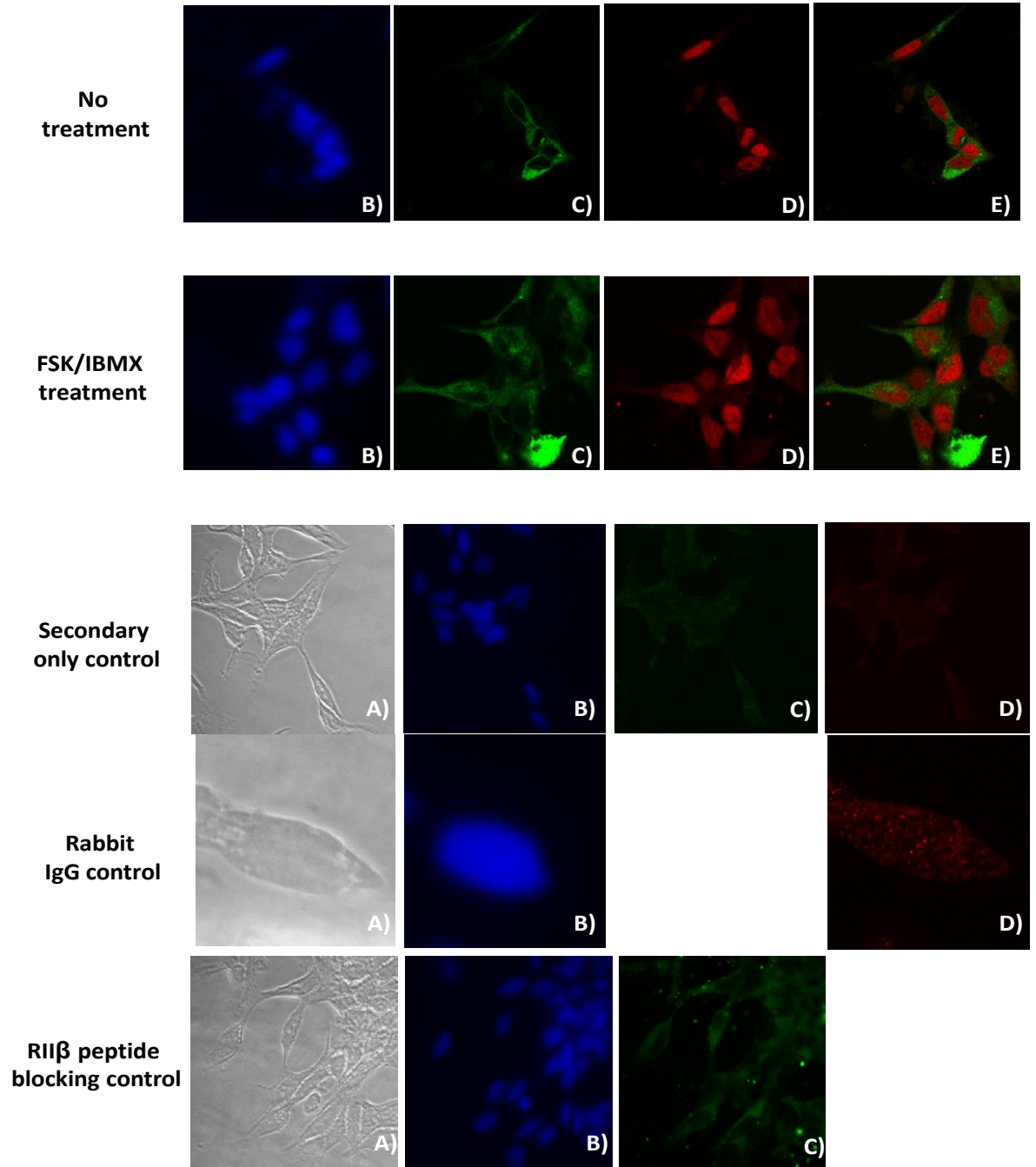


Figure 4.13: Co-localisation experiments using confocal microscopy
 Cells were plated onto glass cover slips, coated in rat tail collagen, and incubated in normal growth medium prior to fixing. Cells were fixed using 4% paraformaldehyde and then permibilised. Cells were subjected to immuno-probing by primary PKA RII β (BD Bioscience® [Green]) and AR (Santa Cruz® [Red]) antibodies, and subsequent Alexa®

fluorophore secondary antibodies; anti-mouse- 488 and anti-rabbit- 594 (molecular probe®). Slips were mounted onto slides using Gold+Dapi (Invitrogen®) and analysed using confocal. A) Cells under light microscope B) Nuclear Dapi C) RII β D) AR E) Co-localised image of RII β and AR. Row 1 shows cells with no treatment. Row 2 shows cells incubated with 100 μ M FSK/IBMX 10 minutes prior to fixing. Row 3 shows Alexa fluorophore secondary only control. Row 4 shows Rabbit IgG to identify any none specific binding of the AR antibody. Row 5 shows RII β incubated with RII β purified protein to identify any none specific binding of the RII β antibody.

This revealed a lack of endogenous co-localisation of PKA RII β and AR in the untreated cells (FIG 4.13, row 1). Additionally treatment with FSK/IBMX was unable to invoke a change in the localisation pattern of either protein (FIG 4.13, row 2). Rigorous negative controls were used in this experiment to control for non-specific antibody binding. All 3 controls employed (FIG 4.13, rows 3-5) show only a background signal, showing antibody specificity for both primary (Figure 4.13, rows 4-5) and secondary antibodies (Figure 4.13, rows 3).

Furthermore, the androgen receptor appears to be mostly translocated to the nucleus. When AR is in the nucleus it is thought to be active and carrying out its transcriptional function. Surprisingly there doesn't appear to be an increase in AR translocation after FSK/IBMX treatment. As discussed many studies have shown that increase FSK/IBMX results in the increase transcription activity of the AR [76, 142]. However, with large expression already displayed in the nucleus of the cell any additional translocation maybe negligible. In addition, RII β is mainly located in the cytoplasm and again exhibits very little change when treated with FSK/IBMX. RII β cellular localisation is mainly controlled via binding to AKAP domains and therefore is usually expressed in specific locations in the cell [227, 228]. I have shown that RII β is specifically located within the cytoplasm of the cells, with area of increase expression which looks to be localised to the cell membrane. While, PKA RII β and AR co-localization could be induced via another mechanism e.g. DHT; co-localisation via FSK/IBMX treatment alone does not occur.

4.3 Discussion

Post-translational modifications, for example acetylation and sumoylation are shown to have an influence on the transactivation of the AR [75, 204]. However, it is unclear what effects, if any, are orchestrated by PKA mediated AR phosphorylation. It has been shown that the AR is a substrate for many different kinases and that additional phosphorylation of the AR can be induced when cells are exposed to androgens [205, 212]. Phosphorylation occurs predominantly at serine residues [205].

Other members of the steroid superfamily can be activated via phosphorylation. It has been shown that the human oestrogen receptor can be activated in the absence of steroids after treatment with PKA activators such as FSK or PKA specific 8-Bromo-cyclic AMP. In addition, other members of this superfamily, for example the human progesterone and glucocorticoid receptors, can be activated in a synergistic fashion by steroids and kinase stimulators [229, 230]. These co-treatment effects can be inhibitory or synergistic. This is no different within the AR pathway. In the case of the rat AR, there is a proposed synergism between the PKA pathway and the steroid pathway, to stimulate transcriptional activation rather than a steroid-independent activation of the AR [215, 231]. In addition Gioeli et al [205] reported that upon treatment with FSK in LNCaP cells, the overall phosphorylation of the AR was increased. Sadar et al [76] demonstrated that treatment with FSK increased the PSA mRNA levels, suggesting AR activation. It is also reported that treatment with AR antagonists can block this PKA-dependant activation and downstream PSA increase, suggesting that although activation is driven by PKA, AR is required for transcription [76, 215].

Some studies have endeavoured to explain these results by looking at PKA activating events and their downstream effects on AR function. Despite the obvious link between PKA and AR signalling, it is yet to be shown conclusively that PKA can directly phosphorylate the AR. In this study, I have endeavoured to show the phosphorylation status of AR in relation to activated PKA signal transduction pathway, in a step towards understanding PKA's effect on AR transcription/regulation and how this may contribute to prostate cancer progression.

The AR has been shown to have 16 phosphorylated residues and they have been linked to different effects on the receptor. Some sites require ligand binding and some do not and most are located in the N-terminal domain. These 16 sites of phosphorylation have been linked to dimerization, transactivation, localisation, transcriptional activity, degradation and stability of the AR receptor [223] confirming that phosphorylation has an important role within AR function.

Within this study, I have shown that AR is able to become directly phosphorylated by PKACB *in vitro*. In addition, I have identified S791 as a novel phosphorylation site for PKA.

Currently phosphorylation of S791 is thought to be AKT dependent. A phosphomimetic mutant study (S791D) exhibited reduced binding of ligand, a decrease in nuclear translocation, and reduced transcription via lack of AR binding to its promoter. In addition, this phosphomimetic mutation at S791 in addition to S213 (S213 is an ATK dependent site), resulted in an impaired translocation of AR to the nucleus in COS1 cells [232]. These data suggest phosphorylation at this site could be important in decreasing the translocation and transcription of the AR. Furthermore, AR stability was decreased when S791 was phosphorylated and this was restored following treatment with the proteasome inhibitor MG132. These results suggesting that phosphorylation of AR at S791 plays a role in the ubiquitination of AR and modulates its degradation via the proteasome. Moreover, S791 is the only modified residue within 50 amino acids of the ubiquitinated lysine 845 and 847 [232]. AKT and PKA are structurally very similar and studies have shown them to share the same phosphosites [233, 234]. Thus S791 could also be a phosphosite for both kinases and PKA could also play a role in regulating the half-life of the AR. However I was unable to follow this area of research due to time constraints.

My data suggests that the kinetics of phosphorylation at S791 are slow following FSK/IBMX treatment. PKA is rapidly dissociated from the R subunits upon cAMP binding and nuclear translocation of PKA catalytic unit can begin within 3-5 minutes. While nuclear translocation doesn't peak until 30 minutes after cAMP elevation, the AKT study discussed above, suggests that phosphorylation of S791 inhibits AR translocation and thus in theory should occur in the cytoplasm. Conversely, Gioeli et al [205] stated that most of the sites phosphorylated on the

AR, weren't maximal until 2hrs after hormone treatment and in the case of S81 phosphorylation, it was still increasing after 6hours. S791 wasn't included in this study; however delayed overall phosphorylation of the AR was shown. Furthermore, these slow kinetics are in parallel to the delayed hormone-dependent phosphorylations that have been shown on progesterone receptor [235].

AR translocation to the nucleus after ligand binding is rapid, occurring 15 minutes after treatment. This suggests that AR phosphorylation is likely to play a role in a late phase of transcriptional regulation or receptor recycling, which correlates with the proposed function of S791 phosphorylation. However, a longer time course would be required to further investigate the phosphorylation of AR by PKA, as the phosphorylation event described is only weakly bound by site-specific antibody and so no conclusions can be made from this data alone.

PKA phosphorylates and activates AKT. Treatment with FSK/IBMX will lead to the hyper-activation of PKA and thus increase phosphorylation of AKT. As AKT has been shown to phosphorylate at S791 to play a role in ubiquitination and turnover of the AR, late stage activation of AKT may occur via PKA signalling. Future studies should consider an increase AKT activation via PKA as a possible mechanism for FSK/IBMX induced phosphorylation at S791.

Finally, I tried to demonstrate a interaction between PKA RII β and the AR. PKA regulatory units have been investigated as a signalling mechanism in many prostate cancer studies [50, 169, 171, 191].

R unit isoforms demonstrate distinct subcellular localizations via A-kinase anchoring proteins (AKAP) that can specifically bind the N-terminal domain of the regulatory subunits. Numerous AKAPs have been identified, and they are suggested to facilitate the compartmentalization of PKA isoforms to discrete intracellular localizations [227]. The localization of PKA plays a crucial role in determining which substrates are phosphorylated. In addition, RI and RII subunits show considerable differences in expression between tissues, and changes in the ratios of PKA I and PKA II play an important role in processes like cellular differentiation and cancer development. The overexpression of PKA II due to the up-regulation of the regulatory subunits type II of PKA has shown to have a

protective effects in cancers owing to the decrease in proliferation and invasion correlating with its expression increase [167]. Whilst RI overexpression has been linked to poor patient outcome. In prostate cancer, this is also true. Cho et al [50] demonstrated the over-expression of the RII subunit in various cancer cells, including prostate adenocarcinoma. This over-expression resulted in a reversion of the transformed phenotype. As discussed, the AR has a pivotal role in prostate cancer progression and thus I hypothesized that RII β up-regulation in the AS cells may interact with AR to exert its effects.

RII β and AR co-IPs showed that RII β could form a complex with endogenous AR in AS cell line. However we couldn't reproduce these effects with confocal microscopy. RII β lays in the vicinity of the heavy chain (50kDa) on a western blot. Use of secondary antibodies that recognise the heavy and light chain of the primary antibody used to pull down a target protein can therefore affect the signal of the protein of interest, in this case RII β . In this study, light chain only secondary antibodies were implemented. These antibodies should circumvent this problem, however it is still possible that antibodies can recognise non-target proteins in a non-specific manner. Therefore, it could be argued that the positive signal from the IPs is due to specificity problems with the secondary antibody. Additionally, upon sequence investigation, no conventional AKAP consensus sequence for PKA RII anchoring exists on the AR.

In conclusion I doubt if PKARII β directly binds to the AR, but exerts its effects via indirect downstream signalling.

5 Exposing the role of PDE4D7 in Prostate Cancer Progression

5.1 Introduction

5.1.1 PDE4s and links in Prostate Cancer

PDE families have long been considered as possible therapeutic targets in many disease states. Prostate cancer is no exception [236]. As with most tumour microenvironments, prostate cancer is a forever changing environment of stimulatory and inhibitory signals that requires the expression and regulation of secondary messenger pathways to respond and interpret this environment. As PDEs are the only known way to degrade cyclic nucleotides and therefore control the spatial and temporal components of these signalling pathways, it was suggested that these enzymes maybe differentially regulated in prostate cancer [236, 237]. Despite the number of papers that implicate cAMP signals as having an effect on prostate cancer progression, the literature is particularly lacking in details of a mechanistic role for PDE enzymes in prostate cancer progression.

Uckert et al have carried out many studies to analyse the distribution and effects of phosphodiesterases within the prostate to determine whether PDE inhibition could be a potential treatment for urinary tract disease and BPH [238-242]. Uckert et al confirmed the presence of mRNA specifically encoding for PDE4A, PDE4B, PDE4C, and PDE4D within the distinct anatomical regions of the prostate, using PCR [240]. He went on to show the importance of PDE4's in prostate function and the co-localization of PDE4's and isoforms of PKA in smooth and glandular areas of the prostate [238, 239]. However, the potential significance of PDE signalling and control of human prostate function wasn't comprehensively investigated.

Another study by Wheeler et al investigated PDE expression in tissues of the urinary tract and describes the presence of all PDE families within the prostate, with the exception of PDE6 [243]. Although interesting, this work does not describe the PDE complement of the prostate in a cell specific fashion.

Work by Rahrmann and co-workers [244] utilised a transposon based mutagenesis screen to implicate PDE4D as a critical factor in the induction of epithelial proliferation and hyperplasia in the prostate after mutagenesis. They went on to investigate the putative role of PDE4D in prostate cancer. It was suggested that PDE4D was overexpressed in prostate cancer samples and cell lines and that changes in PDE4D isoform expression was detected in prostate cancer progression. Furthermore, they suggested that knock-down of PDE4D by shRNA also reduced the proliferation of DU145 prostate cancer xenografts in rats and also effected migration by wound healing assays. Once again, these studies were relatively descriptive and failed to provide the molecular mechanism that was underpinned by PDE4D activity and resulted in the phenotypic changes.

Further to these studies, a comprehensive analysis of PDE isoform expression in prostate cancer has been carried out by our laboratory [179]. Within this study 19 prostate cancer cell lines and xenographs were used, 10 AS and 9 AI, to provide an expression profile for each PDE within prostate cancer and its possible fluctuation in abundance in prostate cancer progression. The RT-qPCR analysis of these prostate cancer samples identified PDE3B, PDE4B, PDE4D, PDE7A, PDE8A, PDE8B and PDE9A as PDE isoforms that are the most abundantly expressed within the prostate and that members of the PDE4D family showed the highest significant change in regulation from AS to AI cancers. In particular, this study identified PDE4D7 as a possible biomarker for prostate cancer progression with a significant 40 fold decrease in expression between AS and AI samples (see further explanation below).

5.1.2 PDE4D7

Since PDE4D7 was first discovered by Wang et al, the understanding of the contribution to the control of intracellular cAMP and signalling events have not been greatly expanded upon [245]. Wang showed PDE4D7 expression in the brain, placenta, lung and kidney. However, one study linked ischemic stroke to small nucleotide polymorphisms of PDE4D in the Icelandic population [246]. They reported that mutations in the region surrounding the PDE4D7a exon are positively correlated with incidence of ischemic stroke. Furthermore, they also suggested that these mutations can lead to a reduction in the expression of the PDE4D7 isoform. However, this remains to be thoroughly proven.

As mentioned above, a study [179] to isolate a prostate cancer biomarkers identified PDE4D as being significantly over expressed in AS prostate cells lines and xenographs. In addition, the isoform PDE4D7 exhibited the highest degree of expression in AS and the largest amount of down-regulation in AI samples than any other PDE4D isoform. To further characterise the role of PDE4D7 in prostate cancer, the report went on to pinpoint the sub-cellular localisation of the isoform at the plasma membrane and utilise FRET-based, targeted cAMP reporters to show that PDE4D7 contributes a significant proportion of rolipram sensitive PDE4 activity at the plasma membrane of AS cell lines.

As prostate cancer progresses, there is an increase in the proliferation enhancing effects of cAMP signalling, thus I hypothesise that PDE4D7 is important in controlling compartmentalisation of cAMP signalling at the sub-plasma membrane, where it is in prime position to modulate cAMP generated by plasma membrane associated adenylyl cyclases. In addition, it is plausible to extrapolate the notion that PDE4D7's compartmentalisation at this locale may require the presence of binding partners and/or induce other signalling pathways. While PDE4D7 is a putative biomarker for prostate cancer progression, nothing is known about its regulation, binding partners or crosstalk with downstream signalling pathways. This may be the key to understanding the mechanism by which PDE4D7 exerts its control over the proliferative effects of cAMP mediated pathways in prostate cancer. This chapter seeks to investigate the role of PDE4D7 in prostate cancer signalling using a range of biochemical, molecular biology and proteomics techniques.

5.2 Results

5.2.1 Using VCaP as a model to investigate PDE4D7 function in PC.

For this section of my study, the VCaP cell line was selected to represent PC AS phenotype. VCaP cells express the highest level of PDE4D7 mRNA and PDE4D5/7 protein, out of all the cell lines examined in this study [179]. VCaP cells exhibits many of the characteristics of clinical prostate cancer as it expresses a functional wild type AR, PAP, and large amounts of PSA [180, 182]. VCaP cells grow in distinct colonies on plastic, making them harder to transfect than the LNCaPs used earlier in this study (unpublished observation) and also take 50-100 hours to double [180, 181]. This observation mirrors the situation in vivo where AS versus AI growth in xenografts of the cell line exhibit a similarly different growth pattern. Since its isolation, the VCaP cell line has increased in use within the prostate cancer field, in part due to the fact it is derived from a bone metastasis and PC patients have metastasis primarily or exclusively in bone [59].

5.2.2 PDE4D7 constructs

Plasmid constructs used during this study were produced in house[179]. The first of which was produced by the sub-cloning of a wild-type PDE4D7 construct in order to express the vesicular stomatitis virus (VSV) epitope tag (YTDIEMNRLGK) on the C-terminal end of the isoform. The tag was placed on the C-terminal end of the protein away from the unique N-terminal region of PDE4D7 , which is known to be the unique targeting domain of all PDE4s. The second construct produced was a dominant negative (DN) version of the PDE4D7 VSV construct. The Houslay/Baillie group has excelled in the use of the dominant negative approach to gain insight into unique cellular roles of PDE4 isoforms. This approach requires that PDE constructs be mutated at a single position within the catalytic site. The catalytic site is essential for the hydrolysis of the phosphodiester bond of cAMP, and thus this mutation rendering the enzyme catalytically inactive. These constructs are useful in defining the function of a particular PDE isoform as it displaces the endogenous, functional protein with the inactive, DN form. This has the benefit of only affecting the displaced, targeted, isoforms allowing local cAMP levels to rise around the original site of

the displaced isoform only, while not affecting global cAMP levels or the functioning of untargeted PDE isoforms [7]. A singular D559A mutation within the catalytic site of PDE4D7 rendered the enzyme unable to hydrolyse cAMP.

The PDE4D7 constructs were transfected into HEK293 cells and the resulting cell lysates were assayed for PDE activity. This assay was performed in order to ensure the inactive nature of the dominant negative PDE4D7 construct and the active nature of the VSV fused PDE4D7 construct. This assay showed that the VSV tagged construct retained catalytic activity while the dominant negative construct exhibited no increase over basal PDE activity.

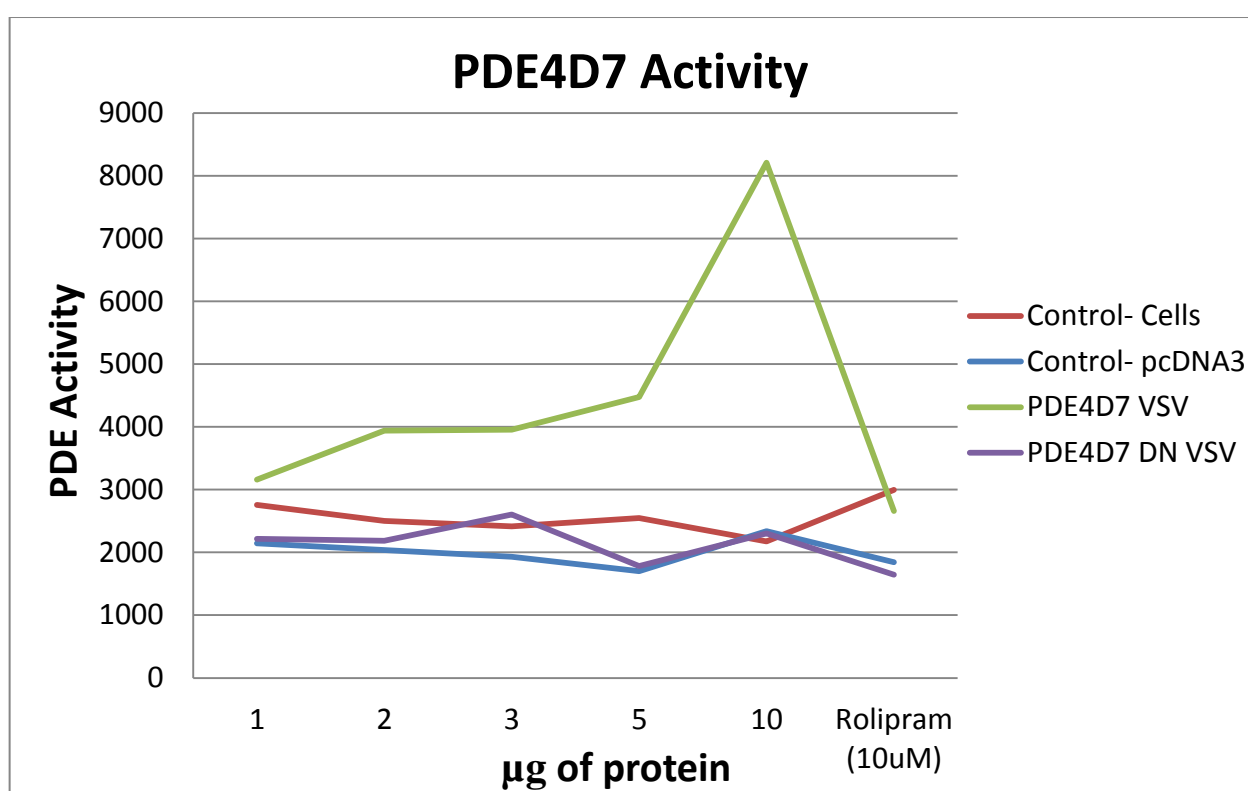


Figure 5.1 PDE activity of PDE4D7 constructs transfected into HEK293
A PDE assay was conducted on HEK293 cells transfected with PDE4D7 VSV or Dominant Negative PDE4D7 VSV constructs. For activity calculation, see 'material and methods' section.

5.2.3 The use of high-throughput screens

The use of high-throughput screens allow for the investigation of multiple molecular targets at any one time at either the DNA, RNA or protein level. This has multiple advantages over conventional methods; the speed of analysis, the relatively low amount of sample used, the consideration of effects on entire signalling cascades and the very large amount of molecular targets that can be

analysed in a single experiment. By exploiting this approach, we are able to investigate the influence of PDE4D7 on many different cellular molecules and signalling systems within prostate cancer.

5.2.4 RT-qPCR

The RT² ProfilerTM PCR arrays used for this high-throughput screen were purchased from Qiagen®. These arrays use Sybr-green technology instead of the Taq-man primer/probe set that were used earlier in this study.

5.2.4.1 Sybr-green vs Taq-man

SYBR green is a small cyanine dye which changes its fluorescence spectrum when bound to double stranded DNA (dsDNA) [247]. As the amplification of target genes increases during the RT-qPCR reaction, initiated via gene-specific primers, this change in fluorescence can be monitored [248]. Sybr-green technology is a widely used PCR technique due to its ease of use and low running costs.

However, due to the non-specific fashion in which the SYBR green dye binds to dsDNA, any off-target amplification can lead to a false result. A post-assay melting point analysis can be used to ensure that the observed change in fluorescence signal is representing only the transcript of interest. During this analysis, the PCR reaction product is exposed to a graduated temperature range which causes further changes in the fluorescence reading as the double stranded amplifications dissociate at specific melting points. The melting point of the specific amplifications can be calculated from its sequence, and thus any change in fluorescence above or below this temperature indicates off-target amplification and a false result. The amount of false positive can be significantly reduced by the careful design of primers and full validation of PCR products [248, 249]. Therefore, in this study, I have used RT² ProfilerTM PCR high-throughput arrays and associated probe sets from SABioscience (Qiagen®). These arrays contain primers that have been carefully designed and fully validated to reduce false positives. I have also run melting curves for the initial screen to authenticate the Sybr-green primers.

PDE4D7 VSV and DN PDE4D7 VSV constructs were transfected into VCaP cells, and overexpression was confirmed via RT-qPCR and PDE4D7 Taq-Man®

primer/probe set prior to use of the RT² Profiler™ PCR arrays (Figure 5.2). Cells were also transfected with empty vector pcDNA3 controls, which as expected, showed no PDE4D7 overexpression.

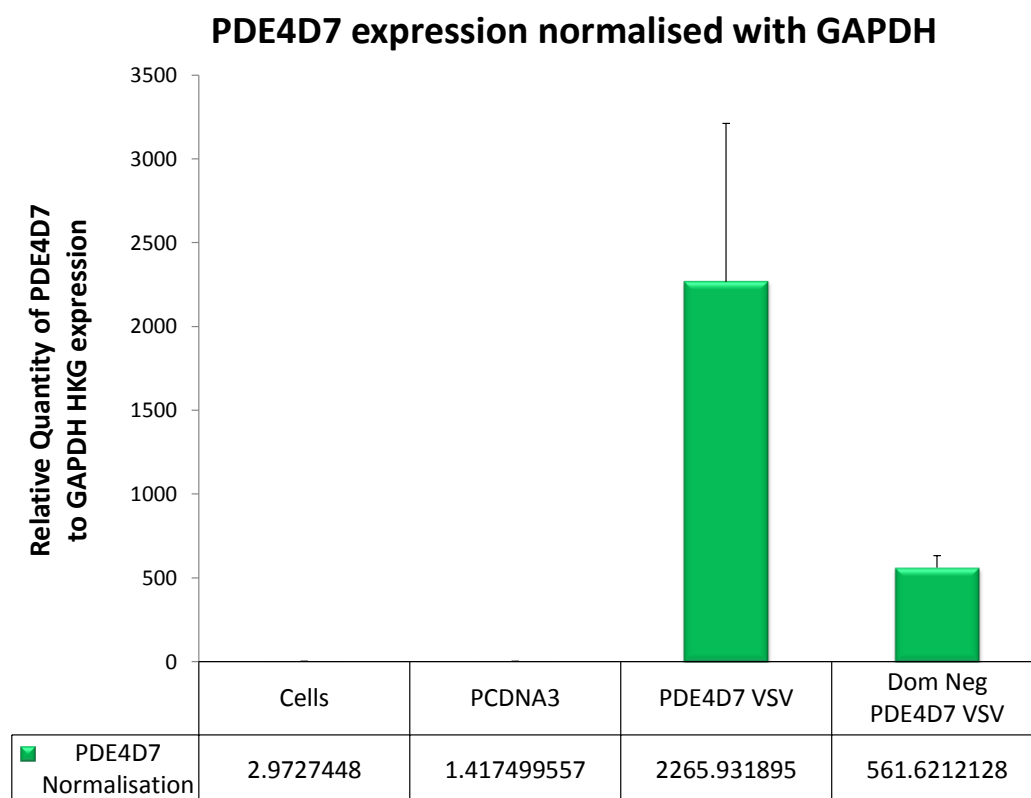


Figure 5.2 Expression of PDE4D7 constructs transfected into VCaP cell
VCaP cells were transfected with pcDNA3, PDE4D7 VSV and dominant negative PDE4D7 VSV constructs. Cellular lysates were subjected to RT-qPCR with PDE4D7 and GAPDH Taq-Man® probes. Cells transfected with PDE4D7 VSV and dominant negative PDE4D7 VSV constructs show an up-regulation in PDE4D7 compared to pcDNA3 construct and untransfected cells. Values are plotted as relative quantities to the expression of GAPDH.

5.2.4.2 RT² Profiler™ PCR arrays

In this study RT² Profiler™ PCR arrays were used to provide insight into the action of PDE4D7 in PC by identifying novel interacting pathways/proteins. The 3 arrays that were selected were; Prostate Cancer array, Cancer PathwayFinder array and Focal Adhesions array. Four conditions were carried out for each array; Cells only, pcDNA3 transfection control, PDE4D7VSV transfected and DN PDE4D7 VSV transfected cells.

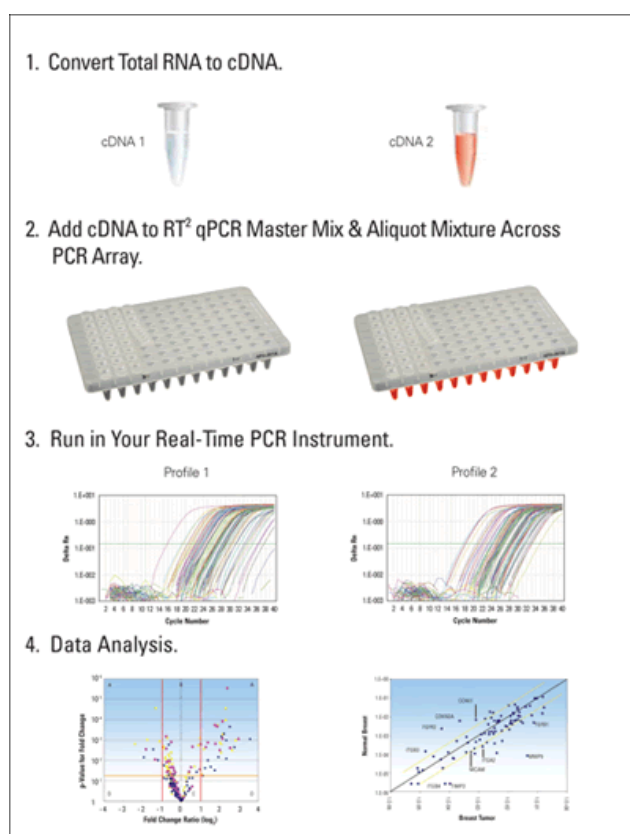


Figure 5.3 Diagram explaining RT² Profiler™ PCR array technique

Cells only control was used to assess fold changes in relative expression between samples e.g. all experimental samples were compared to cells only control and plotted as relative fold change. Figures 5.4, 5.5, 5.6, show genes that are expressed with a fold change above 2.

The prostate cancer arrays contain Sybr-green primers for key genes that are often involved in the development of prostate cancer. These 84 genes include; genes involved in AR, AKT and PTEN signalling as well as genes associated with metastatic potential, cells cycle and apoptotic pathways. In addition, the array included genes that are known to change in methylation profile in PC and genes that have been detected routinely in PC samples to be dysregulated. All these genes are known to be important in prostate cancer initiation, progression, and metastasis. Thus in an attempt to unveil the mechanism by which PDE4D7 exerts its control over cAMP mediated pathways in prostate cancer, this study focused on the changes in expression of a panel of genes following PDE4D7 overexpression or displacement via the dominant negative approach. Figure 5.4

displays the fold regulation of these genes in each test condition with relative expression to untreated cells alone.

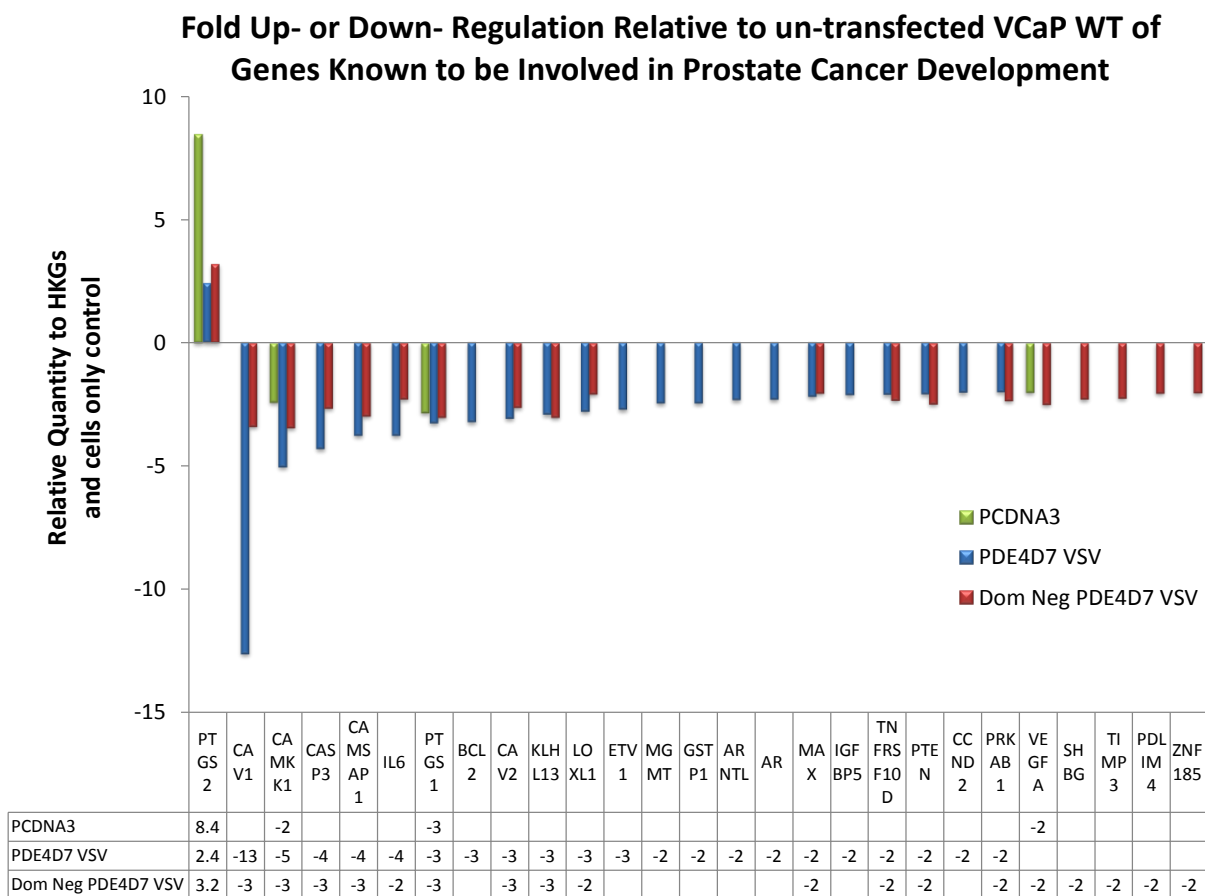


Figure 5.4 Fold regulation of RT² ProfilerTM prostate cancer PCR array
RT² ProfilerTM prostate cancer PCR array was conducted under 4 conditions; Cells only, pcDNA3 transfection control, PDE4D7VSV transfected and DN PDE4D7 VSV transfected cells. Data is expressed relative to VCaP cells only control and is displayed as relative fold change greater than 2.

The Cancer PathwayFinder arrays contain Sybr-green primers for key genes that are often involved in transformation and tumourgenesis. 84 genes represent 9 different biological pathways that regulate specific aspects of cell growth. During oncogenesis, dysregulation of these key pathways can occur due to an increase in gene mutation and expression changes. A myriad of different genes can potentially be affected during tumourgenesis and the profile can sometimes be indicative of a specific cancer type. As the mechanisms behind PC are not fully understood, I wanted to investigate the possible interaction of all common genes involved in oncogenesis with PDE4D7. The 84 genes encompassed within this array represent these 9 pathways that are often affected in oncogenesis;

apoptosis, cell cycle, DNA damage/repair, cellular senescence, telomere maintenance, angiogenesis, epithelial-to-mesenchymal transition, hypoxia and metabolism. PDE4D7 interaction with any of these pathways could be the key to understanding how PDE4D7 exerts its effects in PC. Figure 5.5 displays the fold regulation, with relative expression to cells only, of these 84 genes.

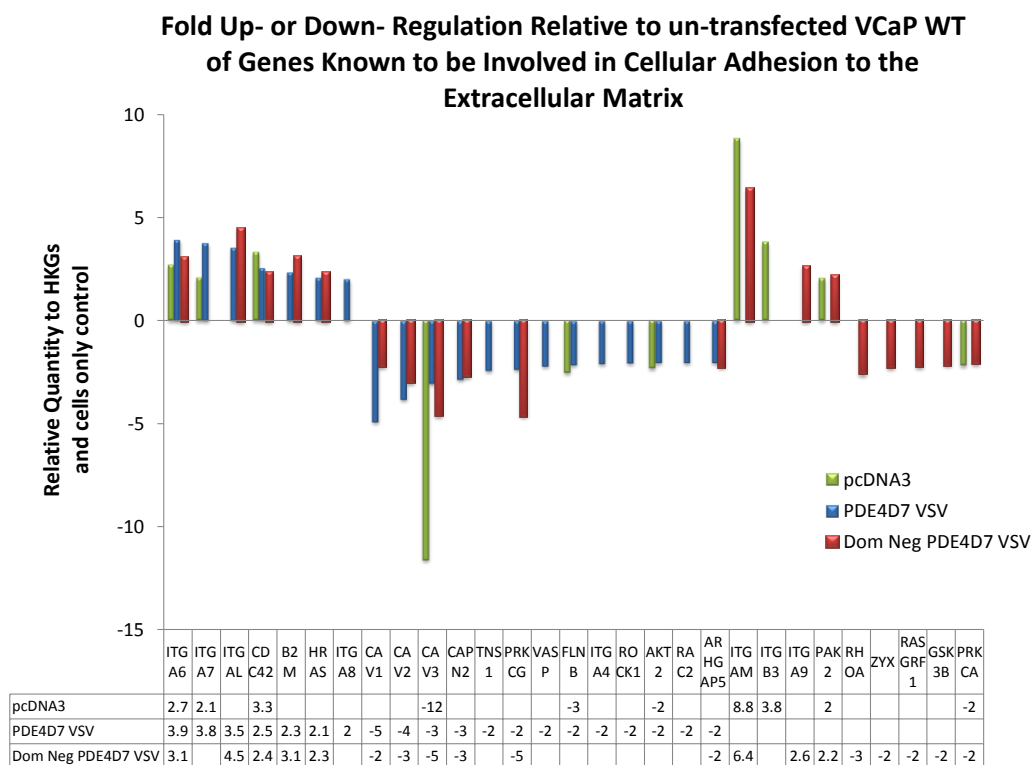


Figure 5.5 Fold regulation of RT² ProfilerTM cancer pathway finder PCR array. RT² ProfilerTM cancer pathway finder PCR array was conducted under 4 conditions; Cells only, pcDNA3 transfection control, PDE4D7VSV transfected and DN PDE4D7 VSV transfected cells. Data is expressed relative to VCaP cells only control and is displayed as relative fold change greater than 2.

The focal adhesions arrays contain Sybr-green primers for key genes that are often involved in cellular adhesion to the extracellular matrix (ECM). Focal adhesions form around the intracellular domains of integrins that are bound to components of the ECM, such as those found in the basal lamina underlying epithelial cells. Focal adhesions connect the intracellular domains of integrins to actin filaments. These structures regulate several key biological processes including angiogenesis, anchorage-dependent cell survival, cell cycle, cell migration, and wound healing. Dysregulation of focal adhesion function and integrity plays a key role in the pathophysiology of diseases such as fibrosis and epithelial-to-mesenchymal transition during tumour metastasis. Within Prostate

Cancer, many focal adhesion proteins have been linked to advancing disease. For example the overexpression of focal adhesion kinase (FAK), which mediates cellular processes like growth, proliferation, adhesion, migration and survival, has been implicated in tumour development and maintenance. FAK overexpression in androgen insensitive cells increased the survival and proliferation of cells, whereas knockdown diminished this effect [250, 251]. Furthermore, FAK has been documented to form a complex with RACK1 and PDE4D5 to contribute to cell polarisation and directional migration [252]. In the study by Serrels et al, disruption of the FAK/RACK/PDE4 complex, by knockdown of either RACK1 or FAK or increase of cAMP, resulted in reduced polarisation and migration. In addition, FAK and the cAMP signalling pathway have been shown to interact in breast cancer studies [253]. This suggests that interactions between the cAMP pathway and focal adhesion signalling proteins could represent a pivotal point of crosstalk in prostate cancer. Although this is just one example of the importance of focal adhesion (FA) proteins in prostate cancer progression, it shows how FA molecules can be linked to different signalling pathways and cAMP, and how these can be exploited in cancer progression. Therefore, I can hypothesize that such proteins may be involved in a signalling axis that impinges on the proliferative effects of cAMP in PC and influences PDE4D7's control over these effects. Figure 5.6 displays the fold regulation of these genes. pcDNA3 control is not displayed for this array series as the genomic DNA negative control amplified and was therefore discarded as it was deemed to be contaminated. The remaining 3 plates showed no amplification within the negative control wells.

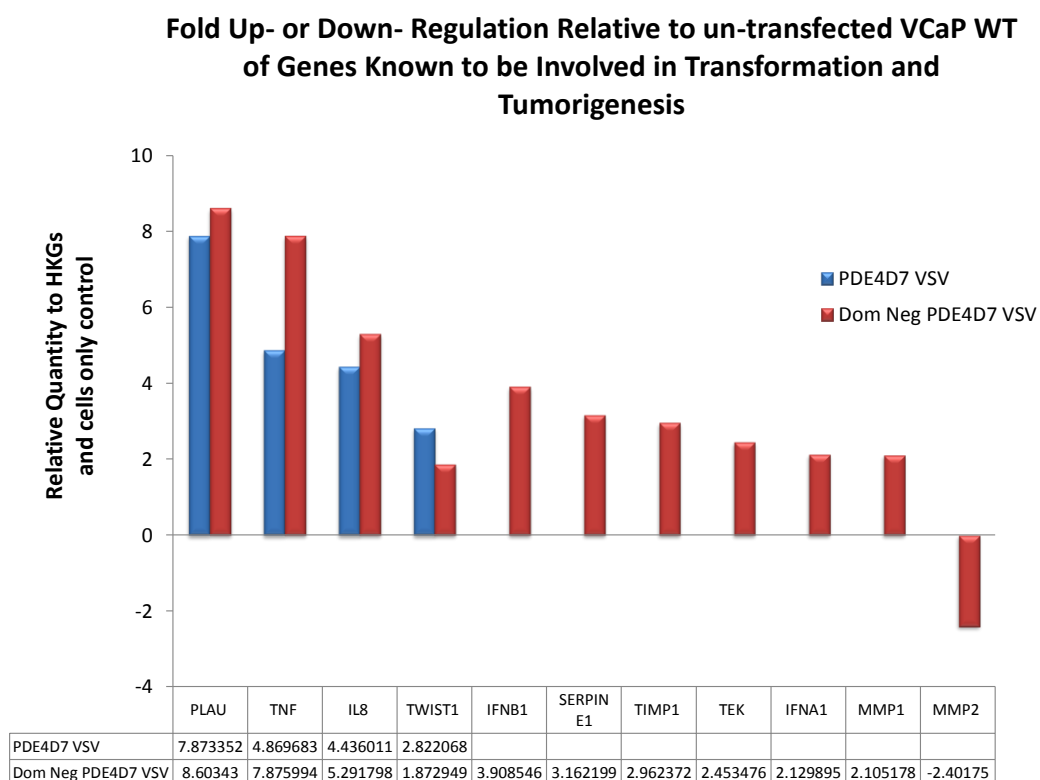


Figure 5.6 Fold regulation of RT² Profiler™ focal adhesion PCR array
RT² Profiler™ focal adhesion PCR array was conducted under 4 conditions; Cells only, pcDNA3 transfection control, PDE4D7VSV transfected and DN PDE4D7 VSV transfected cells. Data is expressed relative to VCaP cells only control and is displayed as relative fold change greater than 2.

The data above suggests that I have managed to isolate some potentially interesting genes/signalling pathways that are affected by increased expression of PDE4D7 and displacement of endogenous PDE4D7 using dominant negatives. Worryingly, some genes showed similar trends towards increased expression following transfection of the both the DN construct and the catalytically active PDE4D7. One would expect opposite effects resulting from ectopic expression of these two constructs. This could be a transfection effect, where high amounts of PDE4 overexpression (both WT and DN) could be affecting the stichiometry of protein complexes that are not regulated or affected by PDE4 activity. Alternatively, as the DN molecule and the catalytically active PDE4D7 share the same unique N-terminal region, I could hypothesize that effects seen are due to binding or scaffolding effects. However, one must be mindful that this is a high throughput screen with a low number of biological and technical replicates and will favour false positives. With this in mind, genes with high fold change when transfected with the catalytically active construct were cross referenced with

the literature and 6 genes were chosen for further analysis based on their links to (prostate) cancer progression, metastasis or survival and possible links to the cAMP signalling pathway.

5.2.4.3 CAV

The caveolin family is made up of caveolin 1, 2 and 3. They are predominantly found at the plasma membrane as part of caveolae structures (invaginations in the plasma membrane), however they are also expressed in the golgi, endoplasmic reticulum, vesicles and cytosolic locations. Caveolins are ubiquitously expressed but levels vary depending on tissue type. Caveolin 2 is co-expressed with caveolin 1 and requires it for membrane targeting. These are found mainly in differentiated cell types, such as endothelia and smooth muscle cells, whereas caveolin 3 is mainly expressed in muscle cells, such as skeletal and cardiac myocytes [254, 255]. Caveolin 1 has been linked to tumour suppression in early stage cancers. However, it has also been implicated in the regulation of endothelial cell proliferation and angiogenesis, and evidence suggests that caveolin 1 is upregulated in many drug-resistant and metastatic cell lines and tumours, positively correlating with tumour stage and grade [256]. Both Caveolin 1 and 2 have shown links to prostate cancer progression. Expression of caveolin 1 has been associated, in prostate cancer, with high Gleason score, metastases and disease recurrence [255, 257, 258]. Caveolin 1 exhibited a proportional increase from primary tumour to lymph metastasis [257] and overexpression has been predictive of progression and poor clinical outcome [255]. Unlike caveolin 1, caveolin 2's role is less clear. Nevertheless, it has been shown to be essential for the assembly of caveolae and acts as a positive regulator of caveolin 1 in human prostate cancer cell lines. In addition, a study by Sowa et al demonstrated that Cav 2 was shown to be expressed at very low levels in LNCaP cells, but the expression levels were distinctly elevated in androgen-independent PC3 cells, as compared to normal prostate epithelial cells. Overall, this data suggest that changes in the plasma membrane involving caveolin could be imperative to prostate cancer progression [259, 260]. In addition, caveolin 1 has also been linked to G-coupled receptors and serine/threonine kinases which interact with caveolin through the cav-1 scaffolding domain. Interaction with this domain then mediates the generation of platforms for compartmentalisation of downstream signalling events [261].

Furthermore, caveolin has been shown to decrease endogenous cAMP concentrations, and treatment of cells with FSK or IBMX leads to an dose-dependent decrease in caveolin mRNA levels [262].

5.2.4.4 CASP3

Caspase 3 is a protease that is activated during programmed cell death. Caspases are members of the cysteine protease family and 14 different caspases have been identified in humans. Caspase 3 is initially expressed as a pro-inactive enzyme, which is activated via selective cleavage of the amino bond following a certain aspartate residues to form an active heterotetrameric enzyme [263, 264]. Caspase 3 is responsible for the execution of apoptosis (along with caspase 6 & 7) by cleavage of the downstream end of the DNA repair enzyme poly(ADP-ribose) polymerase, which is essential for the initiation of apoptosis [264]. Activation of caspase 3 in prostate cancer cells leads to the execution of apoptosis in the cells and blockage of caspase activity within LNCaP cells leads to the reduced effectiveness of androgen-ablation induced apoptosis [265]. Thus it is not a surprise that immunoreactivity of caspase 3 is significantly decreased in prostate cancer [264]. Loss of expression of this key caspase could protect the prostate cancer cells against programmed apoptosis. cAMP activation has also been linked to caspase activity. In vascular cells it was shown that activation of adenylate cyclase via FSK treatment resulted in a decrease in caspase 3 activation [266]. Furthermore, cAMP elevation also protected against apoptosis and promoted growth in colorectal cancer. Here the elevation of cAMP levels decreased the activity, but not the production of caspase 3 [267].

5.2.4.5 BCL2

The main function of BCL-2 or B-cell lymphoma-2 is to decrease apoptosis in cells. BCL-2 acts to inhibit pro-apoptotic family members, which induce permeabilisation of the outer mitochondrial membrane and cause the subsequent release of apoptogenic molecules and caspase activation [268]. BCL 2 has been found to be involved in a wide range of cancers including prostate cancer. BLC-2 has been extensively linked to prostate cancer progression, with studies showing that BCL-2 is considerably increased in androgen independent vs androgen dependent cancers. In addition, an increased level of BCL-2 is linked to

metastasis and poor response to radiotherapy [269]. BCL-2 and the cAMP pathways are known to have points of crosstalk in prostate cancer signalling mechanisms. For example, a decrease in PKA R1 α subunit results in an increase in pro-apoptotic BCL family members and that this reduction in PKA subunit also inhibited tumour growth in nude mice. As BCL-2 acts to inhibit these pro-apoptotic BCL members, it could be suggested that a link could exist between the cAMP pathway and BCL-2 [188].

5.2.4.5.1 ETV1

ETV1 is a member of the ETS transcription factor family. There are 28 ETS genes that have been isolated in humans and these are separated into 12 groups. One of the defining characteristics of the encoded proteins is the ETS domain, which binds to DNA sequences with a 5'-GGA(A/T)-3' core. ETS proteins assemble distinct sets of coactivators or corepressors, and so the ETS protein bound to the DNA will influence and modulate gene transcription in different ways. In prostate cancer, the majority of tumours display a chromosomal translocation involving ETS (frequently the ERG gene, but here we will discuss the less frequent but still established, ETV1 gene) and TMPRSS2 gene (a trans-membrane protease serine enzyme). This translocation results in the generation of a TMPRSS2-ETS fusion gene. In this case, the ETV1 protein is controlled by the TMPRSS2 gene promoter/enhancer, which is under androgenic control and is highly expressed in prostate tissue. As a result of this control point, ETV1 undergoes androgen dependent expression in prostate cells and subsequent ETV1 overexpression in prostate cancer. All fusion proteins created in this way, retain the ETV1 DNA binding domain and thus cause dysregulation of gene transcription. Furthermore, cells with this translocation that are subjected to ETV1 down-regulation, display impaired cell proliferation, invasion and tumour formation in nude mice. The counter is also true, that overexpression of ETV1 in immortalized, non-transformed prostate epithelial cells can lead to enhanced proliferation and invasion [270].

It is also noteworthy that PKA has been shown to phosphorylate ETV1 on several sites, including serine 334, during in vivo studies. Phosphorylation on this site severely reduces the DNA-binding ability of ETV1 [271, 272].

5.2.4.6 IL6

IL-6 is a pleiotropic cytokine that regulates a wide range of biological actions within immune regulation, inflammation and oncogenesis. IL-6 's primary function is in acute state response and inflammation, and is secreted by monocytes. It has also been shown to interact with activated B-cells to induce terminal differentiation into anti-body secreting cells [273]. However, it does have other functions and can also be secreted by osteoblasts and skeletal muscle cells [274]. In prostate cancer, IL-6 levels are elevated in cancer tissues and PIN, and increased in circulating levels have been shown in metastatic prostate cancers. In the prostate cancer cell line, LNCaP, IL-6 has been suggested to have both growth promoting and inhibiting activities. Studies have indicated that IL-6 can mediate growth arrest in cells, as well as acquisition of NE characteristics, however these studies are contradicted by reports that IL-6 can increase androgen-induced growth rates by either autocrine or paracrine mechanisms [275, 276]. In vivo, cytokine signalling occurs in the context of other interacting pathways. One study showed that the co-treatment of LNCaP cells with agents that increase the activity of PKA and IL-6 expression caused a promotion of the NE phenotype above that seen with single agents. The author suggested that this indicates that PKA and IL-6 signals cooperate to produce gene transcriptional alterations that result in the acquisition of NE changes in LNCaP cells [275].

5.2.4.7 Validation of candidates using RT-qPCR

The genes described above were pulled from a high throughput screen and hence I wanted to validate them by using individual Sybr-green primers (SA Bioscience ®) and VCaP cells transfected as before with three constructs, pcDNA3 transfection control, PDE4D7VSV and DN PDE4D7 VSV. The pcDNA3 transfection control was used to assess fold changes in relative expression between samples. RNA purity, integrity and RIN were assessed via Agilent 2100 bioanalyzer and NanoDrop ® prior to use. cDNA expression of PDE4D7 was confirmed via RT- qPCR and PDE4D7 Taq-Man ® primer/probe set prior to use. This was repeated for each biological replicate.

A graph showing RQ to GAPDH HKG and pcDNA3 transfection control of various genes

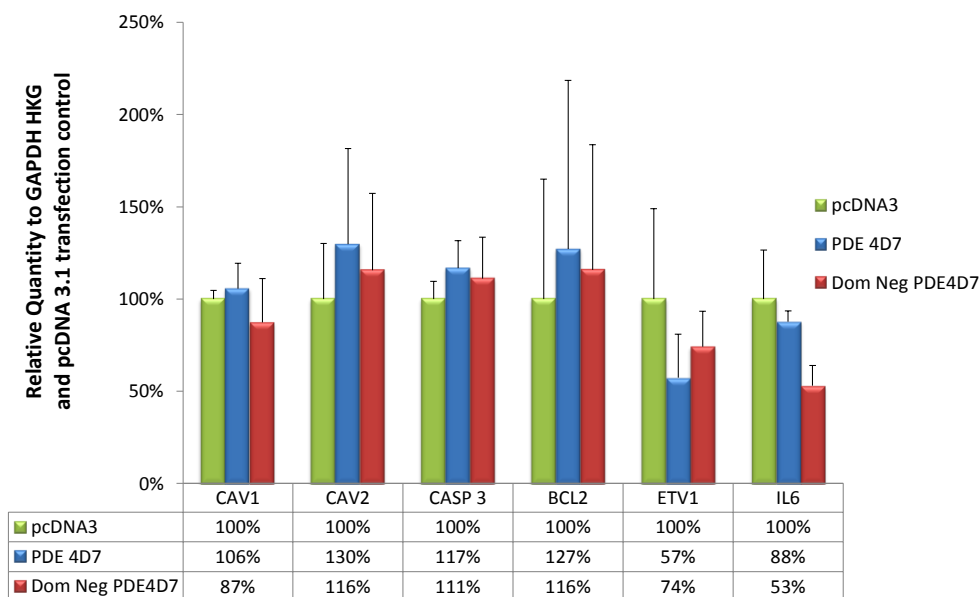


Figure 5.7 Validation of the genes isolated for potential interaction with PDE4D7 VCaP cells were transfected with pcDNA3, PDE4D7VSV and DN PDE4D7 VSV constructs. RT-qPCR was carried out with Sybr® green primers towards the indicated genes. Results are expressed as relative expression to GAPDH and pcDNA3

Candidate genes that had previously been selected from the of RT² Profiler™ screen were reprobred using RT-qPCR in order to confirm differential regulation following overexpression of WT and DN PDE4D7 constructs.. Unfortunately, none of the genes pinpointed during the high-through-put study, showed significant differences between over-expressed PDE4D7 and controls during the secondary assay. A trend towards ETV-1 down regulation is seen, however, due to variability of the experimental data, this change was not deemed significant. To control for potential housekeeping gene variability, 3 housekeeping genes were used in this validation study (see appendix).

Due to a highly disappointing failure of any of my candidates to repeat in the secondary assay, none of the “hits” were taken forward for further analysis. In a way to try and explain the failure to repeat results in the validation assay shown in the initial screening, one has to consider that while high through-put screening assays are a useful tool, they do concede a low number of biological and technical replicates and will favour false positives. Therefore, although care was taken by cross referencing results with the literature to reduce the risk of

selecting a falsely positive result, it is plausible that the proteins selected could not be effected by PDE4D7 overexpression or the effect could be less than in the initial screening and so is lost in the experimental noise. In addition, as previously suggested in the initial high through-put screen, the transfection of DN and active PDE4D7 constructs exhibited similar changes in protein expression insinuating that these effects were caused by binding or scaffolding effects. I could theorise that this scaffolding effects could be shown due to an over saturation with the transfected constructs. Therefore with multi-biological replicates and slightly changing transfection efficiency, this scaffolding “noise” maybe reduced.

5.2.5 Luciferase reporter arrays

In an attempt to circumvent problems associated with the lack of reliable data from the RT-qPCR experiment, we decided to use a different but complementary technique, Luciferase reporter assays. Luciferase reporter arrays were purchased from SA Biosciences ® and were employed as a method to reveal pathways influenced by PDE4D7 activity in prostate signalling. The array relays on dual luciferase reporter technology to provide a pathway-focused, transcription factor responsive readout of transcription factor binding.

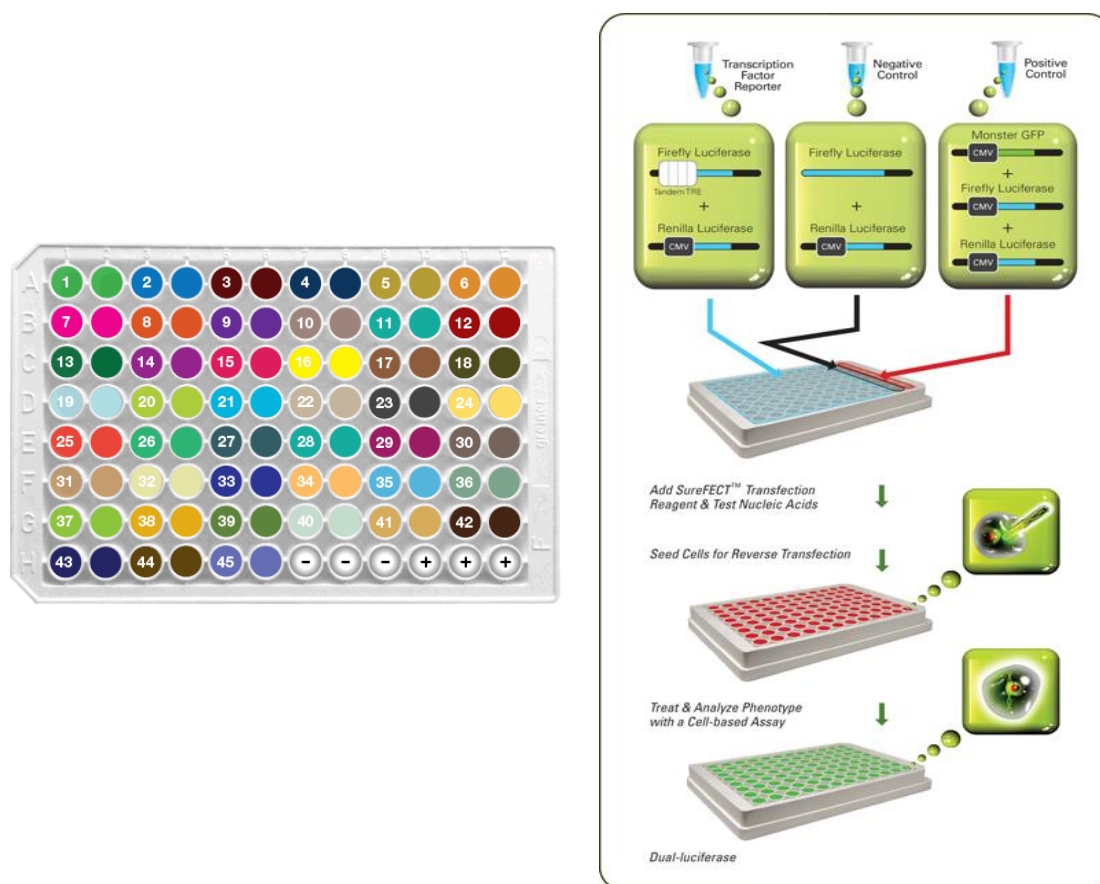
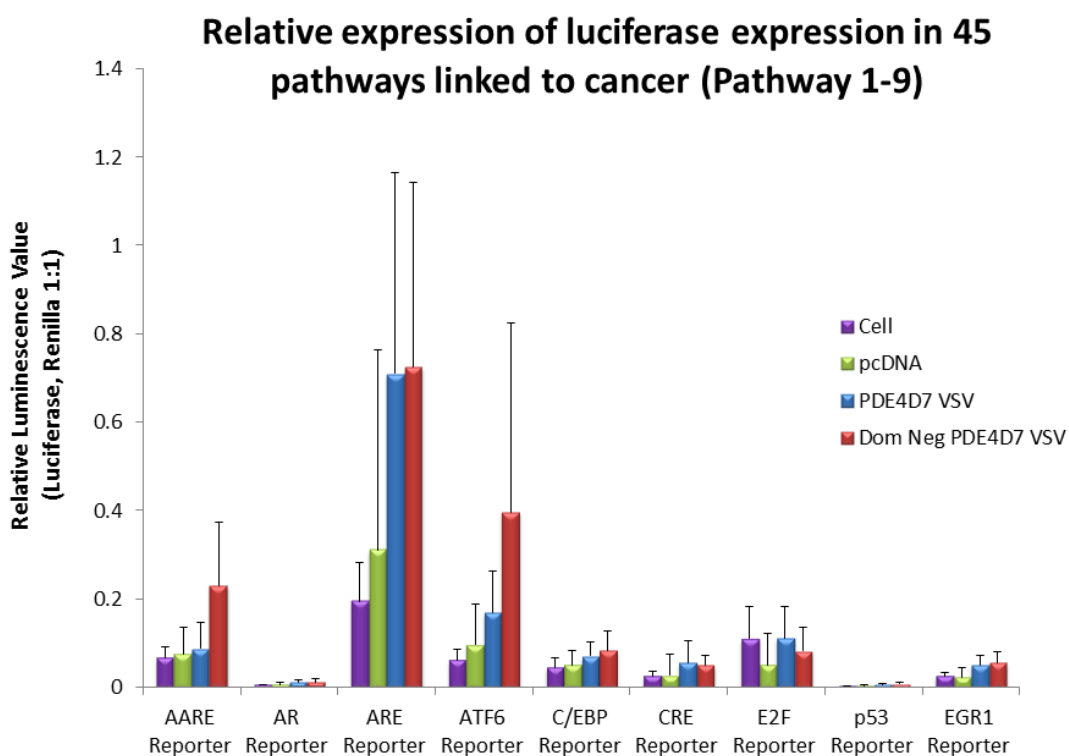


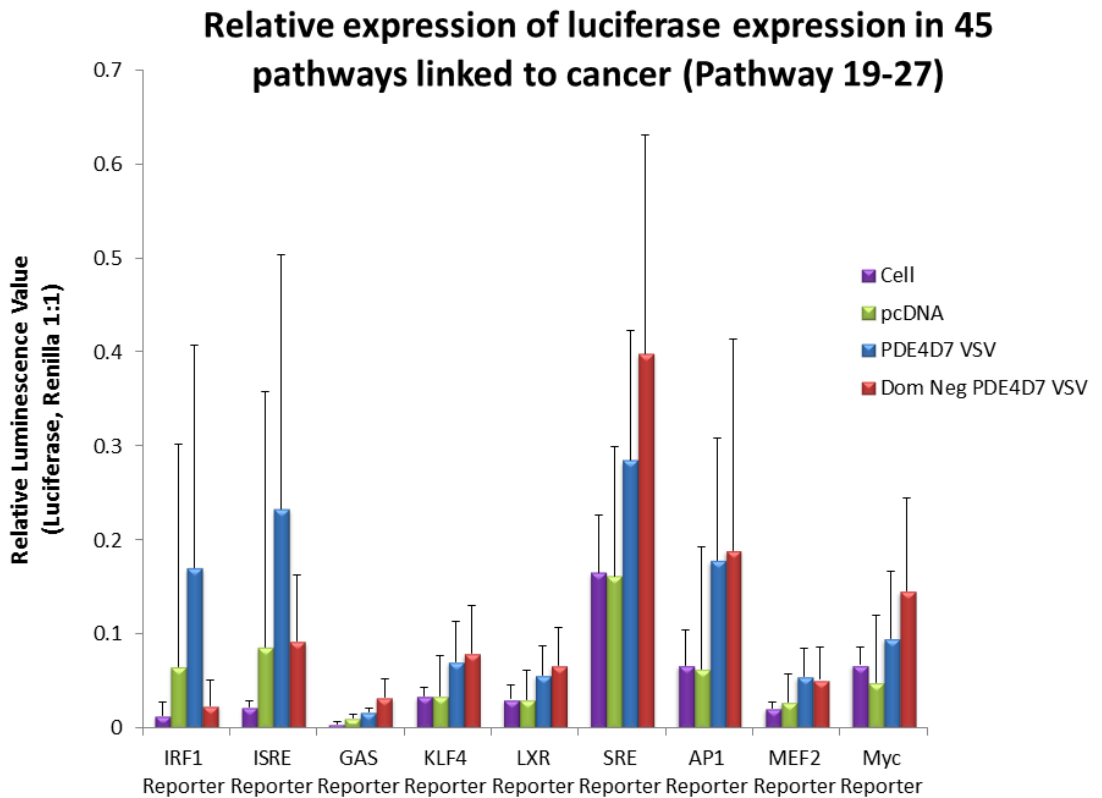
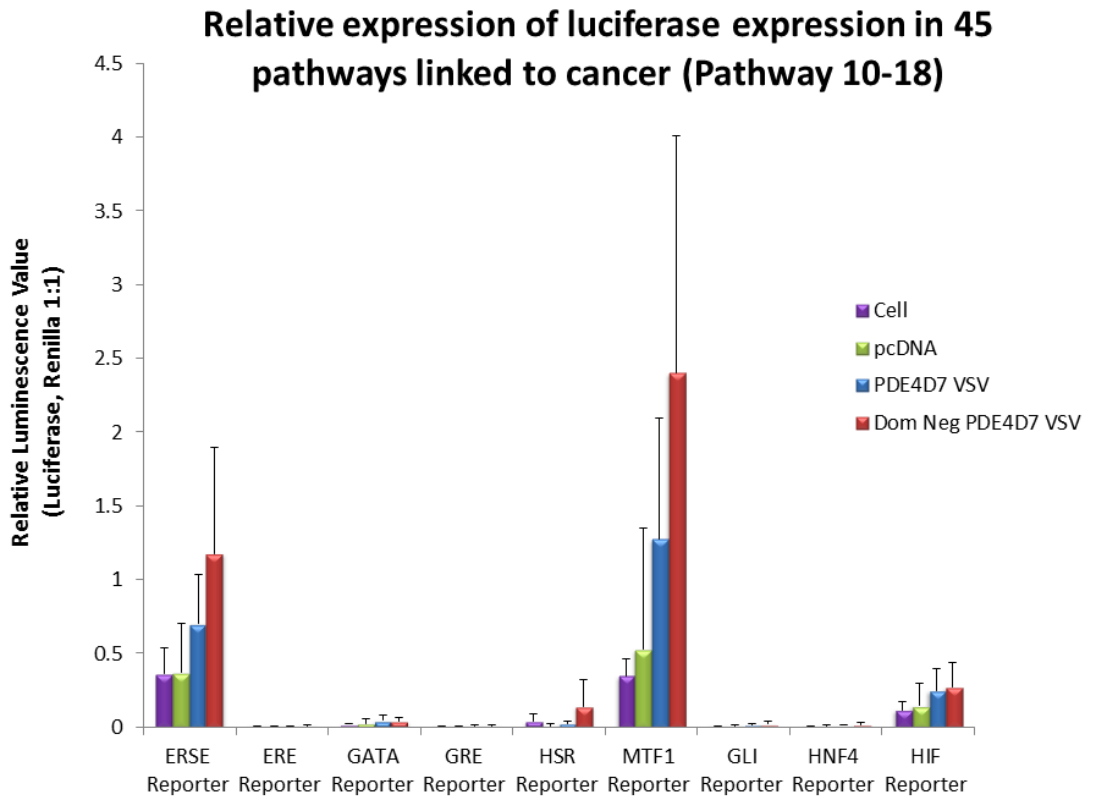
Figure 5.8 Diagram demonstrating the layout and procedure for the use of luciferase reporter arrays (SA Biosciences®).

As transcription factors play a central role in cellular processes and regulate gene expression, they can be used to provide readouts for the activation status of certain signalling pathways. The luciferase reporter arrays used in this study exploits this by combining a luciferase gene with a specific transcription factor binding site and basic promoter elements. Thus, when a signalling pathway is influenced, changing the activity of the downstream transcription factor, the level of expression of the luciferase gene is altered. Therefore, changes in luminescence intensity directly correlate with events that modulate transcription activity. The array contains 45 different firefly luciferase reporters each specific to a particular transcription factor. In addition, the array comprises a negative control, which is a non-inducible firefly luciferase, a positive control, which is a mixture of constitutively expressing GFP and a constitutively active firefly luciferase. Each well of the array also contains a constitutively expressing Renilla luciferase as an internal control. This acts to normalise for unwanted variability between wells by as Renilla utilise different

substrates when catalysing a luminescent reaction, and as a result does not interfere with the test, firefly luciferase luminescence (Figure 5.8).

As with the RT-qPCR experiments, the arrays were carried out using VCaP cells under four transfection conditions; transfection reagent only, pcDNA3, PDE4D7 VSV and DN PDE4D7 VSV. Unfortunately, no significant changes were shown between the transfection control and test treatments across all of the 45 reporters (Figure 5.9).





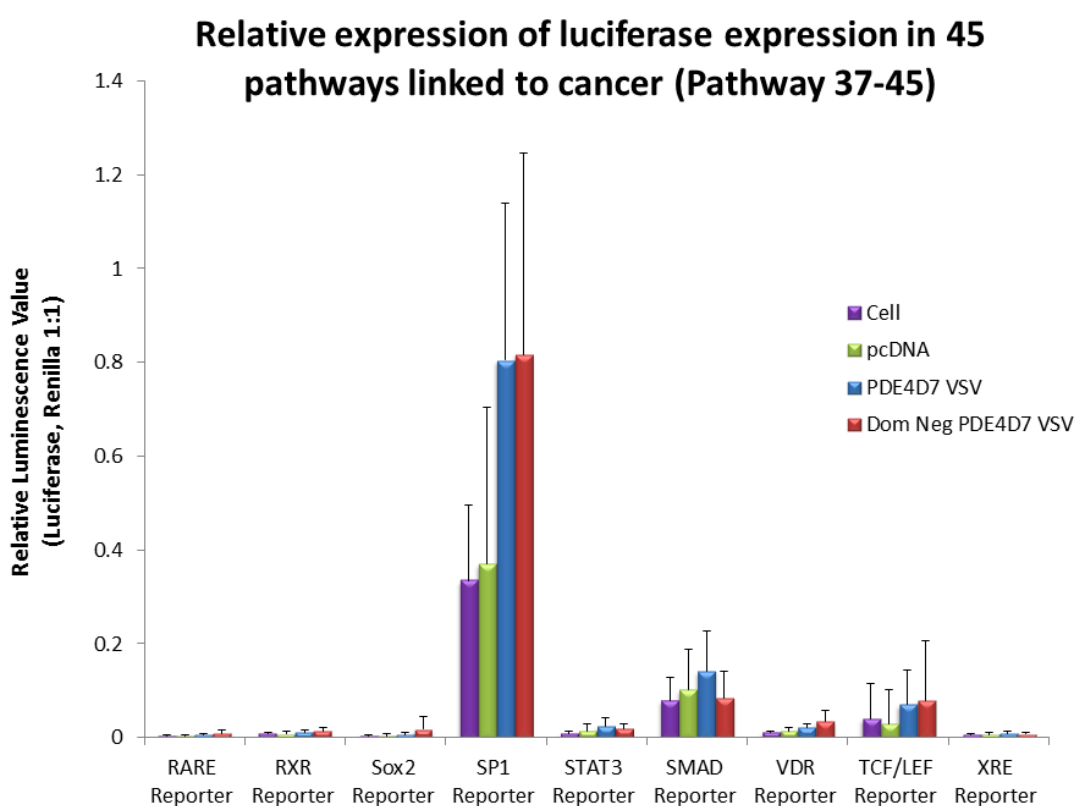
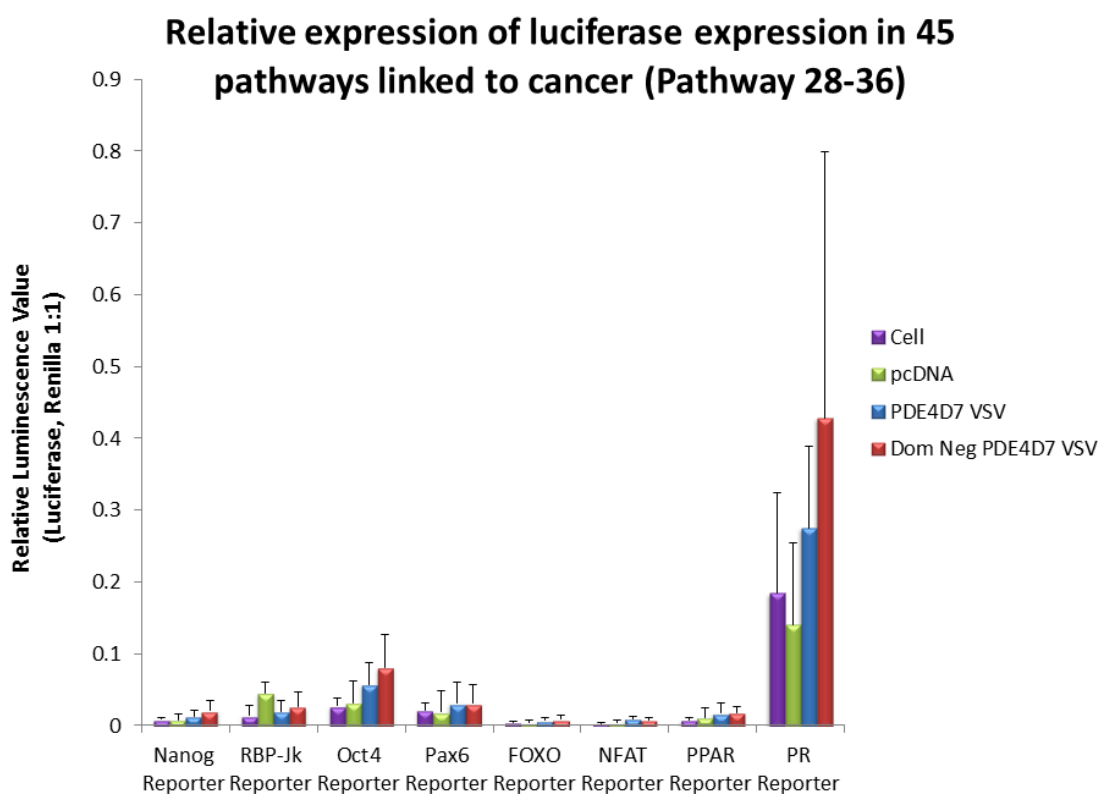


Figure 5.9 Luciferase reporter array results

Each graph contains 9 different transcription factor reporters. VCaP cells were transfected with pcDNA3, PDE4D7VSV or DN PDE4D7 VSV constructs plus Luciferase and Renilla reporter constructs. Luciferase luminescence was normalised using Renilla luminescence.

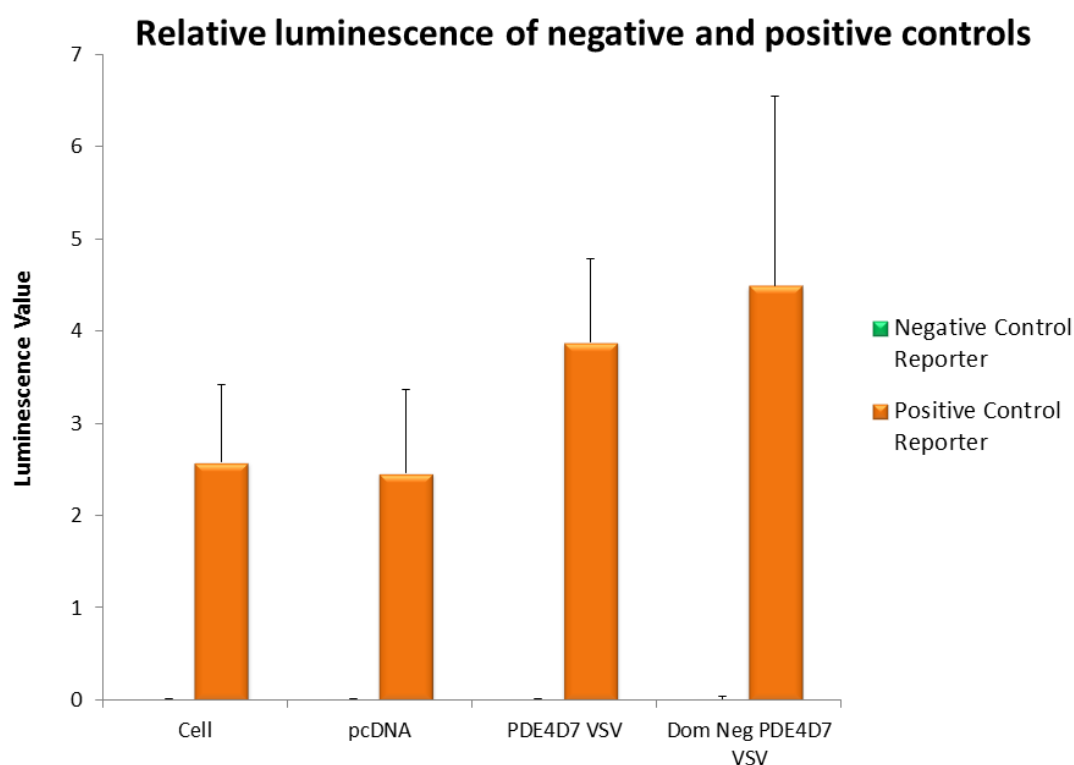


Figure 5.10 Positive and negative controls for the Luciferase reporter arrays.

The negative and positive controls of each array worked, indicating that changes in the test wells were not due to problems with the luciferase constructs, transfection of the constructs or the transfection reagent (Figure 5.10). By way of explanation as to why we failed to observe any significant changes, it is worth remembering that PDE4D7 is just one PDE in an array of compartmentalised micro-environments within the cell established by many different PDE isoforms (25 PDE4 isoforms in one family). Therefore, it is conservable that PDE4D7 upregulation alone could have small effects on downstream transcription factors and thus these changes could be swallowed by the ‘noise’ of the system. In addition to this, the VCaP cells used in this experiment already convey overexpression of PDE4D7 endogenously. Any concurrent downstream signalling effects on transcription factors could therefore be saturated within the cells only and pcDNA transfection controls, thus any potential additional effects of PDE4D7 transfection would be small and undetectable by this technology.

However, both of these theories are conjecture and we have to consider that PDE4D7 expression may not affect the transcription factors within this array.

5.2.6 RPPA

As I have been unable to implicate any signalling pathway using the above molecular techniques, I decided to move to a novel proteomics technique that allows analysis of a “snapshot” of signalling changes caused by an alteration in the chemical environment or genetic make-up of cells. RPPA (Reverse Phase Protein Array) is a high-throughput proteomics technology that allows the analysis of protein expression levels of a large number of biological samples. The coverage of proteins can include native or modified species (e.g. Phosphorylated) and depends on the selection of primary antibodies used in the first detection step.

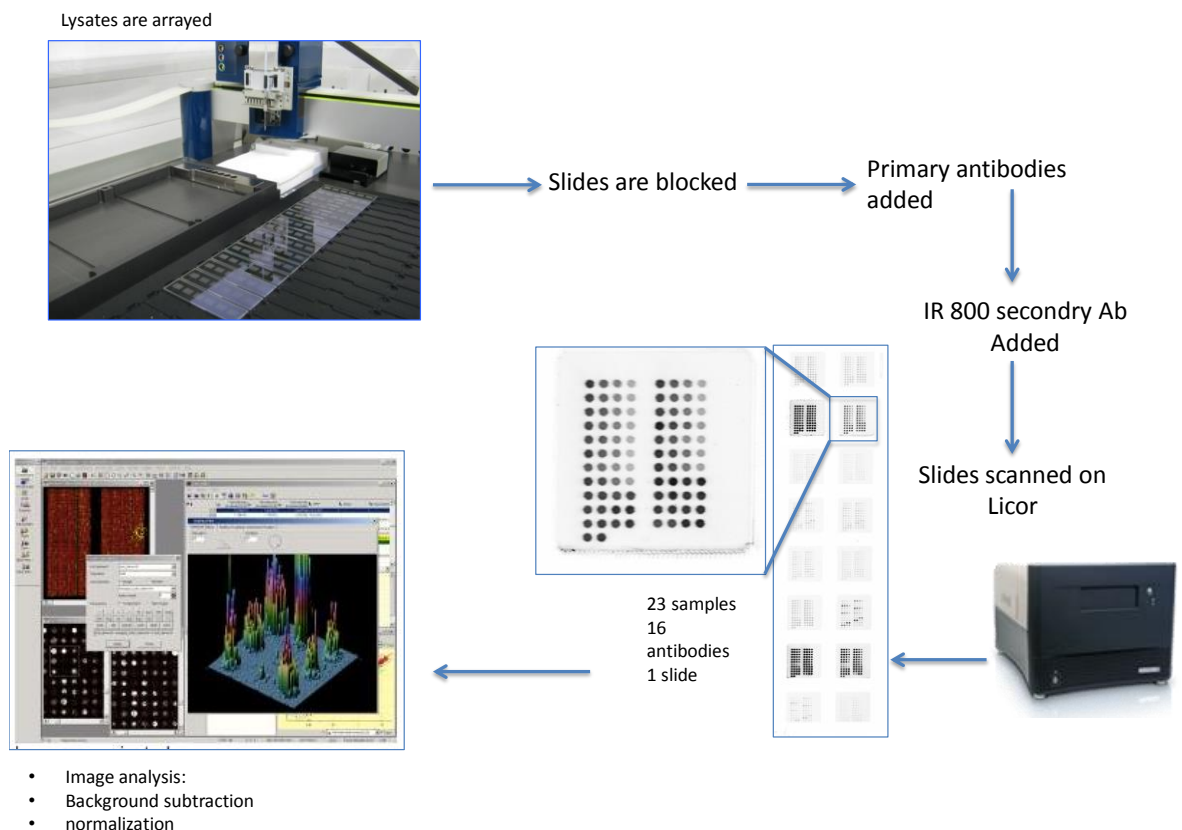


Figure 5.11 Diagram outlining the Reverse Phase Protein Array procedure

Cellular lysates were deposited as individual spots in an automated manner onto microarray slides. Proteins of interest were then detected using a large range of specific antibodies. Only small amounts of biological material are deposited per spot, and many samples can be analysed simultaneously on the same slide. Detection was carried out using a secondary antibody labelled with fluorescence. As this technology uses antibody technology, it shares the majority of the benefits and draw backs as western blotting techniques. With the foremost issue been antibody problems such as, cross-reactivity, sensitivity and specificity. To try to circumvent such issues, this screening was carried out by Dr Bryan Serrels (University of Edinburgh) who has a fully validated database of antibodies routinely used for this technique. VCaP cells were transfected with pcDNA3 transfection control, PDE4D7 VSV, dominant negative PDE4D7 VSV and cells/transfection reagent only.

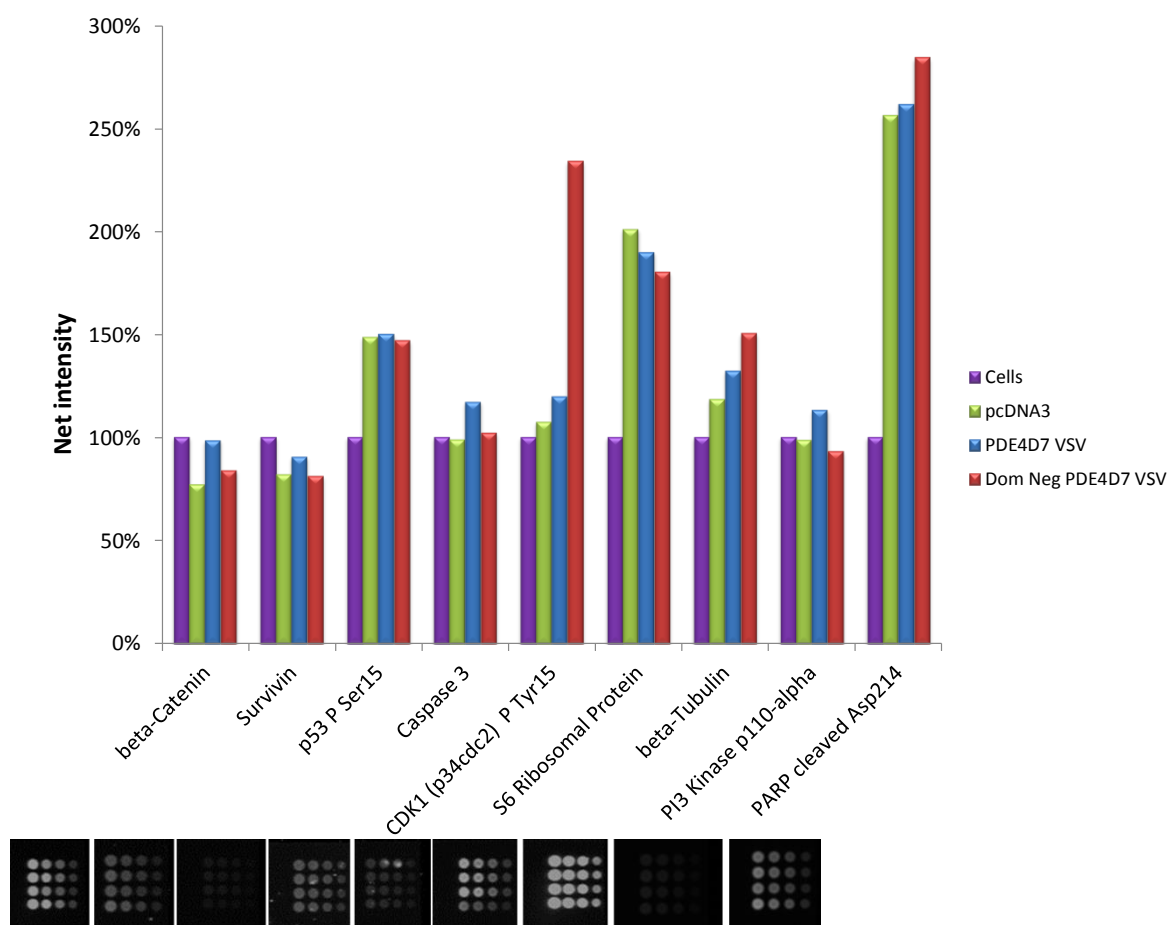


Figure 5.12 PDE4D7 transfected VCaP RPPA protein expression profile

VCaP cells transfected with pcDNA3 transfection control, PDE4D7 VSV, dominant negative PDE4D7 VSV and cells/transfection reagent only, spotted onto microarray slides and overlaid with different antibodies. Values are net intensity of fluorescence relative to cells only. (Screen carried out by Dr Bryan Serrels- University of Edinburgh)

Analysis for the RPPA experiment was conducted by Dr Bryan Serrels. Figure 5.12 shows proteins identified by the analysis software as potentially noteworthy (For full screen see appendix). Unfortunately none of the proteins show 2 fold or over increase or decrease in protein expression levels compared to both controls. DN PDE4D7 control is constitutively inactive construct (as previously described) and so I would expect this construct to cause similar effects on protein expression as the cell only and transfection controls. However, in some cases (Figure 5.12) DN PDE4D7 transfection elicits a much larger change in protein expression compared to either control, I could hypothesize that this increase could be due to scaffolding effects of the protein but as this effects is not shown with the active construct also this is unlikely.

Caspase 3 and PI3 kinase suggest that PDE4D7 transfection may have a small effect on these proteins. Caspase 3 was previously explored using RT-PCR (Figure 5.4), however changes in this protein, due to PDE4D7 overexpression, couldn't be validated (Figure 5.7). Validation of these proteins via western blot wasn't undertaken due to time and money constraints.

5.2.7 Celluspot arrays

CelluspotTM peptide array technology utilises arrays that are spotted with short peptide sequences. The individual peptides are covalently linked to cellulose and then spotted onto a membrane. This technology is able to form a 3D structure that is able to hold 1000 times more peptides than conventional peptide arrays, allowing low affinity protein-protein interactions to be detected. Here, pre-made arrays containing a variety of short, well documented kinase substrates, as well as consensus sequences for both, tyrosine and serine/threonine kinases were purchased from Intavis ®. The tyrosine kinase chip has 384 peptide substrates and the serine/threonine kinase substrates come as two chips with 768 peptides in total, each printed in duplicate.

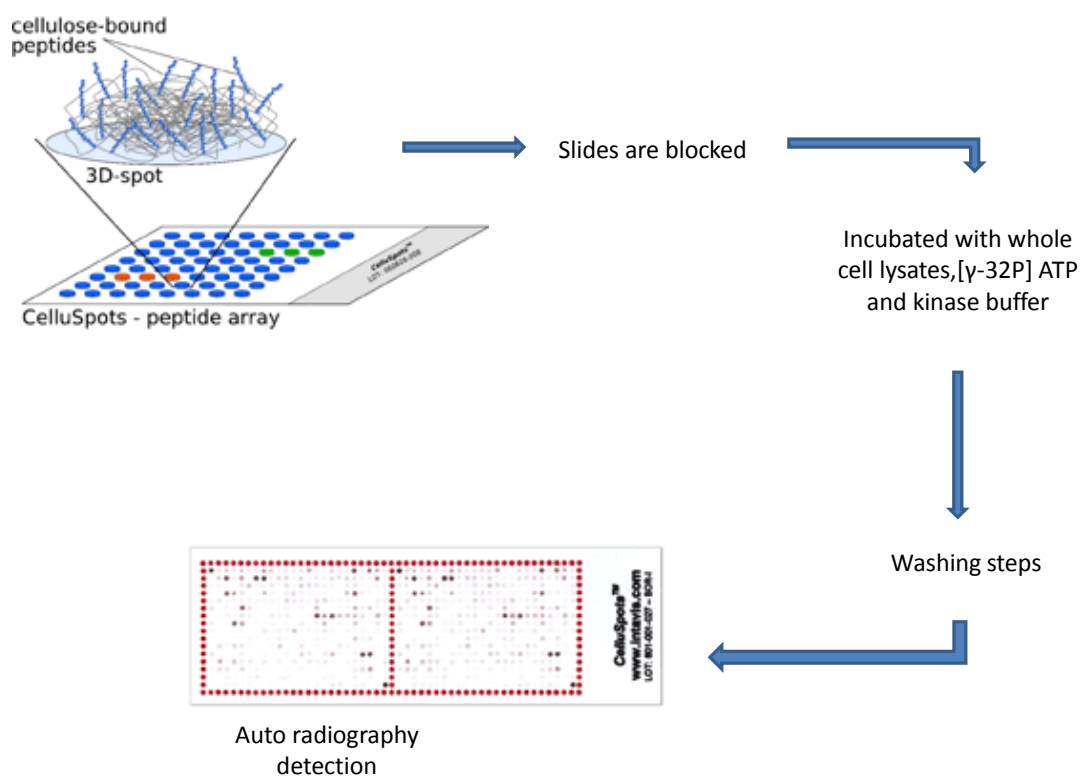


Figure 5.13 Diagram outlining the Celluspot array procedure

Lysates, transfected as previously discussed, were overlaid on the arrays with the appropriate kinase buffer and $[\gamma\text{-}^{32}\text{P}]\text{ATP}$ with the notion that a “snapshot” of kinase activation from the 4 cell treatment conditions (untreated, pcDNA3, PDE4D7 and DN PDE4D7) could be observed. Phosphorylation was detected by autoradiography and analysed using image J software. As expected several peptides were phosphorylated in all test conditions (see Appendix). Therefore, phosphorylated peptides with a fold change above 2, between PDE4D7 and pcDNA3 transfection control, and low internal variability, were cross referenced with the autoradiograph images to identify the short list that is displayed in Figure 5.14 (For full screen see Appendix). This list also demonstrated similar phosphorylation levels for DN PDE4D7 overexpression as pcDNA3 transfection control, showing that all increased phosphorylation activity displayed with overexpression of PDE4D7 is due to the catalytic activity of the enzyme.

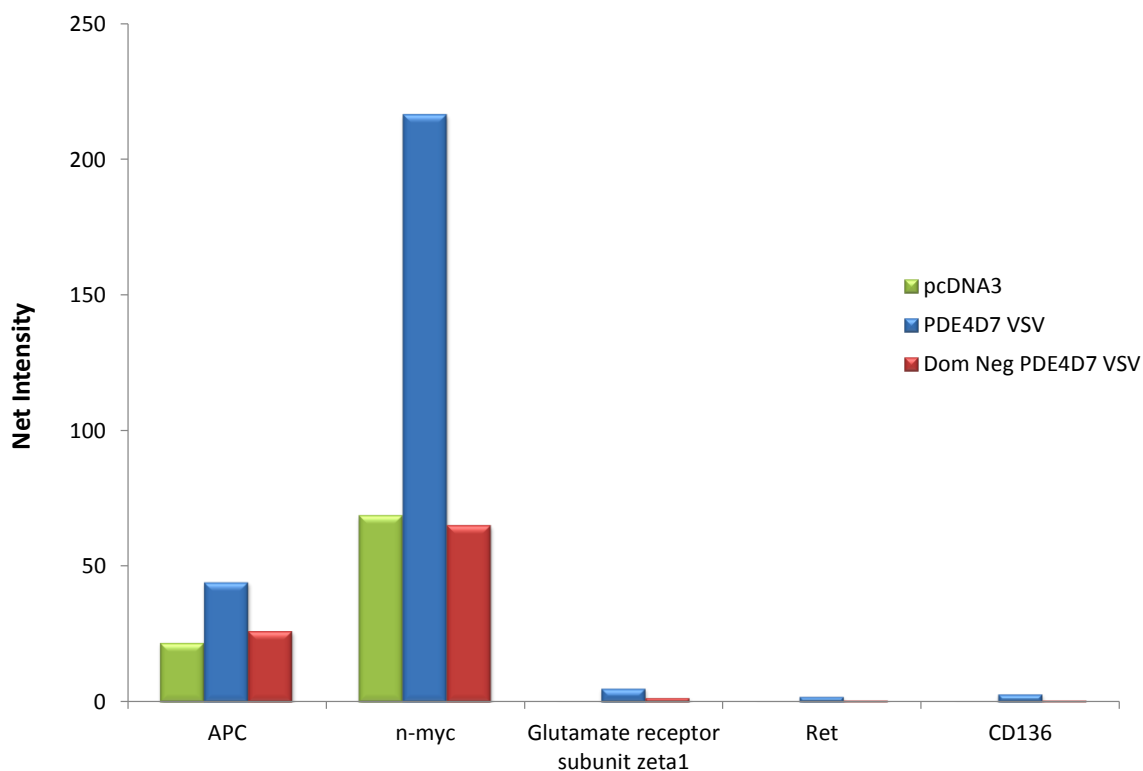


Figure 5.14 CelluSpot peptide array phosphorylation analyses with PDE4D7 transfected VCaP lysates

CelluSpot peptide arrays overlaid with VCaP lysates transfected with; pcDNA3, PDE4D7 VSV or dominant negative PDE4D7 VSV. Lysates were mixed with the appropriate kinase buffer and [γ - 32 P]ATP. Detection was carried out via autoradiography.

This short list of proteins potentially changed via PDE4D7 increase was then cross referenced with the literature. However, due to time constraints further analysis and validation was not carried out.

5.2.7.1 APC

Adenomatous polyposis coli or APC protein is a multifunctional protein that can contribute to a number of basic cellular processes, including cytoskeletal and transcriptional regulation. It is involved in Wnt-regulated degradation of β -catenin and can also regulate cytoskeletal proteins, consequently effecting cell migration, cell adhesion, and mitosis. The best-characterized function of APC is as a scaffolding protein. It forms a multiprotein complex with a variety of proteins including GSK3 β , β -catenin, axin, and numerous kinases and phosphatases. This signalling hub is essential for Wnt signalling. In the absence of

Wnt signals, GSK3 β in the complex is able to phosphorylate all three other complex proteins, leading to an increase in their interaction and subsequent destruction of β -catenin by the proteasome. In the presence of a Wnt signalling molecule, Dishevelled (Dsh), GSK3 β activity ceases and thus, the kinase activity in the complex drops, leading to a build-up of β -catenin in the cell. In general, accumulation of β -catenin correlates with deregulation of target gene transcription and potential changes in the proliferation and differentiation state of cells [277, 278]. Truncations in the APC gene are found in >80% of sporadic colonic tumours and are also accountable for Familial Adenomatous Polyposis (FAP), an inherited form of colon cancer. APC has also been detected in other cancers such as breast cancer [277, 279]. In prostate cancer, changes in the Wnt/ β -catenin signalling have been linked to cancer progression. In mouse studies, deletion of APC leads to elevated levels of β -catenin. Tumours that are induced via this deletion are highly proliferative, fully penetrant and follow normal cancer progression patterns [280].

5.2.7.2 N-Myc

N-Myc is a member of the Myc family. Myc family proteins function as transcription factors, and their broad transcriptional and biological activities regulate cell growth and proliferation, as well as activities such as stimulating angiogenesis and vasculogenesis, and blocking differentiation. Thus, this family of proteins is exploited and over-regulated in a range of cancers [281]. In human prostate cancer, an increased Myc gene copy number is often observed. MYC has also been shown to increase relevant to Gleason score, in protein and mRNA studies. The mechanism behind this increase in expression still remains elusive. However, some studies have shown that increased levels of MYC could be correlated with its activation via increased levels of β -catenin [282].

5.2.7.3 Glutamate Receptor Subunit Zeta1

Glutamate Receptor Subunit Zeta1 or NMDAR1/ GRIN1 is a ligand-gated ion channel that has a role in the control of synaptic plasticity and memory function. As a result, its effects have been widely studied in neuronal diseases, such as Alzheimer's disease and neuroblastoma's [283, 284]. Blockage of this channel has been reported to have many effects on calcium influx, kinase and

phosphatase regulation, translation and transcription, suggesting that NMDA receptor is coupled with many signalling pathways [285]. NMDAR1 like most cellular proteins can also phosphorylated, and this action has been shown to regulate discrete cellular processes. NMDAR1 can be phosphorylated by both PKC and PKA. It is phosphorylated by PKC on two residues (S890 and S896) and PKA on one (S897). Phosphorylation of S890 disrupts the clustering of the NR1 subunit, whereas S896 phosphorylation alone has no effect on GRINR1 clustering. However, when phosphorylated together with PKA phosphorylation of S897, receptor surface expression is increased [286]. In our study, peptides containing S890, S896 were available for phosphorylation on the chip.

In addition to neuronal malignancies, the channel subunit has been shown to be expressed in high-grade breast tumours, that, when treated with NMDAR1 antagonists, showed significant decrease in tumour growth [287]. In terms of prostate cancer, very little is known, however an immunohistochemical study by Abdul et al [284] showed a higher percentage staining in prostate cancer samples. They also showed that upon treatment of prostate cells with NMDAR antagonist it reduced growth of all cancer cell lines tested.

5.2.7.4 Ret

RET is a proto-oncogene that encodes a receptor tyrosine kinase which is most expressed in neural, kidney and urogenital cells. Is it required for the maturation of many cells in the nervous system and spermatogenesis. RET acts as a signalling receptor of a complex that binds the growth factors of the glial cell line-derived neurotrophic factor (GDNF) family and GFR α s ligand-binding co-receptors.

RET can activate several intracellular signalling cascades, which regulate cell survival, differentiation, proliferation, migration, chemotaxis, branching morphogenesis, neurite outgrowth and synaptic plasticity [288] and thus can often be exploited in cancers. The catalytic and signalling activities of RET, are regulated by the autophosphorylation of tyrosine residues in the cytoplasmic region. Some studies have revealed possible autophosphorylation sites within this region [289]. In our celluSPOT experiment, Y806 and Y809 were available for phosphorylation. Mass spectrometry studies show that both the kinase activity

and transforming activity of RET was impaired in Y806F and Y809F mutants .In prostate cancer, RET is suggested to be overexpressed in both high-grade PIN and in carcinoma [290].

5.2.7.5 CD136

CD136 or MST1R/RON is a proto-oncogene tyrosine kinase receptor, that binds macrophage-stimulating protein (MSP). On binding of this protein, autophosphorylation occurs on the intracellular section of the receptor, Y1238/1239 which regulates the catalytic activity of the enzyme and Y1353/Y1360 which provides a docking site for downstream signalling molecules [291]. These phosphorylations allow CD136 to affect many physiological processes including cell survival, migration and differentiation. These functions can be exploited in cancer, and CD136 has been shown to respond to other growth factors to promote cell survival. CD136 expression has been found in many epithelial human tumours including colon, and exhibits increased expression in a significant number of human breast cancer tissues and established breast cancer cell lines. Further studies have shown that this overexpression correlates with poor prognosis and aggressive disease [292, 293]. Furthermore, in prostate cancer, CD136 has been shown to be highly expressed in cancer tissue, compared to normal prostate tissue, and is also highly expressed in androgen-insensitive cell lines. In vivo, mice lacking functional CD136 presented decreased prostate tumour size and prostate vasculature [294, 295]. In this study, transfection of PDE4D7 increased the phosphorylation of Y1238/Y1239 phosphorylation site compared to pcDNA3 and DN controls, suggesting effects on CD136-tyrosine kinase catalytic activity.

5.3 Discussion

This study was undertaken to find interacting pathways/proteins for PDE4D7 in order to gain a better understanding of the molecular function of PDE4D7 in developing prostate cancer. As previously mentioned, a large amount of evidence exists surrounding cAMP signalling and its effects on prostate cancer progression. In comparison, there is a paucity of information for putative roles for PDEs. Studies by Uckert et al, reported on RT-PCR analysis of PDE expression in various anatomical regions of the prostate gland and found PDE 1A, 1B, 2A, 4A, 4B, 4C, 4D, 5A, 7A, 8A, 9A and 10A in each different histological region. In addition PDE4 and PDE5 hydrolytic activities were shown in the cytosolic fraction of the tissue, suggesting conversion of mRNA to active enzymes. Furthermore, immunostaining implied that the occurrence of these isoenzymes was not evenly distributed [239, 240]. These studies however, were of histological regions and lacked the precision of expression in differing cell types.

To further the knowledge regarding PDE expression within prostate cancer and its changes within cancer progression, a study was conducted by former laboratory member [179]. This study described PDE expression in 19 different cell lines and xenographs and isolated PDE4D isoforms, specifically PDE4D7, to be significantly downregulated between AS and AI prostate cancer samples. In correlation with this finding, using FRET sensors, they also observed a decrease in the ability to hydrolyse cAMP in AI cell lines suggesting that this change in mRNA expression translates into comparable changes in protein levels. In addition they localised PDE4D7 expression to the plasma membrane in AS cell line, suggesting that PDE4D7 is important in controlling compartmentalisation of cAMP signalling at the sub-plasma membrane.

However, this study failed to address why these changes in PDE4D7 regulation occur during prostate cancer progression and how these changes affect downstream signalling to execute cellular changes. We endeavoured to address this absence in knowledge by using several different high-through-put screens to try to expose interacting partners or downstream signalling effects of PDE4D7 over expression.

The RT² Profiler™ PCR arrays studies identified some interesting genes that are key in prostate cancer progression. Furthermore, these genes have been linked to cAMP signalling molecules in prostate, prostate cancer or cancer signalling.

Unfortunately these changes in gene regulation could not be validated. ETV1 shows possible trend towards downregulation when PDE4D7 is overexpressed, however as these genes are not highly expressed and thus, due to the low levels of transcript abundance they are more susceptible to fluctuations in expression, this causes an increase in variability within the experiment. In addition, unpublished work from the Baillie laboratory [179] showed that VCaPs shows the highest abundance of PDE4D7 isoform compared to other AS cell lines used in this study. As PDE4D7 is already highly expressed in this cell line, it has to be considered that this low level of transcript abundance could be a result of PDE4D7 endogenously causing dysregulation of these pathways and thus further overexpression is unable to cause much further downregulation of these genes. ETV1, as discussed, has been shown to be involved in chromosomal translocation with the TMPRSS2 gene which is highly expressed in prostate cancer. Downregulation of the ETV-1 gene can impair proliferation, invasion and tumour formation [270]. The TMPRSS2:ETS fusion proteins, however, are under androgenic control due to the TMPRSS2 gene promoter and subsequently is overexpressed in androgen sensitive cancerous tissues. As the AR has a pivotal role in prostate cancer, but few AR gene mutations have been shown, it could be hypothesised that other gene mutations could contribute to progression.

The VCaP cell line, used in this study, is often used as a model for TMPRSS2:ERG gene fusion. Cases with ETS fusions are often grouped together for simplicity, however, although there is functional overlap among ETS family members, individual ETS genes have distinct roles and can vary through development and oncogenesis. A recent study shows a difference in regulation between ETV1 fusion genes and ERG and their effects in cancer signalling. It was shown that ERG causes negative regulation of androgen receptor transcription, while ETV1 aids AR signalling by favouring the activation of AR transcription. Furthermore, they suggested that ETV1 expression, promotes autonomous testosterone production that is not shown with ERG [296]. ETV-1 transcriptional activity is increased following phosphorylation by PKA on the edge of the DNA-binding domain [270, 297]. The DNA-binding domain is highly-conserved between family members and

thus, it can be extrapolated that PKA has the same effect on ERG activity. As PDE4D7 would decrease PKA activity, it could be suggested that PDE4D7 overexpression could play a role in decreasing the transcriptional activity of ETS fusions. Given more time, I would have explored this novel signalling axis.

ETV1 downregulation via PDE4D7 signalling could be the key to explain how PDE4D7 exhibits its protective effects over regulation and how dysregulation of this pathway could lead to aggressiveness in AI disease. However, we have to take into account that no PDE4D7 siRNA knockdown model or AI cell line has been used to compare changes in gene regulation to an environment with low PDE4D7 expression. In addition, many other signalling events, such as phosphorylation, can affect protein function and thus trends in gene regulation by qPCR can't be fully relayed upon. All in all, further work into ETV1 and cAMP signalling maybe warranted but no clear conclusions can be drawn from this study.

As PDEs affect global cAMP levels and shape cAMP gradients in response to extracellular stimuli, they also indirectly affect the function of many signalling kinases. In this light, Celluspot array studies were employed to examine the phosphorylation status of signalling molecules in relation to PDE4D7 over expression. PDE4D7 is a long cAMP specific PDE and so acts to degrade cAMP. This method has identified proteins which have a distinctive increase in phosphorylation status with an increase in PDE4D7 suggesting a downstream, and not direct effect, of cAMP signalling. However these results are yet to be verified and much more work has to be conducted to ascertain how PDE4D7 over-expression contributes to this increase in phosphorylation and their effects in prostate cancer.

Despite high-through-put screen being a powerful tool for systematic identification of transcription changes or protein-protein interactions, they do have limitations. They are costly and thus often can only be carried out once. Also, due to the systematic nature of the screening methods used, no set of screening substituents can be complete, hence there will always be a set of untested substrates/binding partners/signalling systems. While high-through-put screens are useful in screening large amounts of interacting pathways with low starting materials, the drawbacks discussed and lack of time hindered my

evaluation. Given more time, a thorough validation of all of the proposed “hits” would have been done as this may provide novel insight into the functional role of PDE4D7 in prostate cancer signalling.

6 Discussion

6.1 Aims

cAMP signalling dynamics have often been implicated in prostate cancer signalling. In particular, the effects of increased cAMP on prostate cancer phenotype have attracted attention for over 40 years. This project looks at two major cAMP signalling molecules in the context of prostate cancer development and as such, the project was divided into two parts: 1) the profiling of PKA isoform expression in prostate progression and subsequent characterisation of the direct effects on AR; 2) the isolation of interacting pathways with PDE4D7 in advancing prostate cancer, to establish how changes in PDE4D7 regulation can effect prostate cancer signalling.

6.2 cAMP Signalling Molecules and Prostate Cancer

Cancers are no longer regarded as isolated masses but rather that their properties relay on the complex interactions of the surrounding micro-environments. In prostate cancer, this involves complex interaction between the stromal and epithelial cellular compartments resulting in the drive of tumour progression [298]. This ever changing complex environment of stimulatory and inhibitory factors, changes in secondary messenger molecules are paramount for cells to interpret this environment. PKA is the 'classical' effector molecule of cAMP and PDEs are the only known means which to degrade cAMP signal, thus these two signalling molecules together can underpin the majority of cAMP signalling and compartmentalisation in cells [9, 32].

6.2.1 PKA Sub-Unit Regulation Change

6.2.1.1 Regulatory subunits

In the first part of this study I have shown the expression pattern of PKA regulatory and catalytic isoforms within androgen sensitive and insensitive cells. Here, I showed that PKA RII β and RI α subunits are expressed inversely in prostate cancer cells and their ratio switch in AI cells vs AS cell lines. This is in keeping with other cancer studies [50, 160, 163, 169]. In addition, I have shown that RII β

expression diminishes in cells no longer under androgenic control, leading to the hypothesis that RII β may have a direct effect on AR signalling. Upon testing whether RII β exerts control on the AR via direct binding, I showed that this was improbable and another indirect mechanism was likely. Although I mainly focused on PKARII β isoform, I also examined the expression of all other PKA regulatory subunits. My study showed that, in addition to RII β , PKARI α and PKARI β also significantly change in regulation as prostate cancer progresses. PKARI α has been shown extensively to be up-regulated as cancer progresses [163, 171, 299]. This disruption in isoform balance is associated with tumorigenesis and tumour proliferation [160, 161, 163]. Furthermore, PKARI α has been isolated as a potential biomarker for prostate cancer progression and in recent years PKARI α antisense molecules in addition to androgen deprivation therapy, has shown an enhanced decrease in tumour volume and significant increase in tumour apoptosis [171, 299]. However, despite this significant research, the mechanism of how PKARI α isoform exerts its action has still not been fully investigated. As RII β and RI α ratio is obviously important in prostate cancer progression, if more time was allowed it may be prudent to further explore my hypothesis that RII β is effective in AR signalling, but in a less direct manner. This research may lead to an understanding of how the switch from RII β to RI α is important in prostate cancer progression and lead to the uncovering of the mechanism whereby RI α shows its effects in an AR free environment.

6.2.1.2 Catalytic subunit

Additionally, the first part of this study highlighted PKAC β as significantly down regulated in AI vs AS prostate cells. This initial data is concurrent with data expressed in a study by Kvissel et al, in which PKAC β 2 is shown to be down regulated in AI tumour cells [169]. A proposed synergism between cAMP and steroid pathways or activation of AR via FSK treatment has been shown in studies [215, 229-231], thus I went onto show that PKAC β mRNA is downregulated upon androgen ablation and mRNA levels are again decreased in AI differentiated LNCaPs. This suggested that PKAC β protein regulation is directly linked to androgens and androgen receptor function. Using novel peptide array technology I was able to identify possible phosphorylation sites on the AR by PKAC β and

using phospho-antibodies produced to isolate the putative phosphorylation site as pS791.

However, the kinetics of phosphorylation at S791 are slow following FSK/IBMX treatment. As PKA is rapidly dissociated from the R subunits upon cAMP binding and nuclear translocation of PKA catalytic unit can begin within 3-5 minutes, it is unclear why this is the case. This type of slow kinetics have also been shown in the progesterone receptor, and studies into androgen receptor phosphorylation have suggested that most phosphorylation sites show a delay in hormone dependant maximal phosphorylation [205, 235]. Furthermore, AR has been shown to destabilise upon phosphorylation of S791 by AKT and restored following treatment with the proteasome inhibitor MG132. These results suggest that phosphorylation of AR at S791 plays a role in the ubiquitination of AR and modulates its degradation via the proteasome [232]. PKA and AKT have been shown to share the same phosphorylation site due to their structural similarities [233, 234]. Thus I could hypothesize that the phosphosite maybe monopolised by both kinases. However, significant amounts of further research are required to delineate the function of this PKA phosphorylation site during early prostate cancer. A longer study with FSK/IBMX treatment may prove to be enlightening.

Due to the obviously important enzymatic activity of PKAC β in prostate cancer, one may also postulate it may be a target for therapeutic intervention during the progression of prostate cancer. Certainly if my hypothesis is correct, and phosphorylation of this site causes de-stabilization of the AR, small molecules tailored to this site could be used to decrease androgen receptor function in prostate cancer thus leading to a less invasive therapeutic approach compared to conventional methods and could be worth investigating. However, the data presented in other studies suggest that FSK treatment and activation of PKA leads to the progression of prostate cancer and activation of PKA may actually be of detriment to prostate cancer patients [76].

In conclusion further study is required to delineate the function of the PKA isoforms in PC. However, this is an exciting area of research which, with more work, may help us better understand the progression of prostate cancer from AS to AI.

6.3 PKA RII β and PKAC β as Biomarkers

In the context of using PKAC β and RII β isoforms as biomarkers, the expression of protein and mRNA in the initial screening does exhibit a significant change in transcript levels between AS and AI prostate cancer phenotypes. However there is an inherent problem when using intracellular proteins as biomarkers: How are they measured? Without a biopsy of the tissue it is difficult to specifically measure expression of these proteins. Therefore if a biopsy is needed then what significance are these proteins as an initial diagnostic tool? Biopsies of patients is common practice, however at this stage immunohistological studies can be conducted which are very accurate at determining stage and prognosis of the prostate tumour. It could be plausible to use these proteins alongside conventional staging methods to assess the androgen sensitivity of the samples and potentially defining populations of AI cells, prior to clonal selection by androgen withdrawal therapy.

Furthermore, if one takes into account that PKAC β and PKARII β are both upregulated between normal prostatic epithelial cell line, PNT1, and androgen sensitive cells (Chapter 3), which is further correlated in tumour studies by kvissel et al [169], thus although I first proposed these proteins as biomarkers due to their decrease into androgen independence, they're potential for use as a diagnostic tool may actually be in determining their increased expression during tumourigenesis and use as a marker for prostate cancer progression. For instance, they may be used as markers for remission or the development of AI disease in patients treated with androgen ablation therapy.

To solve the problem of how to detect PKAC β and RII β in order to use them as a clinical biomarker a new method that has shown initial promise with PDEs could be tested and potentially implicated for use with these proteins also. This method involves the use of urine sediments; phosphodiesterases are also intracellular enzymes that are not secreted into the extracellular environment. However, urinary sediments contain dislodged cells from the urinary tract and the prostate [300]. Initial data by Researchers at Philips Research Centre (Eindhoven) has shown that PDE4D7 mRNA can be detected from these dislodged cells [179]. This could be a potentially interesting technique that could be

utilised to detect PKAC β or RII β in urine, rendering these molecules promising biomarkers.

6.4 PDE4D7 Compartmentalised Signalling Dynamics and Interactive Pathways

Continuing on from work previously carried out in the laboratory, the second section of my thesis (chapter 5) investigates the interacting pathways/proteins for PDE4D7 in order to gain a better understanding of the molecular function of PDE4D7 in developing prostate cancer.

Previous work described PDE expression in 19 different cell lines and xenographs and isolated PDE4D7, to be the highest downregulated between AS and AI prostate cancer samples. In addition, it was shown that PDE4D7 expression was localised to the plasma membrane in AS VCaP cell line, suggesting that PDE4D7 is important in controlling compartmentalisation of cAMP signalling at the sub-plasma membrane. However, this study failed address why these changes in PDE4D7 regulation occur during prostate cancer progression and how these changes affect down-stream signalling to execute cellular changes.

In order to address these questions, I used a varied range of high-through put screens which look at the messenger, protein or activity levels of various proteins when PDE4D7 is overexpressed in VCaP prostate cancer cell line. Unfortunately changes in gene regulation shown could not be further validated, or due to time constraint, weren't validated. One may want to consider that as VCaPs cells have the highest abundance of PDE4D7 compared to other AS cell lines used in this study [301], that PDE4D7 is already highly expressed in this cell line and so low level of transcript abundance or protein expression could be a result of PDE4D7 endogenously causing dysregulation of these pathways and thus further overexpression is unable to cause much further downregulation of these genes. Therefore siRNA knockdown model may be useful in further validations of potential 'hits'.

Despite high-through-put screen being a powerful tool for identification of transcription changes or protein-protein interactions, they do have limitations. Due to the systematic nature of the screening methods, not all of the potential

interacting proteins can be screened. In addition, the quality and variability of the screen itself is also a major limitation. While every effort was taken to overcome these draw backs (i.e. picking relevant proteins and buying in the high-through put kits), the sample size is still relatively small compared to the size of libraries screened by pharmaceutical companies which often constitutes millions of potential partners. Given more time, a thorough validation of all of the proposed “hits” would have been carried out, including a knockdown model for PDE4D7. This may potentially provide novel insight into the functional role of PDE4D7 in prostate cancer signalling.

Appendices

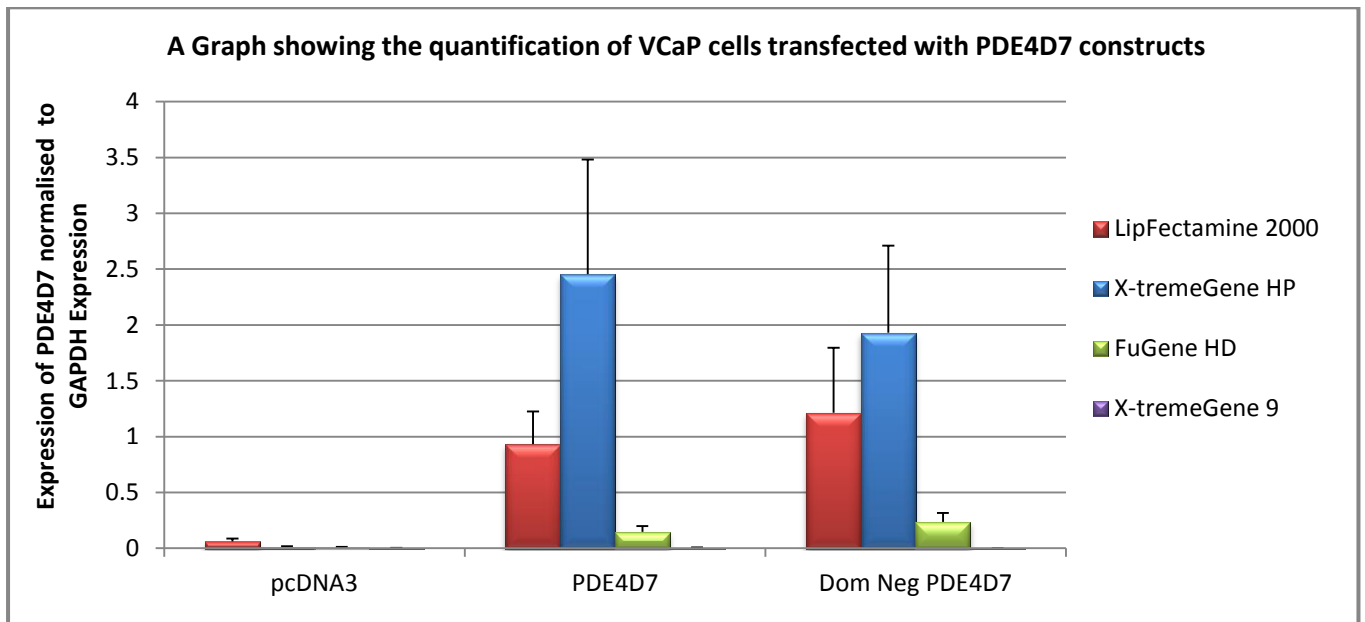


Figure 7.1 Quantification of VCaP cells transfected with PDE4D7 constructs

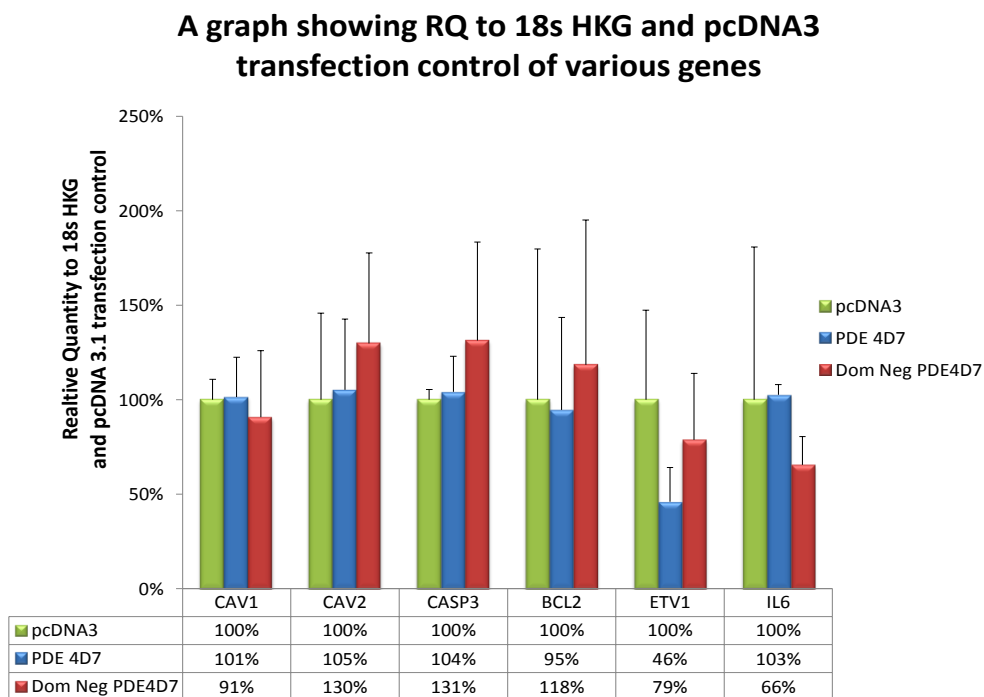


Figure 7.2 Validation of the genes isolated for potential interaction with PDE4D7 (18s HKG)

A graph showing RQ to B-Actin HKG and pcDNA3 transfection control of various genes

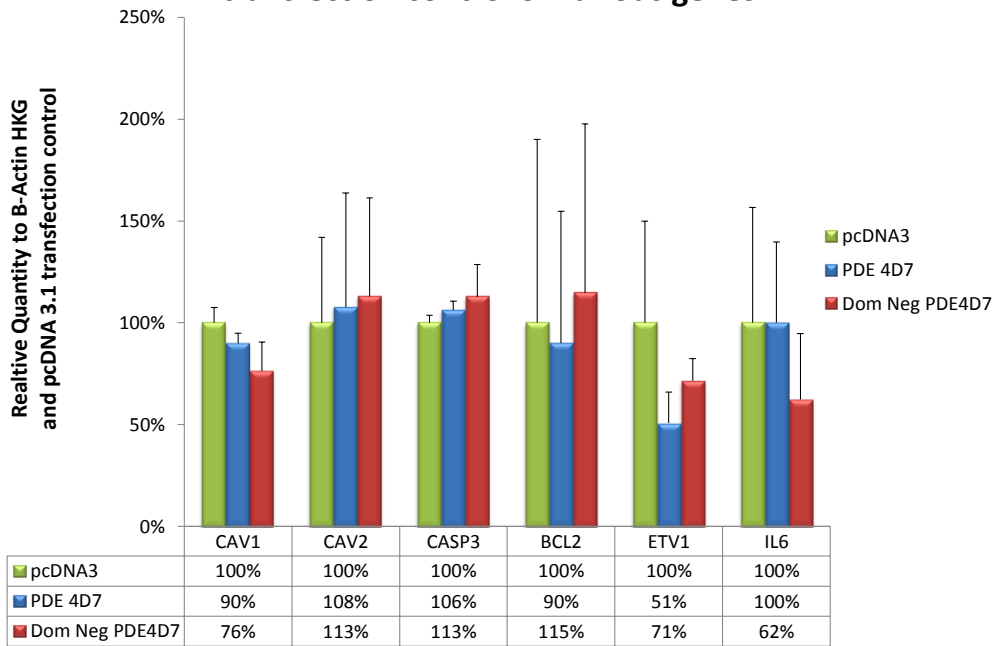


Figure 7.3 Validation of the genes isolated for potential interaction with PDE4D7 (β -actin HKG)

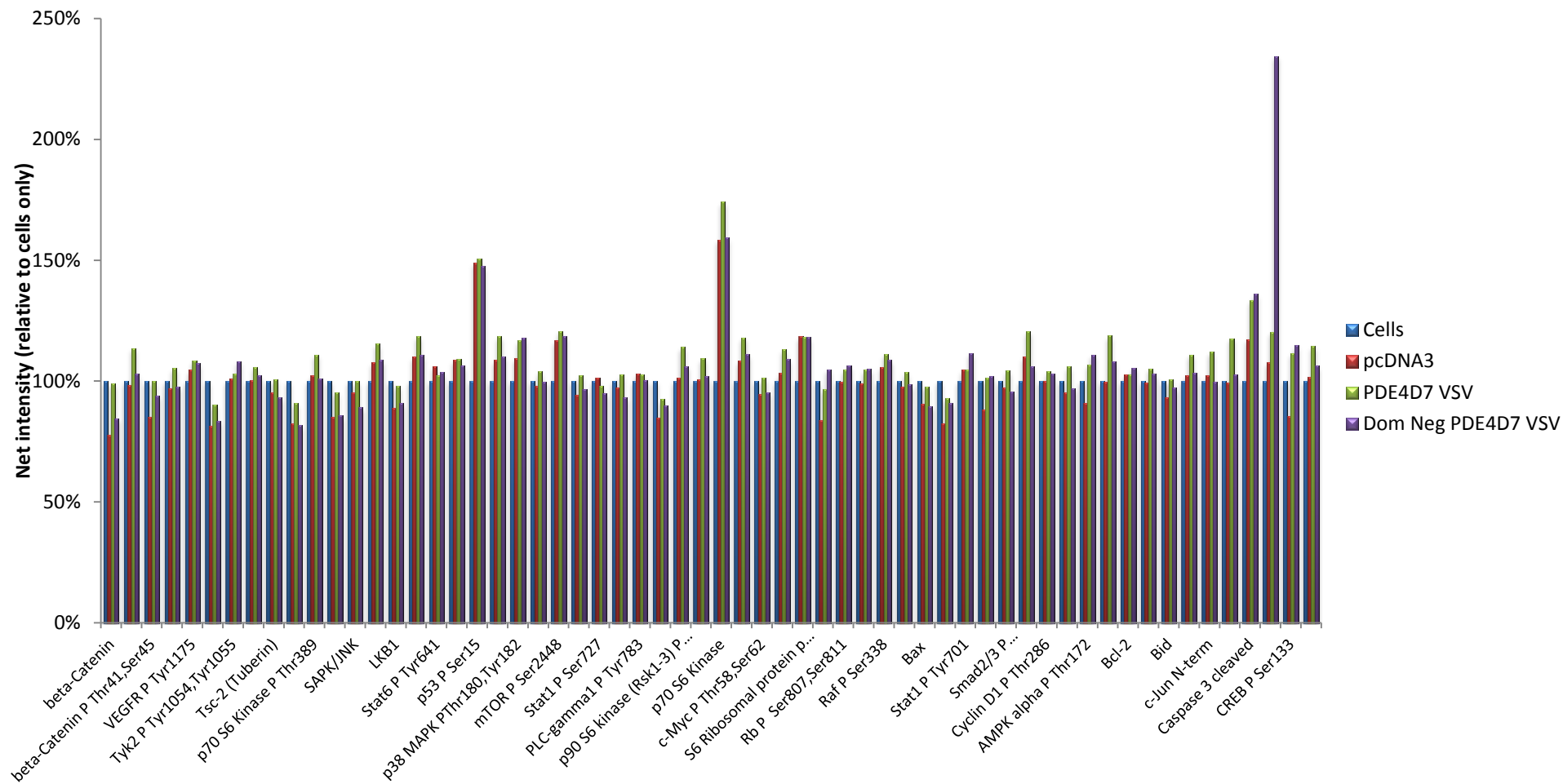


Figure 7.4 PDE4D7 transfected VCaP RPPA protein expression profile (Full Screen Part 1)

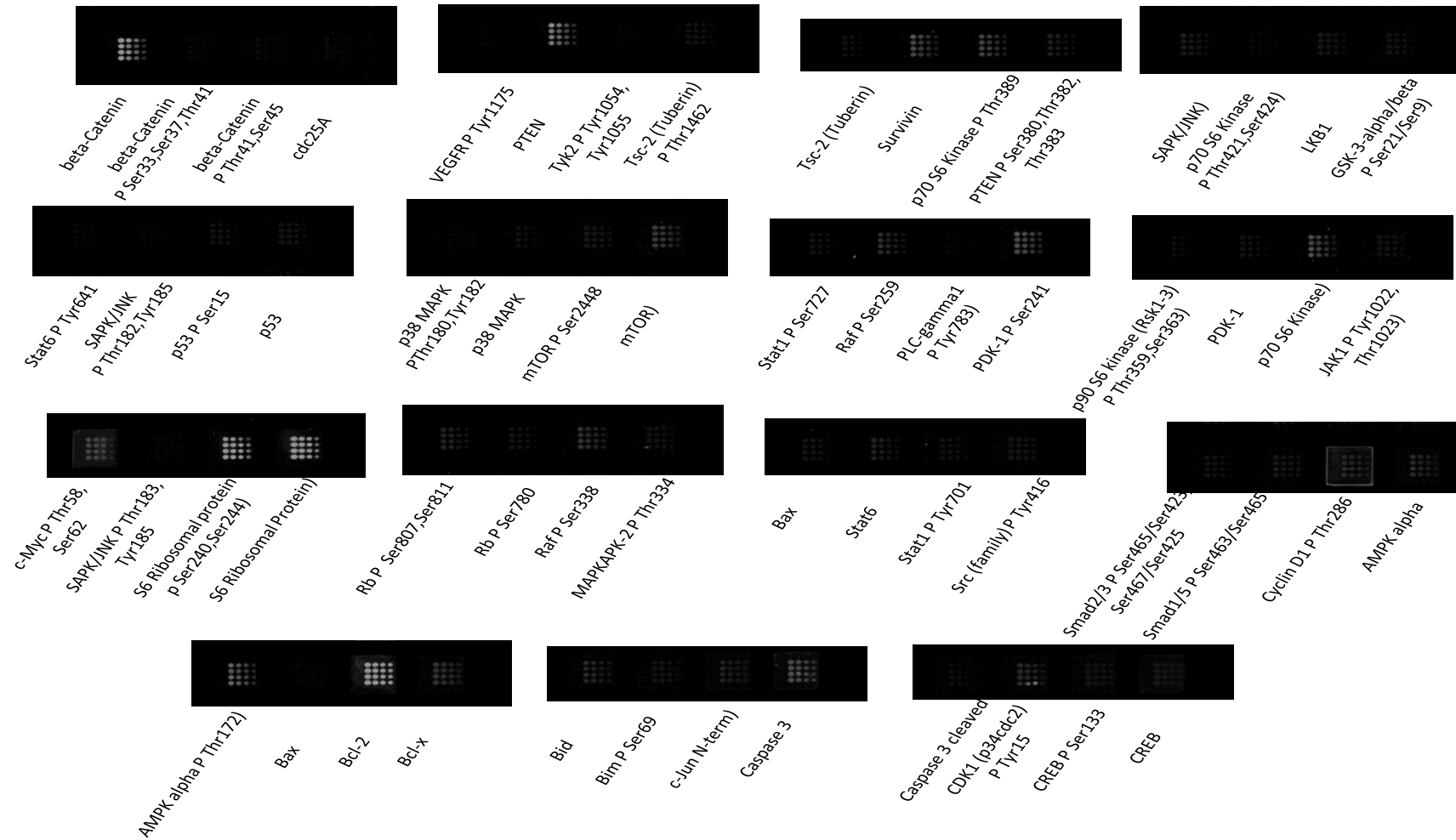


Figure 7.5 PDE4D7 transfected VCaP RPPA protein expression images (Full Screen Part 1)

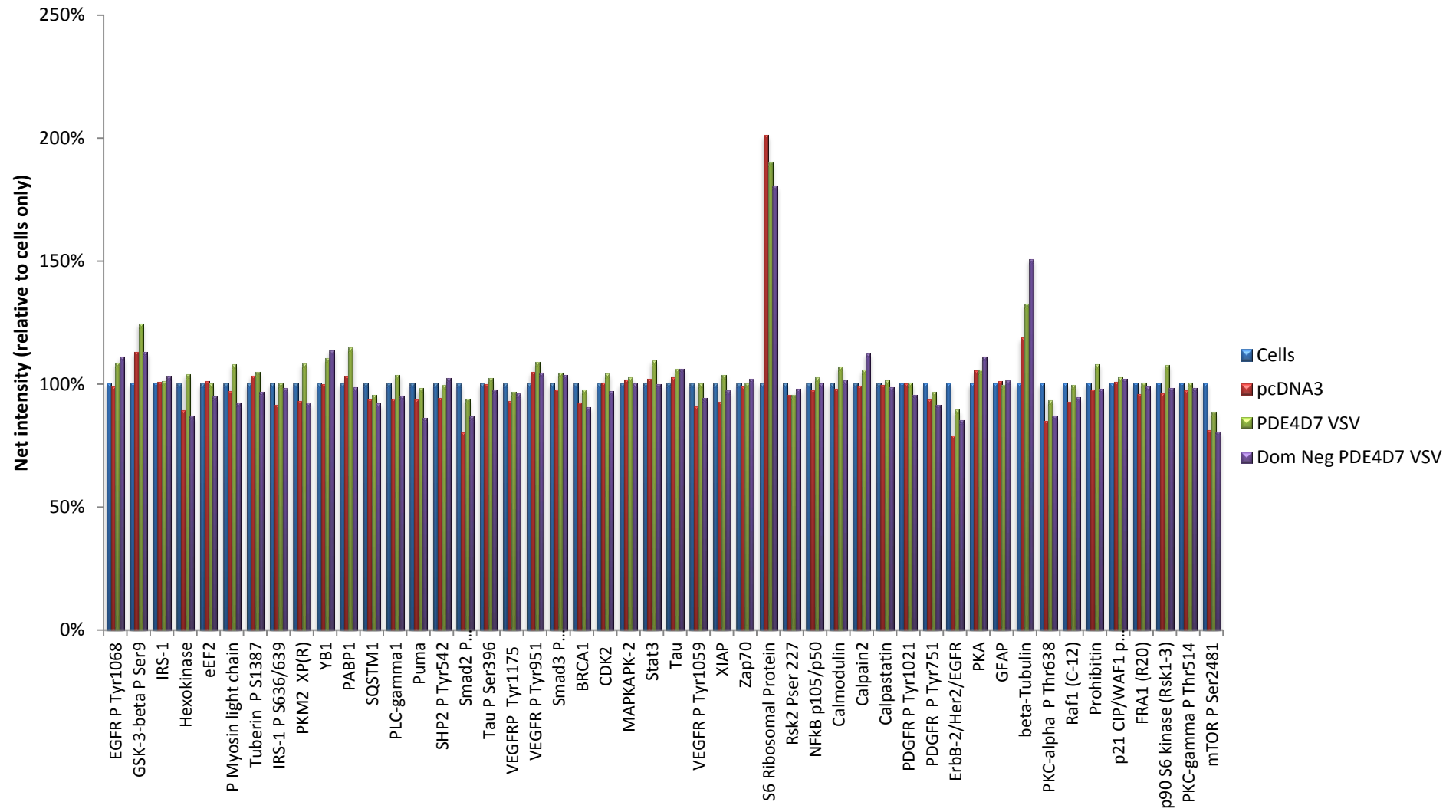


Figure 7.6 PDE4D7 transfected VCaP RPPA protein expression profile (Full Screen Part 2)

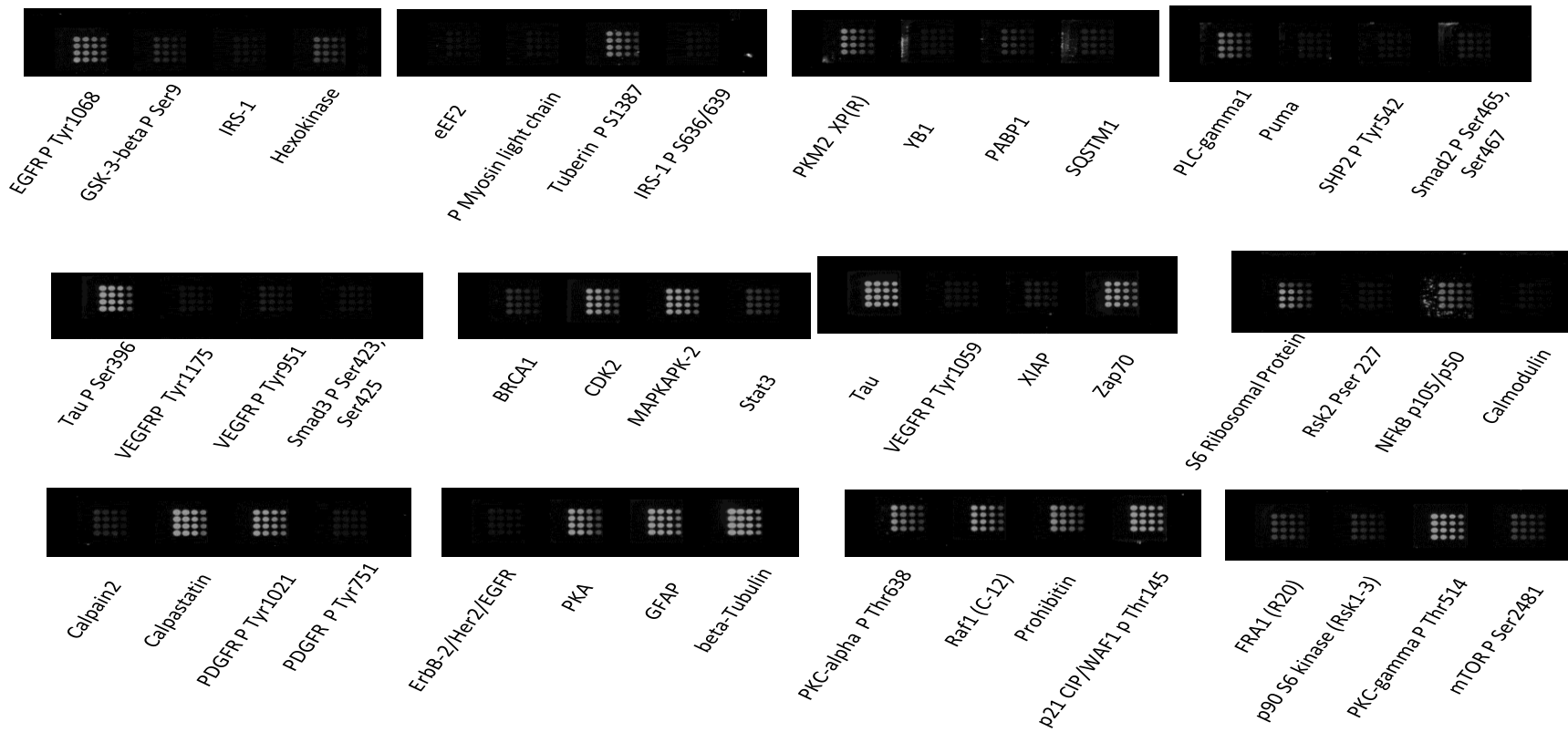


Figure 7.7 PDE4D7 transfected VCaP RPPA protein expression images (Full Screen Part 2)

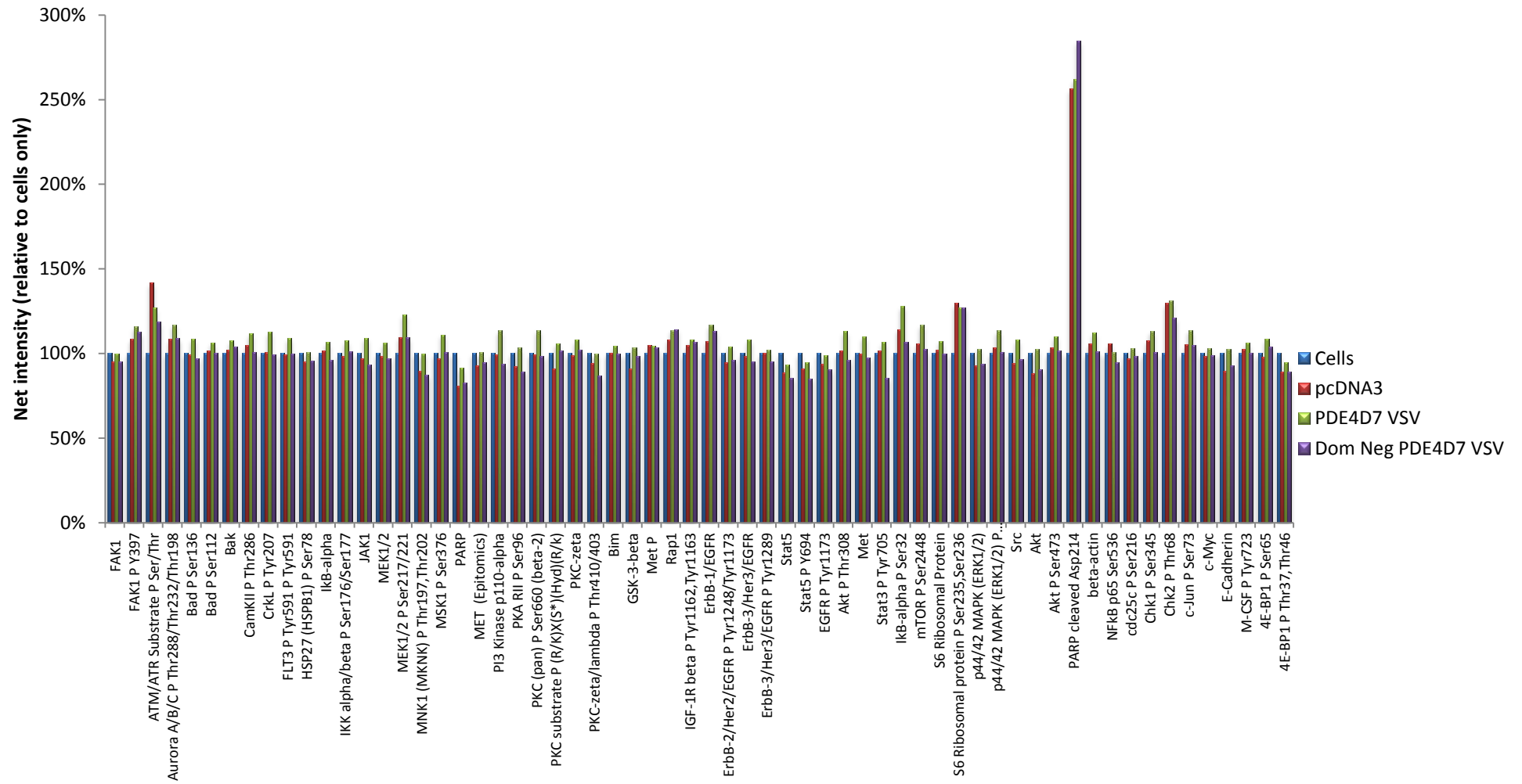


Figure 7.8 PDE4D7 transfected VCaP RPPA protein expression profile (Full Screen Part 3)

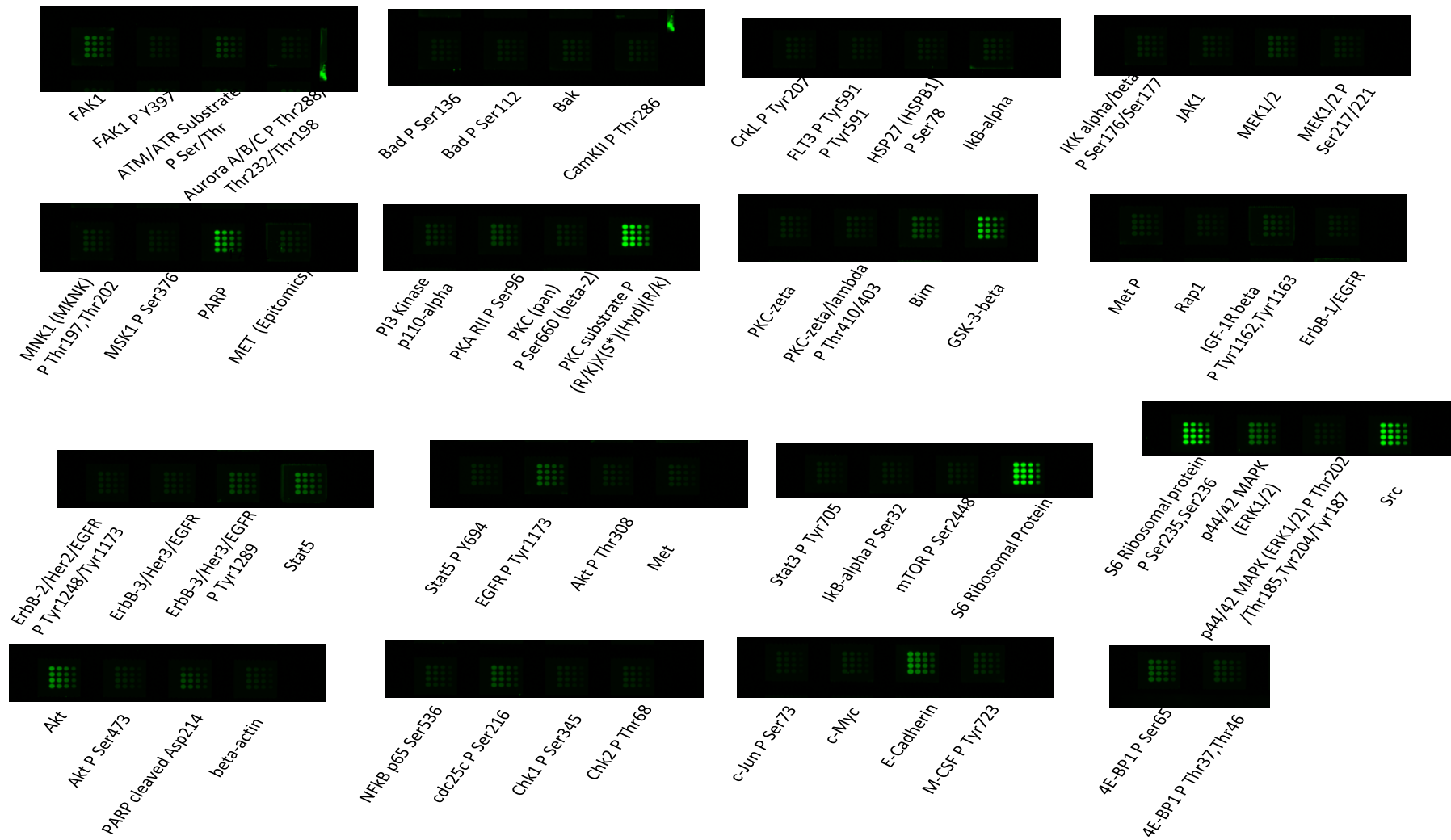


Figure 7.9 PDE4D7 transfected VCaP RPPA protein expression images (Full Screen Part 3)

List of References

1. Daniel, P., W. Walker, and J. Habener, *Cyclic AMP signaling and gene regulation*. ANNUAL REVIEW OF NUTRITION, 1998: p. 353-383.
2. Sassone-Corsi, P., *The cyclic AMP pathway*. Cold Spring Harb Perspect Biol, 2012. 4(12).
3. Cooper, D.M. and A.J. Crossthwaite, *Higher-order organization and regulation of adenylyl cyclases*. Trends Pharmacol Sci, 2006. 27(8): p. 426-31.
4. Cooper, D.M., *Regulation and organization of adenylyl cyclases and cAMP*. Biochem J, 2003. 375(Pt 3): p. 517-29.
5. Taylor, S.S., et al., *Assembly of allosteric macromolecular switches: lessons from PKA*. Nat Rev Mol Cell Biol, 2012. 13(10): p. 646-58.
6. Baillie, G.S., *Compartmentalized signalling: spatial regulation of cAMP by the action of compartmentalized phosphodiesterases*. FEBS J, 2009. 276(7): p. 1790-9.
7. Houslay, M.D., G.S. Baillie, and D.H. Maurice, *cAMP-Specific phosphodiesterase-4 enzymes in the cardiovascular system: a molecular toolbox for generating compartmentalized cAMP signaling*. Circ Res, 2007. 100(7): p. 950-66.
8. Manning, G., et al., *The protein kinase complement of the human genome*. SCIENCE, 2002. 298(5600): p. 1912-34.
9. Taylor, S., et al., *PKA: a portrait of protein kinase dynamics*. BIOCHIMICA ET BIOPHYSICA ACTA-PROTEINS AND PROTEOMICS, 2004: p. 259-269.
10. TAYLOR, S., J. BUECHLER, and W. YONEMOTO, *CAMP-DEPENDENT PROTEIN-KINASE - FRAMEWORK FOR A DIVERSE FAMILY OF REGULATORY ENZYMES*. ANNUAL REVIEW OF BIOCHEMISTRY, 1990: p. 971-1005.
11. ChoChung, Y., et al., *cAMP-dependent protein kinase: Role in normal and malignant growth*. CRITICAL REVIEWS IN ONCOLOGY/HEMATOLOGY, 1995: p. 33-61.
12. Gibson, R., Y. Ji-Buechler, and S. Taylor, *Identification of electrostatic interaction sites between the regulatory and catalytic subunits of cyclic AMP-dependent protein kinase*. Protein Sci, 1997. 6(9): p. 1825-34.
13. Walsh, D.A., J.P. Perkins, and E.G. Krebs, *An adenosine 3',5'-monophosphate-dependant protein kinase from rabbit skeletal muscle*. J Biol Chem, 1968. 243(13): p. 3763-5.
14. Newlon, M.G., et al., *A novel mechanism of PKA anchoring revealed by solution structures of anchoring complexes*. EMBO J, 2001. 20(7): p. 1651-62.
15. Brown, S.H., et al., *Novel isoform-specific interfaces revealed by PKA RIIbeta holoenzyme structures*. J Mol Biol, 2009. 393(5): p. 1070-82.
16. Kim, C., N.H. Xuong, and S.S. Taylor, *Crystal structure of a complex between the catalytic and regulatory (RI alpha) subunits of PKA*. Science, 2005. 307(5710): p. 690-696.
17. Cho-Chung, Y.S., *Role of cyclic AMP receptor proteins in growth, differentiation, and suppression of malignancy: new approaches to therapy*. Cancer Res, 1990. 50(22): p. 7093-100.

18. Vigil, D., et al., *Solution scattering reveals large differences in the global structures of type II protein kinase A isoforms*. J Mol Biol, 2006. **357**(3): p. 880-9.
19. Cummings, D.E., et al., *Genetically lean mice result from targeted disruption of the RII beta subunit of protein kinase A*. Nature, 1996. **382**(6592): p. 622-6.
20. Taylor, S.S., J.A. Buechler, and W. Yonemoto, *cAMP-dependent protein kinase: framework for a diverse family of regulatory enzymes*. Annu Rev Biochem, 1990. **59**: p. 971-1005.
21. Hensch, T.K., et al., *Comparison of plasticity in vivo and in vitro in the developing visual cortex of normal and protein kinase A RIIbeta-deficient mice*. J Neurosci, 1998. **18**(6): p. 2108-17.
22. Taimi, M., T.R. Breitman, and N. Takahashi, *Cyclic AMP-dependent protein kinase isoenzymes in human myeloid leukemia (HL60) and breast tumor (MCF-7) cells*. Arch Biochem Biophys, 2001. **392**(1): p. 137-44.
23. Cheng, X., C. Phelps, and S.S. Taylor, *Differential binding of cAMP-dependent protein kinase regulatory subunit isoforms Ialpha and IIbeta to the catalytic subunit*. J Biol Chem, 2001. **276**(6): p. 4102-8.
24. Yang, J., et al., *Contribution of non-catalytic core residues to activity and regulation in protein kinase A*. J Biol Chem, 2009. **284**(10): p. 6241-8.
25. KNIGHTON, D., et al., *STRUCTURE OF A PEPTIDE INHIBITOR BOUND TO THE CATALYTIC SUBUNIT OF CYCLIC ADENOSINE-MONOPHOSPHATE DEPENDENT PROTEIN-KINASE*. SCIENCE, 1991: p. 414-420.
26. Qi, M., et al., *Impaired hippocampal plasticity in mice lacking the Cbeta1 catalytic subunit of cAMP-dependent protein kinase*. Proc Natl Acad Sci U S A, 1996. **93**(4): p. 1571-6.
27. Chung, S., et al., *Overexpressing PKIB in prostate cancer promotes its aggressiveness by linking between PKA and Akt pathways*. Oncogene, 2009. **28**(32): p. 2849-2859.
28. Brunton, L.L., J.S. Hayes, and S.E. Mayer, *Functional compartmentation of cyclic AMP and protein kinase in heart*. Adv Cyclic Nucleotide Res, 1981. **14**: p. 391-7.
29. Edwards, H.V., F. Christian, and G.S. Baillie, *cAMP: novel concepts in compartmentalised signalling*. Semin Cell Dev Biol, 2012. **23**(2): p. 181-90.
30. Conti, M. and J. Beavo, *Biochemistry and physiology of cyclic nucleotide phosphodiesterases: essential components in cyclic nucleotide signaling*. Annu Rev Biochem, 2007. **76**: p. 481-511.
31. Jeon, Y.H., et al., *Phosphodiesterase: overview of protein structures, potential therapeutic applications and recent progress in drug development*. Cell Mol Life Sci, 2005. **62**(11): p. 1198-220.
32. Houslay, M.D., *Underpinning compartmentalised cAMP signalling through targeted cAMP breakdown*. Trends Biochem Sci, 2010. **35**(2): p. 91-100.
33. Vezzosi, D. and J. Bertherat, *Phosphodiesterases in endocrine physiology and disease*. Eur J Endocrinol, 2011. **165**(2): p. 177-88.
34. Fabbri, L.M., et al., *Roflumilast*. Nat Rev Drug Discov, 2010. **9**(10): p. 761-2.
35. Houslay, M.D., *The long and short of vascular smooth muscle phosphodiesterase-4 as a putative therapeutic target*. Mol Pharmacol, 2005. **68**(3): p. 563-7.
36. Millar, J.K., et al., *DISC1 and PDE4B are interacting genetic factors in schizophrenia that regulate cAMP signaling*. SCIENCE, 2005. **310**(5751): p. 1187-91.

37. Houslay, M.D., P. Schafer, and K.Y. Zhang, *Keynote review: phosphodiesterase-4 as a therapeutic target*. *Drug Discov Today*, 2005. **10**(22): p. 1503-19.
38. Stefan, E., et al., *Compartmentalization of cAMP-dependent signaling by phosphodiesterase-4D is involved in the regulation of vasopressin-mediated water reabsorption in renal principal cells*. *J Am Soc Nephrol*, 2007. **18**(1): p. 199-212.
39. Bolger, G.B., et al., *Scanning peptide array analyses identify overlapping binding sites for the signalling scaffold proteins, beta-arrestin and RACK1, in cAMP-specific phosphodiesterase PDE4D5*. *Biochem J*, 2006. **398**(1): p. 23-36.
40. Sin, Y.Y., et al., *Disruption of the cyclic AMP phosphodiesterase-4 (PDE4)-HSP20 complex attenuates the beta-agonist induced hypertrophic response in cardiac myocytes*. *J Mol Cell Cardiol*, 2011. **50**(5): p. 872-83.
41. Perry, S.J., et al., *Targeting of cyclic AMP degradation to beta 2-adrenergic receptors by beta-arrestins*. *SCIENCE*, 2002. **298**(5594): p. 834-6.
42. Omori, K. and J. Kotera, *Overview of PDEs and their regulation*. *Circ Res*, 2007. **100**(3): p. 309-27.
43. MacKenzie, S.J., et al., *Long PDE4 cAMP specific phosphodiesterases are activated by protein kinase A-mediated phosphorylation of a single serine residue in Upstream Conserved Region 1 (UCR1)*. *Br J Pharmacol*, 2002. **136**(3): p. 421-33.
44. Richter, W. and M. Conti, *Dimerization of the type 4 cAMP-specific phosphodiesterases is mediated by the upstream conserved regions (UCRs)*. *J Biol Chem*, 2002. **277**(43): p. 40212-21.
45. MacKenzie, S.J., et al., *ERK2 mitogen-activated protein kinase binding, phosphorylation, and regulation of the PDE4D cAMP-specific phosphodiesterases. The involvement of COOH-terminal docking sites and NH2-terminal UCR regions*. *J Biol Chem*, 2000. **275**(22): p. 16609-17.
46. Gottesman, M.M. and R.D. Fleischmann, *The role of cAMP in regulating tumour cell growth*. *Cancer Surv*, 1986. **5**(2): p. 291-308.
47. Stratakis, C.A., L.S. Kirschner, and J.A. Carney, *Clinical and molecular features of the Carney complex: diagnostic criteria and recommendations for patient evaluation*. *J Clin Endocrinol Metab*, 2001. **86**(9): p. 4041-6.
48. Yang, W.L., et al., *Interaction of the regulatory subunit of the cAMP-dependent protein kinase with PATZ1 (ZNF278)*. *Biochem Biophys Res Commun*, 2010. **391**(3): p. 1318-23.
49. Stratakis, C.A. and Y.S. Cho-Chung, *Protein kinase A and human disease*. *Trends Endocrinol Metab*, 2002. **13**(2): p. 50-2.
50. Cho, Y.S., et al., *Extracellular protein kinase A as a cancer biomarker: its expression by tumor cells and reversal by a myristate-lacking Calpha and RIIbeta subunit overexpression*. *Proc Natl Acad Sci U S A*, 2000. **97**(2): p. 835-40.
51. Pullamsetti, S.S., et al., *Phosphodiesterase-4 promotes proliferation and angiogenesis of lung cancer by crosstalk with HIF*. *Oncogene*, 2013. **32**(9): p. 1121-34.
52. Murata, K., et al., *Cyclic AMP specific phosphodiesterase activity and colon cancer cell motility*. *Clin Exp Metastasis*, 2000. **18**(7): p. 599-604.
53. Narita, M., et al., *A role for cyclic nucleotide phosphodiesterase 4 in regulation of the growth of human malignant melanoma cells*. *Oncol Rep*, 2007. **17**(5): p. 1133-9.

54. Mouratidis, P.X., et al., *Antiproliferative effects of CC-8062 and CC-8075 in pancreatic cancer cells*. *Pancreas*, 2009. **38**(1): p. 78-84.
55. Goldhoff, P., et al., *Targeted inhibition of cyclic AMP phosphodiesterase-4 promotes brain tumor regression*. *Clin Cancer Res*, 2008. **14**(23): p. 7717-25.
56. Lerner, A. and P.M. Epstein, *Cyclic nucleotide phosphodiesterases as targets for treatment of haematological malignancies*. *Biochem J*, 2006. **393**(Pt 1): p. 21-41.
57. Kumar, V.L. and P.K. Majumder, *Prostate gland: structure, functions and regulation*. *Int Urol Nephrol*, 1995. **27**(3): p. 231-43.
58. Kavanagh, J.P., *Sodium, potassium, calcium, magnesium, zinc, citrate and chloride content of human prostatic and seminal fluid*. *J Reprod Fertil*, 1985. **75**(1): p. 35-41.
59. Balk, S.P., Y.J. Ko, and G.J. Bubley, *Biology of prostate-specific antigen*. *J Clin Oncol*, 2003. **21**(2): p. 383-91.
60. Steers, W.D., *Physiology and Pharmacology of the Prostate*. *Practical Urology: Essential Principles and Practice*, 2011: p. 239-248.
61. Tanaka, M., et al., *Prostatic acid phosphatase degrades lysophosphatidic acid in seminal plasma*. *FEBS Lett*, 2004. **571**(1-3): p. 197-204.
62. Umezu-Goto, M., et al., *Autotaxin has lysophospholipase D activity leading to tumor cell growth and motility by lysophosphatidic acid production*. *J Cell Biol*, 2002. **158**(2): p. 227-33.
63. Kue, P.F., et al., *Lysophosphatidic acid-regulated mitogenic ERK signaling in androgen-insensitive prostate cancer PC-3 cells*. *Int J Cancer*, 2002. **102**(6): p. 572-9.
64. McNeal, J.E., *The zonal anatomy of the prostate*. *PROSTATE*, 1981. **2**(1): p. 35-49.
65. McNeal, J.E., *Normal histology of the prostate*. *Am J Surg Pathol*, 1988. **12**(8): p. 619-33.
66. Liu, A.Y. and L.D. True, *Characterization of prostate cell types by CD cell surface molecules*. *Am J Pathol*, 2002. **160**(1): p. 37-43.
67. De Marzo, A.M., et al., *Inflammation in prostate carcinogenesis*. *Nat Rev Cancer*, 2007. **7**(4): p. 256-69.
68. Cohen, R.J., et al., *Central zone carcinoma of the prostate gland: a distinct tumor type with poor prognostic features*. *J Urol*, 2008. **179**(5): p. 1762-7; discussion 1767.
69. Carson, C., 3rd and R. Rittmaster, *The role of dihydrotestosterone in benign prostatic hyperplasia*. *Urology*, 2003. **61**(4 Suppl 1): p. 2-7.
70. Gao, W., *Androgen receptor as a therapeutic target*. *Adv Drug Deliv Rev*, 2010. **62**(13): p. 1277-84.
71. Azzouni, F., et al., *The 5 alpha-reductase isozyme family: a review of basic biology and their role in human diseases*. *Adv Urol*, 2012. **2012**: p. 530121.
72. Saartok, T., E. Dahlberg, and J.A. Gustafsson, *Relative binding affinity of anabolic-androgenic steroids: comparison of the binding to the androgen receptors in skeletal muscle and in prostate, as well as to sex hormone-binding globulin*. *Endocrinology*, 1984. **114**(6): p. 2100-6.
73. Dehm, S.M. and D.J. Tindall, *Androgen receptor structural and functional elements: role and regulation in prostate cancer*. *Mol Endocrinol*, 2007. **21**(12): p. 2855-63.
74. Katagiri, Y., et al., *Androgen receptor CAG polymorphism (Xq11-12) status and human spermatogenesis: a prospective analysis of infertile*

- males and their offspring conceived by intracytoplasmic sperm injection.* Int J Mol Med, 2006. **18**(3): p. 405-13.
75. Gioeli, D. and B.M. Paschal, *Post-translational modification of the androgen receptor.* Molecular and Cellular Endocrinology, 2012. **352**(1-2): p. 70-8.
 76. Sadar, M.D., *Androgen-independent induction of prostate-specific antigen gene expression via cross-talk between the androgen receptor and protein kinase A signal transduction pathways.* J Biol Chem, 1999. **274**(12): p. 7777-83.
 77. Shang, Y., M. Myers, and M. Brown, *Formation of the androgen receptor transcription complex.* Mol Cell, 2002. **9**(3): p. 601-10.
 78. Doesburg, P., et al., *Functional in vivo interaction between the amino-terminal, transactivation domain and the ligand binding domain of the androgen receptor.* Biochemistry, 1997. **36**(5): p. 1052-64.
 79. Lee, D.K. and C. Chang, *Molecular communication between androgen receptor and general transcription machinery.* J Steroid Biochem Mol Biol, 2003. **84**(1): p. 41-9.
 80. Yang, C.S., et al., *Ligand binding to the androgen receptor induces conformational changes that regulate phosphatase interactions.* Mol Cell Biol, 2007. **27**(9): p. 3390-404.
 81. Coffey, K. and C.N. Robson, *Regulation of the androgen receptor by post-translational modifications.* J Endocrinol, 2012. **215**(2): p. 221-37.
 82. McEwan, I.J., et al., *Natural disordered sequences in the amino terminal domain of nuclear receptors: lessons from the androgen and glucocorticoid receptors.* Nucl Recept Signal, 2007. **5**: p. e001.
 83. Clinckemalie, L., et al., *The hinge region in androgen receptor control.* Molecular and Cellular Endocrinology, 2012. **358**(1): p. 1-8.
 84. Claessens, F., et al., *Diverse roles of androgen receptor (AR) domains in AR-mediated signaling.* Nucl Recept Signal, 2008. **6**: p. e008.
 85. He, B., et al., *An androgen receptor NH2-terminal conserved motif interacts with the COOH terminus of the Hsp70-interacting protein (CHIP).* J Biol Chem, 2004. **279**(29): p. 30643-53.
 86. Callewaert, L., N. Van Tilborgh, and F. Claessens, *Interplay between two hormone-independent activation domains in the androgen receptor.* Cancer Res, 2006. **66**(1): p. 543-53.
 87. Jenster, G., et al., *Identification of two transcription activation units in the N-terminal domain of the human androgen receptor.* J Biol Chem, 1995. **270**(13): p. 7341-6.
 88. Tsai, M.J. and B.W. O'Malley, *Molecular mechanisms of action of steroid/thyroid receptor superfamily members.* Annu Rev Biochem, 1994. **63**: p. 451-86.
 89. Verrijdt, G., et al., *The androgen receptor DNA-binding domain determines androgen selectivity of transcriptional response.* Biochem Soc Trans, 2006. **34**(Pt 6): p. 1089-94.
 90. Zhou, Z.X., et al., *A ligand-dependent bipartite nuclear targeting signal in the human androgen receptor. Requirement for the DNA-binding domain and modulation by NH2-terminal and carboxyl-terminal sequences.* J Biol Chem, 1994. **269**(18): p. 13115-23.
 91. Matias, P.M., et al., *Structural evidence for ligand specificity in the binding domain of the human androgen receptor. Implications for pathogenic gene mutations.* J Biol Chem, 2000. **275**(34): p. 26164-71.

92. Moras, D. and H. Gronemeyer, *The nuclear receptor ligand-binding domain: structure and function*. *Curr Opin Cell Biol*, 1998. **10**(3): p. 384-91.
93. Trapman, J., *Interaction of the Androgen Receptor Ligand-Binding Domain with the N-Terminal Domain and with Coactivators*, in *Androgen Action in Prostate Cancer*, J. Mohler and D. Tindall, Editors. 2009, Springer US. p. 375-384.
94. Brinkmann, A.O., et al., *Mechanisms of androgen receptor activation and function*. *J Steroid Biochem Mol Biol*, 1999. **69**(1-6): p. 307-13.
95. Paolone, D.R., *Benign prostatic hyperplasia*. *Clin Geriatr Med*, 2010. **26**(2): p. 223-39.
96. Desgrandchamps, F. and P. Teillac, *The role of growth factors in the pathogenesis of benign prostatic hyperplasia*. *Biomedicine & Pharmacotherapy*, 1994. **48**, Supplement 1(0): p. 19s-23s.
97. Guess, H.A., *Benign prostatic hyperplasia and prostate cancer*. *Epidemiol Rev*, 2001. **23**(1): p. 152-8.
98. Marks, L.S., C.G. Roehrborn, and G.L. Andriole, *Prevention of benign prostatic hyperplasia disease*. *J Urol*, 2006. **176**(4 Pt 1): p. 1299-306.
99. Lin, J., et al., *Qianliening capsule treats benign prostatic hyperplasia via suppression of the EGF/STAT3 signaling pathway*. *Exp Ther Med*, 2013. **5**(5): p. 1293-1300.
100. Simpson, R.J., *Benign prostatic hyperplasia*. *Br J Gen Pract*, 1997. **47**(417): p. 235-40.
101. Nickel, J.C., *Inflammation and benign prostatic hyperplasia*. *Urol Clin North Am*, 2008. **35**(1): p. 109-15; vii.
102. St Sauver, J.L., et al., *Longitudinal association between prostatitis and development of benign prostatic hyperplasia*. *Urology*, 2008. **71**(3): p. 475-9; discussion 479.
103. Dennis, L.K., C.F. Lynch, and J.C. Torner, *Epidemiologic association between prostatitis and prostate cancer*. *Urology*, 2002. **60**(1): p. 78-83.
104. Collins, M.M., et al., *Prevalence and correlates of prostatitis in the health professionals follow-up study cohort*. *J Urol*, 2002. **167**(3): p. 1363-6.
105. Collins, M.M., et al., *Distinguishing chronic prostatitis and benign prostatic hyperplasia symptoms: results of a national survey of physician visits*. *Urology*, 1999. **53**(5): p. 921-5.
106. Nelson, W.G., A.M. De Marzo, and W.B. Isaacs, *Mechanisms of disease: Prostate cancer*. *New England Journal of Medicine*, 2003. **349**(4): p. 366-381.
107. Jemal, A., et al., *Cancer statistics, 2006*. *CA Cancer J Clin*, 2006. **56**(2): p. 106-30.
108. Hsing, A.W., L. Tsao, and S.S. Devesa, *International trends and patterns of prostate cancer incidence and mortality*. *Int J Cancer*, 2000. **85**(1): p. 60-7.
109. Gronberg, H., *Prostate cancer epidemiology*. *Lancet*, 2003. **361**(9360): p. 859-864.
110. Nieto, M., et al., *Prostate cancer: Re-focusing on androgen receptor signaling*. *Int J Biochem Cell Biol*, 2007. **39**(9): p. 1562-8.
111. Kolonel, L.N., A.M. Nomura, and R.V. Cooney, *Dietary fat and prostate cancer: current status*. *J Natl Cancer Inst*, 1999. **91**(5): p. 414-28.
112. Bostwick, D., *High grade prostatic intraepithelial neoplasia. The most likely precursor of prostate cancer*. *Cancer*, 2006. **75**(S7): p. 1823-1836.

113. Bostwick, D.G., et al., *High-grade prostatic intraepithelial neoplasia*. Rev Urol, 2004. **6**(4): p. 171-9.
114. Davidson, D., et al., *Prostatic intraepithelial neoplasia is a risk factor for adenocarcinoma: predictive accuracy in needle biopsies*. J Urol, 1995. **154**(4): p. 1295-9.
115. Huggins, C., *Studies on Prostatic Cancer. I. The Effect of Castration, of Estrogen and of Androgen Injection on Serum Phosphatases in Metastatic Carcinoma of the Prostate*. Cancer Res, 1941(1): p. 293-297.
116. Kaarbo, M., T.I. Klock, and F. Saatcioglu, *Androgen signaling and its interactions with other signaling pathways in prostate cancer*. Bioessays, 2007. **29**(12): p. 1227-38.
117. Lamont, K.R. and D.J. Tindall, *Minireview: Alternative activation pathways for the androgen receptor in prostate cancer*. Mol Endocrinol, 2011. **25**(6): p. 897-907.
118. Roberts, R.O., et al., *Serum sex hormones and measures of benign prostatic hyperplasia*. PROSTATE, 2004. **61**(2): p. 124-31.
119. Yao, S., et al., *Serum estrogen levels and prostate cancer risk in the prostate cancer prevention trial: a nested case-control study*. Cancer Causes Control, 2011. **22**(8): p. 1121-31.
120. Miao, L., et al., *Estrogen receptor-related receptor alpha mediates up-regulation of aromatase expression by prostaglandin E2 in prostate stromal cells*. Mol Endocrinol, 2010. **24**(6): p. 1175-86.
121. Ellem, S.J. and G.P. Risbridger, *Aromatase and prostate cancer*. Minerva Endocrinol, 2006. **31**(1): p. 1-12.
122. Thomas, L.N., et al., *Type 1 and type 2 5alpha-reductase expression in the development and progression of prostate cancer*. Eur Urol, 2008. **53**(2): p. 244-52.
123. Bonkhoff, H., et al., *Differential expression of 5 alpha-reductase isoenzymes in the human prostate and prostatic carcinomas*. PROSTATE, 1996. **29**(4): p. 261-7.
124. Shirakawa, T., et al., *Messenger RNA levels and enzyme activities of 5 alpha-reductase types 1 and 2 in human benign prostatic hyperplasia (BPH) tissue*. PROSTATE, 2004. **58**(1): p. 33-40.
125. Godoy, A., et al., *5alpha-reductase type 3 expression in human benign and malignant tissues: a comparative analysis during prostate cancer progression*. PROSTATE, 2011. **71**(10): p. 1033-46.
126. Niu, Y., et al., *Reduced levels of 5-alpha reductase 2 in adult prostate tissue and implications for BPH therapy*. PROSTATE, 2011. **71**(12): p. 1317-24.
127. Wegiel, B., et al., *Molecular pathways in the progression of hormone-independent and metastatic prostate cancer*. Curr Cancer Drug Targets, 2010. **10**(4): p. 392-401.
128. Craft, N., et al., *Evidence for clonal outgrowth of androgen-independent prostate cancer cells from androgen-dependent tumors through a two-step process*. Cancer Res, 1999. **59**(19): p. 5030-6.
129. Scher, H.I. and C.L. Sawyers, *Biology of progressive, castration-resistant prostate cancer: directed therapies targeting the androgen-receptor signaling axis*. J Clin Oncol, 2005. **23**(32): p. 8253-61.
130. Rao, A.R., H.G. Motiwala, and O.M. Karim, *The discovery of prostate-specific antigen*. BJU Int, 2008. **101**(1): p. 5-10.
131. Tangen, C.M., et al., *Improved overall survival trends of men with newly diagnosed M1 prostate cancer: a SWOG phase III trial experience (S8494, S8894 and S9346)*. J Urol, 2012. **188**(4): p. 1164-9.

132. Jia, L., et al., *Androgen receptor activity at the prostate specific antigen locus: steroidal and non-steroidal mechanisms*. *Mol Cancer Res*, 2003. **1**(5): p. 385-92.
133. Jain, S., A.G. Bhojwani, and J.K. Mellon, *Improving the utility of prostate specific antigen (PSA) in the diagnosis of prostate cancer: the use of PSA derivatives and novel markers*. *Postgrad Med J*, 2002. **78**(925): p. 646-50.
134. Lilja, H., et al., *Prostate-specific antigen in serum occurs predominantly in complex with alpha 1-antichymotrypsin*. *Clin Chem*, 1991. **37**(9): p. 1618-25.
135. Jacobsen, S.J., et al., *Incidence of prostate cancer diagnosis in the eras before and after serum prostate-specific antigen testing*. *JAMA*, 1995. **274**(18): p. 1445-9.
136. Labrie, F., et al., *Serum prostate specific antigen as pre-screening test for prostate cancer*. *J Urol*, 1992. **147**(3 Pt 2): p. 846-51; discussion 851-2.
137. Catalona, W.J., et al., *Measurement of prostate-specific antigen in serum as a screening test for prostate cancer*. *N Engl J Med*, 1991. **324**(17): p. 1156-61.
138. Roobol, M.J., et al., *Prostate cancer mortality reduction by prostate-specific antigen-based screening adjusted for nonattendance and contamination in the European Randomised Study of Screening for Prostate Cancer (ERSPC)*. *Eur Urol*, 2009. **56**(4): p. 584-91.
139. Bokhorst, L.P., et al., *Prostate-specific Antigen-Based Prostate Cancer Screening: Reduction of Prostate Cancer Mortality After Correction for Nonattendance and Contamination in the Rotterdam Section of the European Randomized Study of Screening for Prostate Cancer*. *Eur Urol*, 2013.
140. Goo, Y.A. and D.R. Goodlett, *Advances in proteomic prostate cancer biomarker discovery*. *J Proteomics*, 2010. **73**(10): p. 1839-50.
141. Sato, N., et al., *Intermittent androgen suppression delays progression to androgen-independent regulation of prostate-specific antigen gene in the LNCaP prostate tumour model*. *J Steroid Biochem Mol Biol*, 1996. **58**(2): p. 139-46.
142. Sadar, M.D., *The Role of Cyclic AMP in Regulating the Androgen Receptor*. *Androgen Action in Prostate Cancer*, ed. D. Tindall and J. Mohler. 2009: Springer. 465-503.
143. Gleason, D.F., *Histologic grading of prostate cancer: a perspective*. *Hum Pathol*, 1992. **23**(3): p. 273-9.
144. Gleason, D.F., G.T. Mellinger, and G. Veterans Administration Cooperative Urological Research, *Prediction of prognosis for prostatic adenocarcinoma by combined histological grading and clinical staging*. 1974. *J Urol*, 2002. **167**(2 Pt 2): p. 953-8; discussion 959.
145. Shah, R.B., *Current perspectives on the Gleason grading of prostate cancer*. *Arch Pathol Lab Med*, 2009. **133**(11): p. 1810-6.
146. Epstein, J.I., *Update on the Gleason grading system*. *Ann Pathol*, 2011. **31**(5 Suppl): p. S20-6.
147. Epstein, J.I., *An update of the Gleason grading system*. *J Urol*, 2010. **183**(2): p. 433-40.
148. Adolfsson, J., *Watchful waiting and active surveillance: the current position*. *BJU Int*, 2008. **102**(1): p. 10-4.
149. Denmeade, S., Isaacs, JT, *Androgen Deprivation Strategies in the Treatment of Advanced Prostate Cancer*, in *Cancer Medicine*, Holland-Frei, Editor. 2000.

150. Dehm, S.M. and D.J. Tindall, *Molecular regulation of androgen action in prostate cancer*. J Cell Biochem, 2006. **99**(2): p. 333-44.
151. Chen, C.D., et al., *Molecular determinants of resistance to antiandrogen therapy*. Nat Med, 2004. **10**(1): p. 33-9.
152. Perlmutter, M.A. and H. Lepor, *Androgen deprivation therapy in the treatment of advanced prostate cancer*. Rev Urol, 2007. **9 Suppl 1**: p. S3-8.
153. Brawer, M.K., *Hormonal therapy for prostate cancer*. Rev Urol, 2006. **8 Suppl 2**: p. S35-47.
154. Patel, V.R., M.F. Chammas, Jr., and S. Shah, *Robotic assisted laparoscopic radical prostatectomy: a review of the current state of affairs*. Int J Clin Pract, 2007. **61**(2): p. 309-14.
155. Malhotra, V., *Transurethral resection of the prostate*. Anesthesiol Clin North America, 2000. **18**(4): p. 883-97, x.
156. Pieters, B.R., et al., *Comparison of three radiotherapy modalities on biochemical control and overall survival for the treatment of prostate cancer: a systematic review*. Radiother Oncol, 2009. **93**(2): p. 168-73.
157. Nilsson, S., B.J. Norlen, and A. Widmark, *A systematic overview of radiation therapy effects in prostate cancer*. Acta Oncol, 2004. **43**(4): p. 316-81.
158. D'Amico, A.V., et al., *Androgen suppression and radiation vs radiation alone for prostate cancer: a randomized trial*. JAMA, 2008. **299**(3): p. 289-95.
159. Bradford, M.M., *A rapid and sensitive method for the quantitation of microgram quantities of protein utilizing the principle of protein-dye binding*. Anal Biochem, 1976. **72**: p. 248-54.
160. Miller, W.R., *Regulatory subunits of PKA and breast cancer*, in *Protein Kinase a and Human Disease*, C.A. Stratakis and Y.S. ChoChung, Editors. 2002, New York Acad Sciences: New York. p. 37-48.
161. Bradbury, A.W., et al., *Protein kinase A (PK-A) regulatory subunit expression in colorectal cancer and related mucosa*. Br J Cancer, 1994. **69**(4): p. 738-42.
162. Miller, W.R., et al., *Cyclic AMP binding proteins and prognosis in breast cancer*. Br J Cancer, 1990. **61**(2): p. 263-6.
163. Cheadle, C., et al., *Regulatory subunits of PKA define an axis of cellular proliferation/differentiation in ovarian cancer cells*. BMC Med Genomics, 2008. **1**: p. 43.
164. de Leeuw, R., J. Neefjes, and R. Michalides, *A role for estrogen receptor phosphorylation in the resistance to tamoxifen*. Int J Breast Cancer, 2011. **2011**: p. 232435.
165. Cox, M.E., et al., *Activated 3',5'-cyclic AMP-dependent protein kinase is sufficient to induce neuroendocrine-like differentiation of the LNCaP prostate tumor cell line*. Journal of Biological Chemistry, 2000. **275**(18): p. 13812-13818.
166. Sadar, M.D., M. Hussain, and N. Bruchofsky, *Prostate cancer: molecular biology of early progression to androgen independence*. Endocr Relat Cancer, 1999. **6**(4): p. 487-502.
167. Neary, C.L., et al., *Protein kinase A isozyme switching: eliciting differential cAMP signaling and tumor reversion*. Oncogene, 2004. **23**(54): p. 8847-56.
168. Merkle, D. and R. Hoffmann, *Roles of cAMP and cAMP-dependent protein kinase in the progression of prostate cancer: cross-talk with the androgen receptor*. Cell Signal, 2011. **23**(3): p. 507-15.

169. Kvissel, A.K., et al., *Androgen dependent regulation of protein kinase A subunits in prostate cancer cells*. Cellular Signalling, 2007. **19**(2): p. 401-409.
170. Cvijic, M.E., et al., *Extracellular catalytic subunit activity of the cAMP-dependent protein kinase in prostate cancer*. Clinical Cancer Research, 2000. **6**(6): p. 2309-2317.
171. Khor, L.Y., et al., *Protein kinase A RI-alpha predicts for prostate cancer outcome: analysis of radiation therapy oncology group trial 86-10*. Int J Radiat Oncol Biol Phys, 2008. **71**(5): p. 1309-15.
172. Kurien, B.T. and R.H. Scofield, *Western blotting*. Methods, 2006. **38**(4): p. 283-93.
173. Desiniotis, A., et al., *Enhanced antiproliferative and proapoptotic effects on prostate cancer cells by simultaneously inhibiting androgen receptor and cAMP-dependent protein kinase A*. Int J Cancer, 2010. **126**(3): p. 775-89.
174. Pfaffl, M.W., *Quantification strategies in real-time PCR*. 2004: p. 87-112.
175. de Sousa Abreu, R., et al., *Global signatures of protein and mRNA expression levels*. Mol Biosyst, 2009. **5**(12): p. 1512-26.
176. Vogel, C., et al., *Sequence signatures and mRNA concentration can explain two-thirds of protein abundance variation in a human cell line*. Mol Syst Biol, 2010. **6**: p. 400.
177. Heid, C.A., et al., *Real time quantitative PCR*. Genome Res, 1996. **6**(10): p. 986-94.
178. Mori, R., et al., *Both beta-actin and GAPDH are useful reference genes for normalization of quantitative RT-PCR in human FFPE tissue samples of prostate cancer*. PROSTATE, 2008. **68**(14): p. 1555-60.
179. Henderson, D., *Phosphodiesterase Expression During the Progression of Prostate Cancer: The Significance of PDE4D7*, in *Institute of Neuroscience and Psychology; College of Medical, Veterinary and Life Sciences* 2011, University of Glasgow.
180. Sobel, R. and M. Sadar, *Cell lines used in prostate cancer research: a compendium of old and new lines--part 1*. J Urol, 2005. **173**(2): p. 342-59.
181. Sobel, R. and M. Sadar, *Cell lines used in prostate cancer research: a compendium of old and new lines--part 2*. J Urol, 2005. **173**(2): p. 360-72.
182. Korenchuk, S., et al., *VCaP, a cell-based model system of human prostate cancer*. In Vivo, 2001. **15**(2): p. 163-8.
183. Horoszewicz, J.S., et al., *LNCaP model of human prostatic carcinoma*. Cancer Res, 1983. **43**(4): p. 1809-18.
184. Lee, Y.G., et al., *Establishment and characterization of a new human prostatic cancer cell line: DuCaP*. In Vivo, 2001. **15**(2): p. 157-62.
185. Kaighn, M.E., et al., *Establishment and characterization of a human prostatic carcinoma cell line (PC-3)*. Invest Urol, 1979. **17**(1): p. 16-23.
186. Cussenot, O., et al., *Immortalization of human adult normal prostatic epithelial cells by liposomes containing large T-SV40 gene*. J Urol, 1991. **146**(3): p. 881-6.
187. Berthon, P., et al., *Androgens are not a direct requirement for the proliferation of human prostatic epithelium in vitro*. Int J Cancer, 1997. **73**(6): p. 910-6.
188. Cho, Y.S., et al., *Protein kinase A RIalpha antisense inhibition of PC3M prostate cancer cell growth: Bcl-2 hyperphosphorylation, Bax up-*

- regulation, and Bad-hypophosphorylation*. Clin Cancer Res, 2002. **8**(2): p. 607-14.
189. Nesterova, M., et al., *Compensatory stabilization of Rllbeta protein, cell cycle deregulation, and growth arrest in colon and prostate carcinoma cells by antisense-directed down-regulation of protein kinase A RIalpha protein*. Clin Cancer Res, 2000. **6**(9): p. 3434-41.
 190. Nesterova, M.V., et al., *Autoantibody cancer biomarker: extracellular protein kinase A*. Cancer Res, 2006. **66**(18): p. 8971-4.
 191. Pollack, A., et al., *The Importance of Protein Kinase A in Prostate Cancer: Relationship to Patient Outcome in Radiation Therapy Oncology Group Trial 92-02*. Clinical Cancer Research, 2009. **15**(17): p. 5478-5484.
 192. Anand, G.S., et al., *R-subunit isoform specificity in protein kinase A: distinct features of protein interfaces in PKA types I and II by amide H/2H exchange mass spectrometry*. J Mol Biol, 2007. **374**(2): p. 487-99.
 193. Amieux, P.S. and G.S. McKnight, *The essential role of RI alpha in the maintenance of regulated PKA activity*. Ann N Y Acad Sci, 2002. **968**: p. 75-95.
 194. Brandon, E.P., et al., *Defective motor behavior and neural gene expression in Rllbeta-protein kinase A mutant mice*. J Neurosci, 1998. **18**(10): p. 3639-49.
 195. Newhall, K.J., et al., *Deletion of the Rllbeta-subunit of protein kinase A decreases body weight and increases energy expenditure in the obese, leptin-deficient ob/ob mouse*. Mol Endocrinol, 2005. **19**(4): p. 982-91.
 196. Sarwar, M.P., JL, *The Protein Kinase A (PKA) Intracellular Pathway and Androgen Receptor: A Novel Mechanism Underlying the Castration-resistant and Metastatic Prostate Cancer*. Journal of Cancer Science and Therapy, 2011. **S5**(003).
 197. Sun, Y., J. Niu, and J. Huang, *Neuroendocrine differentiation in prostate cancer*. Am J Transl Res, 2009. **1**(2): p. 148-62.
 198. Komiya, A., et al., *Neuroendocrine differentiation in the progression of prostate cancer*. Int J Urol, 2009. **16**(1): p. 37-44.
 199. Harper, M.E., et al., *Vascular endothelial growth factor (VEGF) expression in prostatic tumours and its relationship to neuroendocrine cells*. Br J Cancer, 1996. **74**(6): p. 910-6.
 200. di Sant'Agnese, P.A., *Neuroendocrine differentiation in prostatic carcinoma: an update on recent developments*. Ann Oncol, 2001. **12** Suppl 2: p. S135-40.
 201. Huang, J., et al., *Immunohistochemical characterization of neuroendocrine cells in prostate cancer*. PROSTATE, 2006. **66**(13): p. 1399-406.
 202. Wong, H.Y., et al., *Phosphorylation of androgen receptor isoforms*. Biochem J, 2004. **383**(Pt 2): p. 267-76.
 203. Chymkowitch, P., et al., *The phosphorylation of the androgen receptor by TFIIH directs the ubiquitin/proteasome process*. EMBO J, 2011. **30**(3): p. 468-79.
 204. Poukka, H., et al., *Covalent modification of the androgen receptor by small ubiquitin-like modifier 1 (SUMO-1)*. Proc Natl Acad Sci U S A, 2000. **97**(26): p. 14145-50.
 205. Gioeli, D., et al., *Androgen receptor phosphorylation. Regulation and identification of the phosphorylation sites*. J Biol Chem, 2002. **277**(32): p. 29304-14.
 206. Guo, Z., et al., *Regulation of androgen receptor activity by tyrosine phosphorylation*. Cancer Cell, 2006. **10**(4): p. 309-19.

207. Lange, C.A., *Making sense of cross-talk between steroid hormone receptors and intracellular signaling pathways: who will have the last word?* Mol Endocrinol, 2004. **18**(2): p. 269-78.
208. Lange, C.A., T. Shen, and K.B. Horwitz, *Phosphorylation of human progesterone receptors at serine-294 by mitogen-activated protein kinase signals their degradation by the 26S proteasome.* Proc Natl Acad Sci U S A, 2000. **97**(3): p. 1032-7.
209. Lannigan, D.A., *Estrogen receptor phosphorylation.* Steroids, 2003. **68**(1): p. 1-9.
210. Zhang, Y., et al., *Identification of phosphorylation sites unique to the B form of human progesterone receptor. In vitro phosphorylation by casein kinase II.* J Biol Chem, 1994. **269**(49): p. 31034-40.
211. Webster, J.C., et al., *Mouse glucocorticoid receptor phosphorylation status influences multiple functions of the receptor protein.* J Biol Chem, 1997. **272**(14): p. 9287-93.
212. van Laar, J.H., et al., *Hormone-dependent androgen receptor phosphorylation is accompanied by receptor transformation in human lymph node carcinoma of the prostate cells.* J Biol Chem, 1991. **266**(6): p. 3734-8.
213. Gioeli, D., et al., *Stress kinase signaling regulates androgen receptor phosphorylation, transcription, and localization.* Mol Endocrinol, 2006. **20**(3): p. 503-15.
214. Lin, H.K., et al., *Akt suppresses androgen-induced apoptosis by phosphorylating and inhibiting androgen receptor.* PROCEEDINGS OF THE NATIONAL ACADEMY OF SCIENCES OF THE UNITED STATES OF AMERICA, 2001. **98**(13): p. 7200-7205.
215. Nazareth, L. and N. Weigel, *Activation of the human androgen receptor through a protein kinase A signaling pathway.* JOURNAL OF BIOLOGICAL CHEMISTRY, 1996: p. 19900-19907.
216. Janne, O.A., et al., *Androgen-receptor-interacting nuclear proteins.* Biochem Soc Trans, 2000. **28**(4): p. 401-5.
217. Grossmann, M.E., H. Huang, and D.J. Tindall, *Androgen receptor signaling in androgen-refractory prostate cancer.* J Natl Cancer Inst, 2001. **93**(22): p. 1687-97.
218. Katz, C., et al., *Studying protein-protein interactions using peptide arrays.* Chem Soc Rev, 2011. **40**(5): p. 2131-45.
219. Slagsvold, T., et al., *Mutational analysis of the androgen receptor AF-2 (activation function 2) core domain reveals functional and mechanistic differences of conserved residues compared with other nuclear receptors.* Mol Endocrinol, 2000. **14**(10): p. 1603-17.
220. Graham, F.L., et al., *Characteristics of a human cell line transformed by DNA from human adenovirus type 5.* J Gen Virol, 1977. **36**(1): p. 59-74.
221. Pi, M., A.L. Parrill, and L.D. Quarles, *GPRC6A mediates the non-genomic effects of steroids.* J Biol Chem, 2010. **285**(51): p. 39953-64.
222. Leister, P., et al., *ZIP kinase plays a crucial role in androgen receptor-mediated transcription.* Oncogene, 2008. **27**(23): p. 3292-300.
223. van der Steen, T., D.J. Tindall, and H. Huang, *Posttranslational modification of the androgen receptor in prostate cancer.* Int J Mol Sci, 2013. **14**(7): p. 14833-59.
224. Ziera, T., et al., *Cnksr3 is a direct mineralocorticoid receptor target gene and plays a key role in the regulation of the epithelial sodium channel.* FASEB J, 2009. **23**(11): p. 3936-46.

225. Lin, H.K., et al., *Suppression versus induction of androgen receptor functions by the phosphatidylinositol 3-kinase/Akt pathway in prostate cancer LNCaP cells with different passage numbers.* J Biol Chem, 2003. **278**(51): p. 50902-7.
226. Kim, J., et al., *The role of protein kinase A pathway and cAMP responsive element-binding protein in androgen receptor-mediated transcription at the prostate-specific antigen locus.* JOURNAL OF MOLECULAR ENDOCRINOLOGY, 2005: p. 107-118.
227. Coghlan, V.M., et al., *A-kinase anchoring proteins: a key to selective activation of cAMP-responsive events?* Mol Cell Biochem, 1993. **127-128**: p. 309-19.
228. Pidoux, G. and K. Tasken, *Specificity and spatial dynamics of protein kinase A signaling organized by A-kinase-anchoring proteins.* J Mol Endocrinol, 2010. **44**(5): p. 271-84.
229. Beck, C.A., et al., *The progesterone antagonist RU486 acquires agonist activity upon stimulation of cAMP signaling pathways.* Proc Natl Acad Sci U S A, 1993. **90**(10): p. 4441-5.
230. Moyer, M.L., et al., *Modulation of cell signaling pathways can enhance or impair glucocorticoid-induced gene expression without altering the state of receptor phosphorylation.* J Biol Chem, 1993. **268**(30): p. 22933-40.
231. Ikonen, T., et al., *Stimulation of androgen-regulated transactivation by modulators of protein phosphorylation.* Endocrinology, 1994. **135**(4): p. 1359-66.
232. Palazzolo, I., et al., *Akt blocks ligand binding and protects against expanded polyglutamine androgen receptor toxicity.* Hum Mol Genet, 2007. **16**(13): p. 1593-603.
233. Fang, X., et al., *Phosphorylation and inactivation of glycogen synthase kinase 3 by protein kinase A.* Proc Natl Acad Sci U S A, 2000. **97**(22): p. 11960-5.
234. Michell, B.J., et al., *Identification of regulatory sites of phosphorylation of the bovine endothelial nitric-oxide synthase at serine 617 and serine 635.* J Biol Chem, 2002. **277**(44): p. 42344-51.
235. Zhang, Y., et al., *Identification of a group of Ser-Pro motif hormone-inducible phosphorylation sites in the human progesterone receptor.* Mol Endocrinol, 1995. **9**(8): p. 1029-40.
236. Houslay, M.D. and D.R. Adams, *Putting the lid on phosphodiesterase 4.* Nat Biotechnol, 2010. **28**(1): p. 38-40.
237. Richter, W., S.L. Jin, and M. Conti, *Splice variants of the cyclic nucleotide phosphodiesterase PDE4D are differentially expressed and regulated in rat tissue.* Biochem J, 2005. **388**(Pt 3): p. 803-11.
238. Waldkirch, E., et al., *Expression of cAMP-dependent protein kinase isoforms in the human prostate: functional significance and relation to PDE4.* Urology, 2010. **76**(2): p. 515 e8-14.
239. Uckert, S., et al., *Immunohistochemical distribution of cAMP- and cGMP-phosphodiesterase (PDE) isoenzymes in the human prostate.* Eur Urol, 2006. **49**(4): p. 740-5.
240. Uckert, S., et al., *Characterization and functional relevance of cyclic nucleotide phosphodiesterase isoenzymes of the human prostate.* J Urol, 2001. **166**(6): p. 2484-90.
241. Kedia, G.T., et al., *Evaluating the significance of cyclic adenosine monophosphate-mediated signaling in human prostate: a functional and biochemical study.* Urology, 2012. **80**(4): p. 952 e9-14.

242. Uckert, S., et al., *Phosphodiesterase type 5 (PDE5) is co-localized with key proteins of the nitric oxide/cyclic GMP signaling in the human prostate*. *World J Urol*, 2013. **31**(3): p. 609-14.
243. Wheeler, M.A., et al., *Regulation of cyclic nucleotides in the urinary tract*. *J Smooth Muscle Res*, 2005. **41**(1): p. 1-21.
244. Rahrman, E.P., et al., *Identification of PDE4D as a proliferation promoting factor in prostate cancer using a Sleeping Beauty transposon-based somatic mutagenesis screen*. *Cancer Res*, 2009. **69**(10): p. 4388-97.
245. Wang, D., et al., *Cloning and characterization of novel PDE4D isoforms PDE4D6 and PDE4D7*. *Cell Signal*, 2003. **15**(9): p. 883-91.
246. Gretarsdottir, S., et al., *The gene encoding phosphodiesterase 4D confers risk of ischemic stroke*. *Nat Genet*, 2003. **35**(2): p. 131-8.
247. Marchionni, L., et al., *Impact of gene expression profiling tests on breast cancer outcomes*. *Evid Rep Technol Assess (Full Rep)*, 2007(160): p. 1-105.
248. Arikawa, E., et al., *Cross-platform comparison of SYBR Green real-time PCR with TaqMan PCR, microarrays and other gene expression measurement technologies evaluated in the MicroArray Quality Control (MAQC) study*. *BMC Genomics*, 2008. **9**: p. 328.
249. Ririe, K.M., R.P. Rasmussen, and C.T. Wittwer, *Product differentiation by analysis of DNA melting curves during the polymerase chain reaction*. *Anal Biochem*, 1997. **245**(2): p. 154-60.
250. Johnson, T.R., et al., *Focal adhesion kinase controls aggressive phenotype of androgen-independent prostate cancer*. *Mol Cancer Res*, 2008. **6**(10): p. 1639-48.
251. Figel, S. and I.H. Gelman, *Focal adhesion kinase controls prostate cancer progression via intrinsic kinase and scaffolding functions*. *Anticancer Agents Med Chem*, 2011. **11**(7): p. 607-16.
252. Serrels, B., E. Sandilands, and M.C. Frame, *Signaling of the direction-sensing FAK/RACK1/PDE4D5 complex to the small GTPase Rap1*. *Small GTPases*, 2011. **2**(1): p. 54-61.
253. Spina, A., et al., *cAMP Elevation Down-Regulates beta3 Integrin and Focal Adhesion Kinase and Inhibits Leptin-Induced Migration of MDA-MB-231 Breast Cancer Cells*. *Biores Open Access*, 2012. **1**(6): p. 324-32.
254. Williams, T.M. and M.P. Lisanti, *The caveolin proteins*. *Genome Biol*, 2004. **5**(3): p. 214.
255. Karam, J.A., et al., *Caveolin-1 overexpression is associated with aggressive prostate cancer recurrence*. *PROSTATE*, 2007. **67**(6): p. 614-22.
256. Shatz, M. and M. Liscovitch, *Caveolin-1: a tumor-promoting role in human cancer*. *Int J Radiat Biol*, 2008. **84**(3): p. 177-89.
257. Yang, G., et al., *Caveolin-1 expression in clinically confined human prostate cancer: a novel prognostic marker*. *Cancer Res*, 1999. **59**(22): p. 5719-23.
258. Tahir, S.A., et al., *Preoperative serum caveolin-1 as a prognostic marker for recurrence in a radical prostatectomy cohort*. *Clin Cancer Res*, 2006. **12**(16): p. 4872-5.
259. Sowa, G., *Novel insights into the role of caveolin-2 in cell- and tissue-specific signaling and function*. *Biochem Res Int*, 2011. **2011**: p. 809259.
260. Sowa, G., et al., *The phosphorylation of caveolin-2 on serines 23 and 36 modulates caveolin-1-dependent caveolae formation*. *Proc Natl Acad Sci U S A*, 2003. **100**(11): p. 6511-6.
261. Thompson, T.C., et al., *The role of caveolin-1 in prostate cancer: clinical implications*. *Prostate Cancer Prostatic Dis*, 2010. **13**(1): p. 6-11.

262. Yamamoto, M., et al., *Downregulation of caveolin expression by cAMP signal*. Life Sci, 1999. **64**(15): p. 1349-57.
263. Porter, A.G. and R.U. Janicke, *Emerging roles of caspase-3 in apoptosis*. Cell Death Differ, 1999. **6**(2): p. 99-104.
264. Winter, R.N., et al., *Loss of caspase-1 and caspase-3 protein expression in human prostate cancer*. Cancer Res, 2001. **61**(3): p. 1227-32.
265. Winter, R.N., J.G. Rhee, and N. Kyprianou, *Caspase-1 enhances the apoptotic response of prostate cancer cells to ionizing radiation*. Anticancer Res, 2004. **24**(3a): p. 1377-86.
266. Orlov, S.N., et al., *Activation of cAMP signaling transiently inhibits apoptosis in vascular smooth muscle cells in a site upstream of caspase-3*. Cell Death Differ, 1999. **6**(7): p. 661-72.
267. Nishihara, H., et al., *Inhibition of apoptosis in normal and transformed intestinal epithelial cells by cAMP through induction of inhibitor of apoptosis protein (IAP)-2*. Proc Natl Acad Sci U S A, 2003. **100**(15): p. 8921-6.
268. Youle, R.J. and A. Strasser, *The BCL-2 protein family: opposing activities that mediate cell death*. Nat Rev Mol Cell Biol, 2008. **9**(1): p. 47-59.
269. Catz, S.D. and J.L. Johnson, *BCL-2 in prostate cancer: a minireview*. Apoptosis, 2003. **8**(1): p. 29-37.
270. Oh, S., S. Shin, and R. Janknecht, *ETV1, 4 and 5: an oncogenic subfamily of ETS transcription factors*. Biochim Biophys Acta, 2012. **1826**(1): p. 1-12.
271. Wu, J. and R. Janknecht, *Regulation of the ETS transcription factor ER81 by the 90-kDa ribosomal S6 kinase 1 and protein kinase A*. J Biol Chem, 2002. **277**(45): p. 42669-79.
272. Janknecht, R., et al., *The ETS-related transcription factor ERM is a nuclear target of signaling cascades involving MAPK and PKA*. Oncogene, 1996. **13**(8): p. 1745-54.
273. Heinrich, P.C., J.V. Castell, and T. Andus, *Interleukin-6 and the acute phase response*. Biochem J, 1990. **265**(3): p. 621-36.
274. Febbraio, M.A. and B.K. Pedersen, *Contraction-induced myokine production and release: is skeletal muscle an endocrine organ?* Exerc Sport Sci Rev, 2005. **33**(3): p. 114-9.
275. Deeble, P.D., et al., *Interleukin-6- and cyclic AMP-mediated signaling potentiates neuroendocrine differentiation of LNCaP prostate tumor cells*. Mol Cell Biol, 2001. **21**(24): p. 8471-82.
276. Amorino, G.P. and S.J. Parsons, *Neuroendocrine cells in prostate cancer*. Crit Rev Eukaryot Gene Expr, 2004. **14**(4): p. 287-300.
277. Nathke, I.S., *The adenomatous polyposis coli protein: the Achilles heel of the gut epithelium*. Annu Rev Cell Dev Biol, 2004. **20**: p. 337-66.
278. Goss, K.H. and J. Groden, *Biology of the adenomatous polyposis coli tumor suppressor*. J Clin Oncol, 2000. **18**(9): p. 1967-79.
279. Furuuchi, K., et al., *Somatic mutations of the APC gene in primary breast cancers*. Am J Pathol, 2000. **156**(6): p. 1997-2005.
280. Bruxvoort, K.J., et al., *Inactivation of Apc in the mouse prostate causes prostate carcinoma*. Cancer Res, 2007. **67**(6): p. 2490-6.
281. Hurlin, P.J., *N-Myc functions in transcription and development*. Birth Defects Res C Embryo Today, 2005. **75**(4): p. 340-52.
282. Koh, C.M., et al., *MYC and Prostate Cancer*. Genes Cancer, 2010. **1**(6): p. 617-28.
283. Li, F. and J.Z. Tsien, *Memory and the NMDA receptors*. N Engl J Med, 2009. **361**(3): p. 302-3.

284. Abdul, M. and N. Hoosein, *N-methyl-D-aspartate receptor in human prostate cancer*. J Membr Biol, 2005. **205**(3): p. 125-8.
285. Husi, H., et al., *Proteomic analysis of NMDA receptor-adhesion protein signaling complexes*. Nat Neurosci, 2000. **3**(7): p. 661-9.
286. Chen, B.S. and K.W. Roche, *Regulation of NMDA receptors by phosphorylation*. Neuropharmacology, 2007. **53**(3): p. 362-8.
287. North, W.G., et al., *Breast cancer expresses functional NMDA receptors*. Breast Cancer Res Treat, 2010. **122**(2): p. 307-14.
288. Arighi, E., M.G. Borrello, and H. Sariola, *RET tyrosine kinase signaling in development and cancer*. Cytokine Growth Factor Rev, 2005. **16**(4-5): p. 441-67.
289. Kawamoto, Y., et al., *Identification of RET autophosphorylation sites by mass spectrometry*. J Biol Chem, 2004. **279**(14): p. 14213-24.
290. Dawson, D.M., et al., *Altered expression of RET proto-oncogene product in prostatic intraepithelial neoplasia and prostate cancer*. J Natl Cancer Inst, 1998. **90**(7): p. 519-23.
291. Follenzi, A., et al., *Cross-talk between the proto-oncogenes Met and Ron*. Oncogene, 2000. **19**(27): p. 3041-9.
292. Feres, K.J., I. Ischenko, and M.J. Hayman, *The RON receptor tyrosine kinase promotes MSP-independent cell spreading and survival in breast epithelial cells*. Oncogene, 2009. **28**(2): p. 279-88.
293. Chen, Y.Q., et al., *Overexpression and activation of the RON receptor tyrosine kinase in a panel of human colorectal carcinoma cell lines*. Exp Cell Res, 2000. **261**(1): p. 229-38.
294. Thobe, M.N., et al., *The Ron receptor tyrosine kinase positively regulates angiogenic chemokine production in prostate cancer cells*. Oncogene, 2010. **29**(2): p. 214-26.
295. Thobe, M.N., et al., *The Ron receptor promotes prostate tumor growth in the TRAMP mouse model*. Oncogene, 2011. **30**(50): p. 4990-8.
296. Baena, E., et al., *ETV1 directs androgen metabolism and confers aggressive prostate cancer in targeted mice and patients*. Genes Dev, 2013. **27**(6): p. 683-98.
297. Baert, J.L., et al., *ERM transactivation is up-regulated by the repression of DNA binding after the PKA phosphorylation of a consensus site at the edge of the ETS domain*. J Biol Chem, 2002. **277**(2): p. 1002-12.
298. Corn, P.G., *The tumor microenvironment in prostate cancer: elucidating molecular pathways for therapy development*. Cancer Manag Res, 2012. **4**: p. 183-93.
299. Hensley, H.H., et al., *PKA knockdown enhances cell killing in response to radiation and androgen deprivation*. Int J Cancer, 2011. **128**(4): p. 962-73.
300. Laxman, B., et al., *A first-generation multiplex biomarker analysis of urine for the early detection of prostate cancer*. Cancer Res, 2008. **68**(3): p. 645-9.
301. Henderson, D., *Phosphodiesterase Expression During the Progression of Prostate Cancer: The Significance of PDE4D7*, in Institute of Neuroscience and Psychology; College of Medical, Veterinary and Life Sciences 2011, University of Glasgow. p. 348.